CHARACTERIZING THE GRAVITY RECOVERABLE PLATINUM GROUP MINERALS

Zhixian (William) Xiao

A thesis submitted to the
Faculty of Graduate Studies and Research
In partial fulfillment of the requirement for the degree of
Doctor of Philosophy

Department of Mining and Materials Engineering
McGill University
Montréal, Canada

Your file Votre référence
ISBN: 978-0-494-66618-0
Our file Notre référence
ISBN: 978-0-494-66618-0

ABSTRACT

Modeling gravity recovery of platinum group minerals (PGMs) in the grinding circuit is based on three components: Ore characterization of gravity recoverable platinum group minerals (GRPGM), their behavior in grinding mills and hydrocyclones, and the performance of the gravity recovery units. This thesis focuses on the first two components.

A laboratory methodology to characterize gravity-recoverable platinum group minerals (GRPGMs) in an ore with four incremental liberation and recovery stages was developed. It was applied to quantify GRPGM content of four ore samples from Canada. To measure the behavior of GRPGMs in the grinding circuit, a methodology to characterize the already liberated (or available) GRPGMs in the circuit streams was developed. The availability of GRPGM in streams, such as ball mill discharge, was used to model the behavior of the GRPGMs in the ball mills and hydrocyclones. Combining with the potential GRPGM in an ore, they can be used for design and/or optimization of platinum group mineral recovery circuit.

The GRPGM content measured by this methodology varied from 5 to 81% depending on the ore. The GRPGM size distribution varied from fine (most GRPGM below 37 μm) to coarse (significant content above 212 μm). The stage size-by-size recovery and the total GRPGM content indicate that the methodology can quantify the GRPGM content of ores.

Based on the measurement of the availability of GRPGM in process streams, the behavior of PGMs in ball mills and hydrocyclones is characterized in terms of the less common cumulative selection functions and conventional classification efficiency

curves. Mineralogical analysis indicates that sperrylite ($PtAs_2$) is the dominant platinum mineral at the Clarabelle mill. Its classification efficiency is similar to that of gold, despite its lower density, while grinding rate is significantly higher than gold. The cumulative selection function of platinum and palladium is 1.3 times higher than the ore for size classes above 212 μm and 50 to 70% of the ore below 212 μm.

As a result, sperrylite accumulates in finer sizes than native gold in the grinding circuit. The cumulative selection function of the platinum group minerals was calculated for the Clarabelle grinding circuit based on the survey data and the GRPGM contents in the ball mill discharge, cyclone underflow, and overflow.

The methodology of characterizing the content of GRPGMs in an ore also offers a way to concentrate the minerals for mineralogical study. The use of secondary electron microscopy (SEM), variable pressure SEM and QEM*SEM for qualitative analysis of platinum group mineral mineralogy is presented and discussed. Most of the GRPGMs recovered are well liberated. Qualitative mineralogical analysis of the GRPGM and its associations in ore samples are also discussed.

Résumé

La modélisation et la prédiction de la séparation gravimétrique des minéraux du groupe du platine sont basées sur trois séries de données : la caractérisation des minerais contenant des minéraux du groupe du platine séparables par gravité (GRPGM), la description de leur comportement dans les broyeurs et hydrocyclones et la performance des unités de séparation. Cette thèse s'attache aux deux premières séries de données, celles-ci représentant les aspects fondamentaux pour la modélisation et la prédiction de la séparation des minéraux du groupe du platine par gravité.

Une méthodologie de laboratoire, basée sur quatre étapes de libération et de séparation, a été développée pour caractériser les CRPGM. Elle a été appliquée pour qualifier la proportion de CRPGM dans quatre échantillons de la région de Sudbury (Canada). Une autre méthodologie, visant à quantifier le comportement des CRPGMs dans les broyeurs et hydrocyclones a été développée de façon à caractériser les CRPGM déjà libérés (ou accessibles) dans les courants d'eaux du circuit de broyage. L'accessibilité des CRPGMs dans les courants, comme à la sortie du broyeur à boulets, ou dans les courants supérieurs ou inférieurs des hydrocyclones, a été utilisée pour décrire le comportement des CRGPMs dans les broyeurs et hydrocyclones. Combiné à la teneur potentielle de CRPMG dans un minerai, il peuvent être utilisés pour la justification du design et/ou l'optimisation du circuit de séparation des minéraux du groupe du platine.

La teneur en CRPGM obtenue par cette méthode varie de 5 à 81% d'un minerai à un autre. La distribution granulométrique varie également de fine (la plupart des GRPGM sont en dessous de 37 μm) à grossière (proportion significative sous 212μm). L'analyse de chaque tranche granulométrique séparée et l'analyse totale des CRPGM

indiquent que cette méthodologie est fiable pour la quantification des CRPGM des différents minerais contenant des minéraux du groupe du platine.

Basée sur la mesure de la disponibilité des CRPGM dans les courants, le comportement des PGMs dans les broyeurs à boulets et hydrocyclones est caractérisé en terme de fonctions de sélection cumulatives, cette dernière étant moins utilisée, et de courbes de classification d'efficacité. L'analyse minéralogique indique que la sperrylite ($PtAs_2$) est le minéral dominant du groupe du platine dans le concentrateur de Clarabelle. Sa courbe de classification d'efficacité est très similaire à celle de l'or, bien que sa densité soit moindre. Sa vitesse de broyage est significativement plus élevée que celle de l'or. De plus, la fonction de sélection cumulative pour les minéraux du groupe du platine a été calculée pour le circuit de broyage de Clarabelle en se basant sur les données de contrôle et sur les proportions de GRPGM à la sortie des broyeurs à boulets, au niveau des courants inférieurs et supérieurs des cyclones.

La méthodologie visant à caractériser la proportion des CRPGMs dans un minerai peut aussi être utilisée avec efficacité pour concentrer les minéraux du groupe du platine lors d'études minéralogiques. L'utilisation du microscope électronique à balayage (SEM), du SEM à pression variable (VP) et du QEM*SEM pour l'analyse quantitative des minéraux du groupe du platine est présentée et discutée. La plupart des GRPGMs séparés sont bien libérés. L'analyse qualitative des GRPGM et de leurs associations pour les échantillons de minerais est présentée et discutée.

Acknowledgements

The thesis is dedicated to remembering Professor A. R. Laplante. His sudden pass away was a huge loss to his family and the mining industry, especially to the gold industry. The author is indebted to Professor A. R. Laplante for his keen insight, wise guidance, enthusiasm and constant support for throughout the course of this research.

Deep appreciation also goes to Professor J. A. Finch for his acceptance of continuing the supervision of this thesis. His support makes it possible for me to complete this thesis. The author also deeply appreciates Professor Finch's wise guidance, knowledgeable suggestions for this thesis.

I wish to thank my friends and colleagues in the Gravity Separation group, especially Dr. Huang and lab technician Mr. R. Langlois for their help during my lab tests. Thanks also go to Kelvin Robertson and Helen Campbell for their help with the SEM operation, Annie X. Wang, Dr. Stephanie Somot, Dr. Mitra Mirnezami for their help in the process of thesis submission.

The author also wishes to thank the Natural Sciences and Engineering Research Council of Canada for their research funding, personnel of Falconbridge: Dominique Fragomini, Norman Lotter, Asim Tasum for supplying samples and analysis. Thank also goes to Clarabelle mine for their's support and corporation during the sampling campaign.

Last but not least, I extend my warmest thanks to my sweet daughter Jessica Jianing Xiao for her cooperation and support, it is her who inspires me to finish this thesis while working in USA at the same time, and my family members for their encouragement in the process of writing this thesis.

Table of Contents

List of Figures

List of Abbreviations and Acronyms

EPMA	Electron Probe Micro-Analyzer
SEM	Scanning Electron Microscopy
VP-SEM	Variable Pressure Scanning Electron Microscopy
QEM*SEM	Quantitative Evaluation of Minerals By Scanning Electron Microscope
GRG	Gravity Recoverable Gold
GRPd	Gravity Recoverable Palladium
GRPGM	Gravity Recoverable Platinum Group Minerals
GRPt	Gravity Recoverable Platinum
KC	Knelson Concentrator
KC-MD3	3 inch Manual Discharge Knelson Concentrator
PGEs	Platinum Group Elements
PGM	Platinum group mineral
XRD	X-Ray Diffraction

List of Abbreviations and Acronyms

EPMA	Electron Probe Micro-Analyzer
SEM	Scanning Electron Microscopy
VP-SEM	Variable Pressure Scanning Electron Microscopy
QEM*SEM	Quantitative Evaluation of Minerals By Scanning Electron Microscope
GRG	Gravity Recoverable Gold
GRPd	Gravity Recoverable Palladium
GRPGM	Gravity Recoverable Platinum Group Minerals
GRPt	Gravity Recoverable Platinum
KC	Knelson Concentrator
KC-MD3	3 inch Manual Discharge Knelson Concentrator
PGEs	Platinum Group Elements
PGM	Platinum group mineral
XRD	X-Ray Diffraction

CHAPTER ONE

INTRODUCTION

1.1 Background, Treatment Options and Statement of Problems

The six Platinum Group Elements (PGEs); ruthenium (Ru), rhodium (Rh), palladium (Pd), osmium (Os), iridium (Ir) and platinum (Pt) can be classified into two groups on the basis of specific gravity compared to gold (19.3). The elements less denser than gold are ruthenium, rhodium, and palladium with specific gravity ranging from 12.0 to 12.4. The elements denser than gold are osmium, iridium, and platinum with specific gravity in the range 21 to 22.5. The major PGE reserves and production is in South African, with Russia in second place and Canada third. South Africa's production centers on the Bushveld Complex, where the ores are primarily mined for the recovery of platinum group elements (PGEs). In Canada, PGEs are mainly by-products of nickel-copper extraction, primarily from the Sudbury area deposits (Cabri, 1981). There is one PGE mine in Canada, North American Palladium's Lac des Iles operation in Ontario.

Various data (such as mineralogical, chromite content, grade of PGEs, and sulphur content) are used to classify PGE ores. The world's PGE deposits can be classified into three types. Firstly, where platinum group minerals (PGMs) are the major economic product, e.g. the Bushveld (South Africa) and Stillwater complexes (Montana, USA). Secondly, copper-nickel dominant ores, with PGMs as by-products, e.g. Sudbury and Noril'sk (Russia). Thirdly, placer deposits, such as those in the Urals

(Russia) and Colombia. In the latter type, the PGMs have been derived from the weathering of a PGE-bearing host rock and subsequently concentrated and re-deposited by sedimentary mechanisms.

Treatment methods for recovering platinum group minerals from PGE ores depend on the type of mineralization. Those amenable to gravity separation contain high-density platinum-group minerals with a coarse grain size suitable for gravity recovery techniques (Cabri, 1981a). Ores in this category include magmatic Dunite or Alaskan-type deposits, and alluvial, eluvial and fossil placer deposits. With recent equipment and technology developments in gravity recovery, more deposits can be classified into this category. Ores amenable to flotation contain PGMs occurring in sulphides or as deposits at the grain boundary between sulphides and silicates (Cabri, 1981). Most PGEs occur either as discrete minerals or as solid solution in major sulphides, such as the Bushveld and Stillwater deposits. Another category is ores where PGEs are by-products of Ni-Cu recovery. These ores are processed by methods determined by the nickel and copper minerals.

PGM recovery poses a unique challenge. Unlike gold and major base metals, whose target element is found in a limited number of minerals, there are one hundred and nine PGM species recognized by the International Mineralogical Association (IMA), including sulphides (e.g. braggite, (Pt, Pd)S), tellurides (e.g. maslovite, PtBiTe), antimonides (e.g. sudburyite, PdSb), arsenides (e.g. sperrylite, $PtAs_2$), alloys (e.g. ferroplatinum alloy) and native species (i.e., native Pt nuggets). Several are economically significant. Apart from the multitude of PGMs, their associations are also diverse. The three main base metal minerals associated with PGMs are pyrrhotite, chalcopyrite, and pentlandite, such as in the South African Merensky Reef deposit. The UG-2 Reef contains low concentrations of copper- and nickel-bearing sulphides and a large amount of chromite ($FeCr_2O_4$). In the Stillwater J-M Reef ore body (U.S.A.), the principal sulphide minerals are chalcopyrite, $CuFeS_2$, and pentlandite, $(Ni, Fe)_9S_8$.

Most platinum minerals are associated with the copper sulphides and palladium with the nickel sulphides. The ore contains less than 1% quartz but significant amounts of talc and serpentine, both of which show natural floatability, making their rejection problematic. Platinum was long known to exist in the arsenide form (sperrylite, $PtAs_2$) in the nickel-copper sulphides of the Sudbury area (Cabri, 1981).

Pentlandite and chalcopyrite are generally well recovered (depending on their particle size and degree of liberation), as therefore are any PGEs in their lattice (i.e., in solid solution) or present in PGM blebs. Platinum group elements present as blebs or in solid solution in pyrrhotite may or may not be recovered. For example, in the Sudbury basin, pyrrhotite is now largely rejected to minimize sulphur dioxide removal costs. The Sudbury pyrrhotites contain significant amounts of nickel (anywhere from 0.4 to 0.8%) and accounts for most of the nickel losses in the Clarabelle and Strathcona mill tailings. The very low concentration of PGMs, their fine size distribution, the difficulty of detection and identification, and difficulty in sampling are typical problems when carrying out studies on PGMs.

In a summary, the range of minerals present, their relative densities, shape, particle size, and associations present a challenge to the metallurgist in designing and optimizing the extraction process (Hochreiter et al., 1985). The various ore types (end members) of typical ore deposits, each with their own metallurgical response, heighten this challenge (Hochreiter et al., 1985).

Table 1-1 Some PGM mineral properties (Cabri, 1981 and 2003)

Name	Ideal Formula	General Appearance	Density (g/cm^3) (calculated)	Hardness (mohs)
Borovskite	Pd_3SbTe	Isolated grains up to 0.2 mm included in pyrrhotite and chalcopyrite	8.25	N/A
Braggite	(Pt, Pd)S	Fractured grains up to 8 mm long	9.36	5
Cooperite	PtS	Euhedral to anhedral micrometer to 1.5 mm grains	10.10	4 to 4.5
Froodite	$PdBi_2$	Grains up to about 1 mm	11.62	Brittle
Geversite	$PtSb_2$	As small drop like inclusion	10.91	4.5-5
Insizwaite	$PtBi_2$	As small rounded grains up to 120 μm	12.86-13.59	5
Isoferroplatinum	Pt_3Fe	In placer deposits occurs as various size nuggets, usually containing chromite and many other mineral inclusion, varying from flakes to nugget size	18.23	N/A
Maslovite	PtBiTe	Grain up to 0.120 mm in size	11.23	4-5
Merenskyite	$PdTe_2$	As minute grains, intimately intergrown with other PGM, or as single-phase inclusions	8.30	3.5-4
Michenerite	PdBiTe	Grains from 0.0001 to 2 mm	9.81	4-4.5
Moncheite	$PtTe_2$	Crystals up to 1 mm and minute grains	10.24	3.5
Palladoarsenide	Pd_2As	Long and irregular grains	10.59	4.5
Sperrylite	$PtAs_2$	Micrometer to centimeter size crystals and rounded grains	10.8	6-7 Brittle
Stillwaterite	Pd_8As_3	Grains up to 0.12mm by 0.265 mm	10.95	4.5-5
Sudburyite	PdSb	Elongated inclusions up to 55 μm by 120 μm	9.41	4-4.5
Tetraferroplatinum	PtFe	Irregular grains, rims on other Pt-Fe grains	15.81	N/A
Vysotskite	PdS	As intergrowths and lensoid inclusions in other sulphides	6.74	N/A
Palladium	Pd	Commonly as loose grains, sometimes with a radial fibrous texture	12.0	4.5-5
Platinum	Pt	In placer deposits, it occurs as various size nuggets.	19.1	4-4.5

The PGM species with their theoretical formula are listed in Table 1-1, although composition may vary. The general appearance is based on where the individual PGM was first reported. The density and hardness listed are critical factors as regard gravity recovery, grinding and classification behavior.

There has been renewed interest in the use of gravity concentration to recover PGMs due to their economic importance and the new/improved gravity concentration devices becoming available commercially (Cole and Ferron, 2002, Kozyrev et al., 2003). Flash flotation is also attractive because of the ability to quickly lower

circulating load of PGMs at relatively low installation cost (Laplante et al., 2002). However, there is no method to quantify the gravity recoverable content for design, optimization or simulation purpose. To justify if a gravity method is economical for recovering PGMs, it is desirable to predict or determine how much **G**ravity **R**ecoverable **P**latinum **G**roup **M**inerals (GRPGMs) is present in an ore (or stream). The concept of GRPGMs is analogous to gravity recoverable gold (GRG). As a working definition, it refers to the portion of PGMs in an ore or stream that can be recovered by gravity at a low yield (<1%). It includes PGMs that are totally liberated, as well as PGMs in particles not totally liberated but of such density that they report to the gravity concentrate. Conversely, it excludes liberated PGMs that are too fine to respond to gravity recovery or are present as blebs or in solid solution in other minerals.

1.2 Thesis Objectives

Much work has been done on the flotation recovery of PGMs from primary ores (Cole and Ferron, 2002). Concerted efforts have been made to evaluate the mineralogy of PGMs and to use gravity separation to improve associated recovery in the processing of nickel-copper ores. This is desirable for Sudbury area ores where PGEs are produced as by-products, for example, the platinum recovery at the Clarabelle mill ranges between 75 and 85%. A significant source of platinum losses is fine discrete sperrylite particles, which very likely originates from coarser liberated particles. Similar losses likely occur at the other Sudbury area Cu-Ni mill, Strathcona. Outside Canada, PGE producers have recognized this loss of fines problem and have attempted to address using either flash flotation or gravity recovery, in some cases with significant success (Cole and Ferron, 2002). However, a formal methodology or protocol to determine the best approach to be able to estimate projected recovery from circulating loads in grinding circuits and potential gains in net overall recoveries is still lacking in the PGM industry. This thesis will endeavor to fill this gap by adapting a similar protocol developed at McGill University for gravity recoverable gold (GRG) (Laplante et al.,

1993; Woodcock and Laplante, 1993; Xiao, 2001). The proposed protocol would answer questions such as "how much of each PGM is available for gravity recovery/flash flotation and at which grind size is it liberated?", "what is the probability that a PGM particle not recovered will be presented again to gravity recovery or flash flotation, having 'survived' in grinding and cycloning?", and "how much will a given unit recover a specific PGM in a specific size class?"

Figure 1-1 shows that the GRG protocol for prediction of gold recovery is based on three components, ore characteristics, behavior in grinding and classification units, and recovery unit performance. The proposed GRPGMs protocol will be based on the GRG protocol; because the PGMs are unique and different from gold minerals, some refinements can be expected.

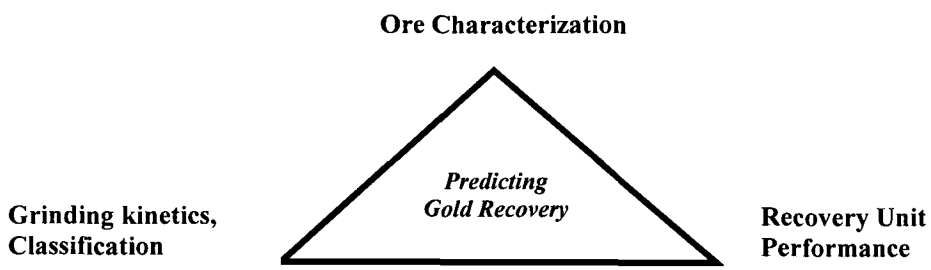

Figure 1-1: GRG Protocol for the Gold Recovery Prediction (Laplante et al., 2004)

The rationale for the transfer of the GRG protocol to GRPGMs is based on the similar specific gravity range of many platinum group minerals (between 10 and 22) to that of gold (between 16 and 19). However, as the PGMs tend to report to finer size classes (Xiao and Laplante, 2003), the GRG protocol will require modification. The modified procedure adds a fourth Knelson Concentrator stage at a higher rotation velocity to the standard GRG protocol. It is also shown that the characterization of the

gravity recoverable platinum group minerals procedure provides an effective preconcentration method for sample preparation for PGM mineralogical studies.

The above suggests that the overall objective will be achieved by pursuing the three components. This thesis focuses on the first two. Firstly, ore characterization is adapted to PGMs, which requires a more intense recovery effort than gold, because of lower specific gravity of the PGMs, and the use of automated mineralogical analysis to quantify the occurrence of various PGMs in the gravity recoverable fraction, as PGM mineralogy is far more complex than gold (Cabri, 1988; Sizgoric, 1985). The occurrence and liberation analysis of platinum group minerals is performed with SEM, variable pressure SEM (VP-SEM) and quantitative evaluation of materials SEM (QEM*SEM) on the gravity concentrates. The results will be present and discussed in Chapter five. Secondly, the already liberated GRPGMs in a stream will be characterized, and then the behavior of PGMs in ball mills and cyclones will be quantified by using the cumulative selection function and classification partition curve combined for the first time in this type of analysis. The third component, recovery unit performance, ideally would require pilot testing of semi-continuous centrifugal concentrator or flash flotation units; this will not be addressed in this thesis.

1.3 Thesis Structure

This thesis consists of seven chapters. Chapter one (this chapter) introduces the background to the program. Treatment methods for platinum group mineral deposits are outlined, as well as the statement of the problem. The objectives of the study and thesis structure are also presented.

Chapter two presents a review of PGM mineralogy and recovery methods, the latter both at bench and industrial scale. The existing GRG characterization protocol is also presented in this chapter.

Chapter three introduces the GRPGM test design. The importance and effect of adding the fourth stage with a high-rotation speed 3-inch Knelson Concentrator are discussed. The results of four ore sample characterization tests are presented, followed by detailed discussion, comparison, and conclusions.

Chapter four introduces characterization of the behavior of PGMs in grinding circuits. The cumulative selection function and classification efficiency curves for platinum minerals from the Clarabelle grinding circuit are presented and discussed. The behavior of other platinum group metals, such as palladium and ruthenium, is touched on. The behavior of gold and platinum is contrasted.

Chapter five introduces the mineralogy component, based on SEM, VP*SEM and QEM*SEM test work. The platinum group minerals species and associations for some ore samples are presented. Most importantly, liberation analysis of some platinum group minerals for a Strathcona ore sample is performed using QEM*SEM.

General conclusions, claims to original work and suggestions for future research are presented in Chapters six and seven, respectively.

CHAPTER TWO

LITERATURE SURVEY AND THEORY

2.1 Introduction

Recovering platinum group minerals (PGMs) in grinding circuits by gravity faces several challenges. The first comes from the complex mineralogy of PGMs, a combination of low grade, a plethora of mineral species and fine size distribution. The mineralogy is reviewed here. The low ore grades almost invariably necessitate upgrading and the approaches are presented. To end there is a section describing typical flowsheets for PGM recovery.

To model the gravity recovery of PGMs in a grinding circuit, three tasks must be completed: characterizing the gravity recoverable platinum group minerals (GRPGMs), their behavior in the grinding mills and hydrocyclones, and their recovery in the gravity concentrator device (Laplante et al, 2004). The approach can be adapted from the approach used for the gold recovery by gravity. The review is divided into three sections: (a) applied/process mineralogy and PGM recovery methods, (b) laboratory methods of characterizing PGMs, and (c) GRG methodology (since it is intended to adapt to PGMs).

2.2 Process Mineralogy and PGM Recovery Methods

There is a relationship between ore mineralogy and metallurgical performance (Petruk and Hughson, 1977; Henley, 1983; Cabri, 1992; Petruk, 1995; Lotter et al., 2002). Not only does mineralogy play a critical role in choosing the recovery method but it also dictates the process flow sheet and plant optimization.

Henley (1983) defines process mineralogy as an integration of mineral processing and mineralogy. In his review, a flow sheet starting from ore body exploration through to optimization of plant operation was proposed. A flow sheet was developed based on mineralogical information, laboratory, and pilot plant testing. After commissioning, an optimization program was followed. The program extended from samples of drill core to samples taken from the operating plant. Petruk (2000) defines applied mineralogy as the application of mineralogical information to understand and solve problems encountered during processing of ores and concentrates. It involves characterizing minerals and interpreting the data with respect to mineral processing. When processing problems are due to the mineralogical characteristics of the ore and/or process products, mineralogical data should be generated to solve the problem(s).

Each platinum-group element ores should be treated using a recovery method based on the mineralogical features. The following briefly discusses several ore types: those amenable to gravity separation, those amenable to flotation, and those where platinum-group elements are by-products of base metal sulphide recovery. Most of the information is drawn from the special volume "Platinum-Group Elements: Mineralogy, Geology, Recovery" edited by Cabri (1981).

2.2.1 Ores Amenable to Gravity Recovery

2.2.1.1 Alaska-type deposit mineralogy and recovery method

The mineralogical features of importance for ores amenable to gravity separation are that the platinum-group elements occur in minerals of high density, that they are free liberated, and that the grain size distribution falls in the region where gravity techniques can be applied successfully (Cabri, 1981a). Ores in this category include magmatic Dunite or Alaskan-type deposits, and alluvial, eluvial and fossil placer deposits. With the development of new centrifuge gravity equipment, more deposits can be classified into this category.

Mineralogy: Primary PGE deposits in Alaska-type ultramafic rocks were found first in the Nizhnii-Tagil district of the Ural Mountains in 1890 (Mertie, 1969). The principal PGMs are Pt-Fe alloys, mostly isoferroplatinum (Pt_3Fe) and to a lesser extent platiniridium (Ir, Pt), according to Razin (1976). This type of deposit also includes the rare PGMs: osmiridium (Ir, Os), iridosmine (Os, Ir), cooperite (PtS), tulameenite (Pt_2FeCu), laurite (RuS_2) tetraferroplatinum (PtFe) and irarasite (IrAsS). Most of the Pt-Fe alloy grains in the Gusevogorskiy deposit are smaller than 0.1 mm; however, grains as large as 3 mm occur sporadically (Begizov et al., 1975).

Recovery method: A typical route is to grind to minus 0.2 mm then subject to magnetic separation followed by tabling (SK-1 concentration tables). The table concentrate is processed again to produce a gravity concentrate in a hydroseparator.

Prior to start of the 20^{th} century, all PGEs were obtained from alluvial deposits. The PGEs occur in these deposits as alloys, usually Pt-rich, in the form of loose grains

and nuggets. There are virtually no published data on the recovery of PGEs from placer mining due to lack of mineralogical data.

2.2.1.2 Norilsk deposit mineralogy and recovery method

The Norilsk Mining Company is one of the largest PGE producers in the world. According to a typical economic classification, Norilsk deposits belong to a group of sulphide copper-nickel ores with associated PGE mineralization (Blagodatin, et al., 2000). The deposit is subdivided into three groups, massive (rich) ore, disseminated ore occurring in host rock, and stringer-disseminated ore occurring in intrusive host rock (Kozyrev, et al., 2003). Another classification method is adopted by Blagodatin et al., (2000): dividing the ores into two groups, one copper-nickel sulphide ores, and another platinum with associated non-ferrous and rare metals, including all kinds of disseminated ores.

Mineralogy: The PGEs in major sulphides (pyrrhotite, pentlandite, and chalcopyrite) and PGE occurrence in many varieties of disseminated ore have been studied at the Research Center of Norilsk Company. The bulk of platinum (90% plus) is in the minerals cooperite (PtS), Pt-Fe alloys, sperrylite ($PtAs_2$), and Pd-rustenbergite $(Pt, Pd)_3Sn$, while minor quantities are dissolved in pyrrhotite, with a maximum concentration of 0.8 ppm. As for palladium, 27% is in discrete mineral form. The PGEs are largely hosted in pyrrhotite, which comprises up to 4.0% of the ore. The +250 μm size fraction contains occasional grains of platinum minerals, whereas size fractions 50-250 μm, appear to be most enriched in these minerals. Palladium minerals occur as fine grains (- 50μm).

Recovery method: The nature of PGE occurrence in the ores dictates the use of modern high-performance techniques of gravity separation to produce high recovery into high-grade PGE concentrates. This makes it possible to process PGE gravity

concentrates directly, avoiding by-product production from copper and nickel concentrates (Blagodatin et al., 2000).

At Norilsk, Knelson Concentrators are widely used; their installation points were selected on the basis of a mineralogical investigation of concentrate products obtained by flotation. From the size analysis of flotation concentrate and tailings, it was found that the bulk of the platinum and palladium mineral grains in the concentrates were below 70 μm, the highest distribution being in the 30-40 μm size fraction with no grains found above 300 μm. In the tailings, no PGM grains were coarser than 100 μm in the non-magnetic fraction and the highest distribution was in the 20-30 μm size fraction. In the magnetic fraction, a significant amount of Pt- and Pd-bearing grains reported to the 100-200 μm size fraction. Such size behavior indicates that flotation cannot completely recover the PGMs and over-grinding may occur. Therefore, the company decided that the gravity separator should be installed after the first grinding stage, thus removing the bulk of PGE minerals from the flotation circuit.

Since June 1998, in both the grinding and tailings reprocessing circuits, Knelson Concentrators (KS-SD 48) have been used. Recoveries of 50-60% Pt, 10-13% Pd, and 17-20% Au are achieved with 400-500 g/t total PGE content in concentrates. These results were obtained from ore assaying 1.1-1.3 g/t Pt, 3.4-4.6 g/t Pd, and 0.16-0.2 g/t Au. The positive results prompted the company to install two additional 48-inch KCs with a modified bowl profile. This resulted in the total PGE content increasing to 1000 g/t, and recovery increasing by 25% (Blagodatin et al., 2000).

2.2.2 Ores Amenable to Flotation Recovery

Flotation might be the most common method to recover PGEs. As is now well known, PGMs often occur in base metal sulphides, often along the grain boundary between sulphides and silicates (Cabri, 1981). Most PGEs occur either as discrete minerals or as solid solution in major sulphides.

In those magmatic deposits where platinum-group elements are intimately associated with the base metal sulphides, flotation is used as the first and often sole recovery process. Although high recovery, usually between 80 and 95%, can be obtained, the concentrate grade is generally quite low, and further upgrading is required.

2.2.2.1 Merensky Reef

Mineralogy: Extensive mineralogical studies have shown that seven PGMs are important in the Merensky Reef although variations occur in different areas and ore types (Vermaak and Hendriks, 1976, Brynard et al., 1976, Schwellus et al., 1976). Three of the PGMs are sulphides: braggite (Pt,Pd)S, cooperite, PtS, laurite, RuS_2; one is a Pt-Fe alloy, one an arsenide (sperrylite, $PtAs_2$) and two are tellurides (moncheite, $PtTe_2$, kotulskite PdTe). The presence and relatively large fraction of platinum minerals and sulphides is unique to this type of deposit which divides into two groups, a silicate ore, and a chromite ore.

The principal sulphide minerals are pyrrhotite, pentlandite and chalcopyrite, in order of decreasing abundance (Vermaak and Hendriks, 1976; Brynard et al., 1976). Minor sulphides include cubanite, mackinawite and pyrite, the latter being more abundant in the chromite-rich bands (Brynard et al., 1976).

The majority of the PGMs occur as idiomorphic inclusions (braggite, cooperite, sperrylite and laurite). A Pt-Fe alloy, especially in those areas where it is an important PGE carrier, commonly occurs as fine intergrowths with base metal sulphides (BMS) or, more rarely, with cooperite (Vermaak and Hendriks, 1976). These authors also pointed out that most PGMs occur at the BMS-gangue contact in the silicate ore, whereas in the chromite ore the PGMs occur mostly in the BMS or in the gangue. The exception to this is braggite, which shows a strong preference for pentlandite. The sperrylite, braggite and cooperite occur "fairly coarse" with moncheite being "much smaller" (Brynard et al., 1976).

Recovery method: Although the basic process used for the Merensky and UG-2 ore is the same, mineralogical features dictate the many subtle differences in each flow sheet. Conventional comminution, including crushing, rod milling, and ball milling or semi-autogenous (SAG) milling, is used for the Merensky ore, while UG-2 ore is not amenable to autogenous milling. The grinding product is classified in hydrocyclones for both ores. Other differences include preconcentration methods, such as the corduroy strake, James table and flash flotation, used for the Merensky ore which shows PGM enrichment in the cyclone underflow. The UG-2 ore is not as amenable to preconcentration because a finer grind is needed to liberate the much finer PGMs and the chromite present can lead to poor gravity separation.

For the Merensky and UG-2 ores, the separation process is a bulk sulphide flotation that recovers sulphide PGMs. Flotation takes place at natural pH (7.5 to 9) with a xanthate collector such as isobutyl xanthate or n-propyl xanthate. Some mines also add another collector, usually Cyanamid 3477 (a dithiophosphate), which is mixed with the xanthate at a ratio of up 7:3. Copper sulphate is added as an activator. The flotation circuit for Merensky ore usually consists of a rougher stage and two cleaner stages in a closed-circuit. To depress the talc, a depressent such as Dextrin or

Carboxymethyl cellulose (CMC) is added to the rougher and cleaner stages. The flotation of the UG-2 ore is similar in general to that of the Merensky ore.

The Northam Merensky concentrator was designed to treat 270 t/h run-of-mine (ROM) ore. The SAG mill discharge is fed to a ball mill operated in a closed circuit. Flash flotation is utilized on the cyclone underflow. The flash flotation cell recovers over 60% of the PGEs. The cyclone overflow goes to flotation after conditioning. Primary flotation is undertaken in a single rougher/scavenger flotation bank. The concentrate of the first cell in the rougher bank is collected as part of the final concentrate. The remaining rougher concentrate is processed through the cleaning circuit (no regrinding) that consists of three column cells operating in series. The cleaner concentrates are the main final concentrates. The cleaner tail is recycled back to the head of the scavenger circuit. The scavenger concentrate can be routed to the head of the rougher bank or to the cleaner circuit. No regrinding is performed on the scavenger concentrate (Cole and Ferron, 2002).

2.2.2.2 The Stillwater Complex, Montana

The Stillwater ore body is referred to as the J-M Reef and is nearly 50 kilometer in length. The PGE mineralization is associated with disseminated base-metal sulphide (BMS) minerals that range from fine- to coarse-grained aggregates that are moulded around and are interstitial to the cumulus or earlier formed silicates.

Mineralogy: Zientek et al. (2002) report that the PGMs include the following palladium, platinum and ruthenium sulphides; Pt and Pd tellurides and arsenides; and Pt-Fe, Pt-Pd-Sn, Pd-Pb, Pd-Hg, Au-Pt-Pd and Rh-Pt alloys. The dominant PGMs are braggite, cooperite, moncheite, vysotskite and isoferroplatinum. Platinum occurs largely as discrete PGMs: 67% as sulphide mineral (braggite, cooperite); 25% as metal alloy (isoferroplatinum); and 8% as telluride (moncheite). Palladium largely occurs in

solid solution in pentlandite; 15% of the palladium occurs in other sulphide minerals (vysotskite, braggite, and cooperite) and 5% is associated with telluride minerals (moncheite). There are some rare PGMs such as rustenbergite (Pd_3Sn), and hollingworthite (RhAsS). The grain size of the PGMs is variable, ranging from micron-size to grains with one side about 200 μm. Of the main PGMs, braggite and vysotskite are the coarsest grained; the Pt-Fe alloy is finer.

The principal sulphide minerals are chalcopyrite ($CuFeS_2$) and pentlandite ($(Ni,Fe)_9S_8$). Most of the platinum minerals are associated with the copper sulphides and the palladium with the nickel sulphides (Thurman et al., 1994). The ore contains approximately 3.5 times more palladium than platinum. Small amounts of gold and rhodium along with the copper and nickel are also found. The ore contains less than 1% free silica, but significant amounts of MgO bearing minerals such as talc and serpentine. The ore is basic with a natural pH of approximately 9.0 (Thurman et al., 1994).

Recovery method: Thurman et al. (1994) and Turk (2001) provide a detailed summary of operations and reagent scheme at the Stillwater Nye concentrator.

A SAG mill / ball mill grinding circuit with hydrocyclones for classification is used for feed preparation. A flash flotation cell is used in the cyclone underflow to produce a final grade concentrate. The cyclone overflow is fed to primary flotation which comprises three stages: rougher flotation, middling flotation and scavenger flotation. There is a regrind stage between the rougher and middling flotation circuit. The middling flotation concentrate is recycled to the head of the rougher circuit while the scavenger flotation concentrate feeds the middling flotation circuit. Cleaning is achieved in three stages operating in a counter-current configuration. The concentrate from the first stage of the first cleaner bypasses the second stage of cleaning and feeds the third cleaner. The tailings from the first part of the first cleaner are reground prior

to further cleaning. The cleaner circuit tails recycle to the feed of the rougher flotation circuit.

Thurman et al. (1994) reported that the reagent scheme is 40.8 g/ton of potassium amyl xanthate and 36.3 g/ton of dithiophosphate and 408 g/ton of Carboxymethyl cellulose (CMC) used for talc depression. The frother MIBC is added for conditioning warrant. Sodium hydrosulfide (NaHS) is added as a sulfidizer and pH is controlled with sulphuric acid.

A bulk sulfide concentrate is produced averaging 1860 – 2170 g/ton of Pt + Pd from ore averaging 24.8 g/ton. Initially the concentrator operated at 500 tpd. But capacity has been steadily increased since the 1987 start-up; concentrator throughput for 1994 was around 1050 tpd, and was 3000 tpd in 2001.

The overall platinum recovery after the flash flotation cell installation improved by 1.5% (Thurman et al., 1994), pushing total Pt recovery to 95%. This improvement in recovery is due to the reduction in over grinding of the Pt minerals. However, because of the extremely short retention time in the flash cell (2-5 min.), Pd recoveries were not affected.

2.2.2.3 Lac des Iles Ore

North American Palladium's Lac des Iles mine began commercial production in December 1993. It has since commissioned a new 15,000 ton per day milling and flotation circuit. The open-pit mine and milling operation is one of only two primary platinum group element producers in North America. The mill treats an ore containing 2g/t palladium (and 0.3 g/t total platinum, gold and rhodium) producing a concentrate assaying 250g/t palladium, at a recovery of roughly 75% (Martin et al., 2003).

Mineralogy: The major sulphide minerals are pentlandite, pyrite, chalcopyrite and pyrrhotite. Galena, magnetite and sphalerite are common minor minerals. Cabri and Laflamme (1979), on the basis of the sample they studied, reported that the principal PGMs are braggite-series minerals (braggite, (Pt, Pd)S, and vysotskite, PdS), kotulskite, PdTe, isomertiete, $Pd_{11}(As, Sb)_4$, merenskyite, $PdTe_2$, sperrylite $PtAs_2$, moncheite, $PtTe_2$; minor PGMs include stillwaterite, Pd_8As_3, and palladoarsenide, Pd_2As. Dunning (1979) reported that vysotskite is the most abundant PGM in the "Roby zone", where it frequently occurs with nickel minerals, especially pentlandite.

Mineralogical studies were performed on five mill feed samples taken at different times during 2002 (Martin et al., 2003). Sample assays ranged from 1.56 g/t to 3.0 g/t Pd+Pt. Using a LEO440 QEMScan system, a total of 444 individual PGM grains comprising twelve distinct PGM species were identified. These were dominated by tellurides, with lesser amounts of arsenides/antimonides, sulphides and alloys. Martin et al. (2003) also reported that the kotulskite-telluropalladinite (Pd(Te,Bi)-Pd_9Te_4) comprised roughly two-thirds of the PGMs grain population. Palladoarsenide (Pd_2As) was the next most abundant PGM species, comprising 20% of the PGMs. Ten other PGM species were observed. PGM particle size ranged from less than 1 μm to 16 μm (equivalent circle diameter). Some 45% of the PGMs occurred as liberated grains, or inclusions within and attachments to sulphides. The remainder occurred as fine inclusions within, and attachments to silicate minerals.

Recovery method: Flotation is the method for recovering the PGMs in Lac des Iles due to their fine size distribution. One SAG mill feeds two ball mills at a rate of 15,000 ton per day. A portion of the SAG mill feed is crushed to –25 mm to increase throughput. Flotation comprises two banks of roughers and scavengers for primary flotation. The rougher concentrate is reground and cleaned in a single stage column. The rougher cleaner tail joins the scavenger concentrate and is reground in three vertimills. Cleaner flotation comprises two stages of cleaning with mechanical cells,

and a third stage using flotation columns, the column tails being scavenged using a bank of mechanical cells. The flotation reagent system consists of amyl xanthate collector, dithiophosphate promoter, MIBC frother and a polymeric talc depressant, usually a form of carboxy methylcellulose.

The expected feed grade to the plant is 2 g/t Pd with a targeted recovery in excess of 80%. However, it is reported that the recovery is around 75% due to problems in the grinding circuit and other factors (Martin et al., 2003).

2.2.3 Cu-Ni Sulphide Deposits with By-Product PGEs

The by-product PGEs from Sudbury Cu-Ni ores were the principal source of PGEs prior to the discovery and subsequent exploration of the PGE-dominant Merensky Reef deposits. The production of Merensky Reef and, later, the Cu-Ni deposits of the Norilsk area reduced Sudbury's share of world PGE production. However, by-product PGEs from Cu-Ni sulphide deposits are still an important source. The Sudbury area and Norilsk-Talnakh area ores will now be discussed.

2.2.3.1 Sudbury Area, Ontario

Mineralogy: Although several researchers have studied the mineralogy of the Sudbury ores, published data are sparse on the PGE content. The principal sulphides are pyrrhotite, chalcopyrite and pentlandite; several other minerals, such as cobaltite, pyrite, millerite, cubanite, galena, sphalerite and magnetite, occur in minor and variable quantities.

Michenerite, PdBiTe, is the principal palladium mineral and sperrylite, $PtAs_2$, is by far the most common platinum mineral for deposits of the South Range (Cabri, 1981). Moncheite, $PtTe_2$, is the principal platinum mineral in deposits with essentially

no sperrylite (Levack West). Froodite, $PdBi_2$, insizwaite, $PtBi_2$, and sudburyite, PdSb, are less common. There are also some rare PGMs. According to Cabri (1981), the PGMs occur mainly as small inclusions, usually less than about 150 μm, but millimeter-size grains of sperrylite are present. Recent studies by Xiao and Laplante (2003b) confirmed the presence of well-liberated sperrylite below 150 μm that is well liberated in Clarabelle mill feed. Although sperrylite characteristically occurs as monocrystalline inclusions or coarse grains, the other PGMs are present more frequently as complex multimineralic intergrowths, often with Bi and Ag tellurides.

Cabri and Laflamme (1976) made a detailed investigation of 150-300 μm sink fractions of hydroseparation. They found that although some PGMs are liberated in this size class, especially sperrylite, the majority of PGMs are still locked. About 5-15% of the michenerite, moncheite, sperrylite and sudburyite grains found in the 150-300 μm sink fraction occurred as inclusions in pyrrhotite or magnetite.

They concluded that the PGE values might be accounted for by discrete PGMs and PGEs in solid solution in arsenides and sulpharsenides. They felt that PGE in arsenides and sulpharsenides, if present, would be important in view of the large tonnages involved, but that conclusive evidence was still required. Detailed mineralogical studies of a second-stage milled sample and metal balance calculations showed that, for the particular sample studied, from 1-4.5% Pt, 22.3-23.3% Pd and 31.2-41.2% Rh are present as solid solutions in cobaltite and gersdorffite (Cabri, 1981).

Cabri (1981) reported that 66% of the sperrylite found in a mill tailing was either liberated or attached to sulpharsenides. Because the sperrylite is the principal Pt mineral in South Range ores and its close textural association with sulpharsenides requires that both be recovered, he suggested that it was worth investigating the flotation characteristics of sperrylite.

2.2.3.2 Massive Ore in The Norilsk-Talnakh Area of U.S.S.R.

According to Kozyrev et al. (2003), this massive deposit is identified as a Kharaelakh orebody, which occurs at the base of a layered intrusion and contains more than 70 vol.% sulphides. The orebody is divided into three groups, namely: pyrrhotite ore, cubanite ore, and chalcopyrite ore. Pyrrhotite ores include pyrrhotite, chalcopyrite-pyrrhotite and cubanite-chalcopyrite-pyrrhotite varieties, and make up 85 vol.% of the Kharaelakh orebody. The cubanite and chalcopyrite ores each make up only 7 to 8 vol.% of the orebody.

Mineralogy: Variability in chemical composition of the ore is manifest in the gradual increase of PGE content from 2.3 to 11.9 ppm up to 20.2 to 111.7 ppm (Kozyrev et al., 2003). The pyrrhotite ore has few PGMs in the -90 μm size fractions. These include isoferroplatinum (IFP), sperrylite, cooperite, rustenbergite, Kotulskite, merenskyite and native gold. The dominant PGM is IFP, which constitutes 99 wt % of the total PGM assemblage (Kozyrev et al., 2003).

Kozyrev (2000) also characterized mineralogy of PGMs in the feed and concentrates of the chalcopyrite-pyrrhotite and cubanite-chalcopyrite ores. It was found that the chalcopyrite-pyrrhotite ore contains 26 PGM species. Palladium minerals are dominant (16 species), Pt constitutes nine minerals while Rh occurs in only one species. Most of the PGMs occur in the –45 μm size fraction (67 to 91 wt %) of the primary ore as well as of the process products. The 45-90 μm size fraction of the nickel concentrate contains 66 wt% of the PGMs. PGMs have not been detected in the tailings.

The major PGMs are amenable to flotation: sperrylite and cooperite report to the copper concentrate (70% and 90%, respectively) and in the nickel concentrate (29% and

8%); stibiopalladinite favors the nickel concentrate (74%) and the pyrrhotite concentrate hosts 70% of isoferroplatinum.

Kozyrev (2000) reported that the cubanite-chalcopyrite-pyrrhotite ore contain most PGMs in the 20-45 μm size fraction (42 to 84 wt%). Twenty-nine PGMs have been identified and these include 18 Pd species and 11 Pt species.

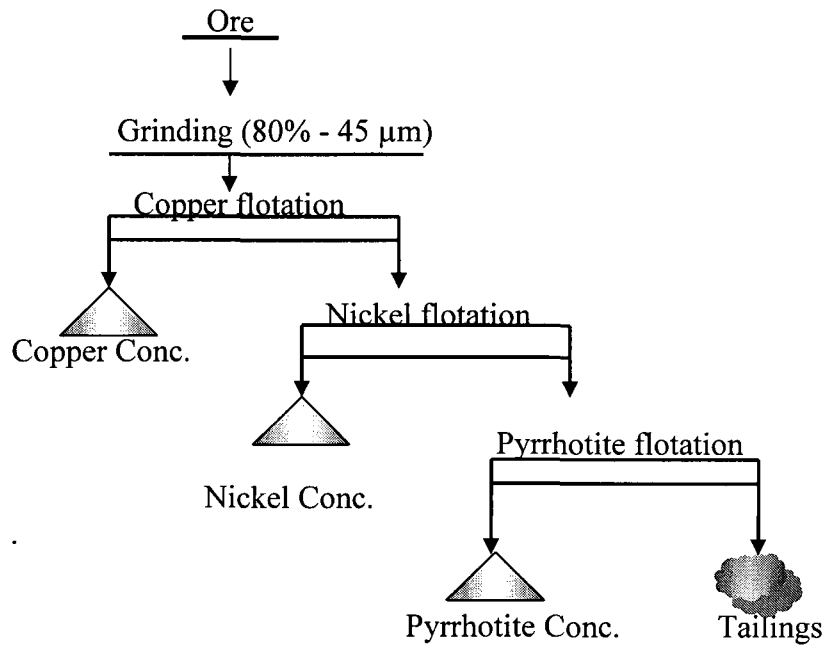

Figure 2-1 Selective Flotation Flow Sheet for Massive Ore

It was reported (Kozyrev, 2000) that the major PGMs in the flotation feed are cooperite (28 wt%), atokite-rustenburgite (24 wt%) and sperrylite (20 wt%); copper concentrate has sperrylite (42%), cooperite (24 wt%) and isoferroplatinum (14 wt%); nickel concentrate contains cooperite (36 wt%), sperrylite (15 wt%), atokite-rustenburgite (23 wt%) and sobolevskite (11 wt%); the pyrrhotite concentrate has

isoferroplatinum (41 wt%) and cooperite (20 wt%) while the tailings have atokite-rustenburgite (54 wt %) and sperrylite (17 wt%). Most of the major PGMs grains in the concentrate are liberated while some occur as complex intergrowths with each other, with sulphides and with silicates.

Recovery method: the massive ores, ground to 85% passing 45 μm, are processed by selective flotation (Figure 2-1) to produce copper, nickel and pyrrhotite concentrates and tailings. In copper flotation, pine oil is used as a frothing agent and butyl dithiophosphate as collector; in nickel flotation, T-80 serves as the frother, potassium butyl xanthate as the collector with sodium dimethyl dithiocarbamate as a depressant, $NaHSO_3$ as a modifier with CaO used to regulate alkalinity.

2.2.3.3 Disseminated Ore in The Norilsk-Talnakh Area of U.S.S.R.

Three varieties of disseminated ores have been distinguished: (1) pyrrhotite ore, the most abundant, (2) cubanite, and (3) chalcopyrite ores. The major sulphide minerals in the pyrrhotite ore are pyrrhotite, chalcopyrite, and pentlandite. Major sulphide minerals in the cubanite ore are cubanite, chalcopyrite, pyrrhotite and pentlandite; minor sulphides include mackinawite, sphalerite, and galena. The chalcopyrite ore includes the following major sulphides: chalcopyrite, pentlandite, pyrrhotite and cubanite with some minor sulphide minerals.

With new technology developed in the past decade, gravity-flotation techniques have been developed to increase the PGM recovery, such as recovering PGMs from concentrates, as well as scavenging from the Norilsk mill tailing (Kozyrev et al., 2003). The Knelson Concentrator has been used by Kozyrev (2002) to study the PGM distribution in the Norilsk mill gravity products. These include:

1) Gravity concentrate of the 12 in Knelson concentrator (laboratory-scale test);
2) Feed of the 48 in. Knelson concentrator;
3) Gravity concentrate of the 48 in Knelson concentrator; and
4) Gravity concentrate of the 20 in Knelson concentrator (processed concentrate of the 48 in. Knelson concentrator).

Table 2-1. PGM distribution (vol.%) by size fraction in disseminated ore, Norilsk I orebody (Kozyrev 2002)

Size Fraction (μm)	Conc. of the 12-inch KC	Feed of the 48-inch KC	Conc. of the 48-inch KC	Conc. Of the 20-inch KC
+250			6.7	
-250+90		7.8	18.6	34.8
-90+45		40.8	29.5	25.4
+74	0.2			
-74+45	32.1			
-45+20	67.7	50.9	45.0	38.6
-20		0.5	0.2	1.2

Mineralogy: Kozyrev (2002) reported that twenty-six PGM species plus alloys of gold and silver have been found in the gravity concentrates of the 12-inch Knelson concentrator and include 19 Pd minerals, 6 Pt minerals and a Rh mineral. Most of PGMs recovered is in minus 45 μm and 45-75 μm size fractions. In the latter size fraction, the most abundant (80 wt%) platinum minerals are isoferroplatinum, rustenbergite, and sperrylite; in the former, Pd species of the atokite-rustenburgite series dominate, with a two-fold decrease in Pt-Fe alloy content. Most PGM grains and

intergrowths (90%) in concentrates are liberated while the rest (10%) are attached to sulphides. The PGMs distribution is shown in Table 2-1.

Table 2-1 shows that PGMs in the feed of 48-inch KC are mainly distributed in the 45-90 μm and 20-45 μm size fraction, 41 vol.% and 51 vol.%, respectively. Thirty-nine PGM species, including twenty-six Pd minerals, twelve Pt minerals and one Rh mineral, have been found. The major PGMs include atokite (28%), sperrylite (16%) and isoferroplatinum (11%) plus other minor PGMs. The main platinum carriers are isoferroplatinum, atokite, sperrylite and tetraferroplatinum; palladium minerals comprise mostly atokite and to a lesser degree, paolovite and taimyrite. Most of the major PGM grains are free while the rest occur as intergrowths with other PGMs, Au-Ag alloys, sulphides and silicates.

The PGMs in the concentrates of a 48-inch Knelson concentrator are mainly distributed in the 90-250 μm (25%), 45-90 μm (29%), and 20-45 μm (45%) fractions. A total of twenty-eight PGM species, plus Au and Ag minerals, has been found. The major PGMs include isoferroplatinum (41%), tetraferroplatinum (18%) and atokite (15%) plus (3 to 9%) sperrylite, rustenbergite and taimyrite. More than half of the Pt is contained in isoferroplatinum, as well as tetraferroplatinum, sperrylite and rustenburgite.

The major PGMs consist of isoferroplatinum (35%), tetraferroplatinum (20%) and atokite (20%) plus minor sperrylite, rustenburgite and taimyrite (3 to 9%). Based on the information provided, it is clear that the main Pt and Pd carriers in this product are much the same as those in the 48-inch Knelson product. Table 2-1 suggests that the recovery of PGMs below 20 μm is negligible. It is unclear whether this is because the KC failed to recover these species or their concentration in the circuit was low, which appears likely.

Recovery method: In practice, disseminated ores are preconcentrated by gravity methods and are then processed by selective bulk flotation (Figure 2-2). Some of the discrete PGMs are skimmed off by gravity in the grinding circuit. The fineness of grinding is about 55% minus 74 μm. Gravity concentration uses Knelson Concentrators of various capacities to separate the noble-metal minerals. Bulk flotation produces a concentrate that undergoes further grinding to further liberate the minerals. Cleaning stages are used to produce higher-grade concentrates, which are processed further into copper and nickel concentrates. For flotation, potassium butyl xanthate and sodium butyl dithiophosphate serve as collectors, T-80 as a frother and CaO as a pH regulator and depressant.

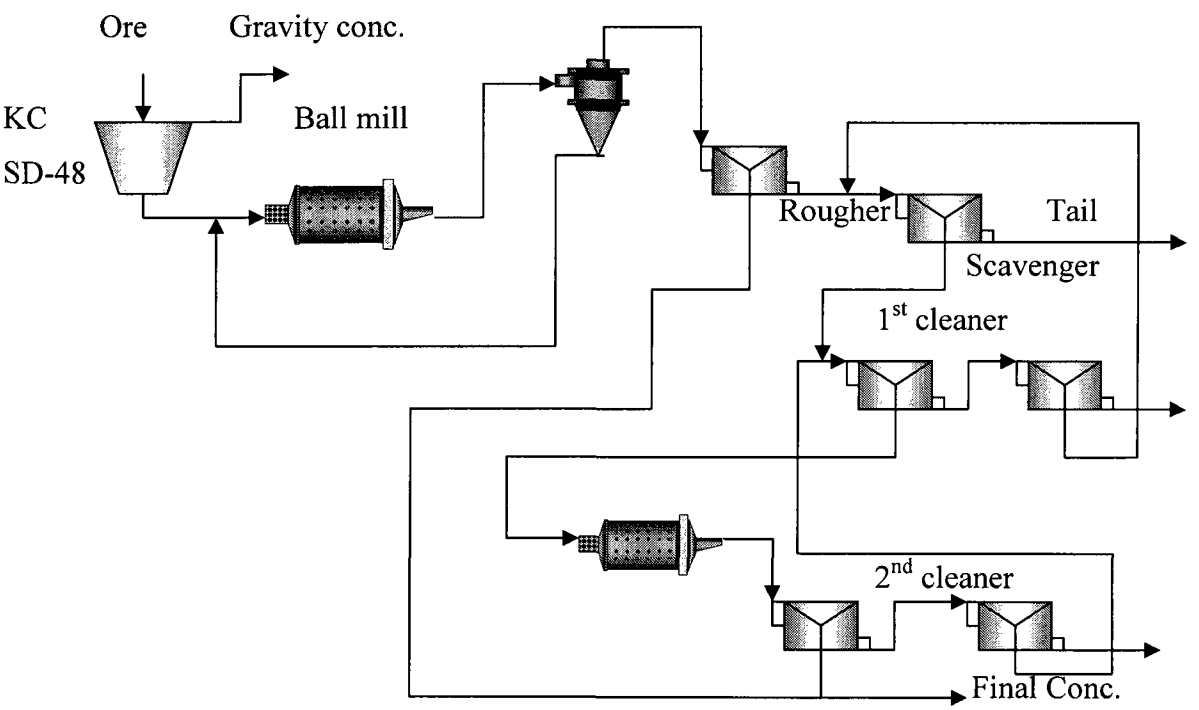

Figure 2-2 Norilsk Flow Sheet for Processing the Disseminated Ore

2.3 Laboratory Methods for Characterizing PGMs

Although applied mineralogy is now a well-established discipline, there is a distinct problem when characterizing PGMs in an ore, which stems from their low grade (often less than 1-2 g/t) and fine size distribution. Finding PGMs in a polished section may be compared to finding a needle in a haystack (Cabri, 1981). Fortunately, this problem can be reduced using pre-concentration techniques such as gravity. These methods will be reviewed.

Zhou and Zhang (1975) gave a detailed account of their comminution and separation techniques for a PGM-bearing chromite ore. Their method involved a large sample size of 1060 kg. The original sample was processed as follows: coarse, medium, and fine crushing; splitting out a 1000-kg sample for grinding and sieving (grinding was used to liberate enough minerals for subsequent concentration), with the balance split further for chemical analyses and back up. The final product, reported to contain only 5% unliberated PGMs, was distributed as follows: 37% +150 μm, 17% -150+106 μm, 4.2% -106+100 μm, 2.8% -100 +74 μm, and 39% -74 μm. The sized samples were processed with a high frequency superpanner (320-800 vibration/min). The first concentrates were considered to be PGM concentrates. The second concentrates and middlings were ground further and the superpanner used to recover more PGMs. The superpanner concentrates were combined with the first concentrate. Chromite concentrates, middling, and tailings were also obtained from this operation. They reported a 50% recovery of PGMs with the superpanner, increasing to more than 70% for high-grade feeds. The PGMs and chromite concentrates were subjected to magnetic separation, first with a weak field to remove strongly magnetic minerals (including some PGE-alloys) and subsequently with increasing field. Finally, a selective dissolution and heavy liquid fractionation were used for further separation to obtain the final PGM and chromite concentrates.

The reported recovery was only 50% (up to 70% for some higher grade ores). The size distribution of PGMs, and some information about source of PGMs was lost due to the selective dissolution process for assaying (this procedure was also extremely time consuming).

Cabri and Laflamme (1976) and Cabri (1981) developed a different mineral separation technique using heavy media elutriation to separate small samples (less than 500 g) of unconsolidated rock or mill samples. They tested this new recovery method on sized synthetic samples of sperrylite mixed with purified and sized pyrrhotite, chalcopyrite and pentlandite. They reported excellent recoveries down to about 53 μm, but recoveries fell off steeply in fractions in finer fraction.

The inability to recover sperrylite below 53 μm, as well as the relatively small masses processed, must be considered handicaps for this approach.

Williamson and Savage (1965) reported a recovery method suited for low grade PGEs in placer ores. The Witwatersrand Au-U fossil placers contain small quantities of by-product PGEs, and the PGMs are considerably finer than those of usual placers, partly due to the grinding of the ore to 80% less than 74 μm (Feather, 1976; Reimer, 1992). Williamson and Savage (1965) therefore used flotation rather than gravity recovery, on 11.3 kg (25-lb) lots of gravity concentrates. Final cleaning operations were carried out in an 800-g Fagergren cell. Feather (1976) reported that twenty-two PGM species were found in this deposit; 80% by weight were Ir-Os-Ru alloys and sperrylite and isoferroplatinum made up 15-20%. Williamson and Savage (1965) reported that the flotation of Ir-Os-Ru alloys is pH-sensitive, with an optimal pH of 1.5 to 3.5. Their recovery in PGEs was reported to be close to 100%, as determined by adding known quantities of irradiated "osmiridium". The final pyrite-rich flotation concentrate was still too large (2-4% of original weight) for their purposes, so they used pyrometallurgical techniques to remove the pyrite.

Knauf and Kozyrev (2002) used a Knelson Concentrator to study the mineralogy of Cu-Ni ores (both the ore fed to the KC and the tailings). They reported that when a primary ore sample of about 40 kg with a top size of 0.5 mm was fed to the KC, 80 g of concentrate was obtained.

Samples of primary ore and KC tailings were investigated. They were screened first to size fraction (SF) of 250-90 μm, 90-37 μm and –37 μm, and each sample was separated using a hydroseparator. Six heavy concentrates (HC) were obtained. Microprobe analysis by size fraction was prepared from the HC. The PGMs were identified and their volumetric area abundance in the polished section estimated.

They concluded that PGM grains are effectively extracted: grains larger than 70 μm were extracted completely, the grains within a size of 30-70 μm were extracted partially and that grains smaller than 30 μm were lost. They also concluded that the distribution of the PGMs by grain size yields all necessary information for the choice of processing flowsheet for PGM recovery. They argued that pre-concentration was helpful for mineralogical investigation and that mineralogical data were among the most important factors to determine the processing route. Their approach yielded significant upgrading ratios, which would contribute to more reliable mineralogical examination. However, the partial PGM recovery below 75 μm and total lack of recovery below 30 μm remain handicaps.

2.4 GRG Methodology

The GRG methodology is reviewed as it will be adapted to the GRPGM case for some PGMs of specific gravity close to gold. One of the objectives of the GRG methodology is to model gold recovery in grinding circuits for purpose of prediction or optimization.

2.4.1 GRG Ore Characterization

The GRG content in ore samples is characterized using a three-stage progressive liberation and recovery protocol (Laplante et al., 1994). To date, this protocol has been applied to over 180 ore samples at McGill University alone with results varying from a GRG content of 3% to 97%. A prominent centrifuge unit manufacturer also now uses the method systematically. Examination of GRG concentrates using an automated SEM technique, the Mineral Liberation Analyzer (MLA), has shown that below 75 μm, gold particles recovered in stage 1 of the test were well liberated (Guerney, Laplante and O'Leary, 2003). Particles above 150 μm for stage 1 can have various degrees of liberation, but average liberation is high (more than 90% of the gold by weight is present in particles of more than 90% gold in gold-silver alloy). Concentrates from stages 2 and 3 were also found to have a high degree of liberation. Figure 2-3 shows three typical GRG contents (coarse, intermediate, fine GRG) as a function of particle sizes.

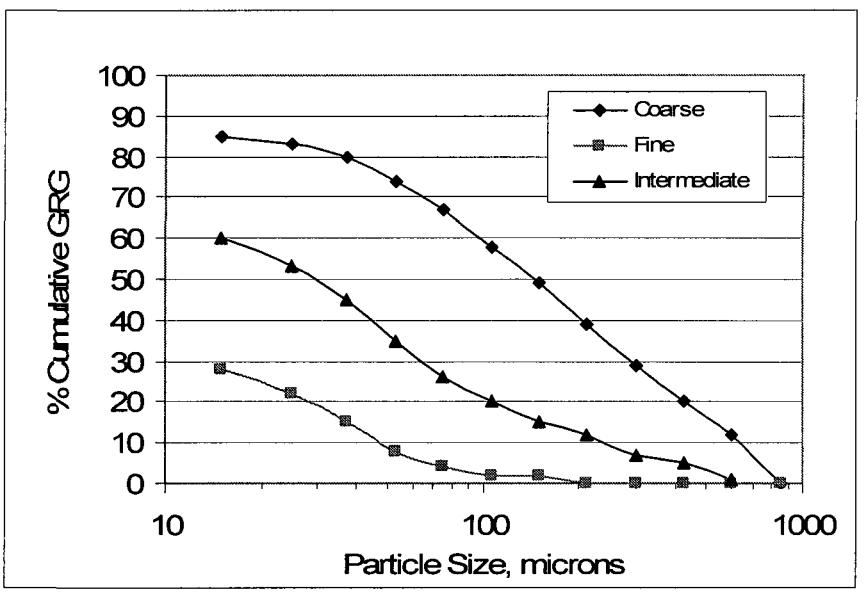

Figure 2-3 Cumulative GRG Contents as a Function of Particle Sizes (Xiao, 2002)

2.4.2 GRG Behaviour in Grinding and Classification Units

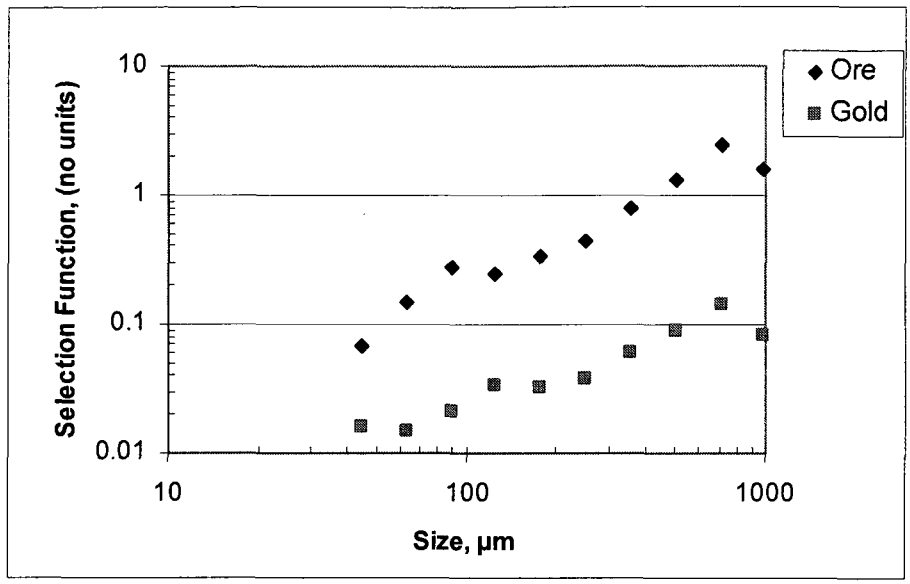

Figure 2-4 The Selection Function of Gold and Ore from Banisi

The behavior of gold and GRG in grinding mills and hydrocyclones has been studied by Banisi (1991), both at bench scale and in the grinding circuit of the Golden Giant Mine. No other study of gold grinding kinetics at full-scale has been completed since, partly because such studies must be completed in the presence of abundant coarse gold in the absence of gravity recovery units, a combination that is now rarely encountered. Figure 2-4 describes the grinding kinetics of gold and ore (Banisi et al., 1991; Laplante et al., 1994): the relative gold over ore grinding rate ranges from 1: 6 at fine size to 1: 20 at coarse size. In other words, gold grinds much slower than the ore.

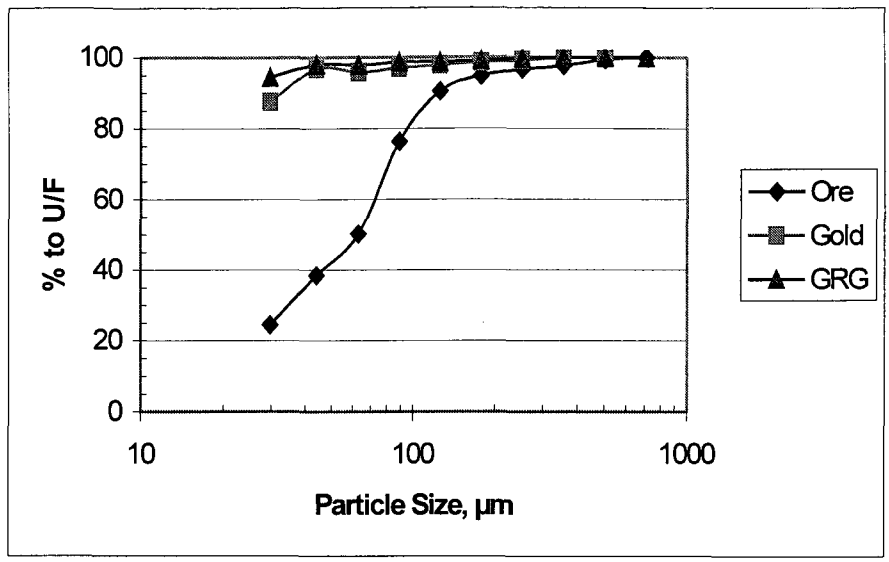

Figure 2-5 Typical Partition Curve for Gangue, Gold and GRG

In the case of cyclone partition curves, a number of studies have been performed (Laplante, Liu and Cauchon, 1990; Banisi, Laplante and Marois, 1991; Laplante and Shu, 1992; Putz, Laplante and Ladouceur, 1993; Woodcock and Laplante, 1994). Figure 2-5 shows typical results of partition curve of gold, GRG and ore.

As a rule of thumb, the GRG partition curve has a lower sharpness of separation (0.8 to 1.1), according to the Plitt's model (1976), with a corrected d_{50} which is from 8 to 10 times lower than that of ore (Laplante et al., 1996).

2.4.3. GRG Recovery

Recoveries for gravity and flash flotation units also have been characterized by a number of researchers (Putz et al., 1993; Laplante et al., 2002). Figures 2-6a and 2-6b show gold recoveries as a function of particle size for the Knelson Concentrator and

flash flotation cell, respectively. They show that the two units complement each other over a wide range of particle sizes.

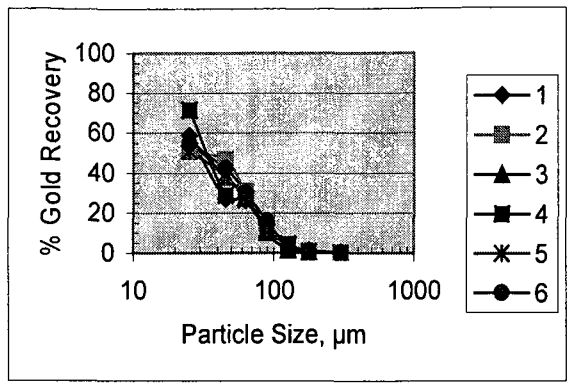

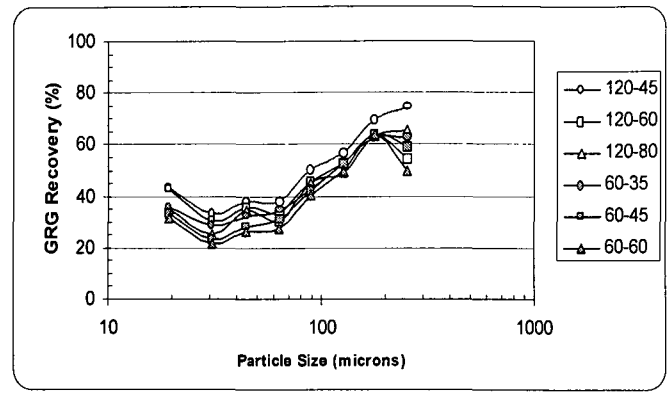

a b

Figure 2-6a and b. Gold Recovery in a Flash Flotation Cell (a) and GRG Recovery in a Knelson Concentrator 20XD (b) (a: six different sampling tests under similar operating conditions; b: Knelson operated at either 60 or 120 G at fluidization flows of 35 to 80 USgpm, as per first and second numbers in legend)

2.4.4 Modeling GRG Recovery

Once the data corresponding to the three corners of Figure 1-1 (see chapter 1) have been generated, they can be incorporated into a model that predicts how much GRG will build-up in the circulating load and how much of each size class will be recovered (Laplante, 1996). When the primary gravity unit processes a bleed of the ball mill discharge, recovery is equal to:

$$\underline{D} = PR^* [I - BC (I - PR)]^{-1} * \underline{F} \qquad \text{Equation 1}$$

where $\underline{D}$ is a column matrix of the GRG flow rate into the concentrate for each size class, P is the diagonal matrix for primary recovery and R gold room recovery, B is a grinding matrix and C the classification matrix, and F is the column matrix for GRG in

the feed. Because Equation 1 requires manipulation of 11 x 11 matrices, Xiao (2001) developed a simplified approach using multi-linear regressions to predict the gold recovery. The model has been used for designing gravity recovery flowsheets in grinding circuits. It also can be used to predict and optimize the gold recovery in the grinding circuit by providing the size distribution of GRG content and CGR classification partition curve.

Recovering PGMs is expected to be more challenging than for gold, as many PGMs have a specific gravity that is significantly lower than that of gold, and the mineral are brittle rather than malleable.

CHAPTER THREE

CHARACTERIZING THE GRAVITY RECOVERABLE PLATINUM GROUP MINERALS

3.1 Introduction

The renewed interest in the use of gravity concentration in recovering PGMs is due to the more efficient gravity concentration devices now on the market (Cole and Ferron, 2002; Kozyrev et al., 2003). Application to recovery of PGMs introduces the need to characterize ***g***ravity ***r***ecoverable ***p***latinum ***g***roup ***m***inerals (GRPGMs). GRPGM, by analogy with gravity recoverable gold (GRG), refers to the portion of platinum group minerals in an ore or stream that can be recovered by gravity at a low yield (<1%). It includes PGMs that are totally liberated, as well as locked PGMs in particles with density such that they report to the gravity concentrates. These species typically have a specific gravity greater than that of the densest sulphides (e.g. galena, 7.5). Conversely, they exclude any very fine, completely liberated PGMs that are not recovered into concentrate on account of their fine size. Also excluded are discrete blebs of PGMs, as well as PGEs in solid solution in carriers such as copper or nickel sulphides.

The interest in GRPGMs is three-fold. Firstly, can the gravity recoverable PGMs of an ore be quantified? Can PGMs be upgraded using a protocol similar to the GRG protocol for mineralogical study in optical or scanning electron microscope? Secondly, for a number of PGMs, is their density high enough that they recover to

cyclone underflow and accumulate in the circulating load? Thirdly, is this accumulation in the circulating load sufficient to achieve significant gravity recoveries by processing part of or the entire circulating load?

Information on GRPGMs in an ore or process stream can be used for different purposes: if gravity concentration is practised, the GRPGM data can be used to optimize the circuit. If gravity concentration is not practiced, the amount of GRPGMs and the size distribution can be used as factors to estimate whether a gravity concentration circuit should be installed.

The behavior of PGMs has never been specifically studied, as methods for isolating PGMs, reviewed in the previous chapter, are either ineffective or too unwieldy to make the process practical. The application of the GRG protocol to PGMs may make these studies possible.

Ore mineralogy plays a critical role in flowsheet design and plant optimization (Cabri, 1981; Henley, 1983; Lotter et al., 2002). Information on the mode of occurrence, grain size distribution, and liberation of the PGMs obtained by mineralogical analysis provides useful starting data. However, there is a problem finding PGMs in a polished section without preconcentration. This problem might be solved or reduced with a GRPGMs test protocol.

Thus, not only the mineralogy of the ore but also the behavior of PGMs in the grinding circuit and their potential response to gravity or flash flotation is critical to circuit design and optimization. Characterizing the gravity recoverable platinum group minerals of an ore, investigating their behavior in grinding and classification and analyzing the mineralogical features are the most important parts of this thesis. This chapter focuses on characterizing GRPGMs. The next chapter focuses on their behavior in grinding and classification.

3.2. Gravity Recoverable Platinum Group Minerals Test Design

The GRG standard test was developed at the beginning of the 1990s (Woodcock and Laplante, 1993) and has been used to characterize over 140 ore samples to date. All results are presented in a sized basis, from minus 20 μm up to 850 μm. The GRG test is most effective when the specific gravity of the gold-bearing mineral is between 16 and 19 (Laplante et al., 1996; Laplante and Dunne, 2002). Since some PGMs have specific gravities close to that of gold-bearing minerals (Table 3-1), the three-stage GRG procedure would seem adaptable to characterize GRPGMs. The test needed modification to account for the fact that most PGMs tend to report to finer size classes (Cabri, 1981; Thurman, 1994; Xiao and Laplante, 2003) and have a lower specific gravity than native gold. The modified procedure includes the standard GRG protocol, but a fourth stage is added at a higher rotating velocity on the Knelson Concentrator to try to recover the fine GRPGMs. Figure 3-1 shows the procedure designed to characterize the gravity recoverable platinum minerals.

Table 3-1: The Density of PGMs and Gold-bearing Minerals

Category	Mineral Name	Formula	Density (g/cm^3)
PGMs	Cooperite	PtS	10.10
	Sperrylite	$PtAs_2$	10.6
	Maslovite	PtBiTe	11.23
	Isoferroplatinum	Pt_3Fe	18.23
	Stillwaterite	Pd_8As_3	10.95
Gold and Gold-Bearing Minerals	Native gold	Au	19.3
	Electrum	Au, Ag	15-19.3
	Auricupride	Cu_3Au_2	11.5

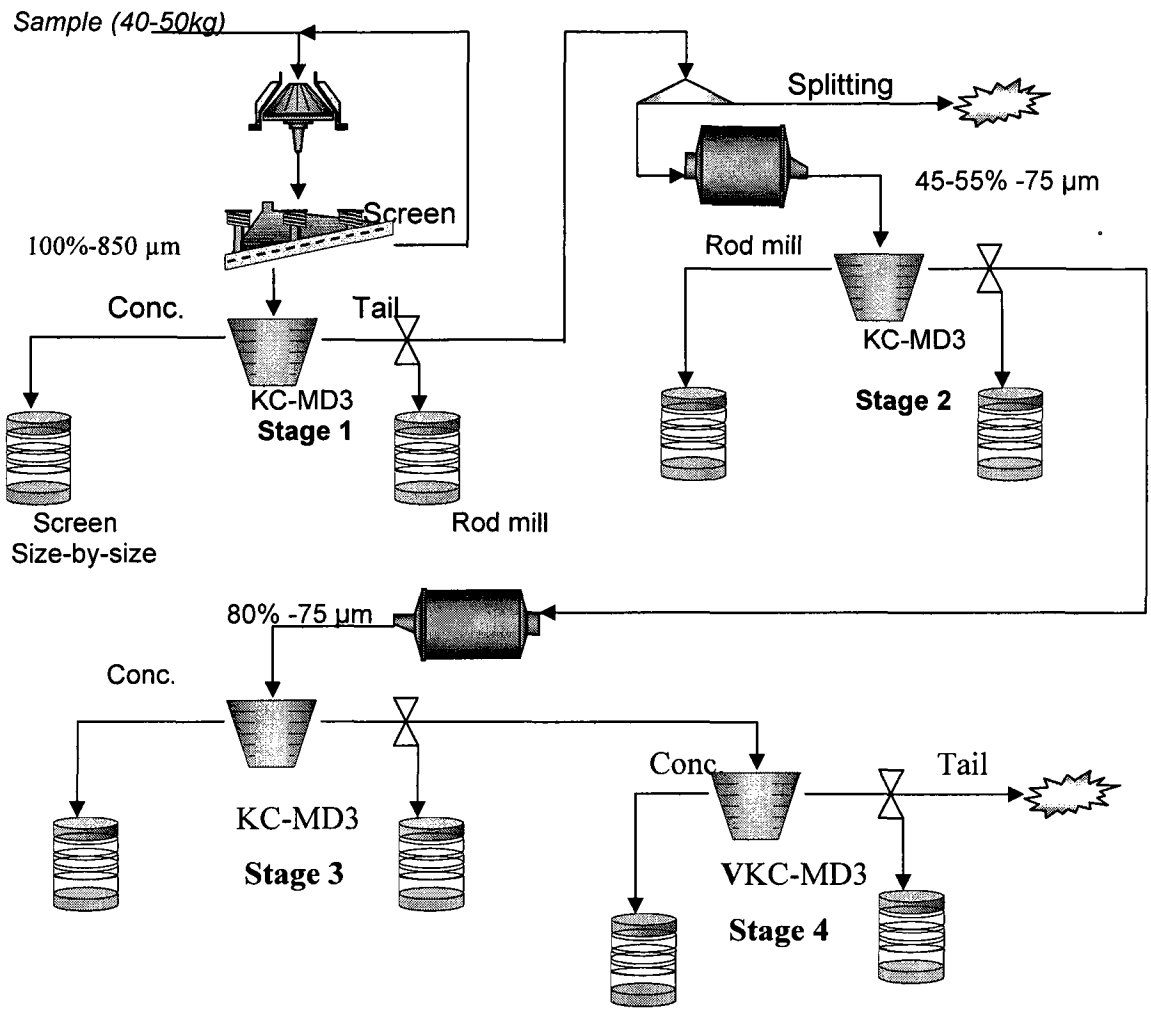

Figure 3-1 Procedure for Measuring GRPGMs Content with a KC-MD3

The GRPGM test is a protocol to progressively liberate and recover PGMs at increasingly finer grinds using a 3-in Knelson Concentrator (KC MD3). In the first three stages, the tailing of the first stage once ground finer becomes the feed to the second, and the tailing of the second once ground finer the feed of the third. However,

for stage 4, all the tailing from stage 3 is directly (i.e., without grinding) fed to the higher rotating velocity KC-MD3 to recover the fine GRPGMs.

The coarser concentrates from stage one (i.e., +600, +425-600, +300-425, and +212-300 and +150-212 μm size classes) are upgraded further using a hydrosizer. Some of the products and concentrates from stage 1 to 3 are used to make a polished section for mineralogical analysis (details in Chapter 5).

3.3 Results and Discussion

Four ore samples from various areas in Canada were processed with the procedure outlined in the previous section (except the sample from Raglan) to characterize the content of GRPGMs, namely, gravity recoverable platinum (GRPt) and/or gravity recoverable palladium (GRPd).

3.3.1 Raglan Ore Sample

Summary: A sample of ore from Raglan mill feed, Québec, was characterized for gravity recoverable platinum group minerals (GRPGMs) content using the standard GRG test (i.e., without the fourth stage added). In this case, gravity recoverable platinum (GRPt) and gravity recoverable Palladium (GRPd) were quantified. The sample, assaying approximately 0.77 g/t of Pt, contained a small amount, 5.1%, or 0.039 g/t gravity recoverable platinum (GRPt). The assay of 1.97 g/t of Pd contained only 2.7% gravity recoverable palladium (GRPd). At 100% -850 μm (F_{80} of 580 μm), only 0.9% of the Pt was recovered and 0.4% of the Pd; GRPt content increased to 3% at a F_{80} of 205 μm, GRPd 1.7%. At a final grind of 79% -75 μm, GRPt and GRPd increased to 5.1% and 2.7%, respectively.

Figure 3-2 presents the size distribution of the feed to the three stages, with corresponding F_{80} of 580, 205 and 78 μm. Feed masses of 54.49, 26.27 and 24.16 kg

were used for the three stages, respectively. Feed rate decreased with decreasing feed size, from 1050 g/min for stage 1 to 280 g/min for stage 3. Fluidization flow rate decreased from 7.2 L/min for stage 1 to 5.5 L/min for stage 3. Sized concentrates (from 25 to 600 μm) and 600-g samples of the tails were assayed for Pt and Pd content.

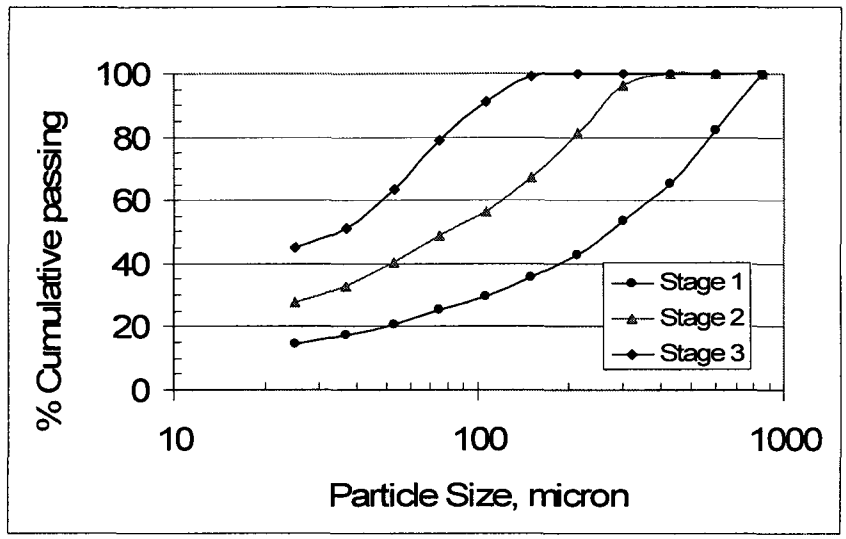

Figure 3-2 Size Distribution of the Feed to Three Stages

3.3.1.1 Stage 1 to 3

Metallurgical balances of Pt and Pd across the hydrosizer for the five coarsest size classes of stage 1 concentrate showed that the upgrading ratio varied from 1.0 to 2.0 for Platinum and 2.1 to 3.5 for Palladium (see on Appendix 1). Although the upgrading ratio of Palladium is higher than for Platinum, it is reasonable to believe that there is no significant difference in specific gravity between the Pd and Pt carriers and the gangue in the same size class. The causes of low recovery of Pt and Pd in this sample is discussed in more detail in the discussion section.

Stage 1: The concentrate mass in each size class below 150 μm was assayed, while above 150 μm the calculated heads from the hydrosizer tests were used.

Appendix 1 shows the metallurgical balance of stage 1 for Pt and Pd, i.e., the first recovery attempt. Because of the high feed rate, and coarse nature of the feed, this first stage is normally aimed at recovering the intermediated to coarsest size of Pt and Pd. The Pt recovery of 0.96%, and Pd recovery of 0.43% are exceptionally low. The feed, at 0.69 g/t Pt and 1.81 g/t Pd, is upgraded to 4.1 g/t Pt and 4.9 g/t Pd, respectively. Platinum does show some modest recovery between 25 and 106 μm, 3 to 7%, whereas palladium shows no recovery other than "background noise" (i.e., recoveries below 1% for all size classes).

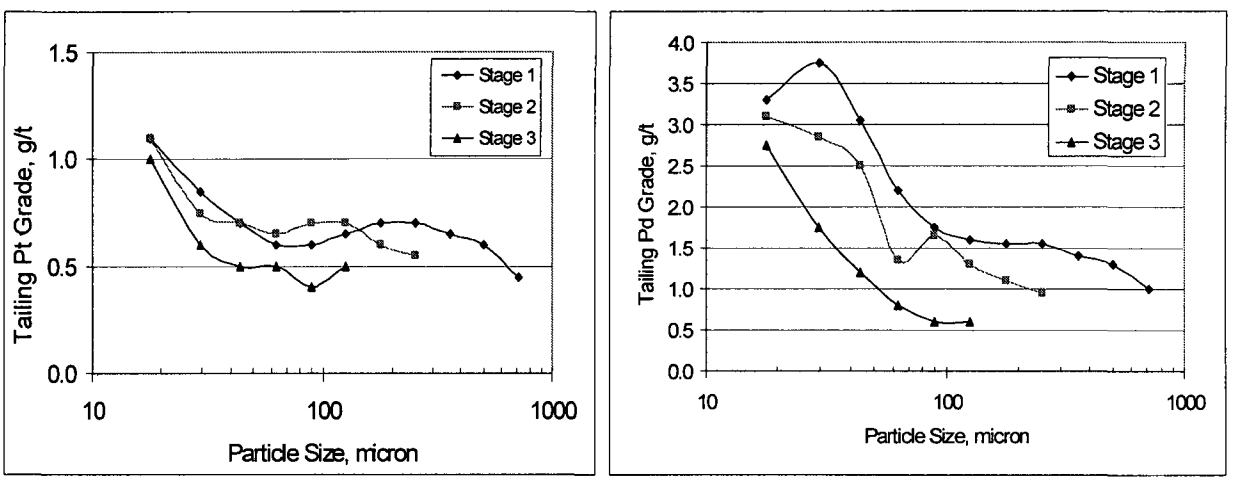

Figure 3-3 Pt, Pd Assays of the Tailing of Stages 1, 2 and 3

Size-by-size data are normally informative, both for the concentrate and tailing fractions. The tailing assays of stage 1 (Figure 3-3) show some consistency: They increase slowly with decreasing particle size, especially below 106 μm.

Concentrate grade shows a different behaviour for Pt and Pd. Whereas Pd grades are slightly upgraded over the full size range, Pt upgrading, which is clearly more significant, takes place predominantly below 106 μm. Head grade increases with decreasing particle size below 53 μm for Pt, whereas the increase is over the full size range for Pd.

Stage 2: Slightly less than half of the tailing of stage 1, once ground to 49% passing 75 μm, was fed to the Knelson for stage 2. The feed rate and size distribution were more conducive to Pt and Pd recovery than stage 1. Nevertheless stage 2 returned a recovery of 2.1% for Pt and 1.4% for Pd. The concentrate grade is 4.4 g/t for Pt and 7.2 g/t for Pd, as shown in Appendix 1. These recoveries are still considered very low.

The tailing fraction assays increase with decreasing particle size over the full range for Pd, and below 75 μm for Pt. Figure 3-3 shows that Pd grades for the same size classes are generally below those of stage 1, despite the very modest recoveries of stage 2.

Concentrate grade increases with decreasing particle size down to the minus 25 μm size fraction for Pt and the 25-37 μm fraction for Pd. Below 53 μm, the grade of Pt increases sharply from 2-6 g/t to 20-58 g/t. The concentrate grade of Pd increasing with decreasing particle size does not show the same trend as Pt does. Platinum recovery is between 1 and 2% above 75μm and then increases to 5-8% between 53 μm and 25 μm. It again drops to 1.4% for the finest size class. The reason is that it is either too fine or not dense enough for effective recovery with the Knelson, or is still unliberated. Palladium recovery decreases with decreasing particle size, down to a very low 0.1% for the finest size class. The Pd assay of the minus 25 μm tailing fraction, 3.1 g/t, is almost the same as that of the feed. The KC is clearly ineffective in recovering Pd in the finest size class, -25 μm.

The calculated head grade, 0.78 g/t Pt, 1.92 g/t Pd, is in reasonable agreement with the measured tails grade of stage 1, 0.68 g/t of Pt and 1.8 g/t of Pd.

Stage 3: This stage returned a recovery of 2.2% for Platinum as shown in Appendix 1- Raglan mass balance, and only 0.98% for Palladium, at a grind of 79% -75

μm. The calculated head, 0.75 g/t of Pt and 1.94 g/t of Pd, is in good agreement with that of the tailing of stage 2, 0.77 g/t of Pt and 1.92 g/t of Pd. Upgrading for Pt from stage 1 to 3 remains almost the same, from around 0.7 g/t in the feed to 4.4 g/t in the concentrate.

Tailing assays show the same trend as stages 1 and 2, but at a lower grade for both Pt and Pd. The lower tailing grade of stage 3, clearly noticeable in Figure 3-3, cannot be explained by the very low recoveries of all stages, but rather by a shift in size distribution to higher-grade finer classes from stage 1 to stage 3.

Concentrate grade of Pd increases steadily from the coarsest to the minus 25 μm size class (typical of stage 3 for gold). Recovery is highest for the 75-106 μm fraction, 4.6%. It drops significantly for the minus 25 μm fraction, to a value of 0.2%. The concentrate grade of Pt also reaches a maximum of 36.8 g/t in the –25 μm size fraction. The maximum recovery appears between 25 μm and 53 μm, 4.2-4.5%.

3.3.1.2 Overall Results

The overall test results present a total GRPt content of 5.1% in a 0.77 g/t feed and GRPd content of 2.7% in a 1.97g/t feed (see Appendix 1- Raglan mass balance).

Another way of representing recovery is as follows: out of 0.77 g/t of platinum in the feed, 0.007 g/t was recovered in stage 1, another 0.016 g/t in stage 2, and 0.016 g/t in stage 3. A total of 0.039 g/t, or 94.9% of the Platinum in the ore, reported to the gravity tailing. Out of 1.97 g/t of palladium in the feed, 0.008 g/t was recovered in stage 1, 0.026 g/t in stage 2, and 0.019 g/t in stage 3. A total of 97.3% of palladium in the ore reported to the gravity tailing.

Overall results can be presented graphically. Figure 3-4 cumulates platinum recovery in two ways. First, platinum is cumulated as percent retained from the coarsest (+850 μm) size class to the finest. The Pt in the finest class (i.e. –25 μm) is assumed to be coarser than 15 μm, but only for the purposes of showing total recovery. Second, platinum is cumulated from stage 1 to stage 3. Thus, the third curve (for stage 3, triangles) cumulates to the total GRG content, 5.1%. The curve is obviously at a low level, but with a shape similar to that of gold ores with a fine GRG component. This fine Pt/Pd component must have a relatively high SG to be recovered.

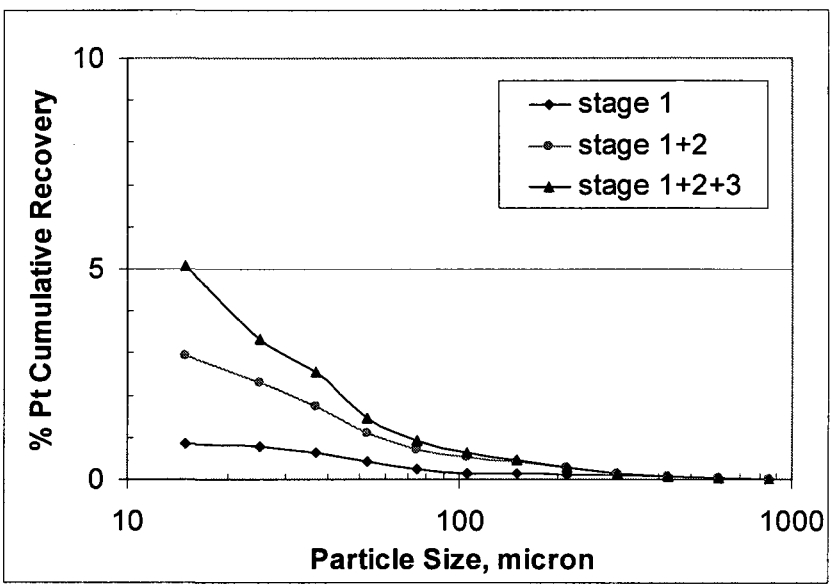

Figure 3-4 Cumulative GRPt Content (100%: total platinum in the ore)

To reveal better the size distribution effect, the data of Figure 3-4 are plotted in Figure 3-5 relative to the total amount of **GRPt** in the ore, rather than the total amount of **Platinum**. All size classes below 75 μm contribute to the GRPt and the absence of GRPt of coarse size (+106 μm) and low head grade makes it a poor gravity application.

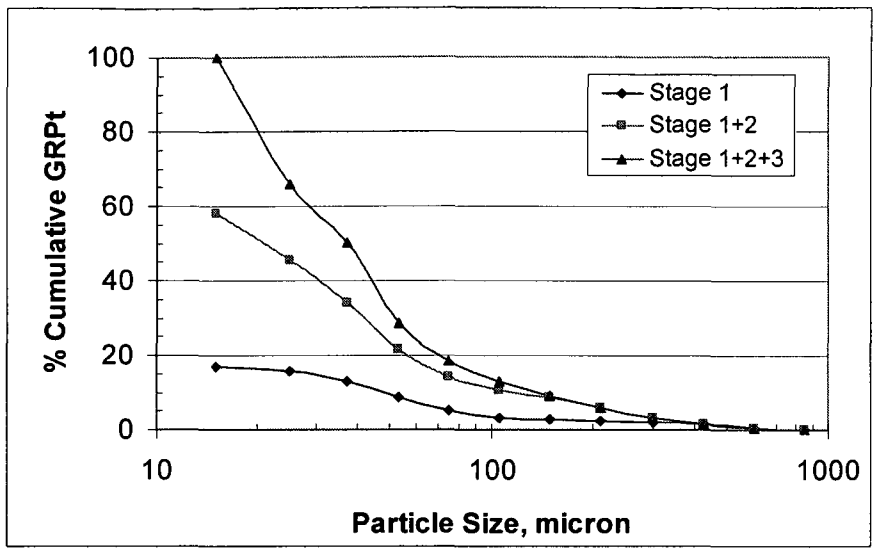

Figure 3-5 Normalized Cumulative GRPt Content (100%: total GRPt in the ore)

3.3.1.3 Discussion and Conclusions

Discussion: Concentrate assaying appears to be quite reliable, the differences between the calculated tailing grade and the head grade of the following stage being small. The head grade of platinum, 0.77 g/t, is in line with the quoted assay for Raglan ore, 0.8g/t (Lotter et al., 2002). The head grade of palladium, 1.8g/t, is slightly lower than the typical value, 1.97g/t. Uncertainty due to sampling, assaying and in the tests does not affect the general findings of the test.

Figure 3-6 shows platinum recovery in each size class for all three stages. The trends are consistent, which adds confidence to the reliability of the test. It is clear from the stage 1 curve that this first stage did not recover much of the GRPt above 106 μm, but the GRPt recovery increased below 75 μm with the highest recovery in the 37-53 μm size fraction. With further grinding, more Pt was liberated and recovered in stages 2 and 3, which is shown at the higher right end of Figure 3-6. This figure also shows

that stages 2 and 3 recovered more GRPt in the finer size classes. This is consistent with the observation that more liberated Pt was found in the finest size class concentrates, such as the minus 25μm fraction.

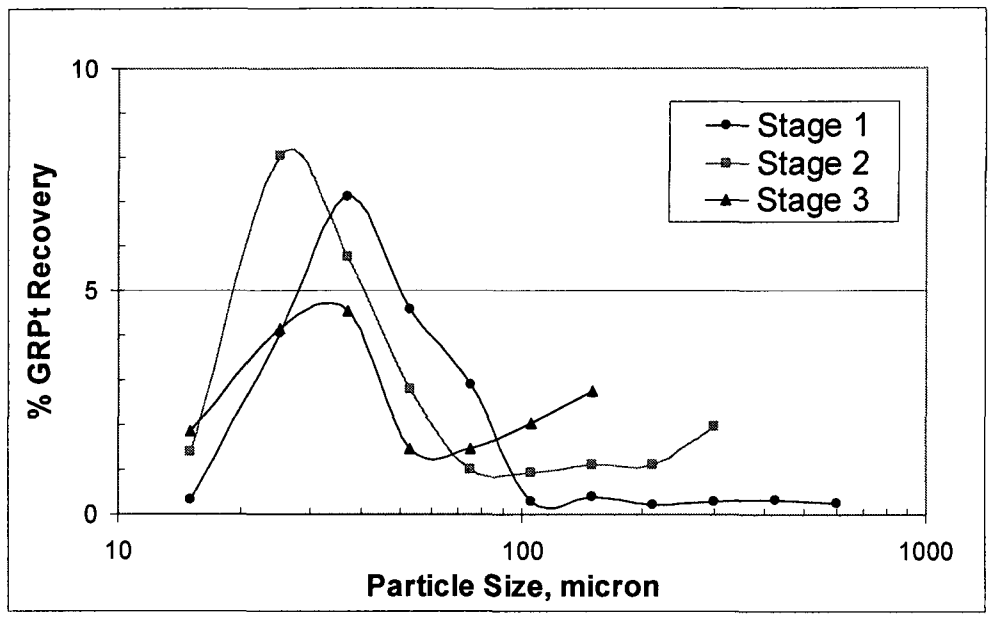

Figure 3-6 Stage Recoveries of Platinum per Size Class

Figure 3-7 shows that stage recoveries for palladium display different trends than those of platinum. Stage 1 is flat which indicates that the lower recovery of all size class might be due to the lower content of coarse Pd, the lower degree of liberation and the finer palladium particles distributed in the Raglan ore sample. Stages 2 and 3 show a strong recovery in the middle size class, from 53 μm to 212 μm, but the recovery drops progressively below 53 μm. This is unusual for a typical GRG test, and suggests a relatively low SG for the palladium-bearing minerals that report to the concentrate is the coarser fractions.

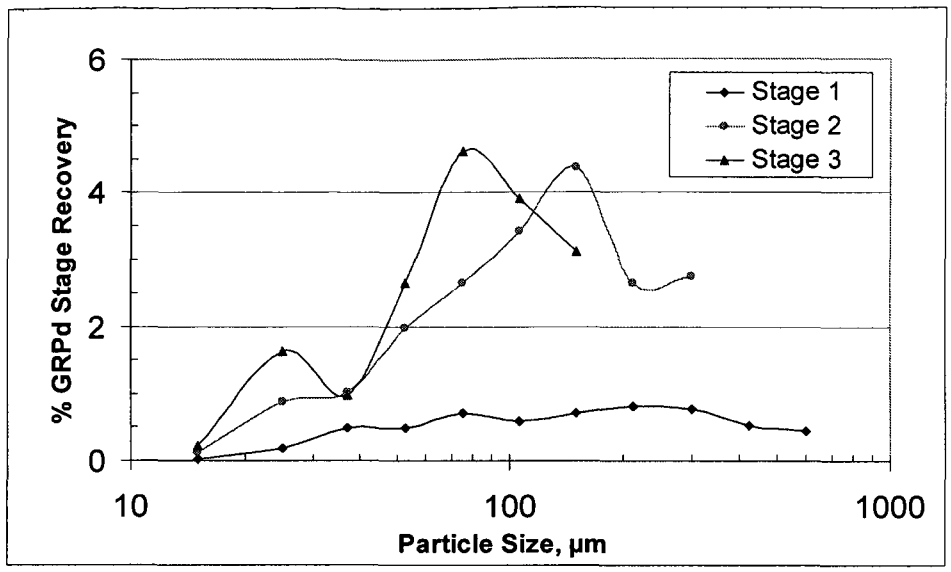

Figure 3-7. Stage Recoveries of Palladium per Size Class

Based on the test, the low grade of Pt and Pd content, the fine size distribution and the small density difference between Pt and Pd carriers and gangue make the Raglan ore a poor candidate for gravity recovery.

Flash flotation could be an interesting alternative based on the fine size distribution of Pt and Pd. But it would have to be justified on the basis of other factors, notably the benefit to copper and nickel recovery. As the Cu- and Ni-minerals are believed to carry most of the Pt and Pd, whatever effect flash flotation has on copper and nickel recovery would also benefit Pt and Pd recovery.

Conclusions: The GRPt and GRPd content of a Raglan mill feed sample assaying 0.77 g/t of Pt and 1.97g/t of Pd were found to be 5.1%, 2.7%, respectively. The very low contents in gravity recoverable platinum and palladium bearing minerals make the Raglan ore a poor candidate for gravity recovery (Xiao and Laplante 2003a).

3.3.2 Strathcona Ore Sample

Summary: A sample of ore from Strathcona mill feed, Ontario, was characterized for its gravity recoverable platinum (GRPt) and palladium (GRPd) contents using the four-stage procedure shown in Figure 3-1. The sample, assaying 0.44 g/t Pt and 0.58 g/t Pd, contained 53% GRPt and 44% GRPd. At 100% -850 μm (F_{80} 530 μm), 16% of the platinum and 17% of the palladium were recovered; GRPt and GRPd contents increased to 38% and 32%, respectively, at F_{80} 175 μm, to reach 53% and 44% at a final grind of 80% -75 μm. GRPt and GRPd were present in all size classes below 600 μm (i.e., 67% of the GRPt and 72% of GRPd were finer than 106 μm). The gravity recoverable gold (GRG) content of 70% was also characterized.

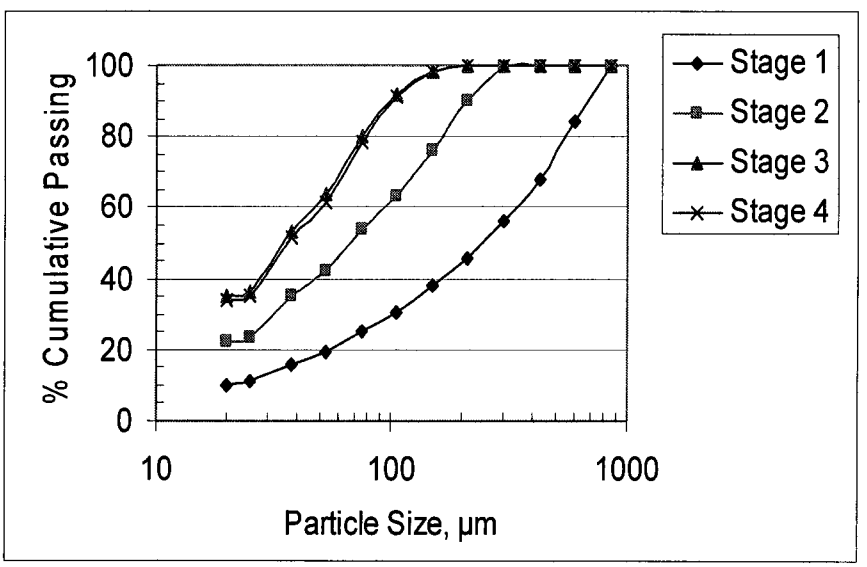

Figure 3-8 Size Distribution of the Feed to the Four Stages

Figure 3-8 presents the size distribution of the feed of the four stages, with F_{80}s of 530, 175 and 78 μm (the same for stages 3 and 4), respectively. The size distribution of stage 4 is slightly coarser than that of stage 3 due to the small loss of some fines

during the handling of stage-3 tails (i.e., siphoning the slurry). Feed masses of 75.39, 27.51 and 25.17 kg were used for the three stages, respectively. The fourth stage used a feed mass of 22.04 kg. Feed rate decreased with decreasing feed size, from 1160 g/min for stage 1 to 296 g/min for stage 3, and 355 g/min for stage 4. Fluidization flow rate also decreased from 7.4 L/min for stage 1 to 5.5 L/min for stage 3 (stage 4: 6.1 L/min). Sized concentrates (from 20 to 600 μm) and 600-g samples of the tails were assayed for platinum and palladium contents at Falconbridge Limited Research Center.

3.3.2.1 Results for stages 1 to 4

Stage 1: Metallurgical balances of the hydrosizing of the five coarsest size classes of stage 1 concentrates for platinum and palladium are shown in Appendix 2, respectively. The upgrading ratio varied from 2.6 for the 300-425 μm fraction to 7.1 (7.3) for the 600-850 μm fraction. The coarsest size class displays the highest upgrading ratio for both platinum and palladium. In each size class, the upgrading ratio is similar for platinum and palladium. Recoveries are high for all size classes above 212 μm for platinum. For the coarsest size class (600-850 μm), the concentrate grade of platinum is so high (800 times of the ore feed grade) that contamination or faulty assaying is suspected. As a result, the Knelson concentrate grade for this size class was set at 1 g/t (this correction will be discussed later).

Metallurgical balance of stages 1 to 4 for platinum and palladium is shown in Appendix 2. The first stage, processing at high feed rate and coarse size distribution, is aimed at recovering mostly the coarsest platinum and palladium minerals or minerals of intermediate particle size that liberate easily. The recoveries of both platinum and palladium are 17 per cent. The feed, at 0.43 g/t platinum and 0.59 g/t palladium, is upgraded to 56 g/t Pt and 79 g/t Pd.

Generally, concentrate grades of both platinum and palladium increase progressively with decreasing particle size down to the 38-53 μm size fraction. For gold, the increase is normally down to the 20-25 μm fraction. The difference is in all likelihood linked to the lower SG of the Pt-bearing and Pd-bearing mineral(s).

Size-by-size recoveries for both platinum and palladium follow the same pattern (Figure 3-9), recovery generally increases as particle size decreases, with a maximum of 47% at 106-150 μm for platinum and 45% at 75-106 μm for palladium, then the recoveries drop significantly, which results in a very low recovery below 20 μm, less than 1% for palladium.

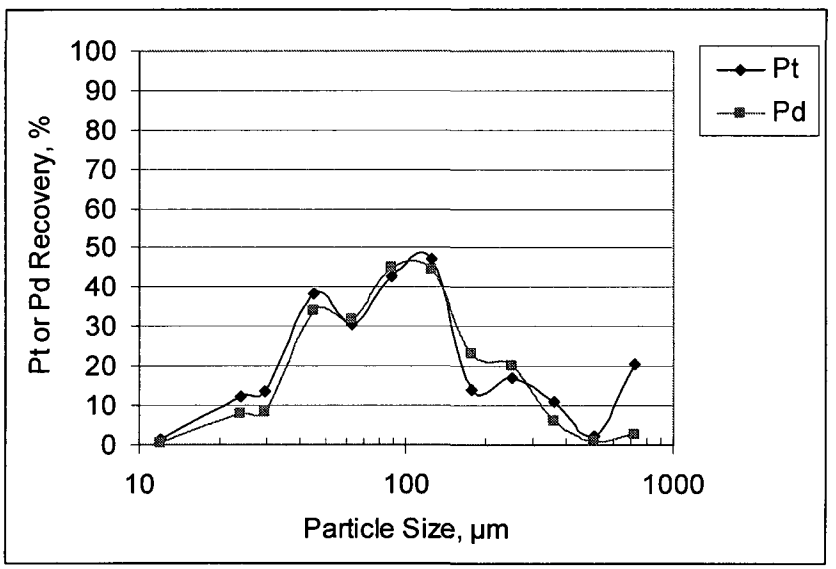

Figure 3-9 Platinum and Palladium Size-by-size Recoveries for Stage 1

Platinum and palladium recoveries in Figure 3-9 are sufficiently similar that it suggests they are in fact contained in the same mineral(s). The mineralogical analysis in Chapter 5 indicates that michenerite (Pd, Pt)(Bi, $Te)_2$, maslovite (Pt, Pd) (Bi, $Te)_2$ are Pt and Pd carries in the Knelson Concentrates.

Stage 2: The tailing of stage 1 was first split, then a sub-sample of 27.51 kg was ground to 54% passing 75 μm, and fed to the Knelson to recover the liberated PGMs. Stage 2 returned a recovery of 24% platinum, yielding a tailing grade of 0.26 g/t, and a concentrate grade of 20 g/t. Stage 2 also recovers 14% palladium, with tailing grade of 0.42 g/t and concentrate of 17 g/t (more details are given in Appendix 2). Concentrate grades increase with decreasing particle size down to the 20-25 μm size fraction for both platinum and palladium. Both platinum and palladium follow almost the same trend, as shown in Figure 3-10: recovery increases with decreasing particle size, up to maximum at the 38-53 μm size fraction, then drops, although there is a "hump" at the 20-25 μm size fraction. The palladium recovery curve is lower than that of platinum possibly due to the lower density of palladium minerals or their lower degree of liberation. Platinum or palladium minerals below 20 μm are either too fine for effective recovery with the Knelson, which explains the drop in recovery. The calculated head grade, 0.34 g/t platinum, is in good agreement with the measured tails grade of stage 1, 0.35 g/t. The calculated palladium head grade, 0.49 g/t, is equal to the measured tails grade of stage 1.

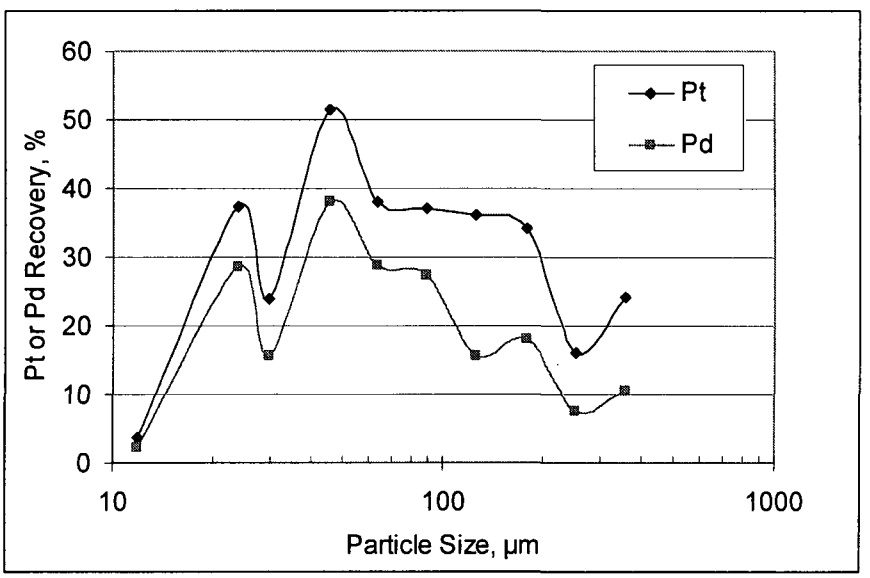

Figure 3-10 Platinum and Palladium Size-by-size Recoveries for Stage 2

Stage 3: This stage returned a 15% platinum and 9% palladium recovery at a grind of 80% -75 μm, the usual grinding target in the GRG test. Figure 3-11 is a comparison of stage recoveries for platinum and palladium. The maximum recoveries for both platinum and palladium are in the 20-25 μm size fraction. The recovery drops to a minimum at the finest size class. Figure 3-11 also shows that both platinum and palladium recoveries follow a similar trend with, on average, less palladium being recovered. The calculated head, 0.29 g/t platinum and 0.43 g/t palladium, is in very good agreement with that of the tailing of stage 2, 0.26 g/t Pt and 0.42 g/t Pd.

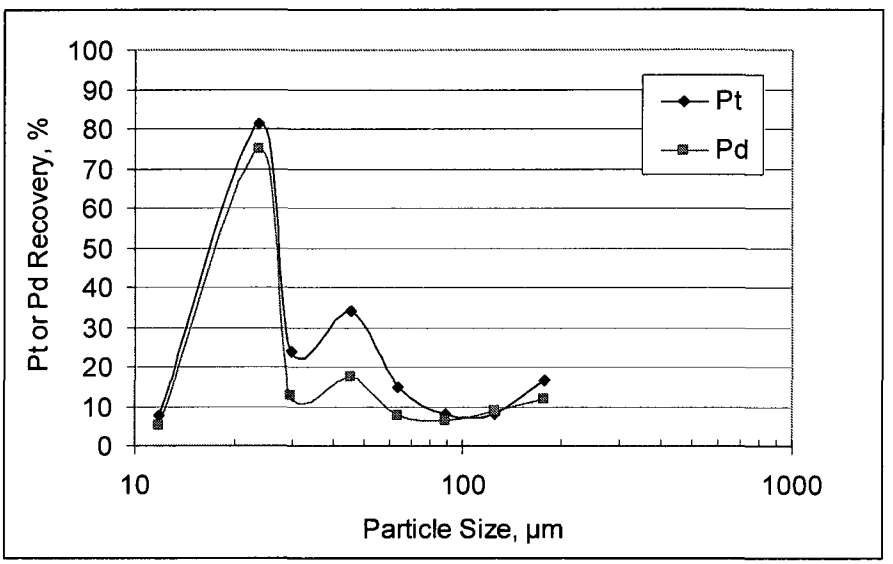

Figure 3-11 Platinum and Palladium Size-by-size Recoveries for Stage 3

Concentrate grade increases steadily from the coarsest size class to the minus 20 μm size class (typical of stage 3 for gold (Laplante et al., 2002)). The highest grade of 80 g/t platinum and 84 g/t palladium occurs in the same size class.

Stage 4: The fourth stage was performed on the tailing of stage 3 using the variable speed KC-MD 3, without regrinding, but at a higher rotation speed

corresponding to 115 G, and a fluidization flow of 6.0 L/min. The feed rate, 355 g/min, was slightly higher than that of stage 3.

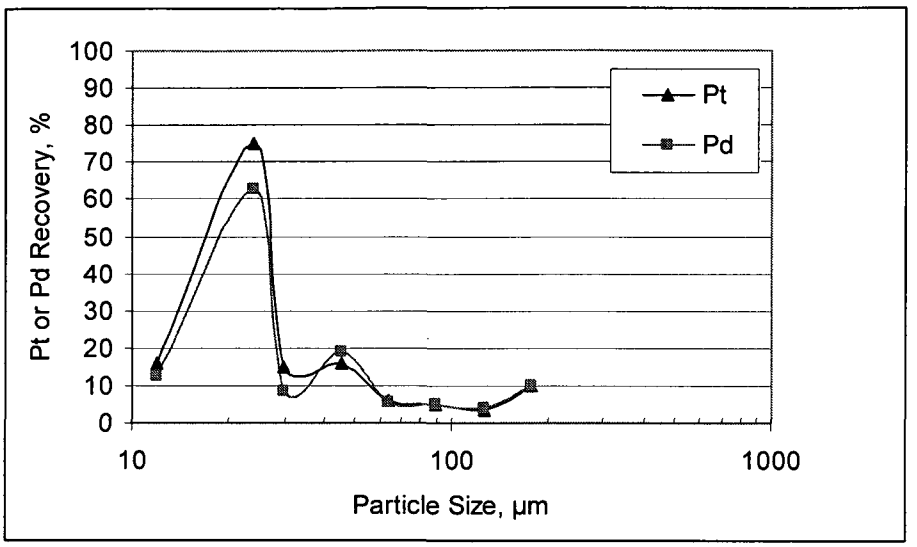

Figure 3-12 Platinum and Palladium Size-by-size Recoveries for Stage 4

This stage had a 26% platinum recovery, upgrading a 0.18 g/t feed (compared to 0.22 g/t in stage 3 tails) into a 9.8 g/t concentrate. Palladium recovery was 12% (Appendix 2). Figure 3-12 compares recoveries size-by-size. There is not much recovered above 25 μm. The recovery of palladium in the 37-53 μm size fraction is slightly higher than that of platinum, the opposite being observed for the 25-37 μm fraction but the difference are not material. The maximum recovery for both platinum and palladium is in the 20-25 μm size fraction.

3.3.2.2 Overall Results

The fourth stage added 8.3% to overall platinum recovery (i.e., GRPt content), over 73% of it being below 25 μm. Overall GRPt reaches 53%. There is a small change for the overall head grade between the three-stage and four-stage overall results. It also added an additional 7.7% to overall palladium recovery, over 77% of it below 25 μm. Overall GRPd stands at 44%. However, the calculated head grade drops from 0.595 g/t to 0.576 g/t due to some assay error on the final tailing.

Figures 3-13A and 3-13B cumulate platinum and palladium recovery size-by-size and stage-by-stage. The fourth curve (for stage 4, crosses) cumulates to the total GRPt content of 53% and GRPd content of 44%. As shown in these two figures, there is some coarse GRPt and GRPd above 150 μm. More platinum was recovered than palladium in stage 2.

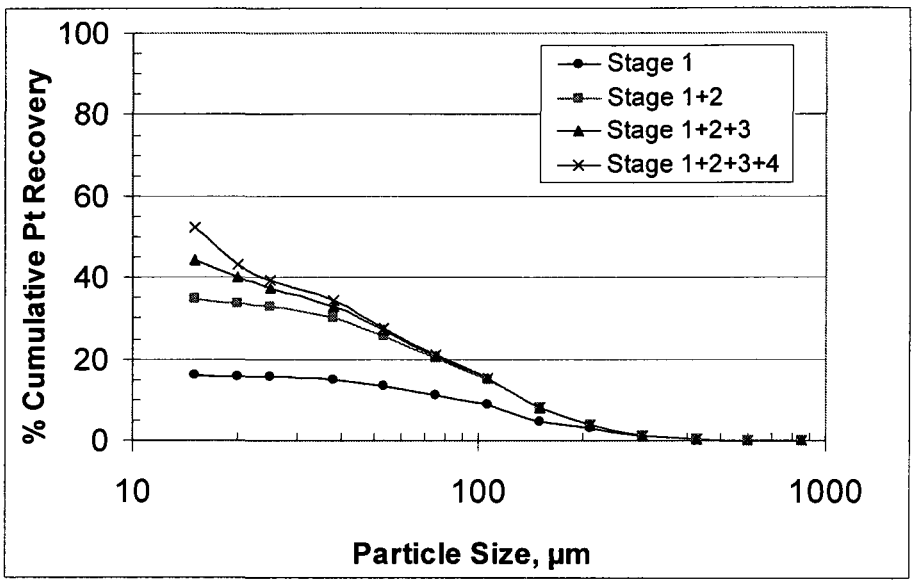

Figure 3-13A Cumulative GRPt Content (100%: total platinum in the ore)

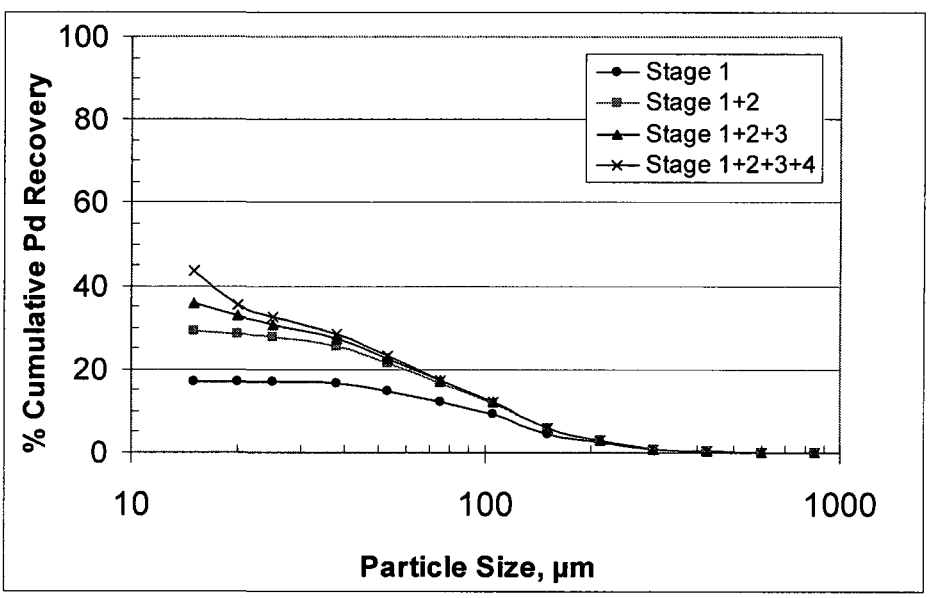

Figure 3-13B Cumulative GRPd Content (100%: total palladium in the ore)

3.3.2.3 Discussion and Conclusions

Discussion: Concentrate assaying appears reliable except for the hydrosizer concentrate of the coarsest size class in stage 1 for platinum, which assays very high (49.3 g/t) compared to the assay of the next size class (2.6 g/t) or that of palladium for the same size class. It was rejected as unreliable and the corresponding grade of the Knelson concentrate was set to a conservative 1 g/t. This correction causes a small drop of 1.5% in total GRPt content.

Tailing assaying shows variation in stage 1 for both platinum and palladium. Other stages follow a stable trend.

As discussed in stage recovery curves, both platinum and palladium recoveries have a different maximum, which moves to finer size as the test progresses and the feed becomes finer. The trends are remarkably consistent, which adds confidence to the reliability of the data.

Table 3-2 Comparison of the tailing grade and the feed grade of next stage

	Pt grade (g/t)		Pd grade (g/t)	
	Feed	Tail	Feed	Tail
Stage 1	0.42	0.35	0.59	0.49
Stage 2	0.34	0.26	0.49	0.42
Stage 3	0.29	0.25	0.43	0.39
Stage 4	0.25	0.21	0.37	0.33

As shown in Table 3-2, the tailing grade of the first three stages is in good agreement with the head grade of next stage for both platinum and palladium. This also confirms the reliability to the test and assaying data.

The test results indicate a degree of liberation for the main Pt minerals and Pd minerals, which needs to be confirmed by quantitative mineralogical analysis. (see Chapter 5). Despite some difficulties associated with the recovery of a lower SG and brittle mineral (compared to gold), the potential for gravity recovery at Strathcona is attractive, the GRPt content being above 50%; another GRPd, at 44%, being the highest of all samples tested. The content of gravity recoverable gold is slightly above the average, 70%, which will add credits for the gravity recovery of precious metals in this ore.

Conclusions: The GRPt content of the Strathcona mill feed sample assaying 0.44 g/t was found to be 53% or 0.23 g/t. The bulk of the GRPt is found below 600 μm, over 70% being finer than 106 μm. The GRPd content was found to be 44% or 0.25 g/t out of a total palladium content of 0.58 g/t. It is the highest content among the four samples tested. The Strathcona ore shows promising for recovery of Platinum and Palladium by gravity. Further investigations, such as the liberation and behavior in the grinding circuit of platinum and palladium are justified.

3.3.3 Nickel Rim South Ore Sample

Summary: A 24.7 kg drill core sample from Ni Rim South (Footwall deposit) was characterized for its gravity recoverable platinum (GRPt) and palladium (GRPd) content. In terms of Platinum, the sample, assaying 3.7 g/t Pt, contained 42%, or 1.5 g/t GRPt. At 100% -850 μm, 8% of the platinum was recovered; GRPt content increased to 22% with further grinding to 62% -75 μm, to reach 42% at final grind of 84%. GRPt was finer than 106 μm. In terms of Palladium, the same sample, assayed 3.9 g/t Pd, and contained 42% GRPd (the same amount of GRPt), or 1.6 g/t GRPd. At 100% -850 μm, 9.5% of the palladium was recovered; GRPd content increased to 24% at grind of 62% -75 μm, to reach 42% at final grind of 84%. The GRPd also was finer than 106 μm.

3.3.3.1 Results for stages 1 to 4

Stage 1: A concentrate of 86 g was obtained for this stage. Metallurgical balances of Pt and Pd of the hydrosizing of the five coarsest size classes of stage 1 concentrate are shown in Appendix 3. The upgrading ratio varied from 2.1 to 4.4 for platinum, and 2.2 to 4.5 for palladium. The trend for the upgrading ratio is similar for both platinum and palladium with the highest upgrading in the 150-212 μm size fraction. Upgrading ratios are lower than typically observed for gold. It is reasonable to assume that the lower upgrading is due to either the lower difference in specific gravity between the Pd and Pt carriers and the gangue, or the absence of liberated Pt and Pd minerals above 150 μm.

The first stage recovery of Pt, 8% and of Pd, 9%, is relatively low (i.e., compared to GRG test). The feed, at 3.7 g/t platinum and 4.0 g/t palladium, is upgraded to 84 g/t platinum and 105 g/t palladium, respectively. The poor recovery of both platinum and palladium can be attributed to the poor performance (ca. 0.5 to 1.8% recovery) of the four coarsest size classes, which carry 43% of Pt and 42% of Pd in the feed. The highest platinum recovery of 41% is in size fraction 38-53 μm, which also gives the highest palladium recovery (45%).

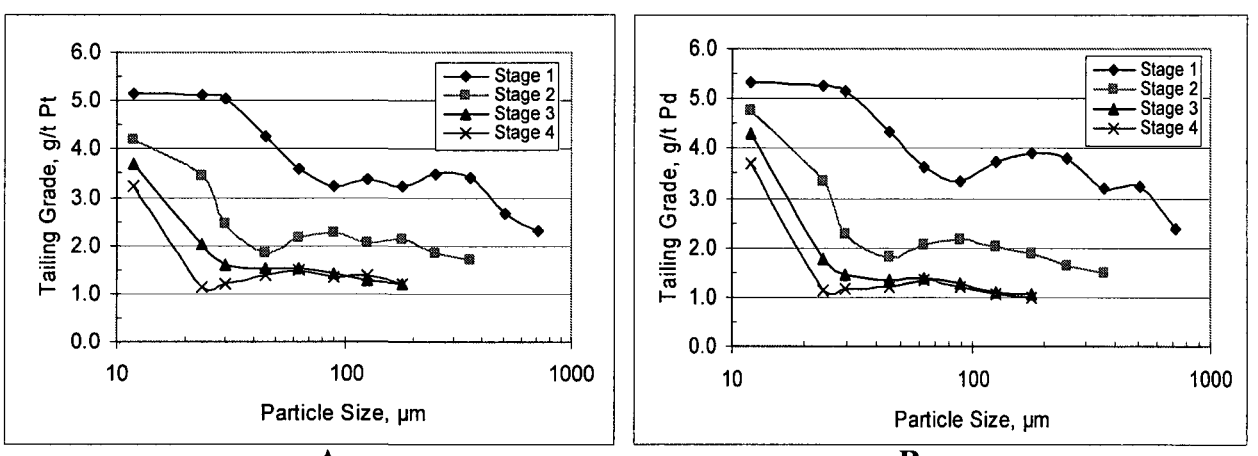

Figure 3-14 Pt and Pd Assays of Tailing of Stages 1, 2, 3 and 4

The tailing assays for platinum of stage 1 (Figure 3-14) show some consistency. They increase slowly with decreasing particle sizes, especially down to 75 μm. Below 75 μm the tailing assays for platinum increase sharply and reach a maximum of 5.2 g/t at the finest size fraction. The same trend is evident for the palladium tailing assay below 75 μm; above 75 μm the grade varies around 2 to 3 g/t. (Note that for the tailing assay data missing due to insufficient mass, the geomean grade of adjacent size classes was taken, or the grade of the next size class when the assay of the coarsest size class was missing.)

Concentrate grade also shows the same behaviour for Pt and Pd. Both progressively increase with decreasing size class down to 38-53 μm. For gold, the increase is normally down to the 20-25 μm size fraction. The difference is in all likelihood linked to the SG of the Pt-bearing and Pd-bearing mineral(s). The grade, consequently, decreases below 38 μm. Palladium upgrading is clearly more significant than Pt upgrading.

Both platinum and palladium head grade increases with decreasing size class down to 38-53 μm with a maximum of 7-8 g/t and the grade decreases to around 5.1-5.3 g/t at the finest size fraction.

Stage 2: All the tailing of stage 1, once ground to 62% passing 75 μm, was fed to the Knelson for stage 2 recovery (although the target fineness was 55% passing 75 μm, it is easy to pass the target due to the ore's brittleness). This stage yielded a concentrate of 112.6 g and a recovery of 15.6% for Pt and 16.5% for Pd. The concentrate grade is 98.5 g/t for Pt and 108.6 g/t for Pd, as shown in Appendix 3.

The tailing fraction assays vary around 2 g/t with decreasing particle size above 75 μm for both Pt and Pd. Figures 3-14A and B show that Pt and Pd grades for the same size classes are generally below those of stage 1, and remain almost the same

trend. The grade of finest size fraction is still high, 4.2 g/t and 4.8 g/t for platinum and palladium, respectively.

Concentrate grade increases with decreasing particle size down to the 20-25 μm size fraction for both Pt and Pd with the highest grade in the 20-25 μm size fraction. Both Pt and Pd recoveries increase with decreasing particle size down to 38-53 μm. The maximum recoveries, around 53 to 55%, are also in the 38-53 μm size fraction. The recoveries decrease to 3.2-3.7% in the finest size class, minus 20 μm. The possible reason is that it is either too fine or not dense enough for effective recovery with the Knelson. The KC's inability in recovering Pt and Pd in the finest size class, where 40 to 44% of the platinum and palladium report, is the main reason for the lower recoveries in stage 2.

The calculated head grade of 3.3 g/t Pt is in good agreement with the measured tails grade of stage 1, 3.4 g/t of Pt. The calculated head grade of 3.5 g/t Pd is also close to the measured tails grade of stage 1, 3.7 g/t of Pd.

Stage 3: A concentrate of 83.2 g was obtained for this stage. It returned a recovery of 11.7% for platinum, and 10.9% for palladium, at a grind of 84% -75 μm. The calculated head, 2.8 g/t of Pt and 3.0 g/t of Pd, is in excellent agreement with that of the tailing of stage 2, 2.8 g/t of Pt and 2.9 g/t of Pd. Upgrading is to 74 g/t for both Pt and Pd.

Tailing assays show the tailing grade increases slowly with increasing size above 38 μm; below 38 μm, it increases quickly up to a maximum at the finest size fraction. The tailing grade is at a lower level for both Pt and Pd compared to stages 1 and 2.

Concentrate grade of both Pt and Pd increases steadily from the coarsest to the minus 20 μm size class (typical of stage 3 for gold). Recoveries are highest for the 20-25 μm fraction, 46.6% for Pt and 45.5% for Pd. The recoveries drop significantly for the minus 20 μm fraction, to a value of 5.8% for Pt and 4.8% for Pd, where the highest Pt and Pd distribution in the feed, 62% and 67% respectively, occurs.

Stage 4: The fourth stage was performed on the tailing of stage 3, without regrinding. A concentrate of 128.8 g was obtained. Appendix 3 shows that stage 4 returned a recovery of 16.1% for platinum and 14.5% for palladium. The calculated head grades, 2.5 g/t of Pt and 2.6 g/t of Pd, are in good agreement with those of the tailing of stage 3, 2.5 g/t of Pt and 2.7 g/t of Pd. Upgrading is from 2.6 g/t to 53.4 g/t for Pt and 2.6 g/t to 49.8 g/t for Pd.

Tailing assays show the same trend as stages 3 above 53 μm; below 53 a lower grade for both Pt and Pd shows the effectiveness of the recovery of variable speed Knelson Concentrator (Figures 3-14A and B). The tailing grade of the finest fraction (minus 20 μm) hardly drops at all, indicating that even a higher rotating velocity does not yield significant recoveries below 20 μm.

Concentrate grade of both Pt and Pd increases steadily from the coarsest size fraction to the minus 20 μm size fraction. Recoveries increase with decreasing particle size for both Pt and Pd, with the highest in the 20-25 μm size fraction, at 55% for Pt and 46% for Pd. Although recoveries drop for the finest size fraction, they are higher than those of the previous three stages at the same size fraction.

3.3.3.2 Overall Results

Tables in Appendix 3 show the overall test results, a total GRPt content of 42.3% in a 3.9 g/t feed and GRPd 42.1% in a 3.7 g/t feed. Note that the overall head

grade increases from 3.58 g/t to 3.65 g/t for platinum (the head grade for palladium is almost unchanged) as a result of an accumulation of errors in tailing assays.

Figures 3-15 and 3-16 cumulate platinum and palladium recoveries in the same way for the previous examples. The total GRPt content of 42.1% and GRPd content of 42.3%, are shown clearly in these two figures (the cross line curves), respectively.

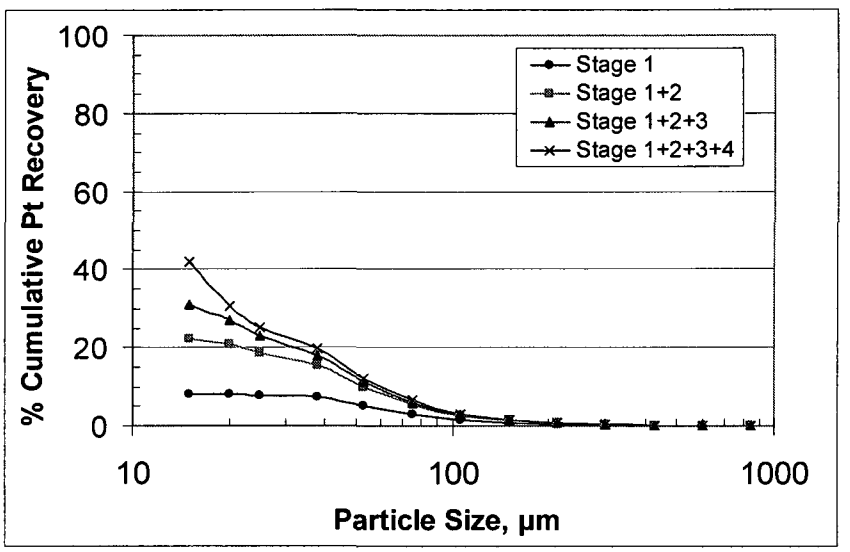

Figure 3-15 Cumulative GRPt Content (100%: total GRPt in the ore)

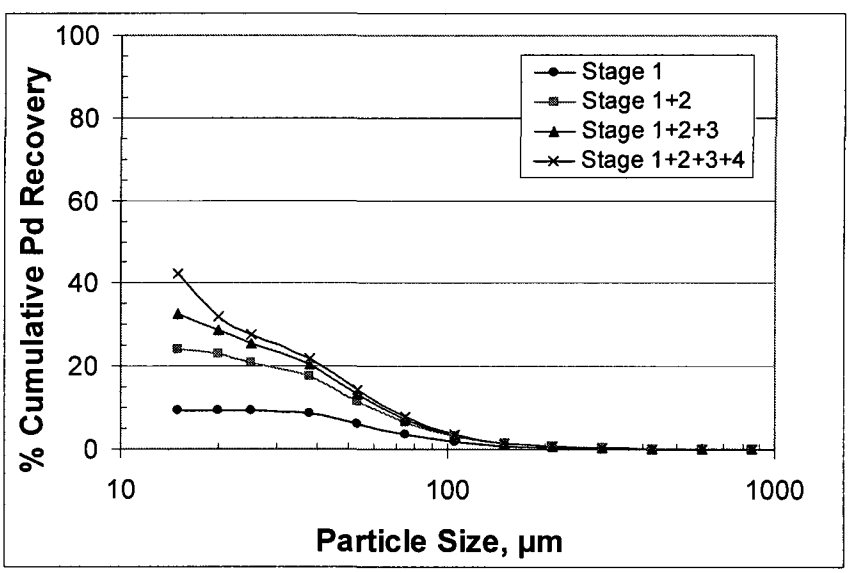

Figure 3-16 Cumulative GRPd Content (100%: total GRPd in the ore)

Comparing the GRPt and GRPd response as a function of particle size shows that, first, both the GRPt and GRPd are finely distributed, 92-93% being finer than 106 μm at final grinding. Second, their behavior is similar. A possible explanation is that the Pt-bearing minerals and Pd-bearing minerals are closely associated. They may also have similar specific gravities, although the difference between the SG of the main platinum-bearing mineral in the sample, maslovite, 11.5 g/cm^3, and the main palladium-bearing mineral, michenerite, 9.5 g/cm^3, suggests a different behaviour.

3.3.3.3 Discussion and Conclusions

Discussion: Although some tailing assays are missing, they do not affect the test reliability. The feed grade of stage 2 is in good agreement with the tailing grade of stage 1, as is the feed grade of stage 3 in good agreement with the tailing grade of stage 4.

Concentrate assaying appears to have been reliable, and the trends in the different stages are clear for both platinum and palladium.

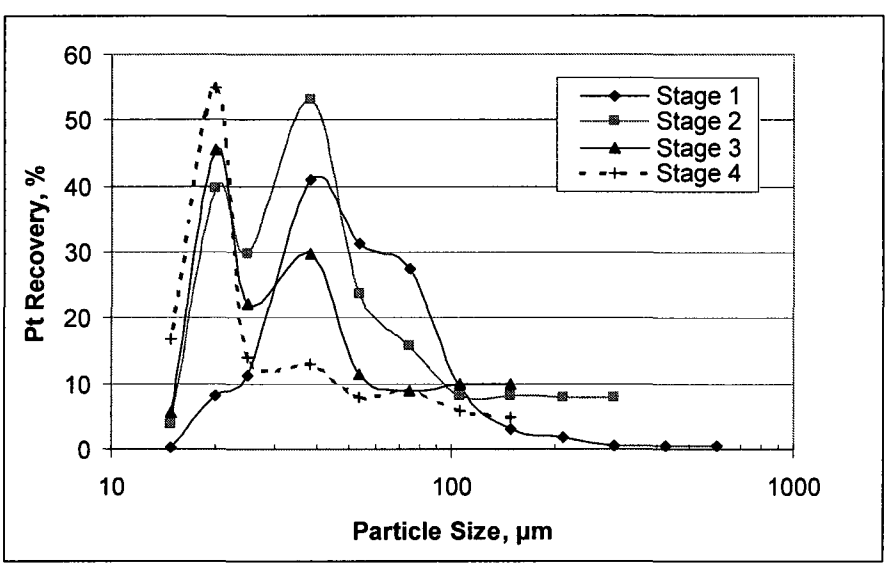

Figure 3-17 Size-by-size Recoveries of Platinum from Stage 1 to 4

Figures 3-17 and 3-18 show platinum and palladium recovery in each size class for all four stages. These trends are remarkably consistent, which adds confidence to the reliability of the test. It is clear from the stage 1 curve that the first stage did not recover most of the GRPt and GRPd above 106 μm, but the recoveries increased below 106 μm. With further grinding, more Pt and Pd were liberated and recovered in stages 2 and 3.

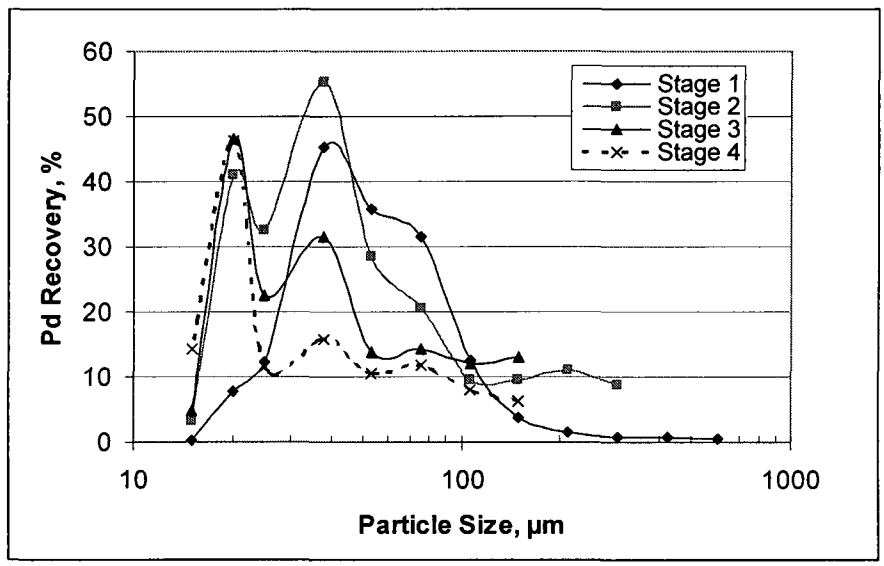

Figure 3-18 Size-by-size Recoveries of Palladium from Stage 1 to 4

Figure 3-17 shows that stage recoveries for platinum display the same trends as those of palladium which were shown in Figure 3-18. The highest recoveries both appear at the 38-53 μm size fraction and there is little GRPt or GRPd recovered above 106 μm. Stage 2 recoveries for both platinum and palladium are almost the same. The maximum recoveries also are in the 38-53 μm size fraction (for gold typically the maximum recoveries move from coarser to finer size fractions when moving from stage 1 to stage 3). The highest recoveries in stages 3 and 4 occur at the 20-25 μm size fraction. Below 20 μm, stage 4 yields the highest recovery, much higher than stage 3, but nevertheless much lower than that of the 20-25 μm fraction.

In summary, both Figures 3-17 and 3-18 show that the recovery is largely confined between 20 and 106 μm. Platinum and palladium recoveries from stage 1 to stage 4 show similar trends.

The proposed flowsheet to process the Nickel Rim South ore includes at least two grinding stages followed by a possible regrind at very fine size (Laplante et al., 2002). Thus there are three possible locations for flash flotation and gravity with P_{80}s of 220 μm, 105 μm and 25 μm.

Within the first grinding loop, it is expected that some density-induced recirculation of PGMs would take place. It would, however, be limited, on account of the relatively fine size of the individual PGM phases. In this first loop, flash flotation could be considered. Gravity processing of the flotation concentrate would be justified only if further cleaning were necessary because some of the Pt and Pd could be lost.

Within the second grinding loop, flash flotation should definitely be contemplated, as undoubtedly there would be a significant build-up of PGMs. The relatively fineness of the circulating load would obviate the need for screening ahead of gravity recovery, which may now also be a viable option. Gravity recovery should also be envisaged to treat this second flash flotation concentrate, which would likely require upgrading.

The third grinding loop calls for very fine grinding and classification, where it is unlikely that gravity recovery can play a significant role. Flash flotation could be used, and would probably be performed in conventional mechanical cells, given the fineness of the circulating load.

Conclusions: The GRPt and GRPd contents of a Ni Rim South ore sample assaying 3.7 g/t of Pt and 3.9 g/t of Pd were the same, 42%. Over 92% of the GRPt and

GRPd contents are finer than 106 μm. The recovery trends and the grade trends of concentrate and tailing for both platinum and palladium appear almost the same from stage 1 to stage 4.

The results indicate that there will be a slight buildup of Pt and Pd in the primary grinding circulating load, and a more substantial one in the secondary grinding circulating load (Xiao and Laplante 2003). For both the use of flash flotation and/or gravity should be evaluated.

3.3.4 Clarabelle Ore Sample

Summary: A sample of ore from Clarabelle mill feed, Ontario, was characterized for its gravity recoverable platinum (GRPt) content. The sample, assaying 0.7 g/t Pt, contained 81%, or 0.55 g/t GRPt. At 100% -850 μm (F_{80} 530 μm), 44% of the platinum was recovered; GRPt content increased to 65% at F_{80} 150 μm, to reach 81% at a final grind of 82% -75 μm. GRPt was finer than 600 μm, and was present in all size classes tested below 600 μm, with 23% of the Pt present as gravity recoverable Pt between 150 and 600 μm.

3.3.4.1 Results for stage 1 to 4

Stage 1: Metallurgical balances of the hydrosizing of the five coarsest size classes of stage 1 concentrate are shown in Appendix 4. The upgrading ratio varied from 6.9 for the 300-425 μm fraction to 8.8 for the 212-300 μm fraction. The coarsest size class did not display any upgrading. Recoveries were high for all size classes above 212 μm, except for the coarsest size class. There is very little GRPt above 600 μm, but the proportion increases dramatically with decreasing size below 600 μm. The grade of the concentrates below 600 μm is high, approximately 1000 to 2000 times that of the ore.

The first stage platinum recovery of 39% is above the average for the other three ore samples tested (Raglan, Strathcona, and Nickel Rim South). The feed, at 0.76 g/t, is upgraded to 163 g/t in slightly more than 0.1% of the feed weight (but much of this mass was subsequently rejected in the hydrosizing step).

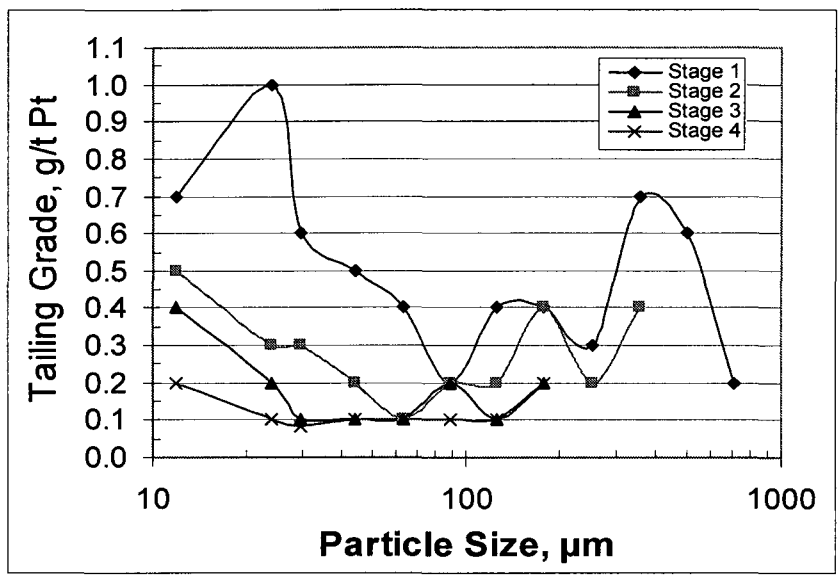

Figure 3-19 Platinum Assay of the Tailing of Stages 1, 2, 3 and 4

The tailing assays (Figure 3-19) show some noise (which is also usual for *gold* in stage 1 of GRG test) at intermediate and coarse size, with an increase at fine size.

Recovery follows a pattern as a function of particle size, with a maximum of 78% at 75-106 µm, with significant drop below this size, which results in a very low recovery below 20 µm, only 1%. Head grade varies erratically with particle size, which is due to the low grades.

Stage 2: Slightly less than half of the tailing of stage 1, once ground to 60% passing 75 µm, was fed to the Knelson for stage 2. This returned a recovery of 34%,

yielding a tailing grade of 0.29 g/t, and a concentrate grade of 32 g/t, as shown in Tables in Appendix 4. This is close to the average performance for all the tests done for stage 2.

The tailing fraction assays are not as noisy as those of stage 1, although the sensitivity of the analysis, ±0.10 g/t, causes some oscillation in the assays.

Concentrate grade increases with decreasing particle size down to the 20-25 μm size fraction. Below 150 μm and above 20 μm, recovery is in the 39 to 67% range. Platinum minerals below 20 μm are either too fine for effective recovery with the Knelson or still unliberated, which explains the drop in recovery. The calculated head grade, 0.43 g/t, is in good agreement with the measured tails grade of stage 1, 0.46 g/t.

Stage 3: This stage returned a 24% platinum recovery at a grind of 82% -75 μm, close to the usual target of 80% passing 75 μm. The calculated head, 0.28 g/t, is in good agreement with that of the tailing of stage 2, 0.29 g/t. Upgrading for stage 3 is fair, from 0.28 g/t in the feed to 15 g/t in the concentrate.

Tailing assays show the same trend as stages 1 and 2, but at a lower grade; in fact, the only assay substantially higher than the others is in the minus 20 μm fraction.

Concentrate grade increases steadily from the coarsest to the minus 20 μm size class (typical of stage 3 for gold of the GRG test). Recovery is the highest for the 20-25 μm fraction, 67%. It drops significantly for the minus 20 μm fraction, to a value of 13%, which is the highest of the three stages for this size fraction.

Stage 4: The fourth recovery stage was performed on the tailing of stage 3, without regrinding. The feed rate was similar to that of stage 3, 300 g/min. This stage returned a 26% platinum recovery, upgrading a 0.18 g/t feed (compared to 0.22 g/t in

stage 3 tails) into a 9.8 g/t concentrate. Tailing grade is relatively independent of particle size at 0.1 g/t, except for the minus 20 μm fraction, in which Pt grade increases to 0.2 g/t. Concentrate grade increases with decreasing particle size, as does recovery, down to the 20-25 μm fraction. The minus 25 μm fraction contributes 75% of the additional recovery, a clear indication that the finer sperrylite (the dominant Pt-mineral, see Chapter 5) is more difficult to recover than native gold at the same particle size.

3.3.4.2 Overall Results

Tables in Appendix 4 show that the fourth stage added 6.5% to overall platinum recovery, more than half of it below 20 μm. Overall GRPt stands at 81%. Note that the overall head grade dropped from 0.72 to 0.68 g/t as a result of normal errors in tailing assays, which are around 0.10 g/t

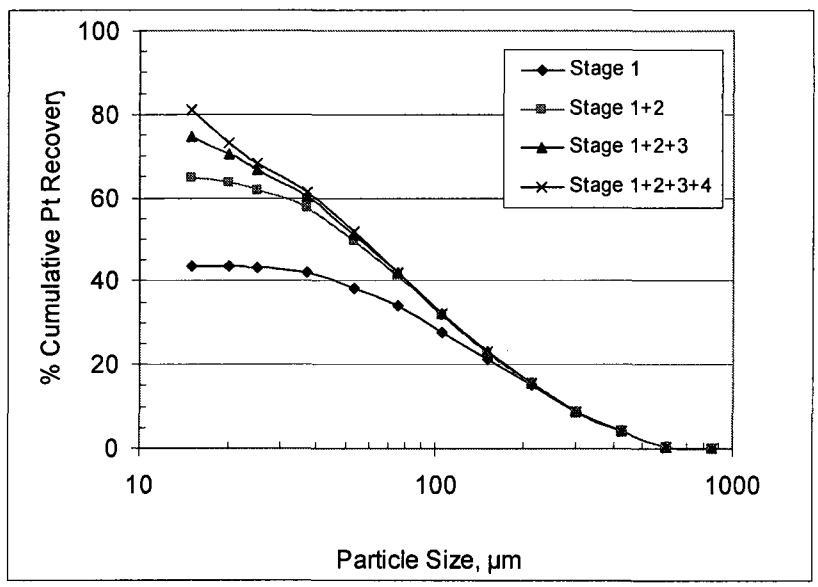

Figure 3-20 Cumulative GRPt Content (100%: total platinum in the ore)

Figure 3-20 cumulates platinum recovery in the same way as for the previous three ores tested. First, platinum is cumulated as percent retained from the coarsest

(+850 μm) size class to the finest. The platinum in the finest class (i.e., –20 μm) is assumed to be coarser than 15 μm, but only for the purposes of showing total recovery (43.5% for stage 1). Second, platinum is cumulated from stage 1 to stage 4. Thus, the fourth curve (for stage 4, crosses) cumulates to the total GRPt content, 81%.

Figure 3-20 is similar to most such figures for typical gold ores, except for the plateau at 15 to 37 μm of stage 1 (at approx. 42% recovery), which is caused by the "low" density of sperrylite (compared to that of native gold).

3.3.4.3 Discussion and Conclusions

Discussion: Concentrate assaying again appears reliable, but tailing grades were too low for accurate assaying. This is particularly apparent for the third stage. It can be concluded that the relative GRPt content is in error by 2 or 3% because of normal experimental limitations. The content in g/t (0.55 g/t) is unaffected by the lack of accuracy in tailing assays.

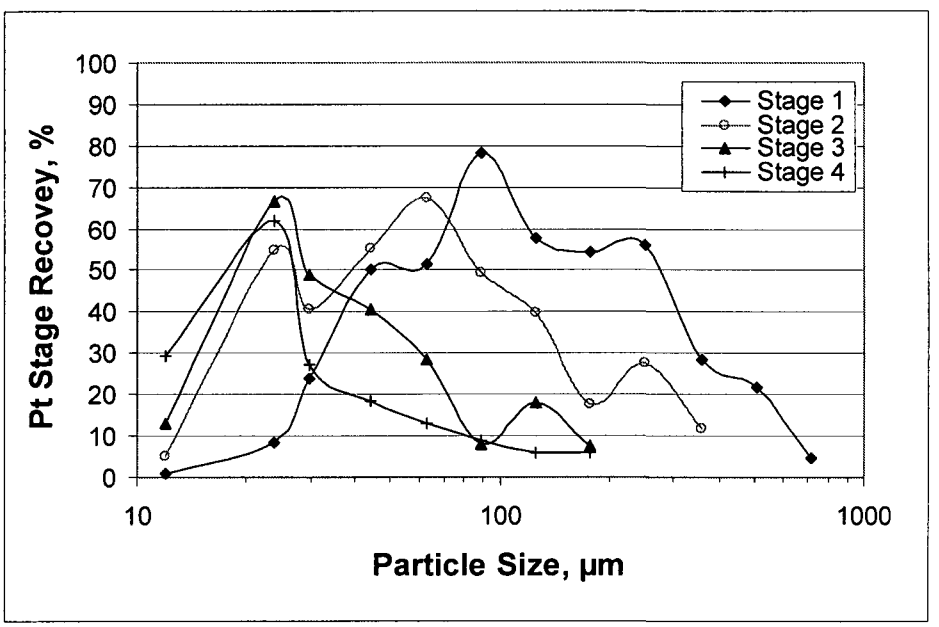

Figure 3-21 Stage Recoveries per Size Class

Figure 3-21 shows platinum recovery in each size class for all four stages. Each stage has a different maximum, which moves to finer size as the test progresses and the feed becomes finer. The trends are remarkably consistent, which adds confidence to the reliability of the data.

Test results show an exceptional degree of liberation for the main Pt-bearer, identified as sperrylite (see Chapter 5). The response of Pt to the test would support this, but identifies the natural size distribution as being coarser than what was thought previously.

If sperrylite had the same grinding and classification behavior as gold, direct gravity recovery from the cyclone underflow would be appropriate. The circulating load of sperrylite in the grinding circuit would also be high relative to the total solids. However, the lower SG of sperrylite and its brittleness compared to gold, as well as the relatively coarse grind size used at Clarabelle, would make gravity recovery, at best, difficult. This will be confirmed in a forthcoming sampling campaign at the mill. It may be that flash flotation will be more effective. This must be tested at pilot scale before any definitive conclusion can be drawn. A research project/or propose needs to address these issues in the future.

Despite some of the difficulties associated with the recovery of a lower SG and brittle mineral (again using gold as the standard), the potential at Clarabelle is attractive because the GRPt content is relatively high with respect to current PGM recovery. Other precious metals are also likely to benefit from the approach (particularly if flash flotation is used), as the same test yielded a gravity-recoverable gold content of 44%, and a palladium content of 35%. The poorest performer was silver, which had a gravity recoverable content of only 6%, despite a head grade of 7 g/t (hence most of the silver is clearly not present as the native metal).

Conclusions: The GRPt content of the Clarabelle mill feed sample assaying 0.68 g/t was found to be 81% or 0.55 g/t. The GRPt is found below 600 μm. Although the GRPt was not examined for mineral liberation, it is likely that any liberation problem would only be found just below 600 μm. By 300 μm, the GRPt recovered should be well liberated (Xiao and Laplante 2003b).

The amount of GRPt and its size distribution suggest that recovery from the grinding circuit (cyclone underflow) should be attempted. Two options, gravity recovery or flash flotation followed by gravity recovery, should be investigated.

3.3.4.4 Comparing All the Ores Tested

As the database grows, it is helpful at this point to compare results. The head grades of these four ores for both Platinum and Palladium are various. Figure 3-22 indicates that the highest Platinum and Palladium head grade is from Ni Rim South ore. There is no correlation between the head grade and the GRPGM contents.

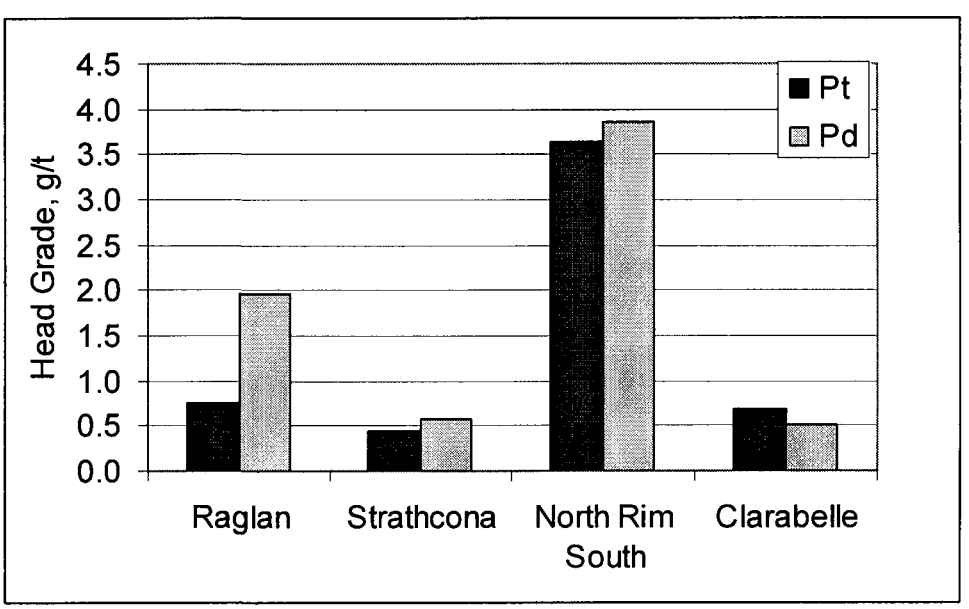

Figure 3-22 Comparison of Head Grade of Platinum and Palladium

The GRPt content, 81%, is the highest among the four ore sample tested. However, the GRPd content, 35% is between the highest and the lowest among the ore samples.

The first test on a sample from Raglan had yielded a GRPt content of only 5% and GRPd 3%. The second test on a sample from Strathcona Mill had yielded an average GRPt content of 53% and GRPd of 44%. The third test on a sample from Ni Rim South deposit in Sudbury area had yielded the same of amount of GRPt and GRPd content, 42%. For the Clarabelle ore, the GRPt content, 81%, is the highest among the four ore sample tested. However, the GRPd content, 35% is between the highest and the lowest among the ore samples as shown in Figure 3-23.

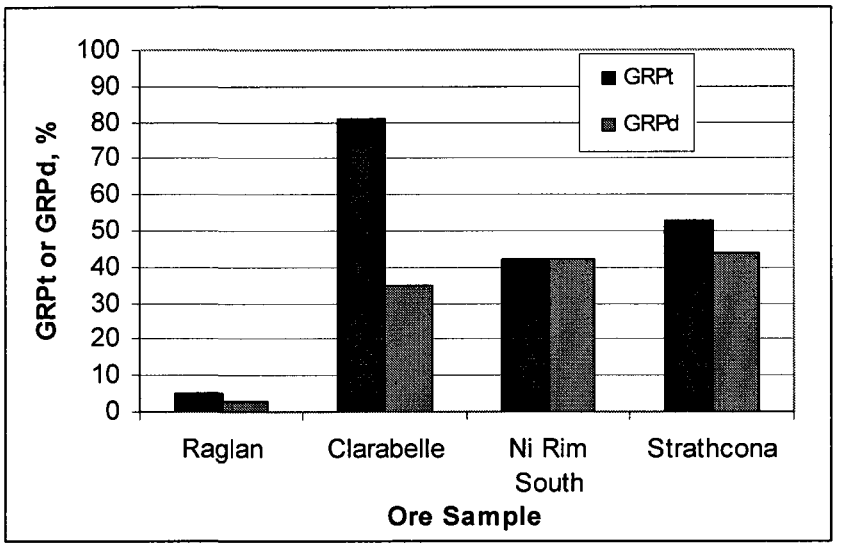

Figure 3-23 Comparison of GRPt or GRPd content in Different Ore Samples

CHAPTER FOUR

CHARACTERIZATION OF THE BEHAVIOR OF PLATINUM GROUP MINERALS IN THE GRINDING CIRCUIT

4.1 Introduction

Analysis of the behavior of PGMs (e.g. breakage and classification behavior) in grinding circuits should be based either on fully liberated PGMs or near-liberated PGMs (i.e., what has been defined as GRPGMs in Chapter one). Of interest are the GRPGMs that are already liberated, rather than those that could eventually be liberated. Thus, the GRPGM protocol could be applied to circuit stream samples. The information generated will be used for characterizing the behavior of GRPGMs in the grinding circuit. The already liberated GRPGMs in the grinding circuit should be measured first to determine their behavior in grinding and classification units.

As is well-known, gold particle breakage, classification, and liberation deportment in a grinding circuit are strongly influenced by gold's malleability and specific gravity. The high malleability reduces grinding rates. Banisi (1991) found that the selection function of silica was more than four times that of gold in a laboratory ball mill and that gold ground six to twenty times slower than the associated gangue at the Golden Giant Mine. For gold (or GRG) classification, the data available to generate cyclone classification curves show that typically over 95% of the GRG reports to the cyclone underflow (Laplante, Liu and Cauchon, 1989; Banisi, Laplante and Marois,

1991; Laplante and Shu, 1992; Putz, Laplante and Ladoucer, 1993; Woodcock, 1994; Noaparast, 1997). Whether the behavior of PGMs in grinding circuit is likely to be different from the other components as is the case with gold (due to differences in density and ductility) has never been investigated. The purpose of characterization of PGM behavior is to understand the breakage behavior (e.g. cumulative selection function), the classification behavior, and the impact of circulating load.

The grinding and classification behavior of PGMs in the Clarabelle grinding circuit was investigated using data from two surveys. The content of the GRPGMs in the various streams (ball mill discharge, cyclone overflow, cyclone underflow, etc.) was characterized first. The size-by-size information from these two surveys was mass balanced for PGMs, GRPGMs and gold. Then grinding kinetics and classification curves were generated. The concept of cumulative selection function (Ramirez and Finch, 1980; Finch and Ramirez, 1981; Laplante, Finch and del-Villar, 1987) is used to describe the breakage behavior of platinum minerals (mainly sperrylite at the Clarabelle mine).

4.2 Methodology

Characterizing the content of GRPGMs in a stream includes measuring how much of the GRPGMs are already liberated (rather than the potential GRPGM content as for the ore). Unlike the GRG protocol, in which samples are processed only once to measure the content of GRG, the GRPGM protocol includes a second or scavenger step. The sampling, lab measurement and analysis protocol is now presented.

To measure the GRPGM content in streams, representative samples (usually between 10 and 30 kg) are extracted and processed with a laboratory semi-continuous centrifuge unit operated to maximize gravity recovery. For this work, a Knelson Concentrator with a 3-inch nominal diameter bowel (KC MD3) was used. As only

GRPGMs that are already liberated are of importance, no grinding is used, and each sample is usually processed only once to simplify the procedure and minimize the risk of recovering non-GRPGMs. Since many PGMs have a slightly lower specific gravity than gold minerals (e. g., sperrylite has a s. g. of 10.6), a variable rotation speed KC MD3 is used to process the tails from the standard Knelson concentrator operation to recover GRPGMs in the finer size classes. This second stage is necessary for GRPGMs due to their relative lower specific gravity.

Two sampling surveys, each two hours in duration, at the Clarabelle mill were completed on November 6, 2002. The six sample points are marked in the following flowsheet, Figure 4-1. All samples were weighed wet, filtered and shipped to McGill. The samples were dried and prepared to measure the content of GRPGMs (as well as GRG for the purpose of comparison).

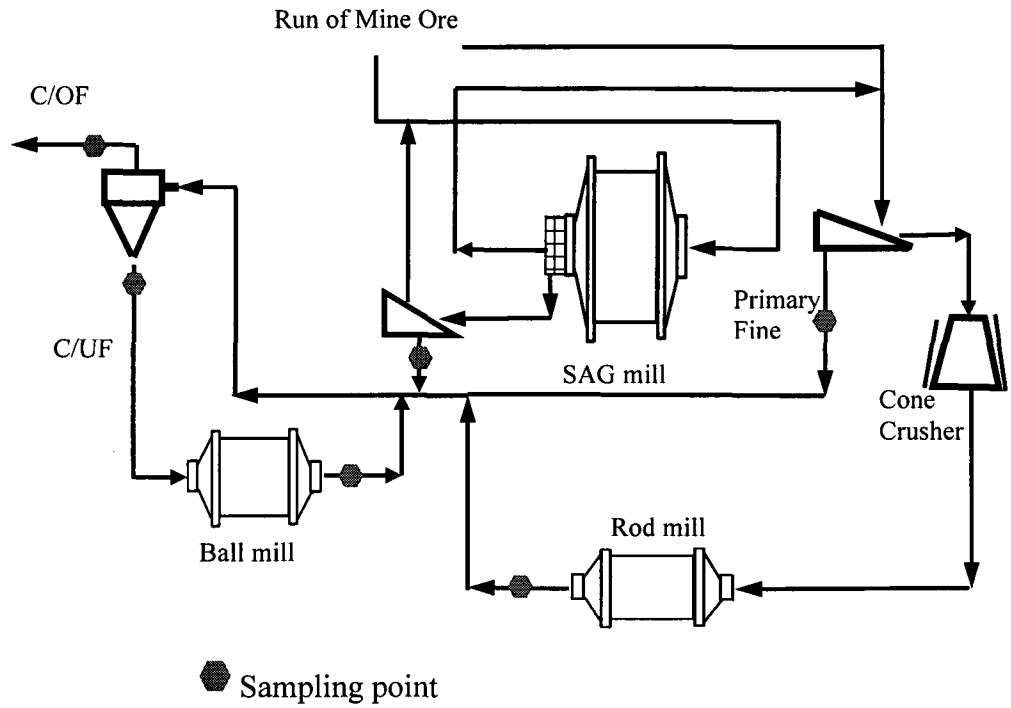

Figure 4-1. Sampling Diagram of the Clarabelle Mill Grinding Circuit

Samples were first screened to collect the plus 850 μm fraction; the minus 850 μm fraction, weighting between 9.5 and 42 kg, was processed with the standard KC MD 3 operated at 60 G, fed at 800 to 890 g/min with a fluidization water flow of 7 L/min. All the concentrate was screened from 600 μm to 20 μm; two 300 g samples of the tailing stream were wet screened at 20 μm and the oversize dry screened from 600 μm to 20 μm. The bulk of the tailing product was dried and screened at 300 μm and the undersize, approximately 8 to 10 kg, was processed with the variable speed KC MD 3, this time at a theoretical acceleration of 115 G, a dry feed rate around 628 g/min and fluidization water flow 6 L/min. The concentrate product and two 300 g sub-samples of the tailing product were processed as in the first recovery step. The various size fractions were analyzed for gold, silver and the six platinum group elements at the Inco Metals Laboratory in Sudbury. Figure 4-2 shows the flowsheet for measuring the GRPGM content of these streams.

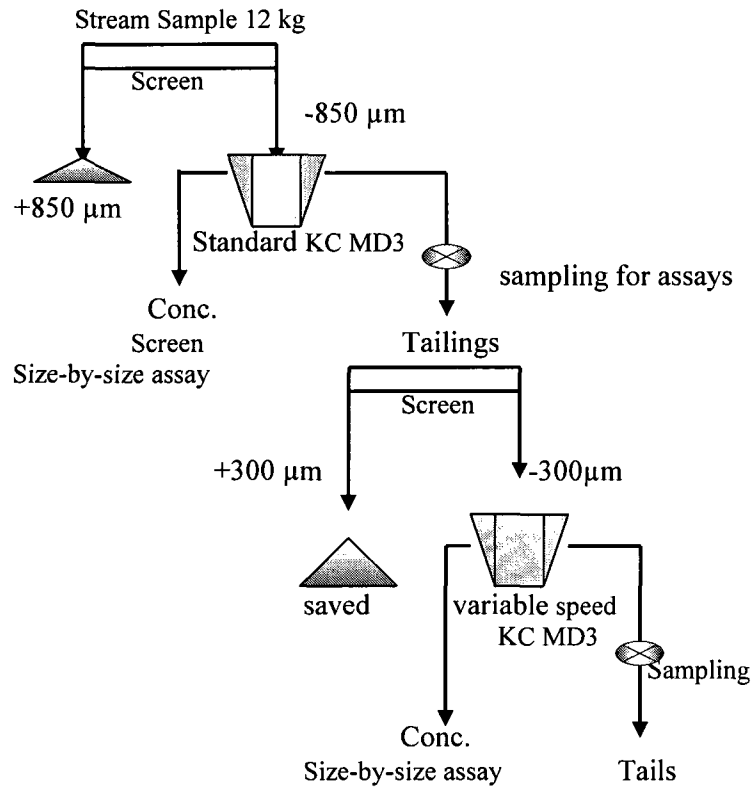

Figure 4-2. Laboratory Flow Sheet for Measuring GRPGM Content of Streams

4.3 Results of Characterizing GRPGMs of Streams in Clarabelle Mill

The sampling survey results, GRPGM content characterized by using the standard and variable speed KC-MD3, are presented below.

4.3.1 The Sampling Results

Table 4-1 shows the sampling survey results.

Table 4-1. Sampling points, weight and screen results for each stream in Clarabelle Grinding circuit

No	Sampling Location	Dry Mass (kg)	Solid (%)	+850 μm mass (kg)	(%)	-850 μm mass (kg)	(%)
1	Ball Mill Discharge (BMD Survey #1)	42.81	75.02	**1.6**	*3.74*	**41.21**	*96.26*
2	Ball Mill Discharge (BMD Survey #2)	32.5	76.99	**1.52**	*4.68*	**30.98**	*95.32*
3	SAG Mill Screen Undersize (SAG u/s Survey #1)	30.21	59.48	**6.60**	*21.85*	**23.61**	*78.15*
4	SAG Mill Screen Undersize (SAG u/s Survey #2)	19.57	62.22	**5.09**	*26.01*	**14.48**	*73.99*
5	Cyclone Overflow (COF Survey #1)	11.13	37.29	**0.01**	*0.09*	**11.12**	*99.91*
6	Cyclone Overflow (COF Survey #2)	12.09	41.37	**0.01**	*0.08*	**12.08**	*99.92*
7	Rod Mill Discharge (RMD Survey #2)	24.3	61.95	**5.50**	*22.63*	**18.80**	*77.37*
8	Primary Fines Survey #1	22.4	41.85	**10.9**	*48.66*	**11.5**	*51.34*
9	Primary Fines Survey #2	16.56	52.43	**7.14**	*43.12*	**9.42**	*56.88*
10	Cyclone Underflow (CUF Survey #1)	30.01	73.74	**3.16**	*10.53*	**26.85**	*89.47*
11	Cyclone Underflow (CUF Survey #2)	43.15	78.73	**6.50**	*15.06*	**36.65**	*84.94*

Rod mill discharge was surveyed only once due to a shut down before the second survey. The solid % of ball mill discharge, SAG mill screen undersize and cyclone overflow are in the range from 60 to 77%. The ball mill discharge is finer than

the cyclone underflow and the finest stream is the cyclone overflow, about 100% passing 850 μm. The coarsest stream is the primary fine stream, about 51-56% passing 850 μm. As mentioned, the fractions of plus 850 μm, ranging from 0.01 to 10 kg, were not processed with KC MD3.

4.3.2 Standard Knelson Concentrator Test Results

The following discusses the results on the ball mill discharge (BMD) sample. Other stream test results are summarized at the end of the section.

The Knelson concentrates (about 100 g) were first screened from 600 μm to 20 μm. Then the five coarser size class fractions (+600, -600+425, -425+300, -300+212, and –212+150 μm) were further upgraded with a hydrosizer. The metallurgical balances of the hydrosizing results are shown in Appendix 5. The enrichment ratio varied from 0.4 for the +600 μm size fraction to 17.2 for the 150-212 μm size fraction. Of the five coarser size classes, the highest calculated head grade of platinum, 137.44 g/t (4.4 oz/st), is in the 150-212 μm fraction, which also has the highest enrichment ratio. The grade of platinum and enrichment ratio of +600 μm and 300-425 μm fractions suggest that there is little gravity recoverable platinum in these two size classes. However, the remaining three size classes are anticipated to contain some gravity recoverable platinum, especially in the 150-212 μm size fraction due to the higher upgrading ratio.

It also can be concluded that there is little GRPt in the coarsest size class of ball mill discharge stream, particularly above 300 μm. The concentrate mass in each size class was assayed below 150 μm; above 150 μm, the calculated heads of the hydrosizer tests were used.

Appendix 5 shows the metallurgical balance of the first recovery attempt with the standard Knelson Concentrator. In order to maximize Pt recovery, the feed rate was

set around 850 g/min, compared to the higher feed rate of 1200 g/min, which is standard for the GRG test, stage 1. This operation is aimed at recovering the well-liberated platinum minerals in medium to coarse size classes. The recovery of 66.7% at a fineness of 27.8% –75 μm is high for Pt recovery; it is higher than the first stage recovery (39%) at the fineness of 25.1% -75 μm for Clarabelle feed ore, which was shown in Chapter Three. The recovery difference between the ore (feed) and ball mill discharge also indicates that the platinum minerals were liberated inside the mill and converted into gravity recoverable minerals. The ball mill discharge sample is upgraded to 203 g/t (6.5 oz/st) from a 2.5 g/t (0.08 oz/st) feed grade in slightly more than 0.8% of the feed weight.

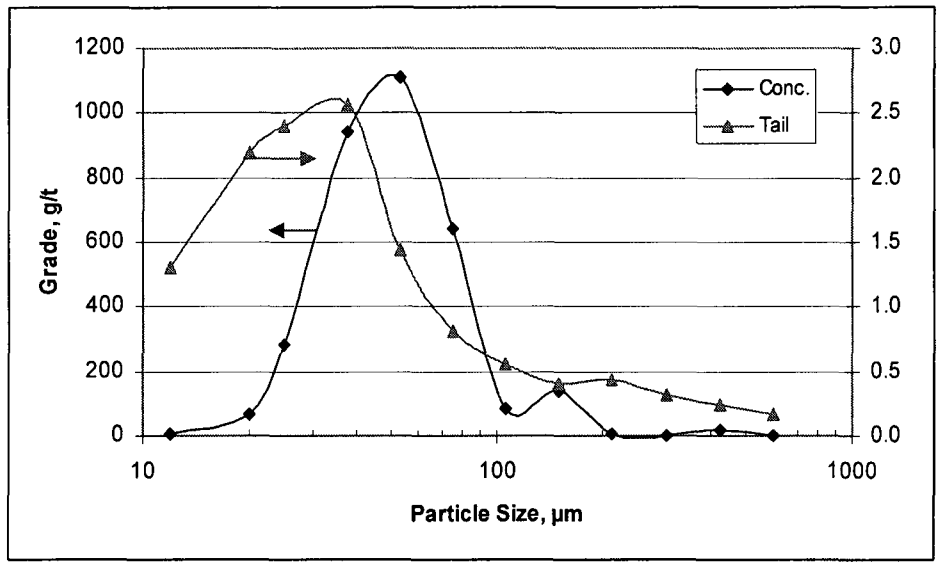

Figure 4-3 Standard KC MD3 Concentrate and Tailing Pt Grade

Figure 4-3 shows the grade distribution for the Knelson concentrate and tailing as a function of particle size. The tailing assays are very consistent as shown by the relatively smooth curve. The grade of Pt increases progressively with decreasing particle size down to the 38-53 μm fraction. The grade decreases significantly at the finer size classes. This suggests that platinum minerals below 38 μm are either absent

or not recovered by the KC MD3. The latter possibility is one reason the variable speed Knelson Concentrator is used to scavenge the tailing.

Concentrate grade is low above 212 μm. It starts to increase from 212 μm down to +53-75 μm fraction. For gold the increase is often down to the 20-25 μm fraction (Laplante et al., 1994). However, for Pt the concentrate grade decreases in the finer size classes. This indicates that it is difficult to recover the finer platinum minerals.

Platinum recovery as a function of particle size is shown in Figure 4-4. The recovery increases with increasing particle size up to the 75-106 μm fraction. The maximum size recovery of ca. 88% appears in the 75-106 μm fraction. The recovery dip at 106-150 μm size class appears due to "noise" in concentrate grade data (see Figure 4-3 of the concentrate grade for size class 106-150 μm). The recovery of 150-212 μm fraction is again high, nearly 80%. However, the recovery drops sharply in 212-300 μm fraction, to around 10%. The recovery of two coarse size classes (+300-425 μm, +600 μm) is below 10%. The recovery of the coarse fraction, 425-600 μm, jumps to 50%, which is believed to be a "nugget" effect.

Figure 4-4 shows that the recovery from size class 38-53 μm to 150-212 μm is high. The data in Appendix 5 indicate that 56 % of GRPt is recovered below 150 μm. It also shows that there is not too much gravity recoverable Pt in the coarse size classes (e.g. plus 150 μm). The recoveries below 38 μm size class drop significantly, particularly below 20 μm. The poor recoveries correspond to the low concentrate grade in these finer size classes which indicates that it is either difficult to recover the fine platinum or not much platinum is in the finest size class.

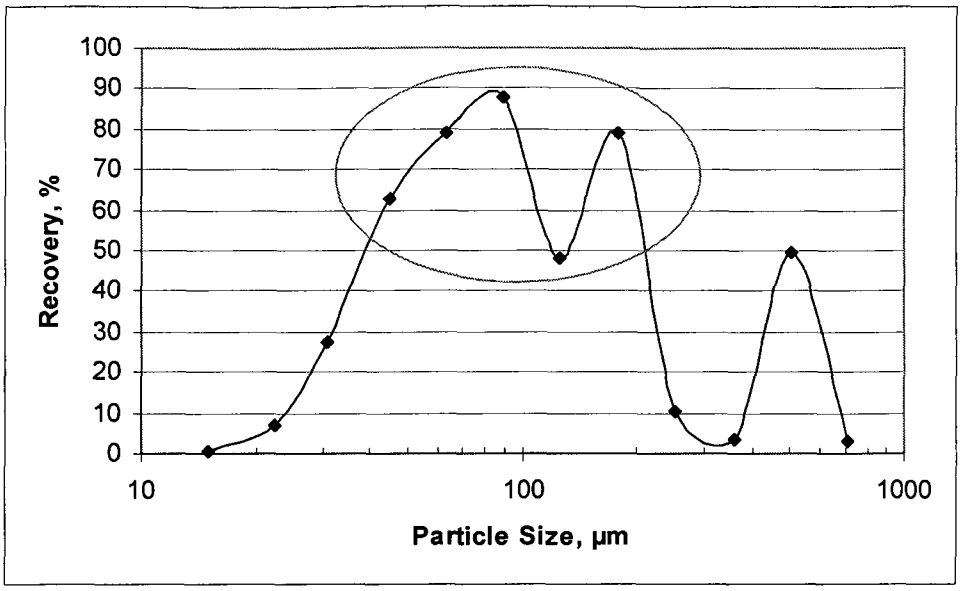

Figure 4-4. Pt recovery as a Function of Particle Size for Standard KC MD3 Operation

4.3.3 Variable Speed Knelson Concentrator Test Results

The metallurgical balances are in Appendix 5. They show that this scavenging step yielded a 56% platinum recovery, upgrading a 0.94 g/t (0.03 oz/st) feed (which is close to the 0.83 g/t (0.027 oz/st) standard KC MD3 tails, bearing in mind that oversize (plus 300 µm) material has been removed) into a 46.88 g/t (1.5 oz/st) concentrate.

Figure 4-5 shows the Pt grade of feed, concentrate and tail in the variable speed KC MD3 test. The feed grade of Platinum is obtained by back calculating from the grade of concentrate and tails. It shows that the Pt feed grade is higher at the fine to intermediate particle size, below 75 µm, with a maximum between 20 and 53 µm. Above 75 µm, concentrate grade is low because most coarser GRPt was already recovered in the standard KC MD3 operation (stage 1).

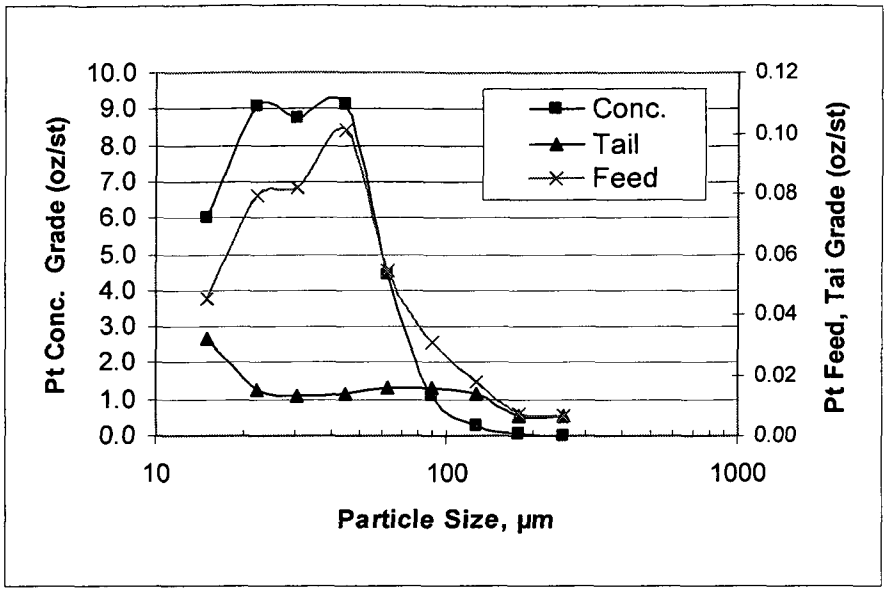

Figure 4-5. Platinum Grades of Feed, Concentrate and Tail of Variable Speed KC Operation

Tailing grade increases slowly with decreasing particle size, being highest, 0.94 g/t (0.03 oz/st), below 20 μm.

The concentrate grade vs. size trends in a similar fashion to the feed grade. The grade increases with decreasing size down to the 20-25 μm, the grades remaining in the "plateau" of 250 to 280 g/t (8-9 oz/st) in size classes 20-25 μm, 25-38 μm, and 38-53 μm, then decreasing slightly in the finest size class, –20 μm. The grade difference between the coarser size classes (e. g. 150-212 μm) and finer size classes (e. g. 25-38 μm) is significant. This also indicates that there is less GRPGM left in the coarse fraction and the variable speed KC can effectively recover the PGMs in the finer size fraction.

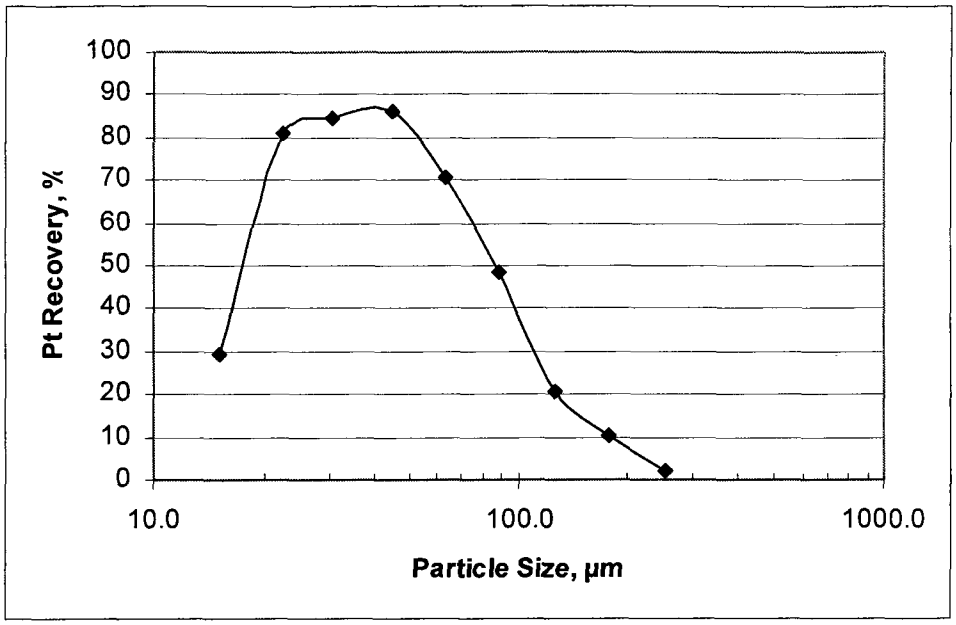

Figure 4-6 Platinum Recovery of Variable Speed Knelson Concentrator as Function of Particle Size

The platinum recovery as a function of particle size is shown in Figure 4-6. It shows good recovery, 81 to 86%, in the finer size classes, 20-25 μm, 25-38 μm and 38-53 μm. Although the recovery decreases below 20 μm, it still reaches 30%. It is worth noting that the "plateau" makes it evident that finer platinum minerals have been recovered in this step. About 98% GRPt is recovered below 150 μm size class.

4.3.4 Overall Results

Figure 4-7 shows the overall platinum recovery as a function of particle size. As shown in Figure 4-7, platinum recovery is the highest in the finer size classes from 20-25 μm to 150-212 μm. Recovery in the coarser size classes is both lower and erratic.

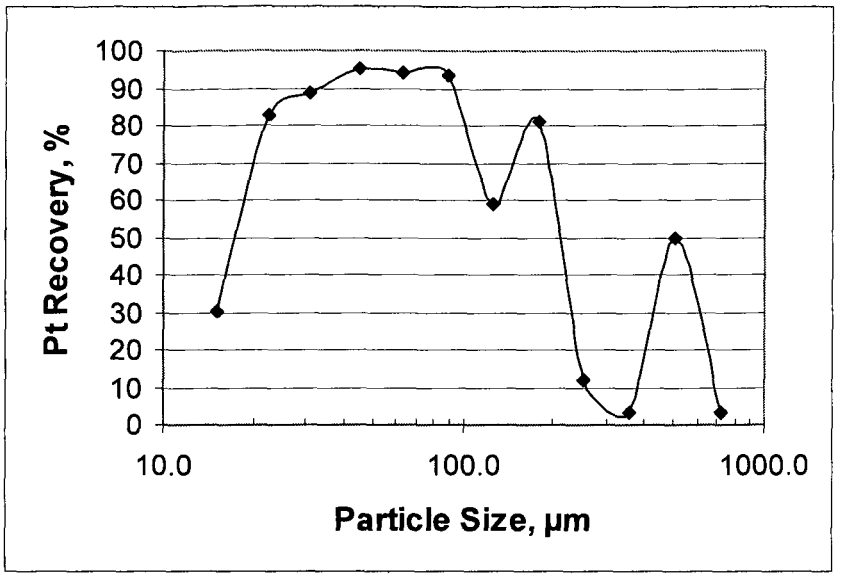

Figure 4-7 Overall Platinum Recovery as a Function of Particle Size of BMD Stream

Overall results can also be shown cumulatively. Figure 4-8 cumulates platinum recovery in two ways. First, platinum is cumulated as percent retained from the coarsest (+600 μm) size class to the finest. The platinum in the finest class (i.e., –20 μm) is assumed coarser than 15 μm in stage 1 for the purpose of showing total recovery, 63.4%, in Figure 4-7. Second, platinum is cumulated from standard KC MD3 operation (here called stage 1) to variable KC MD3 operation (stage 2 or scavenger step). Thus, the second curve cumulates to the total GRPt content, 83.3%. Figure 4-8a also shows that the variable speed KC MD3 recovers a significant amount of platinum in the finer size fractions from 15 μm to 53 μm.

Figure 4-8b shows the GRG cumulative recovery in the same way as Figure 4-8a for the purpose of comparison with platinum. It indicates that more gold is recovered in coarser size fractions than is the case for platinum and there is not much fine gold recovered in stage 2.

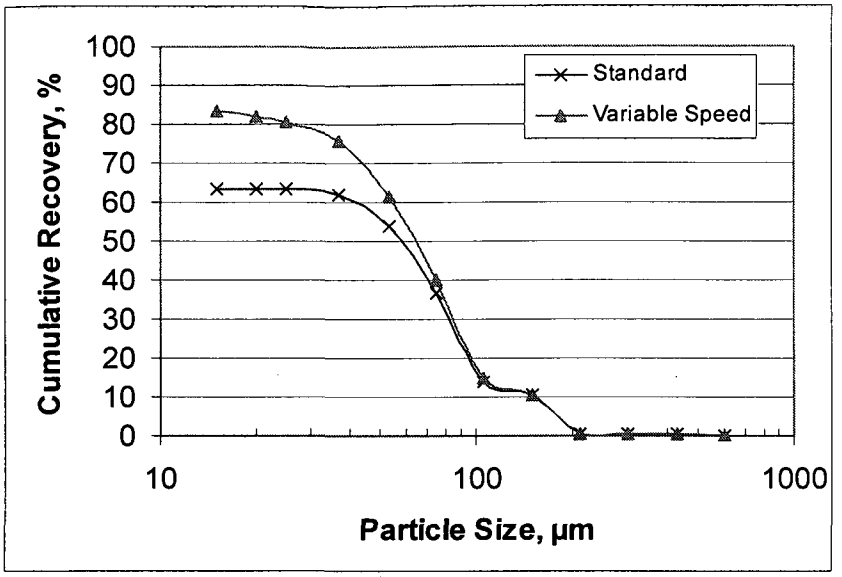

Figure 4-8a. Cumulative GRPt Content for Stream BMD

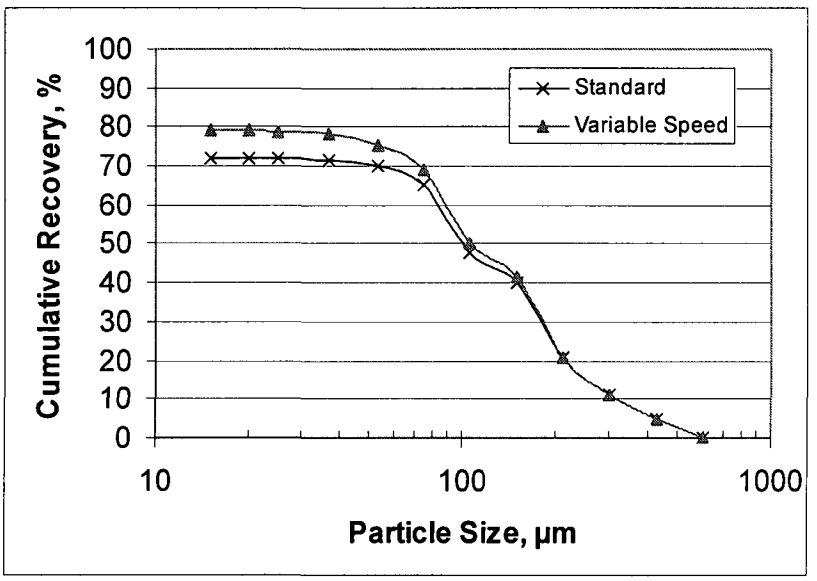

Figure 4-8b. Cumulative GRG Content for Stream BMD (100%: Total Gold in the Stream)

Appendix 5 shows the overall metallurgical balance for stage 1 and 2. There is a small difference in recoveries between the individual and combined calculation, as the +300 μm fraction of the tailing of stage 1 has been removed from the feed of stage 2.

The same protocol was applied to the other five streams, namely SAG undersize, primary fines, cyclone underflow, cyclone overflow, and rod mill discharge. The results of grades and gravity recoverable platinum mineral content of all streams for both surveys are included in Table 4-2.

The availability of GRPGMs in all five streams of the two surveys (except the rod mill discharge of the first survey) was measured and compared. Results are similar, with the exception of the cyclone overflow, which has a lower grade in survey 2. There is a clear upgrading ratio in the circulating load streams (the cyclone underflow and ball mill discharge), but there is also a slight upgrading in the primary fines. The platinum grade of the cyclone underflow is greater than that of the ball mill discharge for the two surveys. The ball mill discharge sample is probably more reliable due to surging in the cyclones.

Table 4-2 Summary of the two Surveys

Stream	First Survey		Second Survey	
	Pt Grade, (g/t)	% GRPt	Pt Grade, (g/t)	% GRPt
SAG U/S	0.73	42.5	0.69	50.2
Primary Fine	1.55	58.9	1.31	56.4
Cyclone Underflow	2.57	77.6	2.29	80.1
Ball Mill Dis.	2.06	82.6	2.03	83.1
Cyclone Overflow	0.67	46.6	0.45	41.1
Rod Mill Dis.	N/A	N/A	0.42	51.5

The GRPt content of the two circulating loads (cyclone underflow and ball mill discharge) is of similar order of magnitude to that of the feed ore (81% GRPt of Clarabelle ore in Chapter 3). Their size distribution, however, are much finer, as shown in the following Figure 4-9.

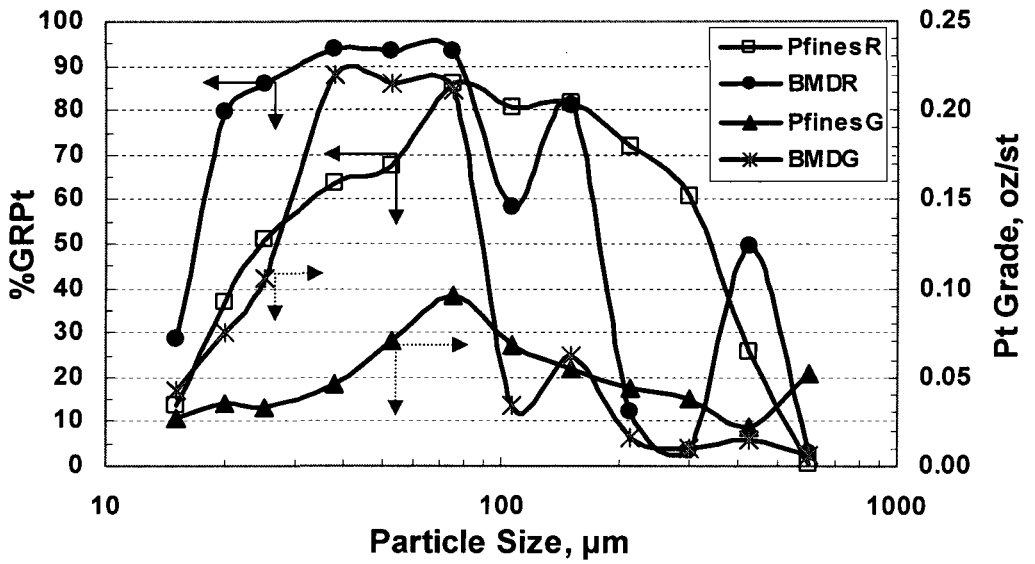

Figure 4-9. Size-by-Size GRPt Data for the Primary Fines and Ball Mill Discharge (Legend: PfinesR—Primary Fines Recovery, BMDR-Ball Mill Discharge Recovery, PfinesG-Primary Fines Grade, BMDG- Ball Mill Discharge Grade)

Figure 4-9 shows typical results for two streams of the first survey, the primary fines, which is not part of the circulating load, and the ball mill discharge. The differences between the two streams at first are not apparent. The primary fines assay, 1.41 g/t (0.045 oz/st), is about twice the overall head grade, whereas the ball mill discharge assay, 1.88 g/t Pt (0.06 oz/st), is about three times the overall head grade. Both have a high gravity-recoverable platinum content, although that of the ball mill discharge is erratic above 100 µm, but clearly higher below 100 µm. It is the platinum grade below 100 µm that distinguishes the two streams, as platinum, most of which is

gravity recoverable, builds up significantly in the circulating load to grades in excess of 6 g/t (0.20 oz/st). It is this platinum that should be targeted for recovery. The recovery data and grade also indicate that the platinum minerals are gradually build up inside the ball mill.

The results of both surveys show that the gravity recoverable platinum and the head grade are close for each stream. It is reasonable to conclude that the survey results are an accurate reflection of the process.

The approach to characterization of the already liberated gravity recoverable platinum in a stream applied here shows it is an effective way to quantify the content of GRPGMs in a stream. The first stage, using standard speed Knelson concentrator, is used primarily for recovering the intermediate and coarse size fraction platinum group minerals. The second stage, using higher speed Knelson concentrator, is used to recover the more finely distributed platinum group minerals. This second step is important because the platinum group minerals usually occur in the finer size classes (Cabri, 1981), which the standard speed Knelson concentrator has difficulty recovering. The second stage contributes more platinum recovery than for gold based on Figures 4-8 (a) and (b).

4.4 Classification Behavior of PGMs in the Grinding Circuit of Clarabelle Mill

The classification behaviour is described using the hydrocyclone classification efficiency curve, which is defined as the percentage of solid, element, or GRPGMs from the feed recovered to the cyclone underflow in each size class.

To start, the size distribution of the cyclone underflow and overflow was obtained by screen analysis. Second, the concentrate and tail of each stream obtained by operating the laboratory Knelson Concentrator MD-3 were sent to assay for gold,

platinum and palladium. Next, the size-by-size data for each stream was mass balanced (using the software NORBAL developed by Noranda) to generate size distributions for gold, platinum and palladium, as well as the GRG, GRPt, and GRPd. Finally, the classification efficiency was calculated for the various components.

Table 4-3 Screen size analysis results for the five streams

Size class (μm)	SAG Discharge	Primary fine	Ball mill discharge	Cyclone underflow	Cyclone overflow
+850	21.69	48.65	3.25	11.02	0.01
600	3.23	6.52	1.62	2.76	0.01
425	5.39	9.3	3.85	5.64	0.29
300	6.29	8.85	7.57	9.3	1.31
212	8.26	8.18	14.43	15.6	4.81
150	7.5	5.1	16.6	16.44	7.87
106	7.93	3.63	17.02	15.68	11.69
75	6.74	2.23	10.12	8.11	12.45
53	7.46	2.08	7.85	5.21	15.02
37	5.79	1.4	4.87	2.7	11.98
20	7.3	1.43	4.99	2.8	13.48
Pan	12.42	2.63	7.83	4.74	21.08
Total	100	100	100	100	100

Table 4-3 shows the size-by-size analysis mass balanced results for the five streams of SAG mill discharge, primary fines, ball mill discharge, cyclone underflow, and overflow.

The gold, platinum, and palladium assay results in each size class for the five streams are shown in Appendix 6. Table 4-4 shows the size-by-size results of the GRG, GRPt, and GRPd in the cyclone underflow and overflow.

The classification efficiency results for the total solids, elements, GRG and GRPGMs are listed in Table 4-5. The classification efficiency of ore is estimated by using the size distribution and cyclone underflow and overflow flowrates measured

during the sampling period. As for the platinum, palladium and gold classification efficiency, the assay for each size class was used in the calculation (Appendix 7).

Table 4-4 Size-by-size results of GRG, GRPt, and GRPd

Size class	Cyclone Underflow			Cyclone Overflow		
(μm)	GRG	GRPt	GRPd	GRG	GRPt	GRPd
999	3.37	1.46	70.51	100	100	100
714	3.37	1.46	70.51	100	100	100
505	70.62	2.18	63.99	100	100	100
357	18.29	1.65	81.87	4.33	5.30	6.22
252	40.58	11.24	59.13	5.86	11.69	25.41
178	34.42	19.54	91.63	9.56	7.48	59.41
126	75.16	36.33	72.30	13.18	10.94	24.41
89	85.70	60.35	91.41	29.26	23.68	49.43
63	93.08	78.10	89.09	58.84	28.65	57.90
44	94.59	86.36	87.86	67.72	45.64	44.89
27	87.83	79.20	75.27	90.52	78.27	75.58
15	26.86	16.52	29.48	26.86	18.43	18.75

The classification curves of the total solid, gold and platinum for the first survey are shown in Figure 4-10. It shows that the classification curve of platinum is similar to that of gold. At the coarser size classes (e.g. above 53 μm), the classification curve of gold and platinum almost overlap. Slightly more platinum reported to the cyclone underflow than gold between the size class of 25-37 μm and 53 -75 μms, whereas the partition of palladium is slightly below that of gold. It is suggested that the flakey shape of gold particles is a hindrance to effective classification, resulting in a cyclone behaviour that is similar to that of platinum minerals of much lower density. The classifications of gold and platinum minerals, it is proposed, are similar in the Clarabelle mill due to the trade-off between specific gravity and particle shape.

Table 4-5 Calculated classification efficiency for survey No. 1

Size Class (μm)	Classification Efficiency (%reported to the cyclone underflow)						
	Solids	Pt	Pd	Au	GRPt	GRPd	GRG
999	99.97	99.98	99.97	99.93	99.40	98.10	99.90
714	99.88	99.92	99.89	99.73	97.64	92.83	99.62
505	98.30	99.03	98.04	97.97	98.64	93.50	96.86
357	95.46	98.75	97.40	99.44	99.70	92.09	99.96
252	90.58	97.19	96.51	99.33	99.58	96.37	99.71
178	86.10	98.41	94.89	97.44	99.55	97.98	98.33
126	79.90	94.89	94.21	95.75	99.06	98.18	98.52
89	65.88	96.33	92.83	97.48	98.72	97.06	98.62
63	50.70	95.59	87.95	94.78	97.16	95.22	96.55
44	40.05	90.54	80.97	80.77	93.04	88.95	89.15
27	38.11	87.18	69.22	74.75	86.84	69.47	74.67
15	40.00	42.77	40.00	47.82	42.77	37.40	59.04

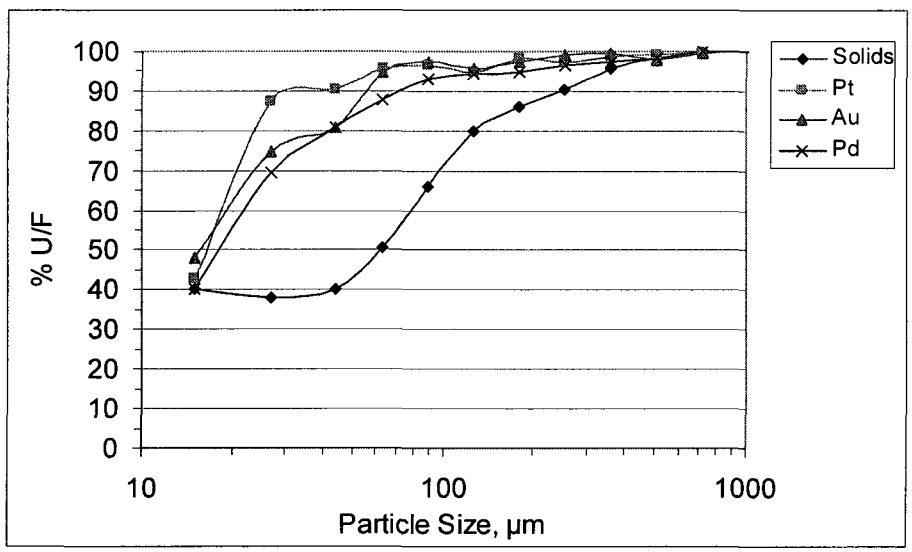

Figure 4-10. Classification Curves of Total Solids, Pt, Pd and Au for the First Sampling Survey #1 in the Clarabelle Mine

The classification curves for the GRG, GRPt and GRPd are shown in the Figure 4-11. They follow a similar trend as for the elements. The classification points for the coarsest size classes show some noise due to the small sample size.

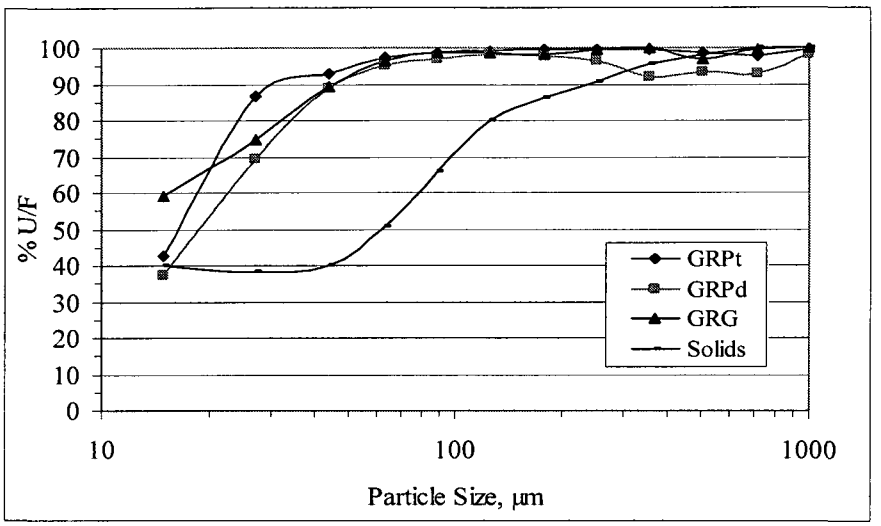

Figure 4-11. Classification Efficiency curves of Total Solids, GRPt, GRPd and GRG for the First Sampling Survey #1 in the Clarabelle Mill

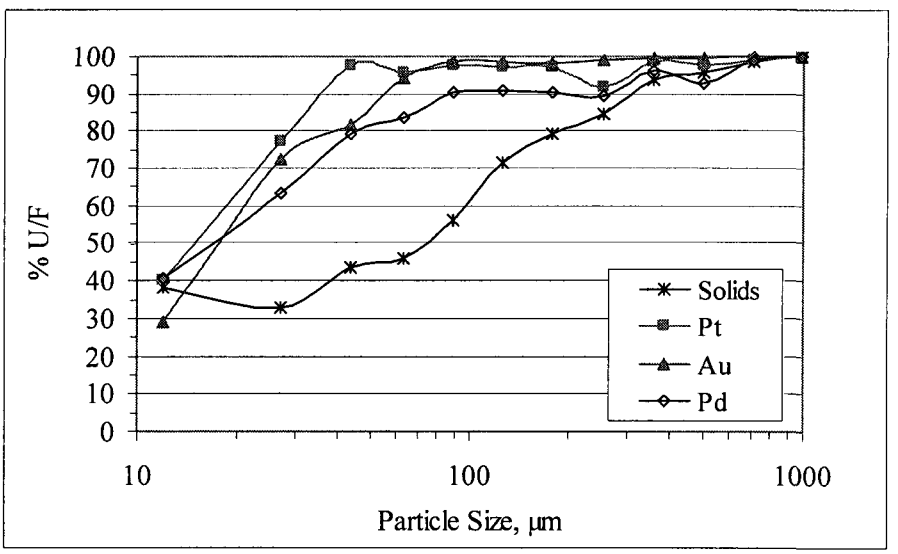

Figure 4-12. Classification Efficiency Curves of Total Solids, Pt, Pd and Au for the Second Sampling Survey #2 in the Clarabelle Mill

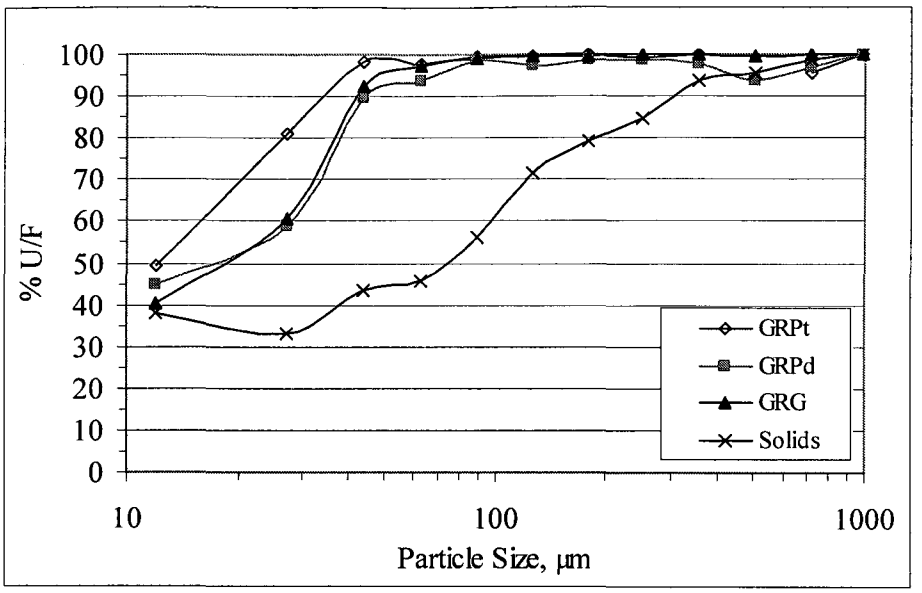

Figure 4-13. Classification Efficiency Curves of Total Solids, GRPt, GRPd and GRG for the Second Sampling Survey in the Clarabelle Mill

The classification efficiency curves almost overlap for GRPt, GRPd and GRG above the 75 μm size class. The differences appear at the finest size classes (i.e., minus 25 μm). The explanation could be related to shape having more impact in the finer size classes although this was not pursued.

Although the second survey results (Figures 4-12 and 4-13) have more variation compared to the first survey results, they confirm the classification behavior.

4.5 Grinding Behavior of the PGMs

Figures 4-14 and 4-15 show the selection functions (specific rate of breakages) estimated from the first and second survey, respectively (see Table 4-6 for the breakage function used). The two surveys show similar trends. The selection function for the ore is roughly log-linear. That of the coarsest size class, the plus 850 μm, is

slightly misleading, since this size class spans many Tyler intervals. The selection function of platinum is calculated twice (Pt(1), Pt(2)), using two breakage function (which has yet to be measured), shown in Table 4-6. The selection function of platinum (which is largely that of sperrylite) is similar to that of the ore above 212 μm, presumably because the liberated sperrylite is expected to be brittle, much like the ore. Below 212 μm, the selection function of platinum is lower than that of the ore. The reason for this is unclear, but Figure 4-15 shows that the second survey returns similar results. It is known that in grinding circuits where the sulphide content is significant (which is the case of the ores in the Sudbury basin), the finer size classes are enriched in the denser, softer sulphides.

Table 4-6 Breakage Function Used to Calculate the Platinum Selection Functions

	b_{21}	b_{31}	b_{41}	b_{51}	b_{61}	b_{71}	b_{81}	b_{91}	$b_{10,1}$	$b_{11,1}$
Pt (1)	0.4804	0.2173	0.1066	0.0581	0.0355	0.0239	0.0173	0.0130	0.0101	0.0079
Pt (2)	0.6054	0.1901	0.0759	0.0397	0.0251	0.0174	0.0125	0.0091	0.0066	0.0049

In Sudbury, the dominant sulphide is pyrrhotite. This suggests that pyrrhotite has a higher specific breakage rate than sperrylite.

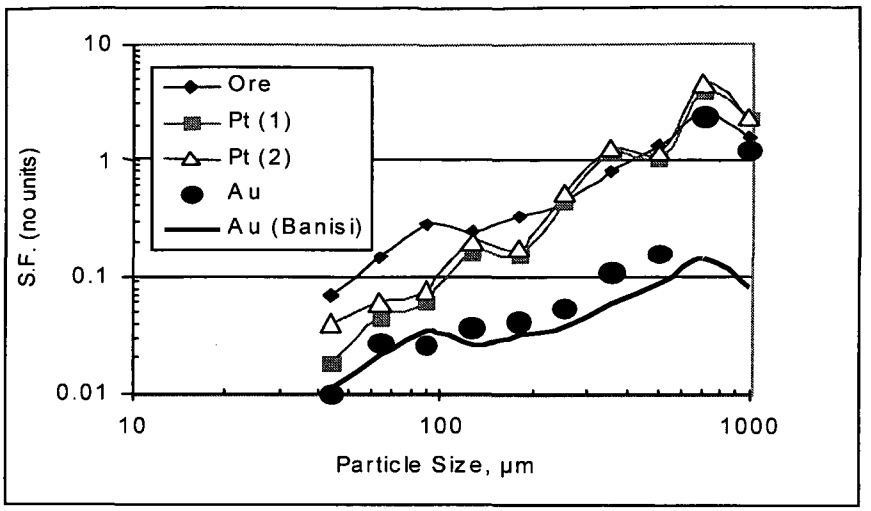

Figure 4-14. Selection Function of Various Species at Clarabelle Mill for the First Survey. (Pt (1) and (2) are calculated using the breakage functions shown in Table 4-6; Au (Banisi) is based on the selection function of ore and the ratios proposed by Banisi et al., 1991)

In Figure 4-14, the behaviour of gold is of particular interest. First, it is noticed that its selection function above 600 µm is indistinguishable from that of the ore, presumably because it is not present as liberated particles (which is what the GRG test on the ore indicates). Liberation takes place below 600 µm and the selection function of gold then assumes values that are in good agreement with those observed by Banisi et al. (1991).

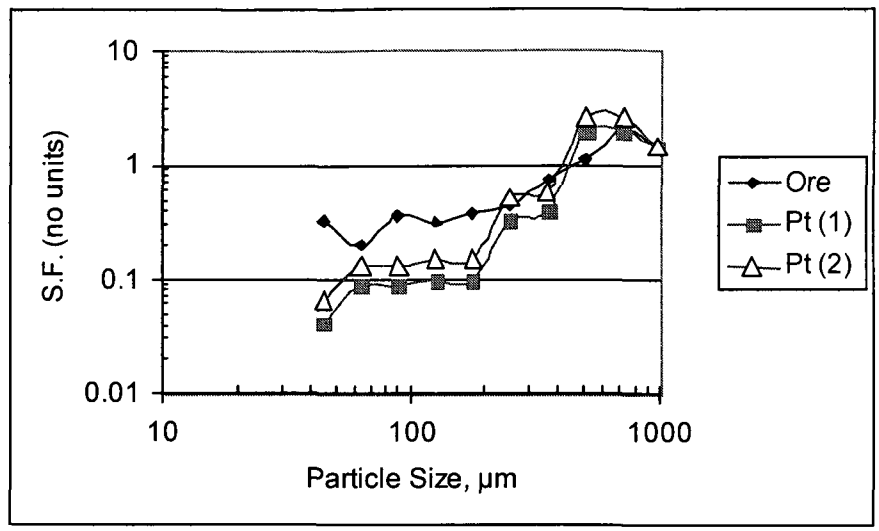

Figure 4-15. Selection Function of Ore and Platinum at Clarabelle Mill for the Second Survey (Pt (1) and (2) are calculated using the breakage functions shown in Table 4-6)

Rather than calculating a selection function from an assumed (or measured) breakage function, Ramirez and Finch (1980), Finch and Ramirez (1981), Laplante, Finch and del-Villar (1987) established that a simple cumulative size selection function, k_x, with plug flow transport is adequate for modeling closed circuit ball mills. The cumulative selection function is a selection function for the cumulative mass of particles coarser than a given size, x, and replaces the breakage function and the selection function. Previous workers (Furuya et. al., 1971; Finch and Ramirez, 1981; Laplante, Finch and del-Villar,1987) had shown that the plug flow assumption is adequate to describe material transport in closed-circuit mills because of the dominating influence of the circulating load. Therefore, the cumulative selection function with plug flow model was used to simulate the behaviors of ore and ore components in the Clarabelle grinding circuit.

Using a cumulative selection function with plug flow transport, the grinding model is simplified to:

$$W_{x(t)} = W_{x(0)} * \exp(-k_x * t) \qquad \text{Equation 4-1}$$

where $W_{x(t)}$ and $W_{x(0)}$ are cumulative mass fraction coarser than size x after grinding times of t and 0, respectively, and k_x is the cumulative selection function for material coarser than x, and t is the retention time.

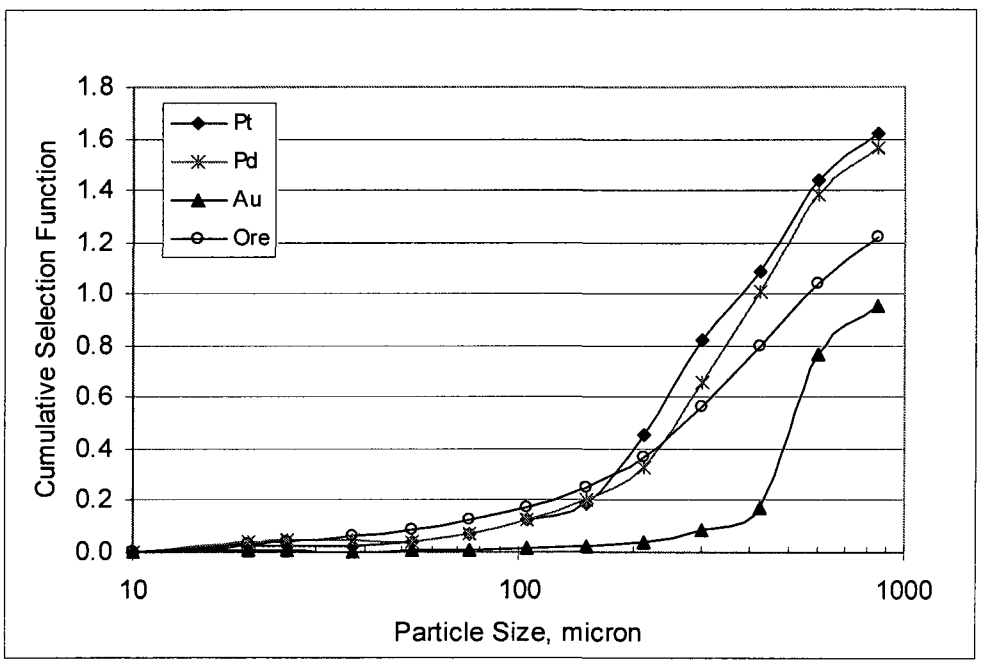

Figure 4-16 Cumulative Selection Function Curves for Survey #1.

Transposing equation 4-1 above, the cumulative selection function k_x for each size x can be calculated, then the cumulative selection function as a function of particle size can be constructed. Figure 4-16 shows the cumulative selection function curves for survey #1. To remind, the cumulative selection function indicates the breakage rate for the cumulative size classes above the quoted size. For example, the cumulative selection function above 600 μm for ore is 1.04 (it has no unit because the residence

time distribution was made dimensionless), which means that the breakage rate for particles above 600 μm is 1.04. The finer the particles the lower the cumulative selection function. The reason is the finer particles breaking more slowly. Therefore, the cumulative selection function decreases as the particle size decreases (as does the discrete size selection function).

Figure 4-16 shows that the cumulative selection function of all size classes for gold is lower than for the ore. However, the trend in cumulative selection function for platinum and palladium appears to be different. They are higher above 212 μm and lower below 212 μm compared to ore, which is consistent with the selection function curves shown in Figures 4-14 and 15. The cumulative selection functions of platinum and palladium are 1.3 times higher than the ore at size classes above 212 μm and are 50 to 70% of the ore's cumulative selection function below 212 μm. The cumulative selection function of gold for all size classes is lower than the ore at Clarabelle Mill due to the known slow grinding kinetics of gold.

CHAPTER FIVE

MINERALOGICAL ANALYSIS OF GRPGMS

5.1 Introduction

The occurrence and distribution of PGEs (platinum group elements) in an ore is directly related to the type of ore (Vermaak, 2005). Usually, PGE deposits can be divided into two categories: one is the deposits containing discrete platinum group minerals and other is that the PGMs are hosted within other minerals. The latter category generally includes the so-called "invisible" portion of the PGE distribution (Oberthur et al., 2002a). The reasons are probably PGEs are present in submicroscopic particles or they occur as a dilute solid-solution.

The examination of the PGMs and the associations qualitatively and/or quantitatively is of importance in order to understand the behavior of PGMs in the grinding circuit and recovery unit. Mineralogical analysis here is used to identify the occurrence and distribution of PGEs (platinum group elements) in the gravity concentrates, as well as the associations.

Maximum recovery at a sellable grade is a constant target of producers. Knowledge of ore characteristics that affect metal recoveries help in achieving this goal. Early determination of whether the PGMs were in sulphides or alloys and whether there is a presence or absence of bismuth, tellurium or arsenic-bearing PGMs will guide the flowsheet design and the method to recover PGMs. PGMs grain size can vary from as

small 1 to 2 μm in UG2 ore from the Bushveld complex to 200 μm for some ores from the JM reef at the Stillwater mine in Montana and greater than 400 μm for some ores from the Sudbury area. As indicated previously, small high specific gravity PGMs particles might behave similarly to large low specific gravity silicate minerals when cycloning is used for classification. This behaviour can lead to recirculation and over-grinding of the PGMs. Identification of the range of PGM grain size can help predict whether or not this problem is likely to occur. Determination of the host (associated) minerals of PGMs and the location of PGM species (intra- vs. inter-grain boundary) normally is critical to analyze to the PGMs liberation. Pyrrhotite can contain PGEs in solid solution or as discrete PGMs locked within pyrrhotite grains (Freeman, 2003). Some copper-nickel ores from the Sudbury, Norilsk, and Raglan districts contain significant pyrrhotite, which needs to be depressed or rejected from the paymetal concentrates. This results in the loss of high unit-value PGMs if the PGMs were locked with the pyrrhotite. The identification of this relationship between PGEs and pyrrhotite can reduce the loss of PGMs during the flotation stage.

To obtain the mineralogical information, a representative sample needs to be available. As noted in Chapter two, various concentrating methods have been used to enrich the PGMs for the mineralogical analysis. The concentration method is especially important for PGMs because they are usually low grade and finely disseminated. In this thesis, the method developed to characterize GRPGMs, is considered an effective way to concentrate the PGMs for mineralogical analysis. All samples for mineralogical analysis were obtained by using the GRPGMs protocol.

This Chapter presents the general mineralogy of PGMs and their associations, as well as the tools used for analyzing their mineralogy. The detailed mineralogical analysis results for the GRPGMs of Raglan, Strathcona and Clarabelle are presented.

5.2 Mineralogy of the GRPGMs and Theirs Associations

5.2.1 Platinum Group Minerals

Unlike gold and major base metals, which are formed a fairly small number of minerals, there were one hundred and nine PGM species recognized by the International Mineralogical Association (IMA) by 2002, ranging from sulphides (i.e. braggite, (Pt,Pd)S) to tellurides (i.e. maslovite, PtBiTe), antimonides (i.e. sudburyite, PdSb) to arsenides (i.e. sperrylite, $PtAs_2$), and alloys (i.e. ferroplatinum alloy) to native species (i.e. native Pt nuggets). Generally, PGMs can be grouped into metals, intermetallic compounds and alloys, notably with Sn, Fe, Pb, Hg, Cu and Ni. The remaining PGMs are formed with Bi, Te, As, Sb and S (Vermaak, 2005). The most common Pt minerals include Braggite (Pt, Pd)S, Cooperite (PtS), Isoferroplatinum (Pt_3Fe), Monchetite ($PtTe_2$), and Sperrylite ($PtAs_2$). According to Cabri (1994), sperrylite is the most common PGM worldwide, and it can be found in every type of geological environment. However, the grain size and grade of sperrylite might vary locally and regionally. The most common Pd minerals include Kotulskite (PdTe), Merenskyite ($PdTe_2$), Michenerite (PdBiTe), Cabriite (Pd_2SnCu), Vysotskite (PdS), and Sudburyite (PdSb) etc.

Generally, PGMs formed with sulphides, arsenides and alloys can be recovered by gravity, as concluded in a report from the Anglo Platinum Research Center (2002). However, PGMs formed with tellurides and oxides can not be recovered by gravity due to the low density and fine grain size distribution.

5.2.2 Associations of Platinum Group Minerals

Apart from the multitude of PGMs, their associations are also diverse. PGMs are usually associated with sulphides, oxides, silicates, sulpharsenides, arsenides and tellurides. The three main sulphide minerals associated with PGMs are pentlandite, chalcopyrite, and pyrrhotite. Pentlandite from Stillwater contains between 8.6% and 12.1% Pd (Cabri, 1992). Reported maximum levels of Pd in Pentlandite in (ppmw) (ppmw refers to parts per million by weight) are: J-M reef (46000), Lac des Iles (6500) and Merensky reef (1164) (Cabri, 1992). Strirny et al., (2000) reported that pentlandite contained 2236 ppmw from the Hartley Mine in the Great Dyke. Lidsay et al., (1998) reported that the mean Pt content of pentlandite is around 10-13 ppmw and 8.5 ppmw from the Merensky reef and the Hartley Mine, respectively. This might indicate that the pentlandite is mainly a Pd carrier. Usually, Platinum minerals are associated with chalcopyrite. Considerable quantities of PGEs can be associated with pyrrhotite in solid solution. Cabri (1988) reported a maximum of 47 ppmw Pd in pyrrhotite from the J-M reef. It is postulated that a significant portion of minute PGMs occurs interstitially in silicates (Sizgoric, 1984). Platinum was long known to exist in the arsenide form (sperrylite, $PtAs_2$) in nickel-copper sulfides in the Sudbury area.

Pentlandite and chalcopyrite are usually readily recovered (depending on particle size and degree of liberation), as are any associated PGEs (i.e. in solid solution or as blebs). PGEs present as blebs or in solid solution in pyrrhotite may or may not be recovered. For example, in milling the Sudbury ores, pyrrhotite is now largely rejected to minimize smelting costs. The pyrrhotite contains significant amounts of nickel (anywhere from 0.4 to 0.8%) and accounts for most of the nickel losses in the Clarabelle and Strathcona mill tailings.

The extremely low concentration of PGMs, their fine size distribution, the difficulty in their detection and identification, and sample representativity are typical problems when carrying out a mineralogical study on PGMs. The range of minerals presented, their relative densities, shape, particle size, and associations present a challenge to the metallurgist in designing and optimizing the extraction process (Hochreiter et al, 1985). The various ore types (end members) of typical ore bodies each with its own metallurgical response heighten the challenge.

5.3 Techniques for Analyzing the Mineralogy of GRPGMs

Several techniques of determining mineralogical characteristics have been developed in the last three decades. The optical microscope can be used to identify many minerals, to observe mineral textures, and to determine mineral quantities by point counting. X-ray diffraction (XRD) is used to identify minerals with a high degree of certainty, and to qualitatively determine mineral content in powdered materials. Development of the electron microprobe (EMP) represented a significant advance in applied mineralogy. Not only can it be used to determine the major, minor, and trace content of minerals in polished sections, but it can also keep the integrity of the mineral grain. The developments of SEM together with the energy dispersive X-ray analyzer (EDX) has enable the mineralogist to nearly instantly identify mineral grains based on backscattered electron images. The development of VP-SEM makes it easy to do the analysis without the need to coat polished sections. With the applications in the mining industry, the following instruments are widely available to the mineralogical department in major mining houses: Scanning electron microscope equipped with an energy dispersive X-ray analyzer (SEM/EDX) or wavelength dispersive X-ray analyzer (SEM/WDX), Variable-Pressure (or Low-vacuum) scanning electron microscope (VP-SEM), electron probe micro-analyzer (EPMA), X-ray diffraction (XRD), quantitative evaluating material by scanning electron microscope (QEM*SEM), and the mineral liberation analyzer (MLA).

Variable Pressure scanning electron microscopy is one of the latest developments in electron beam techniques. It retains most of the performance advantages of a conventional SEM, but removes the high vacuum constraint on the sample environment. Wet, oily, dirty, insulated samples may be examined in their natural state without modification or preparation. It is easy to operate and results can be obtained quickly. The technique can stabilize insulator material sample surface potential close to ground potential during imaging even when high beam voltages, up to 20 kV or more, are employed (Farley and Shah, 1988). The basic difference between the conventional SEM and VP-SEM is the pressure in the specimen chamber. For conventional SEM (the column and specimen chamber share the same vacuum) it amounts to 10^{-3} Pa and for VP-SEM it can be as low as 10^{-3} Pa and as high as 10^{3} Pa (Danilatos, 1991).

The conventional SEM has been used to characterize the polished sample of concentrates while the VP-SEM was used to characterize powder of finer sized concentrates. In order to perform X-ray analysis in the VP-SEM, a high vacuum (10^{-3} Pa) was employed to reduce the so-called "skirt effects" (Robertson et al., 2004).

The conventional SEM, VP-SEM and QEM*SEM developed by CSIRO and the Mineral Liberation Analysis (MLA) developed at the Julius Krusttschnitt Mineral research center are briefly introduced in this thesis because they were used to characterize the mineralogy of GRPGMs from three ores.

5.3.1 Scanning Electron Microscope with Energy Dispersive X-ray Analyzer

The scanning electron microscope (SEM) is one of the most versatile and widely used tools of modern science as it allows the study of both the morphology and composition of materials. Equipped with an energy dispersive X-ray analyzer (EDX), it is used in applied/process mineralogy to analyse polished or thin sections of samples, as well as unmounted pieces of material (Petruk, 2000). By scanning an electron probe

across a specimen, high-resolution images of a specimen, with great depth of field, over a range of magnifications, can be obtained. From a combination of back scattered electron intensities and the identities of most minerals and the size and the relationships among mineral grains can be obtained.

The SEM functions as its optical counterparts except that it uses a focused beam of electrons to "image" the specimen. The gun on the top of SEM column produces an electron beam under high vacuum. The beam, which is confined and focused by apertures and magnetic lenses, is either scanned over the entire sample, or is focused on a spot. The sample, which is coated to prevent surface charging, interact with the electron beam and to produce backscattered electrons (BSE), secondary electrons (SE), X-rays and other signals. The SEM is generally equipped with BSE, SE and EDX detectors.

Backscattered electrons are the incident electrons which are scattered "backward" 180 degree when colliding with an atom in the specimen. The production of BSE varies directly with the mineral's average atomic number. This differential production rate causes higher average atomic number minerals to appear brighter than lower average atomic number ones. For example, most silicate minerals have low average atomic number and appear dark grey in BSE image. In contrast, some PGMs, i.e. sperrylite ($PtAs_2$), michenerite (PdBiTe), maslovite (PtBiTe) have a higher average atomic number and appear in light shades in the BSE image. These features can be used to search for PGMs minerals in the BSE images. The shades of grey between minerals can be either enhanced or reduced by changing the operating conditions on the SEM.

Secondary electrons are ionized electrons which are ejected form the atom with a low energy (5eV) when an incident electron strikes an atom. Due to their low energy, only secondary electrons that are near the surface can exit the sample and be examined.

The SE images can reveal topography of a particle and display details of surface features. The SE image is not as useful as the BSE image for revealing mineral type. The SE image can be produced at a much lower current and voltage than is required for the BSE image.

Characteristic X-rays are caused by the de-energization of the specimen atoms after secondary electrons are produced. Since an electron was emitted from the atom during the secondary electron process, a lower energy shell now has a vacancy. A higher energy electron can "fall" into the lower energy shell, filling the vacancy. As the electron "fall", it emits an X-ray of characteristic energy that is unique to the element from which it originated. These signals are detected with the EDX detector. By combining the resulting element information the mineral can be identified.

5.3.2 Variable Pressure SEM

Variable Pressure scanning electron microscopy (VP-SEM) is one of the latest developments in electron bean microscopy. It retains most of the features of a conventional SEM, but removes the high vacuum constraint on the sample environment. Therefore, wet, oily, dirty, insulated samples may be examined in their natural state without extensive modification or preparation. This high-pressure (low-vacuum) technique can stabilize the insulator sample surface potential close to ground potential during imaging even when high beam voltages up to 20 kV or more are employed (Farley and Shah, 1988). In summary, the basic difference between the conventional SEM and the variable pressure SEM is the pressure in the specimen chamber. For conventional SEM the vacuum is 10^{-3} Pa (the column and specimen chamber share the same vacuum) and for VP-SEM it can be as low as 10^{-3} Pa and as high as 10^{3} Pa (Danilatos, 1991).

When the primary electron beam passes through the gaseous medium of the specimen chamber, collisions of the electrons with atoms and molecules of the gas occur. As a result of these collisions, the electrons lose a portion of their energy and can change the direction of propagation. A portion of the scattered electrons, the so-called "skirt", does not contribute to the image signal. It produces only the background (noise) in the image. The other portion of the electrons of the primary beam, which does not scatter strikes on the specimen at a spot. This portion of electrons creates a useful image signal with sufficient resolution. The air in the sample chamber is ionized by the primary electron beam, conducting electricity sufficiently to allow the electrons absorbed by the sample to leak through the air to a ground contract, so that no coating is needed, even at high accelerating voltages (Maocrieff et, al., 1978).

The same signals as those in the conventional SEM can be detected in the variable pressure SEM. Of interest in mineral processing studies, wet sample can be analyzed so that a slurry sample obtained from a process stream can be analyzed within a very short time after it is collected. The low-vacuum SEM system can easily change the pressure and accelerating voltage settings to obtain good contrast BSE images.

Robinson (1998) pointed out that the low-vacuum SEM is as fast and as easy to use as an optical microscope for an experienced mineralogist. However, the conventional SEM requires a coating, such as carbon, gold and platinum, on the surface of polished section, which is not always possible or desirable (Farley and Shah, 1991). If a PGMs mineral is under study, then it can be only coated with carbon. A coating is not required when using the low-vacuum SEM.

In practice, to ensure that the number of primary beam electrons "lost" due to collisions with the molecules of gases is low, the working distance must be optimized; usually it is set to 15 mm.

5.3.3 Quantitative Evaluation of Minerals by Scanning Electron Microscope (QEM*SEM)

The names QEM*SEM or QEMScan are usually exchangeable. The QEM*SEM was developed by CSIRO in Australia to provide an automatic, off-line, size-by-size and particle-by-particle mineralogical analysis of metallurgical products and exploration samples. It is used widely in mineral processing to analyze ores and mill products to obtain quantitative information about the distribution of minerals in plant and test products.

The system uses a combination of backscattered electron (BSE) images to create an image of a sample reflecting atomic composition, and EDX analysis to provide elemental analysis. The mineral type and composition is obtained by combining with the BSE and EDX database in the computer system. The electron gun is steered within the image frame to scan each particle and to obtain X-ray counts for up to 16 elements at designated pixel points within the particle. The system uses four EDX detectors. The X-ray counts for each element at each pixel position are compared to a reference file to identify the mineral. Each identified point is recorded in a file and displayed on the CRT screen by a false color which represents the mineral. Calculations, e.g. liberation, are performed automatically, and no further image analysis is performed (Pignolet-Brandom and Reid, 1988; Reid and Pignolet-Brandom, 1988). The QEM*SEM has three basic modes of operation:

1) Point scan, this is the most basic mode of QEMScan operation, and is similar to a mineralogical point count. EDX analyses are performed on a grid pattern with equidistant points. Only modal abundance information can be determined from this image.

2) Line scan, the scan grid is set up so that points are closely spaced in the X direction and widely spaced in the Y direction.

3) Areas scan, points are closely spaced in both X and Y directions, this mode is used to determine grind size for liberation in feed samples, diluents in concentrates and losses in tailing samples.

QEMScan is highly automated to ensure reliable and repeatable results. It is gradually being accepted in many operations. The system is much more expensive than the conventional SEM and VP-SEM.

5.3.4 Mineral Liberation Analyzer

The Mineral Liberation Analyzer was developed for the same reasons as the QEM*SEM to provide an automatic, off-line, size-by-size quantitative mineralogy and liberation data for the purpose of assessing an ore body, improving plant performance, and maintaining the quality of product.

Like the QEM*SEM, the system is equipped with backscatter electron imaging and EDX systems, which combined with the MLA software provide high speed and high-resolution BSE imaging, EDX analysis and image analysis which result in accurate mineral identification for particles ranging from 2 to 600 μm. The system takes advantage of the capability of SEM to provide consistent grey-levels for each mineral in

BSE image of a sample. The software "segments" the image into minerals, taking into account cracks, other surface imperfections and "edge effect" around particles. The Xrays are used to confirm the identity of each mineral.

The measurement system is capable of measuring up to 14 samples overnight. Image analysis occurs partly off-line and produces a database of mineralogical results and a set of colored mineral maps. When performing liberation analysis, the quantitative mineralogical information, such as the mineral distribution as volume and weight percent, calculated elemental assay, and particle size distribution, can be easily obtained. When performing a rare phase search, such as for gold or a platinum group mineral, each occurrence, to less than 1 mm in size, is imaged at high-resolution and the associated minerals identified.

Most minerals can be identified from the BSE signal. However, for minerals with similar BSE levels, the EDX is employed. The X-ray spectra of these minerals are stored with the BSE data for off-line image segmentation. In all cases, once subsequent image processing is complete, the SEM can be driven back to view any desired particles by mouse click in order to check mineral identification or to obtain a photographic record of the original particle of interest.

5.4 Results

The Objective of the mineralogical work is to determine the PGM species and mineral associations present in each of the sample analyzed.

The following is the GRPGM mineralogical information for the various samples measured by SEM, VP-SEM and QEM*SEM.

5.4.1 Analysis of GRPGMs from the Raglan Ore with SEM

The GRPGM content of the Raglan ore is low and most is finely distributed. A sub-sample concentrate (stage 2) of the minus 25 μm size class was mounted, polished and searched in backscattered electron mode using a conventional SEM to detect the PGMs. PGMs usually appear as bright objects under this mode due to their high atomic number. Once bright particles were found they were analyzed using the system. Figure 5-1 shows the backscattered images of one PGM particle (A) and some other high atomic number particles.

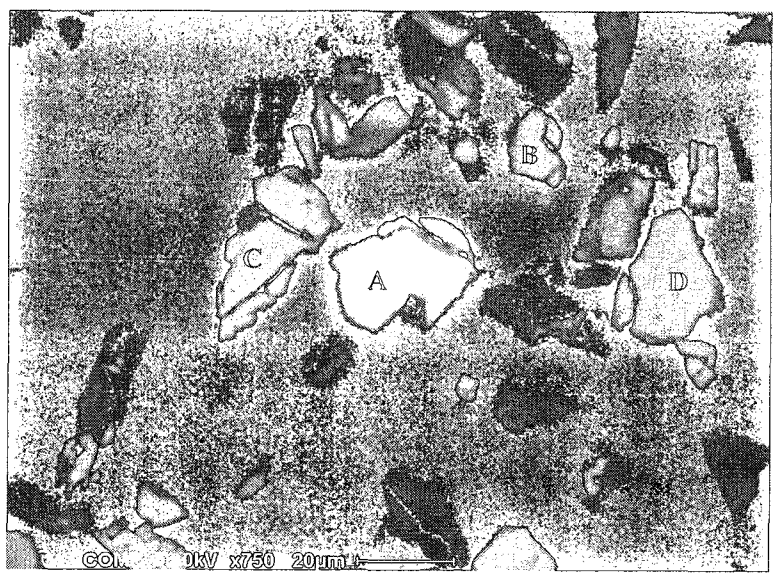

Figure 5-1 Backscattered Electron Image of Concentrates of Raglan Ore Sample

The backscattered electron image of particle A was obtained with 30 kV accelerating voltage and 750x magnification (in the original screen image). Qualitative analysis shows that particle A contains mainly Pt and Te (according to peak height of X-ray spectrum) with Bi and Fe. Analyzing different spots of particle A, similar X-ray spectrum (Figure 5-2) was obtained which means that particle A is probably a single phase. Based on the BSE image, this particle is considered to be liberated.

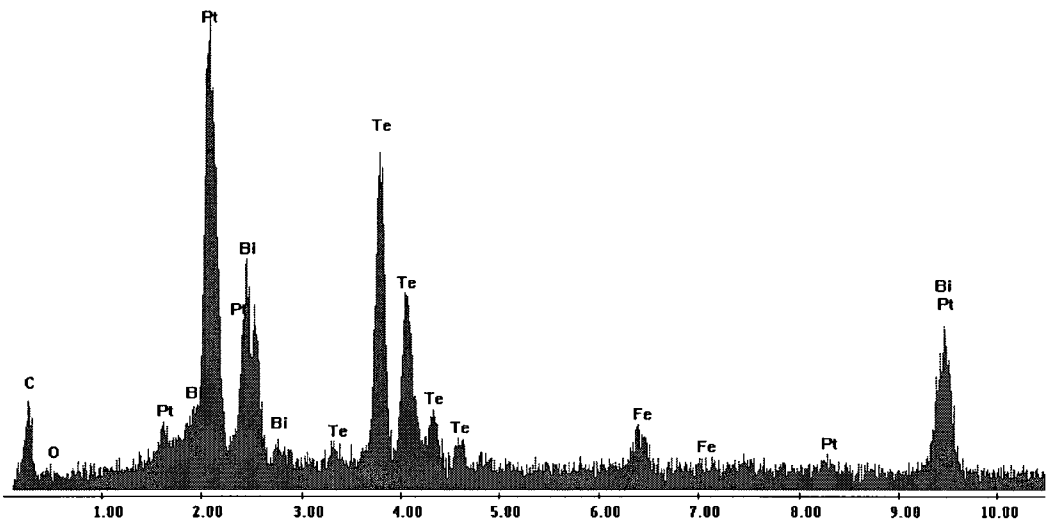

Figure 5-2 Backscattered Electron Image and X-ray Spectra for Particle A

Particles B, C and D in Figure 5-1 were also analyzed using EDX (Figure 5-3). The spectra show that these particles mainly contain Fe, Ni and S elements, the main constituents of pentlandite, which is the dominant nickel mineral in the Raglan ore. The image of particles B, C, and D is darker than that of particles A is due to their lower atomic number.

Some particles consisting of Fe and S were also found in these size classes (presumably pyrrhotite).

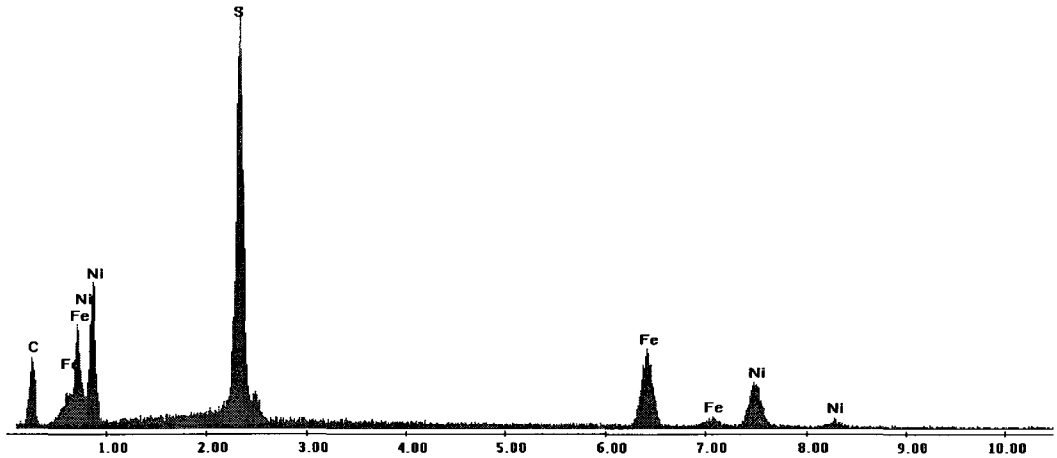

Figure 5-3 The X-ray Spectrum of Particle B, C and D

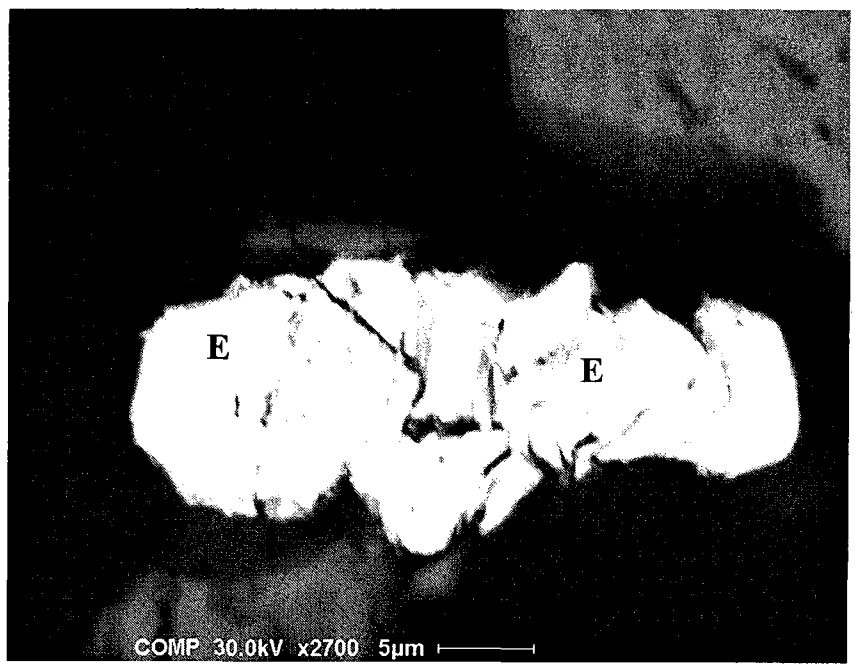

Figure 5-4 Backscattered Electron Image of Particle E (minus 25 µm)

Another PGM particle, E, of the same size class as particle A was found with a 30 kV accelerating voltage and 2700x magnification, shown in Figure 5-4. Particle E

contains Pt, Bi, Te and Fe (C appears here also because of carbon coating, O because of a hole in the section). The particle E contains mostly Pt, Bi and Te, the same components found in the mineral Moncheite ($Pt_{1.01}(Te_{1.96}\ Bi_{0.03})$). Analyzing different spots of particle B confirms its homogeneity.

Based on analysis of the 37-53 μm size class (stage 2 concentrate) polished section, five liberated particles containing Au and/or Pd were found. No particles containing Pt were found in this size class. Most of the darker particles were either pyrrhotite or pyrite. It was difficult to find any liberated PGM particles above 106 μm due to the fine-grained nature of Raglan ore.

The microscopy results show the low Pt and Pd content and the fine size distribution. Combined with the small density difference between Pt and Pd carriers and gangue, indicates that the ore will likely be unresponsive to gravity recovery. The mineralogical information helps explain the low GRPt and GRPd content measured by the GRPGM methodology in Chapter 3.

Flash flotation could be an interesting alternative to gravity separation based on the fine size distribution of Pt and Pd, but again it would have to be justified on the basis of other factors, presumably the benefit to copper and nickel recovery. As these latter minerals are believed to carry most of the Pt and Pd, whatever effect flash flotation has on copper and nickel minerals would also benefit Pt and Pd recovery.

In conclusion, the low content and finely distributed gravity recoverable platinum and palladium minerals make the Raglan ore a poor candidate for gravity recovery.

5.4.2 Analysis of GRPGMs from the Clarabelle Ore with SEM and VP-SEM

Twenty particles in the +600 μm fraction Knelson concentrate of a Clarabelle ore sample were attached directly to carbon tape and examined with the JOEL 840A conventional SEM without polishing. No PGMs (sperrylite) particles were found, most particles being pyrite (FeS_2), pyrrhotite ($Fe_{1-x}S$), Pentlandite $(Fe, Ni)_9S_2$.

Sixteen particles from concentrates of the 425-600 μm size fraction were also checked: one sperrylite particle was found. Figure 5-5 and 5-6 show the BSE image and X-ray spectrum, respectively, as can be seen, the sperrylite particle is brighter than other nearby particles because of its higher average atomic number. This sperrylite particle seems nearly fully liberated with minor other associated minerals (B). Another phenomenon has been observed: when using the tweezers to place the particles onto the carbon tape, there are several small brighter particles around the sperrylite particle, which was also found to be sperrylite. It confirms that that the sperrylite is brittle (Cabri, 1981a).

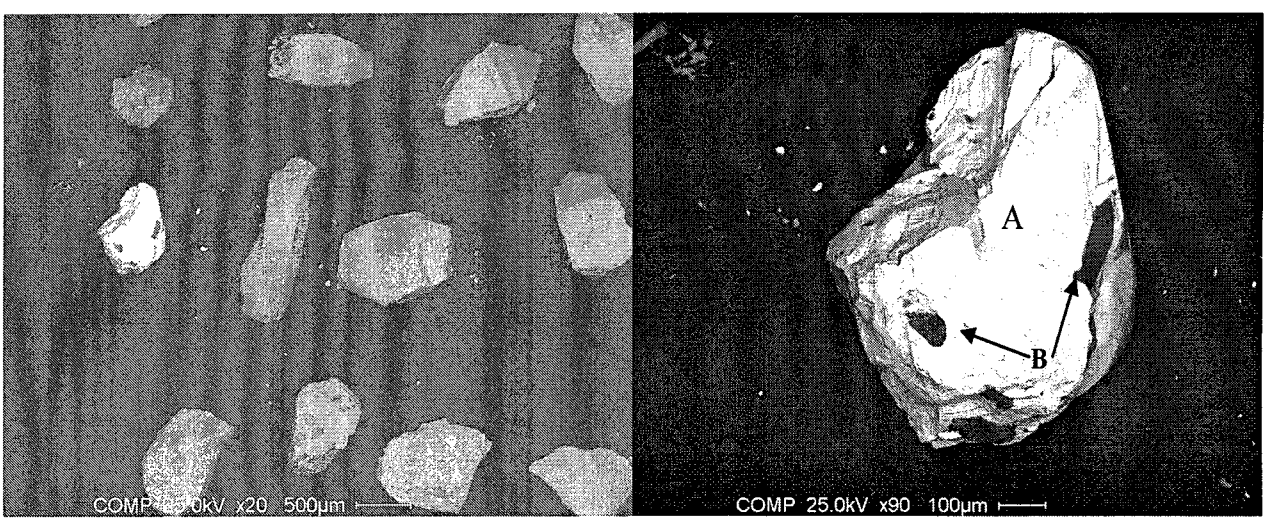

Figure 5-5 BSE Image of Sperrylite Particle in 425 –600 μm Size Fraction

The right side image of Figure 5-5 shows the sperrylite particle under higher magnification. It seems to be associated with other minerals, identified as B.

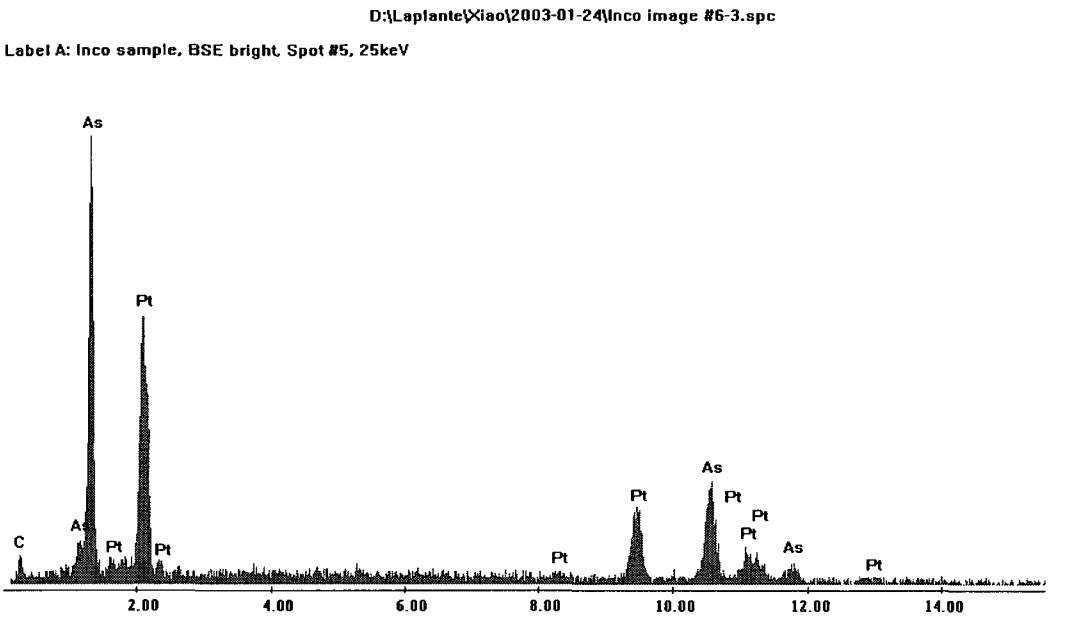

Figure 5-6 X-ray Analysis Spectrum of Spot A and B on Sperrylite Particle

Several spots on this particle were examined with EDX analysis. This confirms that spot A consists of elements As and Pt, as expected with sperrylite. Spot B consists of Oxygen (O), silicon (Si) and iron (Fe) elements.

In the 150-212 μm size fraction examined with a conventional SEM, two sperrylite particles were found, as shown in Figure 5-7.

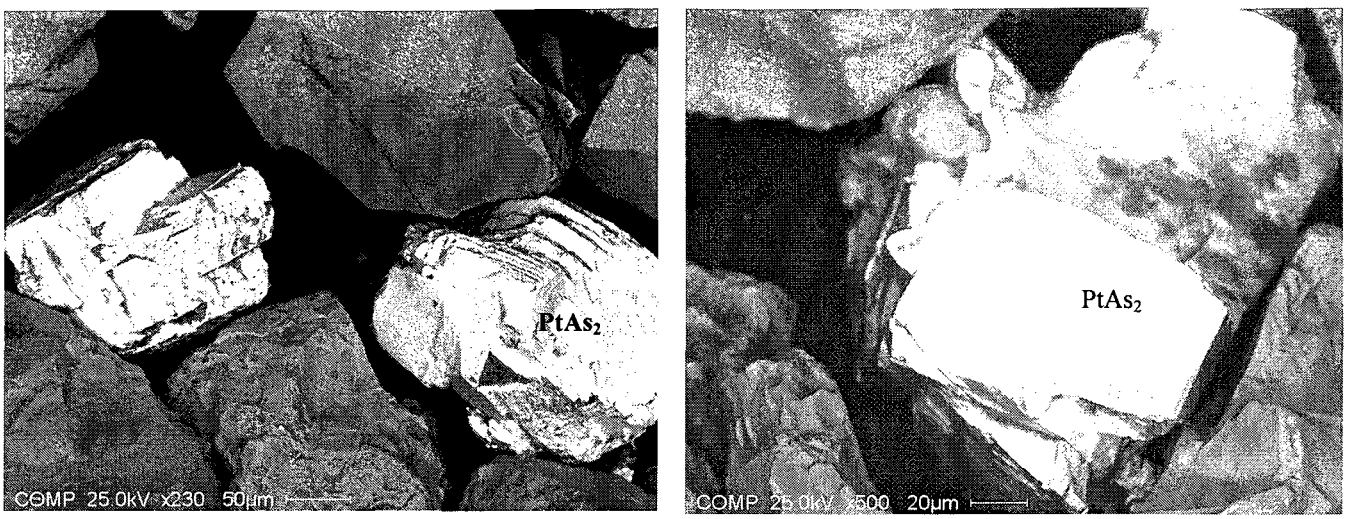

Figure 5-7 BSE images of Two Sperrylite Particles in the Concentrate of the 150 –212 µm Size Fraction

The sperrylite particle in the left image seems well liberated. The layer structure is obvious. The sperrylite particle in the right image seems to be also well liberated while the upper part contains some iron (shadow). All of the above BSE images were obtained at 25 kV and "COMP" mode of SEM. The liberated sperrylite particles found in the coarse size range support why high GRPt content in the Clarabelle ore sample was obtained.

The concentrate and tailings from magnetic separation of the 38-53 µm size fraction Knelson concentrate of the Clarabelle ore sample were examined with VP-SEM at 20 kV and "COMP" mode in high vacuum environment (almost the same as that of conventional SEM). Several sperrylite particles were found in the non-magnetic fraction; Figure 5-8 shows two sperrylite particles found. The structure and tin white color are obvious. Both particles appear to be well liberated.

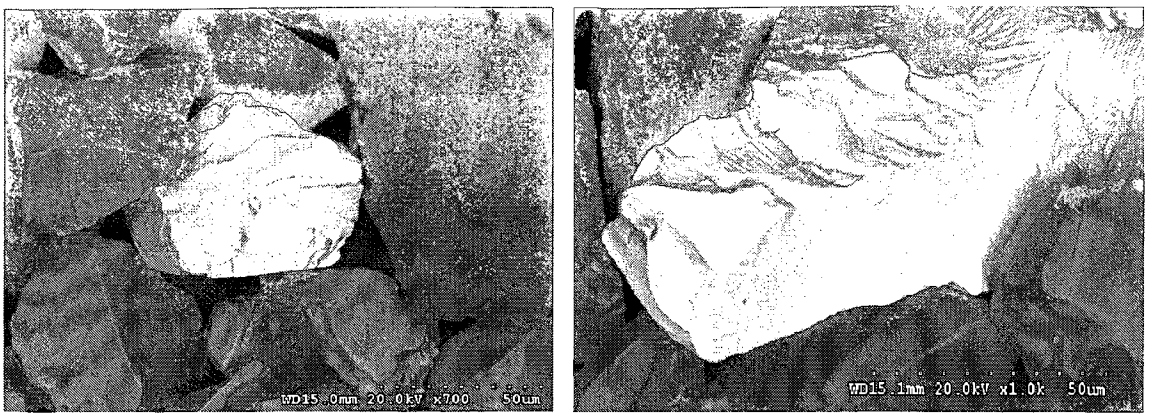

Figure 5-8 Two BSE Images (VP-SEM) of Sperrylite Particles in 38-53 μm Size Fraction Obtained from Non-magnetic of Knelson Concentrate of Clarabelle Ore

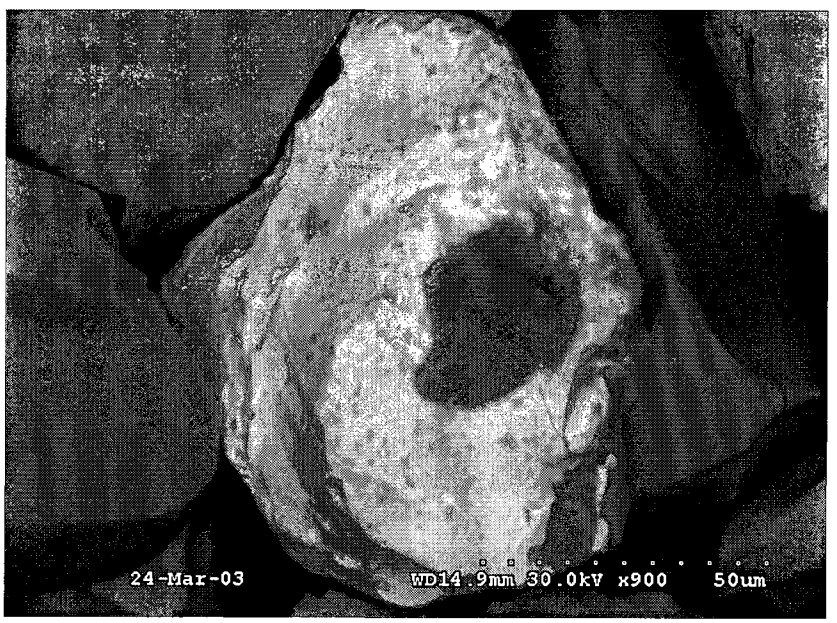

Figure 5-9 A Well Liberated Unidentified PdBiTe Particle in Same Fraction as in Figure 5-8

In the same fraction, an unidentified PbBiTe particle is shown in Figure 5-9, with a small attached gangue particle. Its spectrum is shown in Figure 5-10.

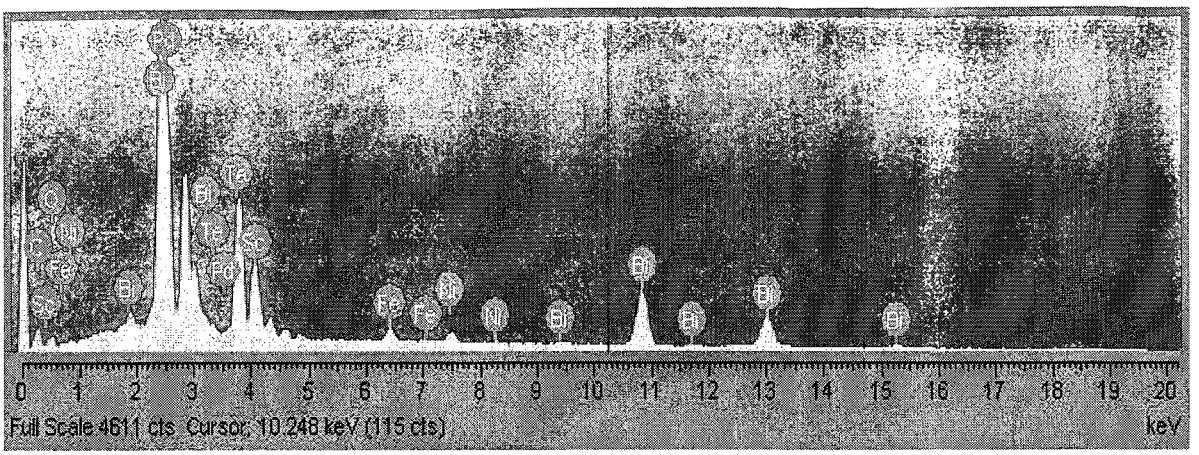

Figure 5-10 Spectrum of the Particle of PdBiTe.

Many liberated sperrylite particles were found in different size classes. Figure 5-11 shows two well-liberated sperrylite particles in the size class of 75-106 μm with the layered and tin white surface.

Figure 5-11 Two Well-liberated Sperrylite Particles in the Size Class 75–106 μm

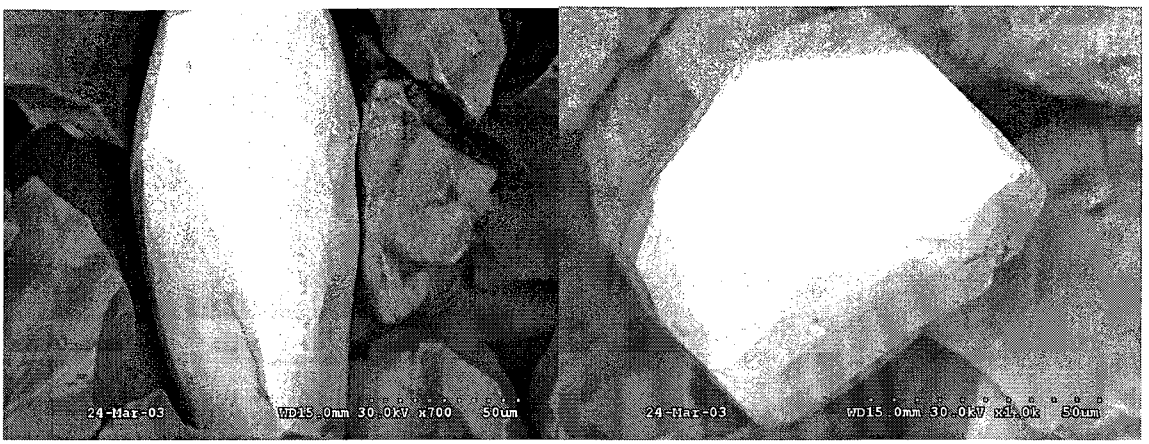

Figure 5-12 Two Well-liberated Sperrylite With Similar Surface Structure in the Size Class 53–75 μm

Figure 5-12 shows two sperrylite particles in the size class 53–75 μm presenting the tin white and smooth surface. It is well liberated and occurs as a single phase.

Sulfide and GRPGM Mineralogy:

The Clarabelle ore typically contains 1.1% Cu mainly as Chalcopyrite $CuFeS_2$ and 1.2% Ni mainly as pentlandite $(Fe, Ni)_9S_8$ (Kerr, et al., 2003). Pentlandite is the most important Ni-bearing minerals in the Clarabelle ore sample. It was found in the gravity concentrates along with chalcopyrite and pyrrhotite ($Fe_{1-x}S$). The latter being the most abundant sulfide mineral in the Clarabelle ore (up to 25%). Many pyrrhotite particles were found in the gravity concentrates by the VP-SEM. A small amount of nickel substitutes for iron in the pyrrhotite lattice. The nickel in solid solution in pyrrhotite typically represents 10% or more of the nickel in the ore (Kerr, et al., 2003). The two major polymorphs of pyrrhotite are hexagonal and monoclinic pyrrhotite, both of which are found in the sample. The dominant form of pyrrhotite in the sample is monoclinic pyrrhotite which is strongly magnetic.

The major platinum group minerals found in the GRPGM concentrates are sperrylite (PtAs2) and to a lesser extent Maslovite (Pt, Pd)(BiTe)2 and michenerite (Pd, Pt)(BiTe)2. The sperrylite is very brittle. There are a lot of small sperrylite particles broken from the sperrylite particle when using twisters to put the particle on the tap as can be seen from the Figure 5-5. Sperrylite starts to liberate at very coarse size, 425-600 μm, this is one of reasons that the content of GRPt is high in the Clarabelle ore. Well-liberated sperrylite particles were also found across the size range from 600 μm to 20 μm.

Several electrum (Au,Ag) particles were found in the size class 53-75 μm. One native Tungsten (W) and Tin (Sn) particles were found in this size class also.

5.4.3 Analysis of GRPGMs from the Strathcona Ore with QEM*SEM

Four size fractions of concentrate of stage 2 from the GRPGM test on Strathcona ore sample including +150μm, +106μm, +75μm and +25μm were measured with QEM*SEM at the Xstrata Process Support (XPS) (Kormos and Whittaker, 2005). All PGM, precious metal (PM), Te and Bi or Sn species are either liberated or occur as multiphase particles with other PGM/PM species. None were locked with either silicateor oxide minerals. The following PGM, PM, Te, Bi and Sn species in Table 5-1 have been identified within these concentrates. (No PGM, PM, Te, Bi, or Sn minerals were identified within the +150 size fraction.)

Four concentrates sample of stage 2 were prepared at McGill and forwarded to XPS for qualitative mineralogical evaluation. The coarsest size fraction for the mineralogical investigation (+150 μm) was upgraded with an additional processing stage in a Hydrosizer. The remaining three finer size fractions were not subjected to this final separation process.

Table 5-1 PGMs and other minerals detected by QEM*SEM from the Strathcona Ore

Mineral	Formula	Size Fraction	Occurs as Liberated Particles	Occurs as Multiphase Particles
Michenerite	$(Pd,Pt)(Bi,Te)_2$	+106, +75	✓	✓
Maslovite	$(Pt,Pd)(Bi,Te)_2$	+106, +75		✓
Froodite	$PdBi_2$	+106, +75, +25	✓	✓
Insizwaite	$PtBi_2$	+106, +75, +25		✓
Niggliite	PtSn	+75, +25		✓
PtPdSnBiTe	unidentified	+75, +25		✓
Hessite	Ag_2Te	+106, +75, +25	✓	✓
Electrum	(Ag,Au)	+75	✓	
Acanthite	Ag_2S	+75		✓
Tellurobismuthite	Bi_2Te_3	+75	✓	✓
Native Bi	Bi	+75, +25		✓
Native Sn	Sn	+75, +25	✓	
Parkerite	$Ni_3Bi_2S_2$	+106, +75	✓	✓
Altaite	PbTe	+75	✓	✓

Sample mass was limited for this study, and most of it was reserved for chemical assay. Normally, mineralogical evaluation at PGM grades averaging 300ppm would require many polished sections per size fraction. Because of the lack of sample, the PGM information presented is qualitative only.

Samples were mounted and polished using the QEM*SEM standard sample preparation procedure. Sections were measured using a Species Indentification Program (SIP) designed for Sudbury ores. Additional PGM species were added to the SIP for this project. The Cameca SX100 Electron Microprobe was used to confirm the identification of a Native Sn particle.

5.4.3.1 Modal Mineralogy

Figure 5-13 shows a small amount of PGMs in the size classes of +106 μm, +75 μm, and +25 μm. This is because of the low platinum and palladium grade in stage 2 concentrate (20 g/t and 17 g/t, respectively). The other minerals include pentlandite, chalcopyrite/cubanite, pyrrhotite, pyrite, silicates, and oxides. Results show a significant difference between the +150 μm size fraction and the three finer fractions. Magnetite (oxide category), with an SG of 5.3, dominates the +150 size fraction, whereas silicates (average SG 2.8) dominate the finer fractions. The overall SG in the +150 μm fraction is higher than in the finer fractions because of this magnetite/silicate distribution. This difference is likely due to the additional processing step taken on the +150 μm fraction.

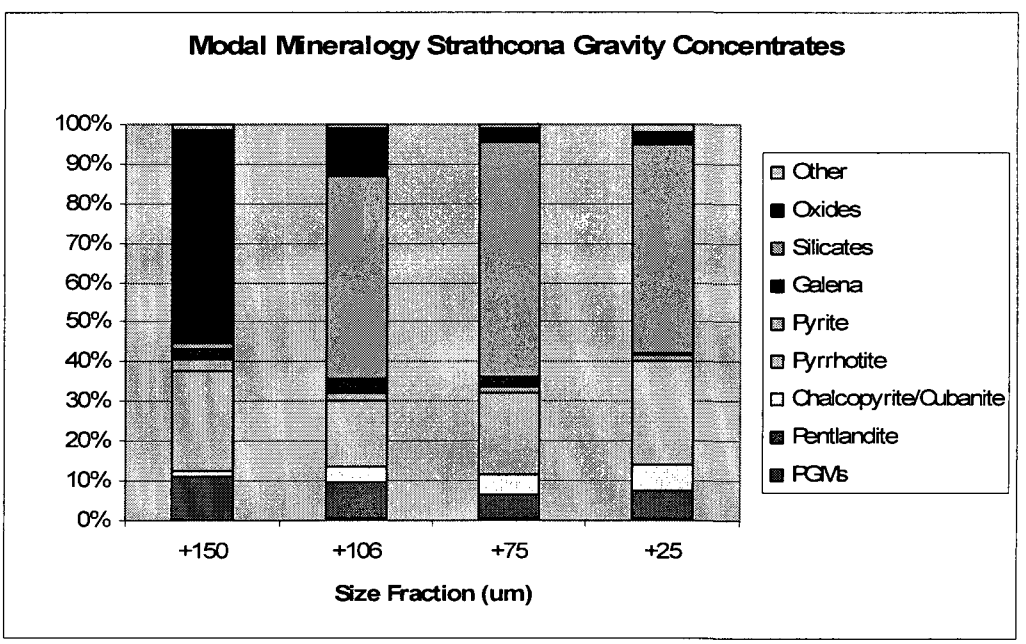

Figure 5-13 Summary of the Modal Mineralogy of the Four Size Fractions.

Trends in the distribution of sulphides were noted. Chalcopyrite (SG 4.2) grades increase in the fine fractions, whilst pentlandite (SG 4.8) grades decrease. Magnetite (SG 5.3) also decreases at the finer size fractions.

Galena, (SG 7.6), occurs in trace amounts within Sudbury ores but has been concentrated in the three coarsest fractions to grades that vary between 2.3% and 3.6%. Pyrrhotite, does not show any pattern in terms of distribution. The two samples containing the highest grades of pyrrhotite are +150μm and +25μm (Kormos and Whittaker, 2005).

5.4.3.2 PGM, PM, Bi and Te Mineralogy

A total of 33 particles in the three size fractions, +106μm, +75μm and +25μm have been identified as PGM, PM or Bi/Te/Sn bearing. No PGM minerals were identified in the coarse +150 size fraction. Assay information suggests that PGMs are present in the +150μm fraction, but insufficient to locate and identify the PGM particles.

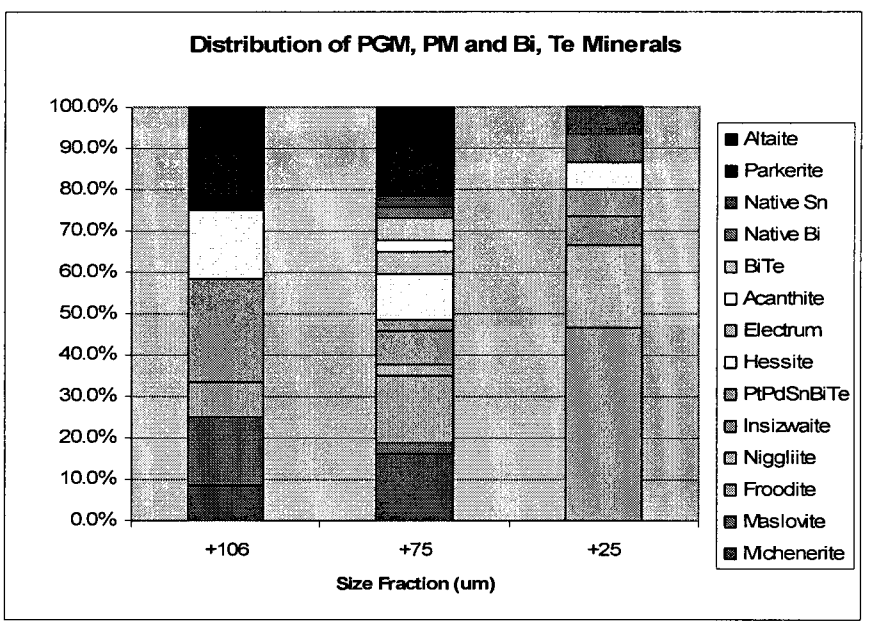

Figure 5-14 Distribution of PGM, PM and Bi, Te Minerals

Figure 5-14 summarises the PGMs, PMs, and Bi-, Te- and Sn-bearing minerals identified in the samples.

Figure 5-14 does not take liberation or locking into account. Therefore in the case where more than one species occurs in a particle, each mineral is counted in the above representation. Comments on liberation and mineral association are made in the following paragraph.

A wide variety of mineral species have been identified. The PGM suite is dominated by bismuthides and tellurides. These include Michenerite, Maslovite, Insizwaite, and Froodite. A number of species, including Niggliite and an unidentified PtPdSnBiTe, contain tin. Silver occurs as Electrum, Hessite and Acanthite. Gold occurs in Electrum which is present in two varieties – one with an almost even split of silver and gold, the other dominated by gold. Finally Native Bi and Sn have also been identified. Native Sn has not been found to date in other Sudbury samples analyzed at FTC; however, native Sn was found in the Clarabelle ore (CVRD Inco) sample.

5.4.3.3 Locking and Mineral Associations of PGM's, PM's, and Bi, Te, Sn minerals

All photomicrographs (backscatter electron images) are presented at the end of this section. In the +106μm size fraction, all PGM/PM particles identified were locked with either other PGM/PMs or with PGM and sulphides.

The +75μm size fraction contained the highest concentration of PGM/PMs. More liberation is noted in this size fraction. Of the 6 Michenerite grains identified, 3 are liberated particles. Of the 6 Froodite grains identified, 4 are liberated particles. Both electrum particles identified are liberated. One out of two Tellurobismuthite particles, a Native Sn particle and 4 out of 5 Parkerite particles are also liberated. Where locking occurs, other PGM/PM associations are common. Particles containing Hessite-Maslovite-Insizwaite-Acanthite-Altaite, Hessite-Froodite-Iinsizwaite-Acanthite-Chalcopyrite, Froodite-Michenerite-Hessite-, and Michenerite-Insizwaite-Tellurobismuthite are examples of the complex multiphase particles identified.

Froodite is the most common PGM identified in the +25μm size fraction, and five out of seven are liberated. Niggliite, Hessite and Native Sn are also present as liberated grains in this size fraction. Some complex multiphase particles were also identified including Froodite-Insizwaite-Niggliite and Froodite-Niggliite-Chalcopyrite.

The following Figures show the backscatter electron images of PGMs of the size fraction 106-150 μm.

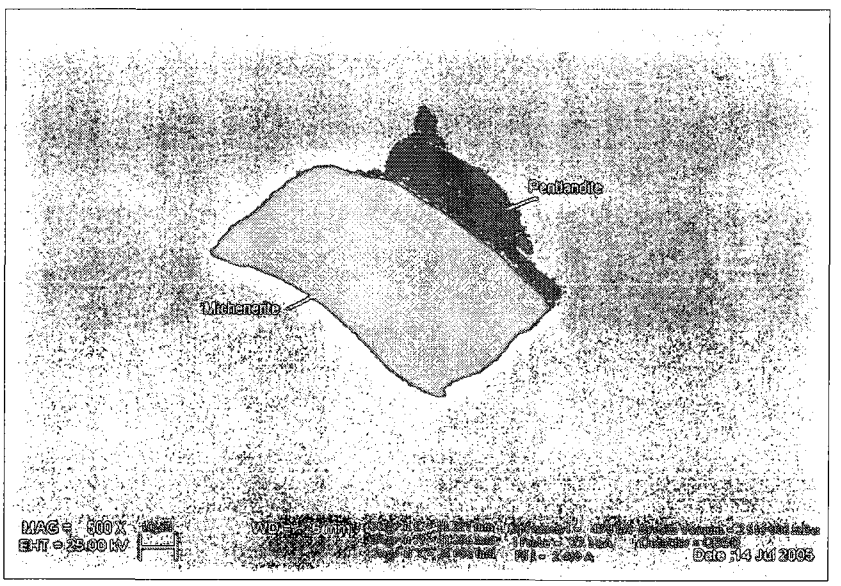

Figure 5-15 Michenerite ((Pd,Pt)(Bi,Te)$_2$) -Pentlandite Grain

Figure 5-15 shows a particle of Michenerite ((Pd,Pt)(Bi,Te)$_2$) associated with the gangue mineral of pentlandite. The particle has two phases and at least 80% liberation in term of the surface area.

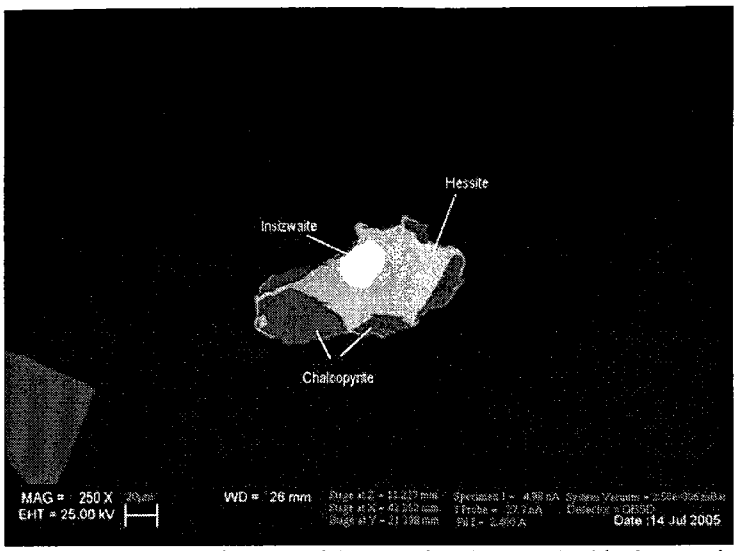

Figure 5-16 Insizwaite ($PtBi_2$)-Hessite (Ag_2Te)-Chalcopyrite Grain

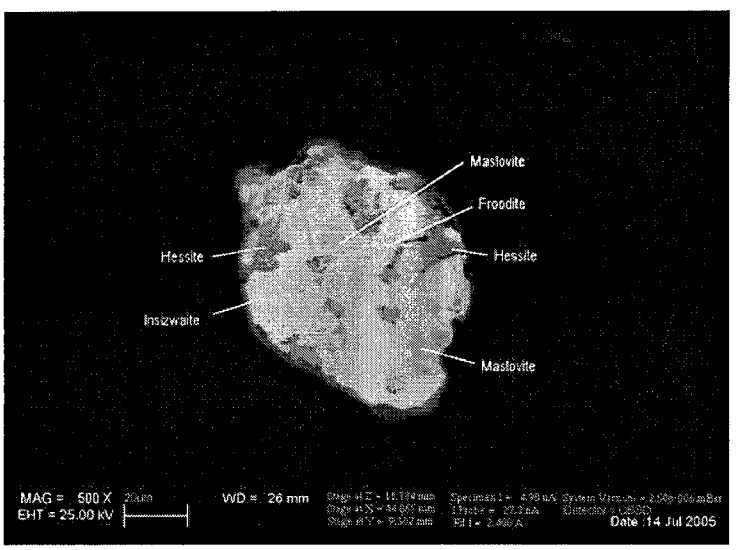

Figure 5-17 Multiphase PGM including grains of Froodite ($PdBi_2$), Maslovite ($(Pt,Pd)(Bi,Te)_2$), and Insizwaite ($PtBi_2$). Hessite (Ag_2Te), in the dark shade of grey is commonly associated with PGM minerals.

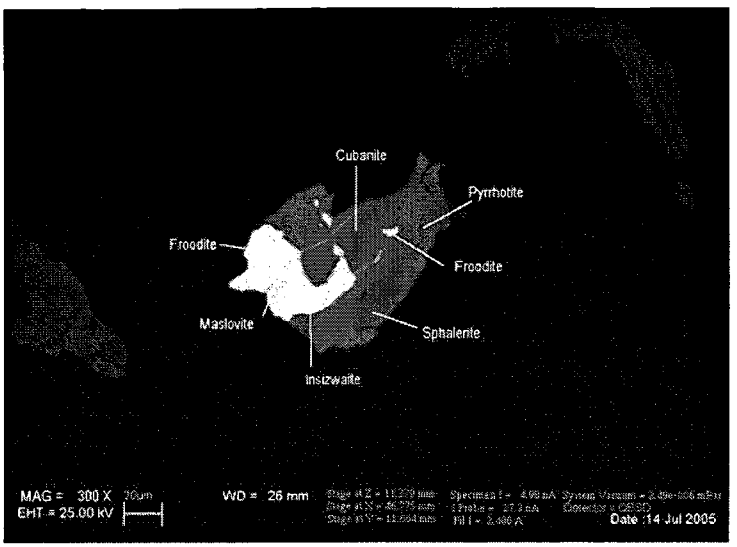

Figure 5-18 Multiphase PGM locked with sulphides. PGMs include Froodite ($PdBi_2$), Maslovite($(Pt,Pd)(Bi,Te)_2$), and Insizwaite ($PtBi_2$)

The following pictures show the backscatter electron images of the size fraction 75-106μm.

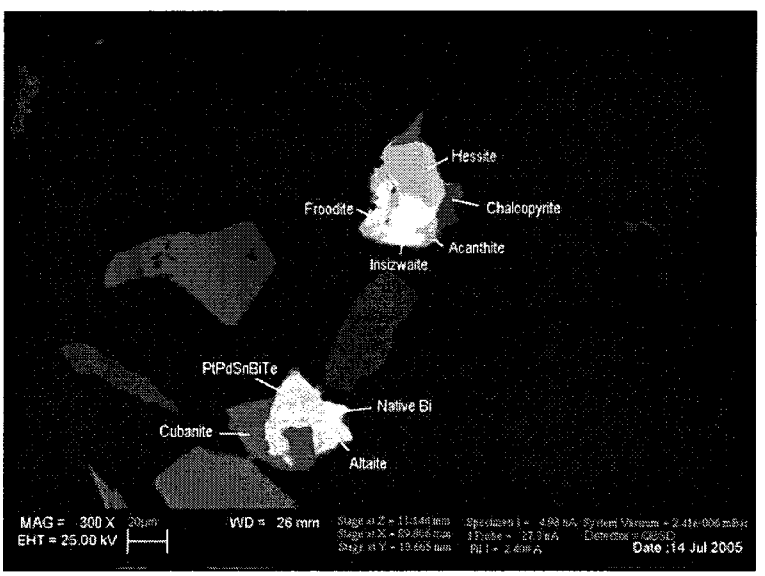

Figure 5-19 Two Multiphase PGM Particles.

Figure 5-19 shows that the top particle contains Froodite ($(PdBi_2)$, Insizwaite ($PtBi_2$), locked with Hessite (Ag_2Te), Acanthite (Ag_2S) and Chalcopyrite. The lower particle contains an unidentified PGM with Pt, Pd, Sn, Bi and Te as well as Native Bi, Atlaite (PbTe) and Cubanite. Both particles are approx. 75μm in length.

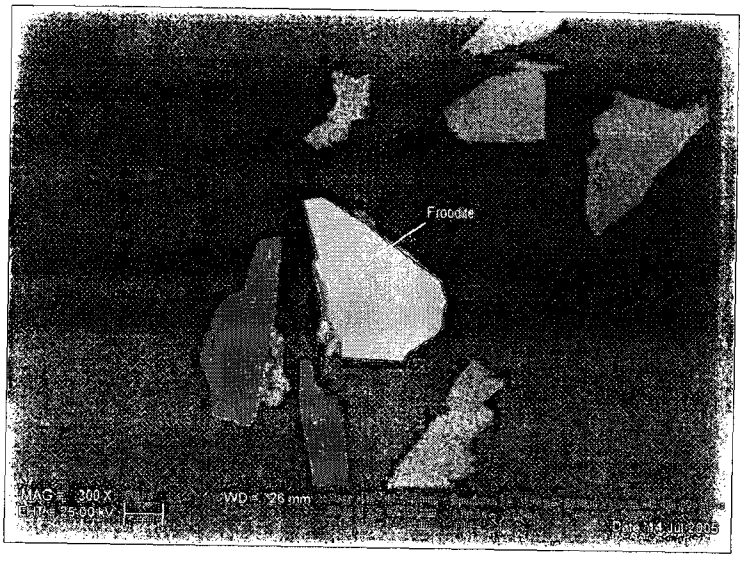

Figure 5-20 Liberated Grain of Froodite (PdBi2)

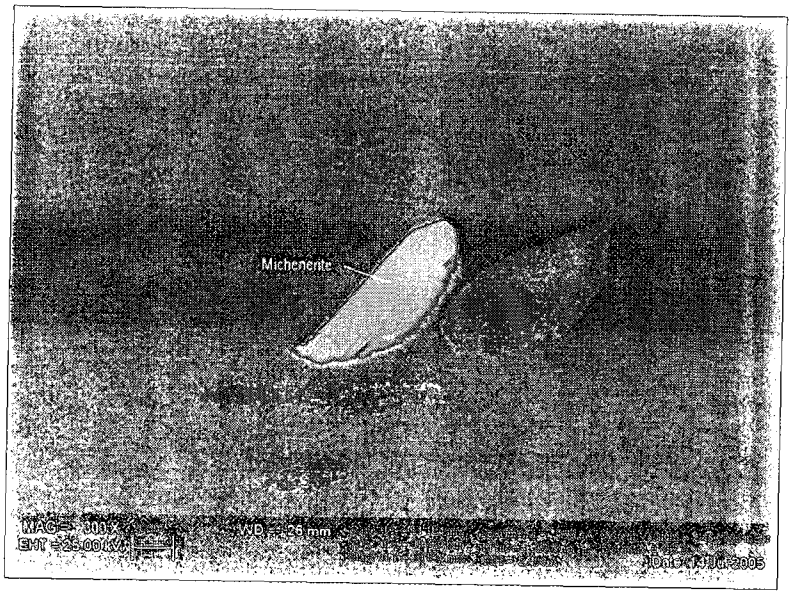

Figure 5-21 Liberated Michenerite ($(Pd,Pt)(Bi,Te)_2$) Grain

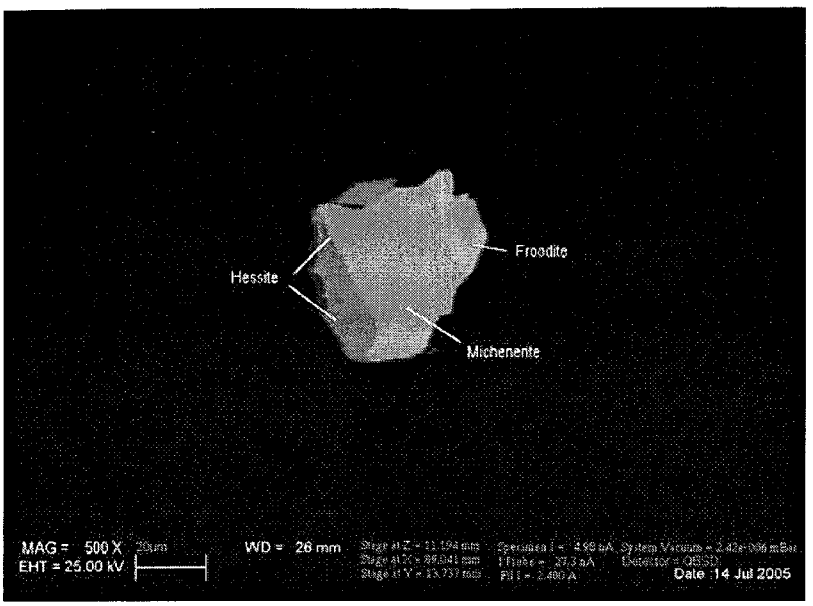

Figure 5-22 Multiphase Particle Containing Froodite ($PdBi_2$), Michenerite ($(Pd,Pt)(Bi,Te)_2$) and Hessite (Ag_2Te).

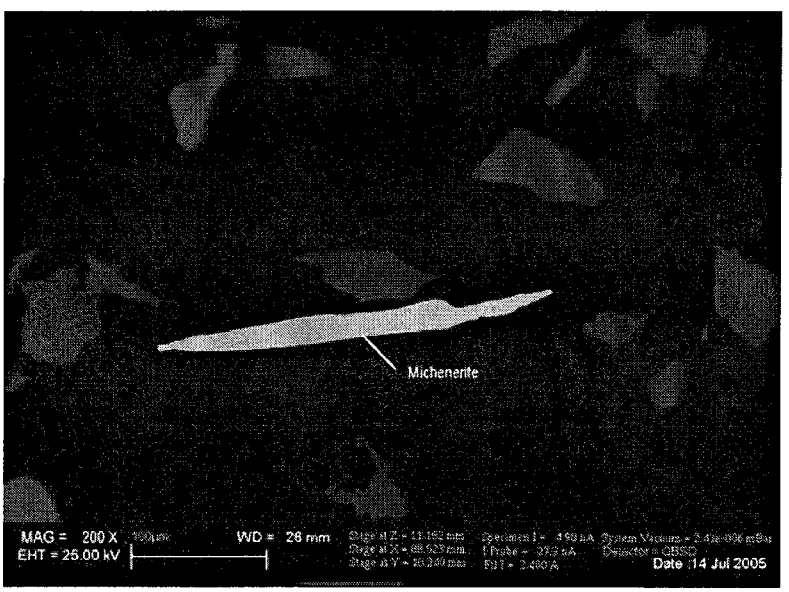

Figure 5-23 Liberated Michenerite ($(Pd,Pt)(Bi,Te)_2$) Grain

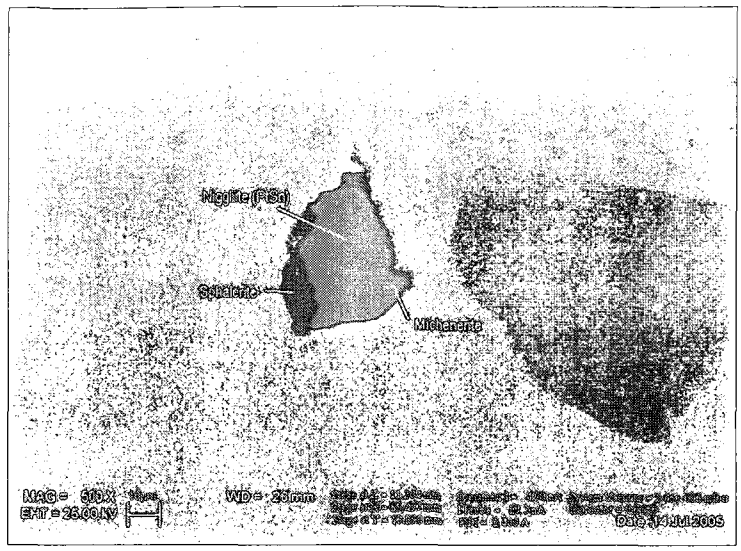

Figure 5-24 Three Phase Particle Containing Michenerite ($(Pd,Pt)(Bi,Te)_2$), Niggliite (PtSn) and Sphalerite.

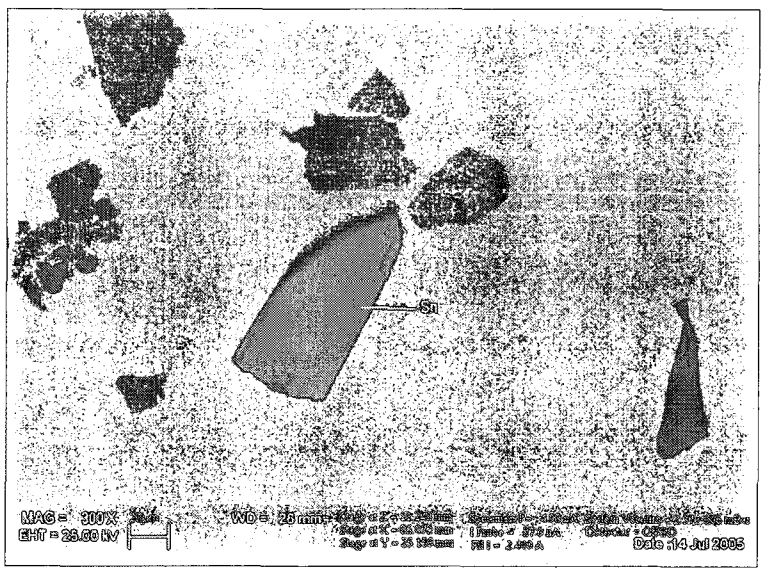

Figure 5-25 Native Sn with Small Grain of Chalcopyrite (Darker Grey) at Lower Edge of Particle

The following pictures show the backscatter electron images of the size fraction 25-38μm.

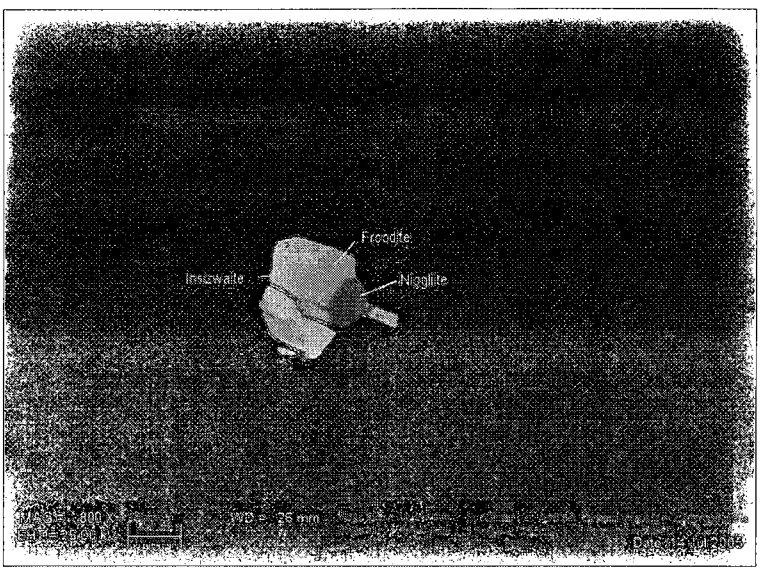

Figure 5-26 Multiphase PGM Containing Froodite (PdBi2), Niggliite (PtSn) and Insizwaite (PtBi2)

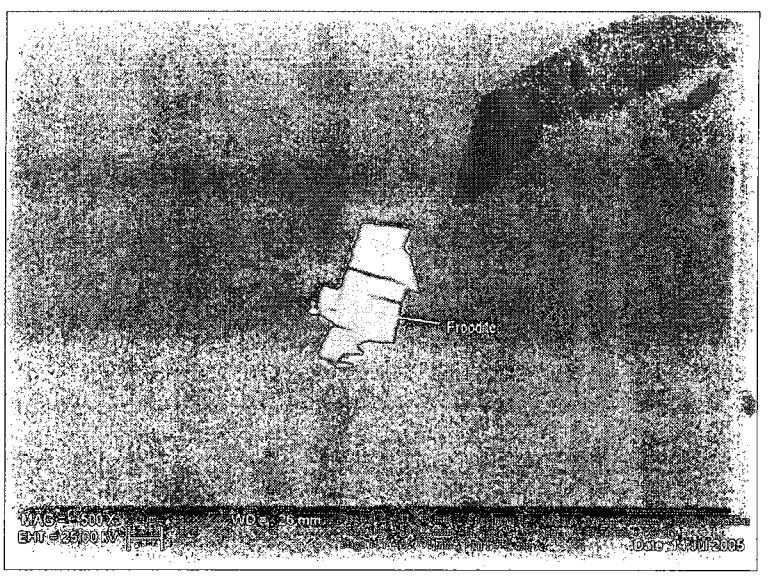

Figure 5-27 Liberated Grain of Froodite ($PdBi_2$), Approximately 40 μm in Length.

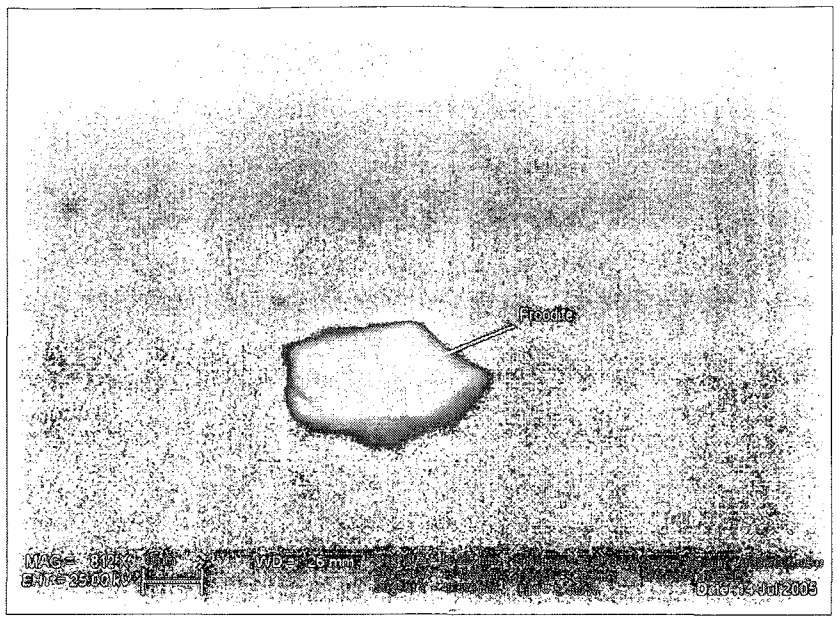

Figure 5-28 Liberated Grain of Froodite (PdBi2)

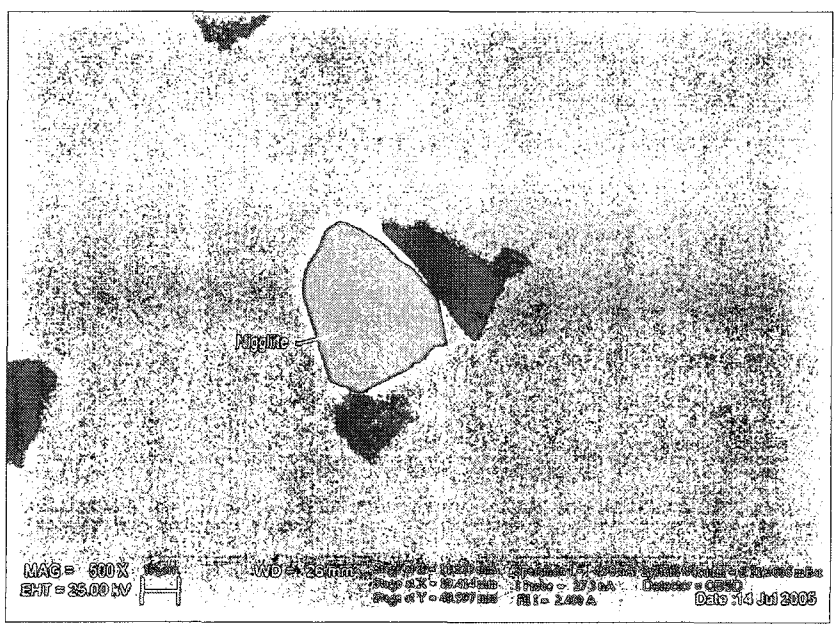

Figure 5-29 Liberated Niggliite (PtSn) Particle

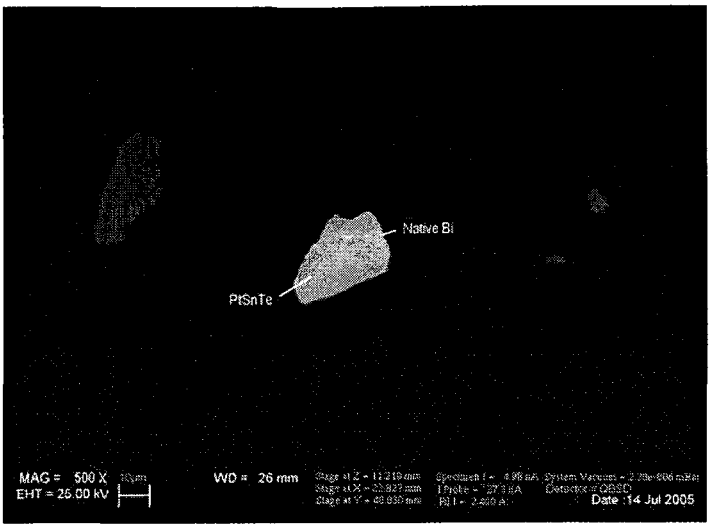

Figure 5-30 Two Phase Particle with Unidentified PtSnTe Mineral, with Small Inclusions of Native Bi

5.4 Conclusions

No liberated GRPGM particles were found above 106 μm for Raglan ore sample. However, those GRPGM particles found in the size class below 53 μm were well liberated. Mineralogical examination indicated that one of the reasons for the low GRPt is due to the fine size distribution of PGMs.

The major platinum group minerals in the GRPGM of Clarabelle ore are sperrylite and to a less extent maslovite, michenerite. Sperrylite particles start to liberate at 425 μm and are well liberated below this size. This is the reason the GRPt content is high for the Clarabelle ore.

The major platinum group minerals in the GRPGM of Strathcona ore sample include froodite, michenerite, maslovite, Insizwaite and Niggliite. Most of these GRPGM particles were locked above 106 μm with other PGMs and/or sulphide. Most of them are well liberated below 53 μm.

CHAPTER SIX

CONCLUSIONS AND CONTRIBUTIONS

6.1 Gravity Recoverable Platinum Group Mineral Methodology (GRPGM) for Ores and Stream Samples

The investigations and tests concluded that the GRG protocol for prediction and modeling of GRG in the grinding circuit could be applied to discrete platinum group minerals, or gravity recoverable platinum group minerals. The methodology is effective to quantify the gravity recoverable platinum group mineral content of a sample. The quantity of the gravity recoverable platinum group minerals can be quantified, which can be used to justify whether gravity separation is an option for recovering the PGMs. The methodology was applied to four ore samples.

- The amount of gravity recoverable platinum (GRPt) and palladium (GRPd) in a sample of Raglan ore is low, 5.1% and 2.7%, respectively, using the three recovery stage protocol.

- The ore sample from the Clarabelle mill contains 82% gravity recoverable platinum (GRPt), and is a promising candidate for a gravity recovery method in the grinding circuit.

- The amount of gravity recoverable platinum (GRPt) and palladium (GRPd) of the Ni Rim South ore sample (Falconbridge) are the same, 42%. Over 92% of the gravity recoverable platinum group minerals are finer than 106 μm.

- The ore sample from Strathcona mill contains 53% GRPt and 44% GRPd. The GRPd content is the highest among the tested ore samples. The potential for recovering precious metals from the Strathcona ore is attractive (53% GRPt, 44% GRPd and the extra 70% GRG).

The fourth stage with the variable speed Knelson Concentrator was able to recover the fine distributed PGMs. However, the contribution to the GRPGM content is moderate.

The two-stage GRPGM protocol for stream samples can be used to characterize the already liberated gravity recoverable platinum group minerals. The second stage for streams is shown to be warranted: Significant recovery of platinum minerals can be achieved in the second stage (more significant than for gold). This also holds true but to a lesser extent for other PGEs. This stems from the relatively coarse size distribution used for stage 1, generally intermediate between the size distribution of stage 1 and 2 for the ore GRPGM methodology.

6.2 Behavior of Gravity Recoverable Platinum Group Minerals

The classification efficiency curves of platinum and palladium are shifted to finer size than that of the total solids for the Clarabelle case. This results from the high density and results in platinum and palladium preferentially reporting to the cyclone underflow which means a build up in the circulating load in the grinding circuit. This is

evident by the higher Pt and Pd grades in ball mill discharge and cyclone underflow compared to the other streams.

The classification efficiency curve of platinum is similar to that of gold. Above 53 μm, the classification efficiency curves of platinum overlap, whereas more fine platinum (below 53 μm) reports to the cyclone underflow than gold. It is that the lamellar shape of gold particles counters the high density effect, resulting in a cyclone behavior for gold that is similar to that of platinum minerals of lower density.

Sperrylite is the dominant PGM in the Clarabelle ore. It is brittle and easily broken. The selection function of platinum is a little higher than that of the total solids above 212 μm, presumably because the sperrylite is liberated at coarser size fractions. Below 212 μm, the selection function of platinum is lower than that of the total solids.

A case is made for using the cumulative selection function. The cumulative selection function of all size classes for gold is lower than the total solids in each corresponding size class for the Clarabelle case. The cumulative selection function of platinum and palladium is 1.3 times higher than the total solids for size classes above 212 μm and 50 to 70% of the total solids below 212 μm.

Sperrylite (the dominant platinum mineral for Clarabelle ore) classification efficiency curve is similar to that of gold, despite its lower density. Its grinding kinetics is significant higher than for gold. As a result, sperrylite accumulates in finer sizes than native gold, but can be recovered by gravity due to its high gravity recoverable content.

6.3 Gravity Recoverable Platinum Group Mineral Mineralogy

The SEM, VP-SEM and QEM*SEM instruments were used to analyze the gravity recoverable PGMs qualitatively. The purpose is to better understand the PGEs distribution between discrete PGMs (gravity recoverable) for the three ore samples from the Sudbury area and the ore sample from Raglan. It is easier to obtain mineralogical information from the VP-SEM compared to the SEM. Mineralogical information, such as the degree of liberation, the associated minerals and the size distribution can be obtained using the QEM*SEM although the procedure is more involved and expensive.

The dominant GRPGM particles of the Raglan ore sample contain the elements Pt, Bi and Te, suggesting the mineral Moncheite ($Pt_{1.01}(Te_{1.96}\ Bi_{0.03})$). The GRPGM particles are finely distributed and well liberated. The low content and fine distribution make the Raglan ore a poor candidate for gravity recovery.

The major platinum group minerals found in the GRPGM Knelson concentrates from the Clarabelle ore sample are Sperrylite ($PtAs_2$) and to a lesser extent Maslovite $(Pt, Pd)(BiTe)_2$ and Michenerite $(Pd, Pt)(BiTe)_2$. The coarsest sperrylite particle was in the size class 425-600 μm and was well liberated. Sperrylite particles were also found in the fine size classes. Several electrum (Au, Ag) particles were found at the finer size class 53-75 μm. One native Tungsten and Tin particle were also found in the same size class.

All GRPGM, precious metal (PM), Te and Bi or Sn species are either liberated or occur as multiphase particles with other PGM/PM species for the ore sample from Strathcona mill. None were locked with silicate or oxide minerals. All GRPGM particles identified in the +106μm size fraction were locked with either other PGM or with PGM and sulfides. The +75μm size fraction contained the highest concentration

of GRPGMs. Higher degree of liberation is noted in this size fraction compared to the +106μm size fraction. Froodite is the most common PGM identified in the +25μm size fraction, and five out of seven Froodite containing particles were well liberated.

6.4 Contributions to Knowledge

The contributions of this research to platinum group mineral recovery are:

- The GRPGM methodology developed can quantify the content of gravity recoverable platinum group minerals of ores and streams. It can also be used to concentrate the platinum group minerals for mineralogical analysis.

- The fourth stage added to the GRPGM methodology for ore characterization and the second stage added for the stream GRPGM measurement protocol is different from the GRG protocol. Their contributions to the recoveries of are significant.

- The description of platinum group mineral behavior in cyclones using the classification efficiency curves and ball mills using the less common cumulative selection function establishes the foundation for modeling the gravity recovery of platinum group minerals in a grinding circuit.

CHAPTER SEVEN

FUTURE WORK

The modified GRPGM protocol for ore samples has yet to be fully evaluated. The contribution of the fourth stage is modest for the ore sample from the Clarabelle Mill. Further investigations could be carried out to verify the usefulness of this fourth stage. One investigation is to use higher speed to replace the standard speed Knelson Concentrator in the fourth stage. The reason is that the particle size is fine for the tailings of stage 3. Another investigation is to grind the tailings from stage 3 then process it by the standard or higher speed Knelson concentrator. The purpose is to ascertain if more PGMs can be liberated and recovered. With these investigations, the usefulness of the fourth stage could be assessed. It should be noted, however, this will yield GRPGM particles that will be difficult to recover by gravity in practice (easier by flash flotation?), not only because of their behavior in gravity recovery units, but also because they are less likely to report to (i.e., concentrate) in the cyclone underflow stream.

In order to use the "triangle" simulation engines as shown in Figure 1-1, the third corner, recovery unit performance, needs to be established. The database of the recovery unit performance of GRPGMs, either by gravity or flash flotation, is simply insufficient at this stage. One solution is to begin building a database for existing applications. A second solution is to use piloting at potential sites to generate data that can be used in the simulation.

The breakage function of the sperrylite is worthy of investigation. A certain amount of well-liberated sperrylite particles could be used in the lab to measure its breakage function. Knowledge of the breakage function is fundamental for interpreting the behavior of the PGMs in the grinding circuit.

The shape effect of PGM particles (compared to the shape of gold) on the classification behavior is critical to understanding the behavior of some minerals. An initial investigation of tungsten with different shapes (irregular vs. spherical) shows that their cycloning behavior is very different. Figure 7-1 shows the different shapes of the tungsten of the size class of minus 38 μm size class and Figure 7-2 shows the results of the Warman cyclosizer at the same operating conditions.

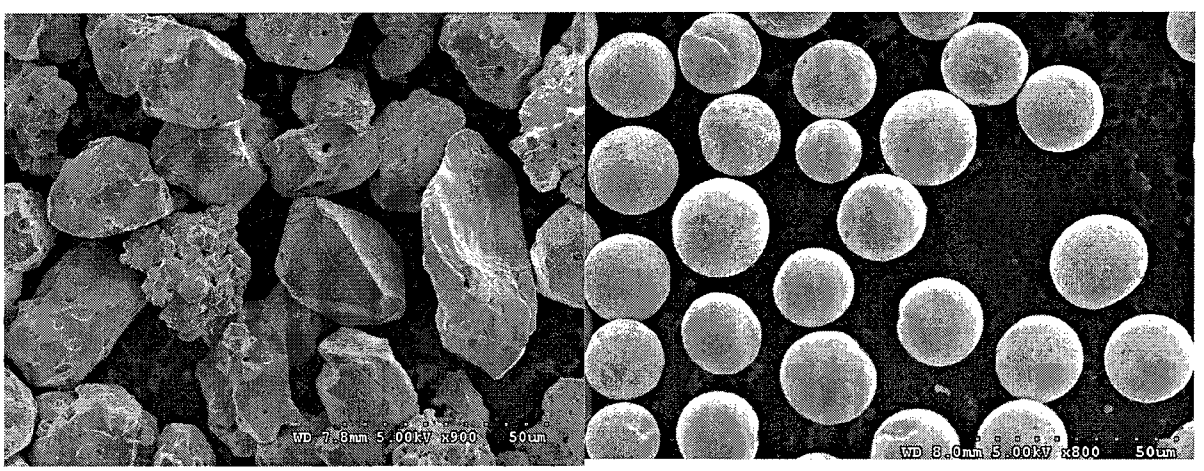

Figure 7-1 Irregular and Spherical Shape of Tungsten

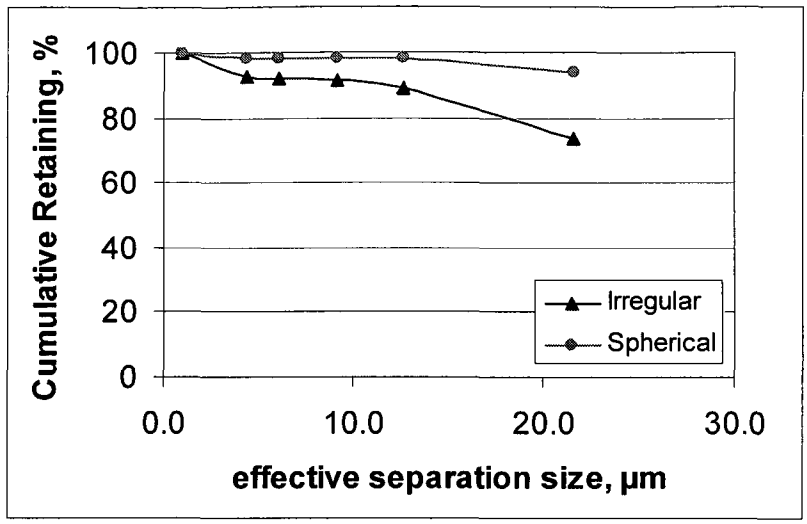

Figure 7-2 Cumulative Retaining of Different Shape Tungsten

Figure 7-2 shows that more spherical shape tungsten was retained while some of the irregular shape tungsten particles can easily reach the overflow of the final cyclone in the Warman cyclosizer. The Warman cyclosizer could be used as a start-point to investigate the shape effect on hydrocyclone performance.

Reference:

1. Banisi, S., 1991. An investigation of the gravity recovery of gold. Master of Engineering Thesis, McGill University, Montreal.

2. Banisi, S., Laplante, A. R., Marois, J., 1991. The behaviour of gold in Hemlo mines Ltd. grinding circuit, CIM Bulletin, Vol. 84(955), pp. 72-78.

3. Begizov, V. D., Borisenko, L. F., Uskov, Y. D., 1975. Sulphides and natural solid solutions of platinum metals from the Ultrabasites of the Gusevogorskiy Pluton, Urals. Doklady Akad. Nauk SSSR, 225: 1408-1411.

4. Blagodatin, Y. V., Distler, V. V., Zakharov, B. A., Sluzhenikin, S. F., 2000. Disseminated ores of the Noril'sk ore district as a potential for increasing output of platinum metals at the Noril'sk mining company, special issue.

5. Brynard, H. J., Villiers, J. P. R. de, Viljoen, E. A., 1976. A mineralogical investigation of the Merensky reef at the western platinum mine near Marikana. South Africa Econ. Geol., vol, 71, pp. 1299-1307.

6. Cabri, L. J., Laflamme, J. H. G., 1979, The mineralogy of the platinum group elements from some copper-nickel deposits in the Sudbury area, Ontario: Econ. Geol., v.71, pp. 1159-1195.

7. Cabri, L. J., 1981. Platinum group elements: mineralogy, geology and recovery, Canadian Institute of Metallurgy. Special Volume, vol. 23, pp. 262-268.

8. Cabri, L. J., 1981a. Classification of platinum-group element deposits with reference to the Canadian Cordillera. Precious Metals in the Northern Cordillera. A.E.G. Special Publish No.10, pp. 21-31.

9. Cabri, L. J., 1988. New developments in determination of the distribution of precious metals in ore deposit, Proceedings of the Seventh Quadrennial IAGOD Symposium, pp 148-152.

10. Cabri, L. J., 1992. The distribution of trace precious metals in minerals and mineral products, mineralogical magazine, vol 56, pp 288-307.

11. Cabri, L. J., 1994. Current status of determination of mineralogical balances for platinum group element bearing ores, Transactions of the Institution of Mining and Metallurgy (Section B: Applied Earth Science), vol 103, pp B4-B-8.

12. Cabri, L. J., 2004. New development in process mineralogy of platinum-bearing ores, Proceedings of the Canadian Mineral Processor Conference, Ottawa.

13. Cole, S., Ferron, C. J., 2002. A review of the beneficiation and extractive metallurgy of the platinum group elements - highlighting recent process innovations. The geology, geochemistry, mineralogy and mineral beneficiation of platinum group elements. Canadian Institute of Metallurgy, Special Volume 54, pp. 811-818.

14. Danilatos, G. D., 1991. Review and outline of environmental SEM at present, Journal of Microscopy, Vol. 162, Pt 3, June 1991, pp.391-394.

15. Dunning, G. R., 1979. The geology and platinum group mineralization, Lac des Iles complex. Northwestern Ontario. M. Sc. thesis, Carleton University.

16. Farley, A. N., Shah, J. S., 1988. A new detection technique for high pressure scanning electron microscopy. Proc. EUREM 88, Inst. Of physics conference series, No. 93, Vol.3 (edited. by P.J. Goodhew and H. G. Dickison), pp. 241-242. IOP publishing.

17. Farley, A. N., Shah, J. S.,1991. High-pressure scanning electron microscopy of insulating materials: A new approach. Journal of Microscopy, Vol. 164, Part 2, November, 1991, pp. 107.

18. Feather, C. E., 1976. Mineralogy of platinum-group minerals in the Witwatersrand. South Africa Econ. Geol., 71, pp.1399-1428.

19. Finch, J. A., Ramirez-Castro, J., 1981. Modelling mineral size reduction in closed-circuit ball mill at Pine Point Mines Concentrator. International Journal of Mineral Processing. 8, pp. 61-78.

20. Freeman, C., 2003. Mineral beneficiation of the platinum group elements: A view through the hand-lens. Engineering & Mining Journal.

21. Furuya, M., Nakajima, Y., Tanaka, T., 1971. Theoretical analysis of closed-circuit grinding system based on comminution kinetics. I &EC Process Design Developm. 10, pp. 449-456.

22. Guerney, P. J., Laplante, A. R., O'Leary, S., 2003. Gravity recoverable gold and mineral liberation analyser. CMP 2003, pp.402-415.

23. Henley, K. J., 1983. Ore-dressing mineralogy: A review of techniques, applications and recent develops. Special publication, Geological Society of South Africa, 7, p. 175-200.

24. Hochreiter, R.C., Kennedy, D.C., Muir, W., Wood, A.I., 1985. Platinum in South Africa, J. S. Afr. Inst. Min. Metall., Vol. 85, no.6, pp. 165-185.

25. Kerr, A., Barret, J., Bouchard, A., Labonte, G., Truskoski, J., 2003. The mill redesign project at INCO's Clarabelle mill. Proceedings 2003 35th annual meeting of the Canadian mineral processors (division of CIM), Ottawa, pp. 29-50.

26. Knauf, V. V., Kozyrev, S. M., 2002. Knelson's concentrator: Extraction Evaluation, website of www. natires.com.

27. Kormos, L., Whittaker, P. J., 2005. QEM*SEM analysis of Strathcona concentrate gravity separates. Communication report for the project of gravity recoverable platinum group mineral for Strathcona mill ore sample.

28. Komarova, M. Z., Kozeyrev, S. M., Simonov, O. N., Lulko, V. A., 2003. The PGE mineralization of disseminated sulphide ore of the Norilsk-Taimyr Region,

geology of platinum group elements: The geology, geochemistry, mineralogy and mineral beneficiation of platinum group elements, Canadian Institute of Metallurgy, Special Volume 54.

29. Kozeyrev, S. M., Komarova, M. Z., Emelina, L. N., Oleshkevich, O. I., Yakovleva, O. A., Lyalinov, D. V., Maximov, V. I., 2003. The mineralogy and behavior of PGM during processing of the Norilsk-Talnakh PGE-Cu-Ni Ores. Canadian Institute of Metallurgy, Special Volume 54. pp. 675-679.

30. Laplante, A. R., Finch, J. A., del-Villar, R., 1987. Simplification of grinding equation for plant simulation. Trans. IMM. (Sec. C), 96, C108-112.

31. Laplante, A. R., Liu, L., Cauchon, A., 1990. Gold gravity recovery at the Mill of Les Mines Camchib Inc., Chibougamau, Quebec, Proceedings, Process Mineralogy Symp., Las Vegas, Feb. 1989, Eds. W. Petruk, R. D. Hagni, S. Pignolet-Brandom and D. M. Hausen, pp. 247-258.

32. Laplante, A. R., Putz, A., Huang, L., 1993. Sampling and sample processing for gold gravity circuits, proceedings, professional development seminar on gold recovery by gravity, McGill University, May, Montreal.

33. Laplante, A. R., Putz, A., Huang, L., Vincent, F., 1994. Practical considerations in the operations of gold gravity circuits. Proceedings, 26th Ann. Meet. Canadian Mineral Processors, Ottawa, January, Paper #23.

34. Laplante, A. R., Shu, Y., Marois, J., 1994. Experimental characterization of a laboratory centrifugal separator, the Canadian Metallurgical Quarterly.

35. Laplante, A. R., Woodcock, F., Noaparast, M., 1994. Predicting gold recovery by gravity, Proceedings, Annual Meeting of SME, Albuquerque, Paper 94-158.

36. Laplante, A.R., Vincent, F., Noaparast, M., Woodcock, F., Boulet, A., Dube, G., and Robitaille, E. J., 1996. Predicting gold recovery by gravity. CMP proceedings, Jan., 1996.

37. Laplante, A. R. Dunne, R. C., 2002. The gravity recoverable gold test and flash flotation. CMP Conference Proceedings, Jan 2002.

38. Laplante, A. R., Xiao, Z., Huang, L., Mejia, N., Fragomini, D., 2004. Recovery of platinum group minerals in grinding circuit: a protocol for predicting. Proceedings 2004, Annual Meeting of Canadian Mineral Processors (division of CIM), Ottawa. pp..301-318.

39. Lidsay, N. M., Sellschop, J. P. E., 1988. Routine SIMS microanalysis: trace Au and Pt sulphides, Nucl. Instr. Meth. Phys. Res. B35, pp 358-362.

40. Liu, L., 1989. An investigation of gold recovery in the grinding and gravity circuits at Les Mines Camchib Inc. Master of Engineering Thesis, McGill University, Montreal, pp. 35-42.

41. Lotter, N. O., Whittaker, P. J., Kormos, L., Stickingand, J. S., Wilkie, G. J., 2002. The development of process mineralogy at Falconbridge Limited and application to the Raglan mill. CMP Conference Proceedings, Jan 2002.

42. Martin, C. J., McKay, N. A., 2003. The role of mineralogical studies in optimizing mineral processing at North American Palladium's Lac Des Iles Mill, 2003 Mineralogy conference, Finland.

43. Mertie, J. B. Jr., 1969. Economic geology of the platinum metals. U. S. Geol. Survey, Prof. Paper 938.

44. Moncrieff, D. A., Robison, V. N. E., Harris, J. B., 1978. Neutralization of insulating surfaces in the scanning electron microscope, J. Physics D: Applied Physics, 12, 2315-2325.

45. Noaparast, M., 1997. The behavior of malleable metals in tumbling mills. Master of Engineering Thesis, McGill University, Montréal.

46. Oberthur, T., Kojonean, K., Weiser, T. W., 2002. Local variations and regional trends in PGE geochemistry and mineralogy in the Main Sulphide Zone of the Great Dyke, Zimbabwe, Proceedings: 9th international Platinum Symposium, Billings, Montana, USA, 21-25 July, 2002.

47. Petruk, W., 2000. Applied mineralogy in the mining industry, Elsevier publish.

48. Petruk, W., 1995. The relationship between mineral textures and extractive metallurgy. Process Mineralogy XIII, ed. R.D. Hagni, TMS, Warrendale, PA, pp. 3-13.

49. Petruk, W., Hughson, M. R., 1977. Image analysis evaluation of the effect of grinding media on selective flotation of two zinc-lead copper ores. CIM Bull. 70 782, pp. 128-135.

50. Pignolet-Brandom, S., Reid, K. J., 1988. Mineralogical characterization by QEM*SEM. Process Mineralogy VIII, EDX. D. J. T. Carson and A. H. Vassoilou, TMS, Warrendale, PA, pp. 337-346.

51. Plitt, L. R., 1976. A mathematical model of the hydrocyclone classifier. CIM Bull. 69, pp. 114.

52. Putz, A., Laplante, A. R., Ladouceur, G., 1993. Evaluation of a gravity circuit in a Canadian gold operation. Proceedings, Randol Gold Forum, Beaver Creek, September, pp. 145-149.

53. Ramirez-Castro, J., Finch, J. A., 1980. Simulation of a grinding circuit change to reduce lead sliming. CIM Bulletin, 73, pp. 132-139.

54. Razin, L. V., 1976. Geologic and genetic features of forsterite dunites and their platinum-group mineralization. Econ. Geol., 71: 1371-1376.

55. Reid, K. J., Pignolet-Brandom, S., 1988. Application of QEM*SEM for beneficiation studies of Minnesota taconite. Process Mineralogy VIII, EDX. D. J.

T. Carson and A. H. Vassoilou, Minerals, Metals and Materials Society, Warrendale, PA, pp. 369-377.

56. Reimer, T. O., 1992. Platinoids in auriferous proterozoric conglomerates of South Africa. Evaluation of Existing Data. N. Jb. Miner. Abh., 135: 287-314.

57. Robertson, K., Gauvin, R., Finch, J. A., 2005. Application of charge contract imaging in mineral characterization. Minerals Engineering, vol. 18, pp. 343-352.

58. Robinson, B.W., 1998. The "GEOSEM" (low-vacuum SEM): an underutilized tool for mineralogy, in modern spproaches to ore and environmental mineralogy, EDX., L.J. Cabri and D. J. Vaughan, Mineral. Association, Can., Short Course 27, 139-151.

59. Schwellus, J. S. I., Hiemstra, S. A., Gasparrini, E., 1976. The Merensky reef at the Atok platinum mine. Environs. Econ. Geol., 71, pp. 249-260.

60. Sizgoric, M. B., 1985. Tracking platinum-group minerals in the milling of Cu-Ni ores at Sudbury. Proceedings of the Ninth International Precious Metals Institute Conference, New York, pp. 923-932.

61. Stribrny, B., Wellmer, F.W., Burgath, K.P., Oberthur, T., Tarkain, M., Pheiffer, T., 2000. Unconventional PGE occurances and PGE minerlization in the Greayke: metalogenic and economic aspects, Mineralium Deposita, Vol 35, pp 260-280.

62. Turk, D. J., 2001. Stillwater mining company Nye concentrator operation, SME Annual Meeting.

63. Vermaak, C. F., Hendriks, L. P., 1976. A review of the mineralogy of the Merensky reef with specific reference to new data on the precious metal mineralogy. Econ. Geol., 71, pp. 1244-1269.

64. Vermaak, M. K. G., 2005. Fundamental of the flotation behavior of the palladium bismuth tellurides. Ph.D. thesis, University of Pretoria etd.

65. Williamson, J. E., Savage, J. A., 1965. The determination of osmiridium in Witwatersrand ores. J. South African Inst. Min. & Metall., Jan., pp. 343-356.

66. Woodcock, F., Laplante, A. R., 1993. A laboratory method for determining the amount of gravity recoverable gold. Randol Gold Forum, Beaver Creek, September 1993, pp. 151-155.

67. Xiao, Z., 2001. Developing simple regressions for predicting gold gravity recovery in grinding circuit. Master of Engineering Thesis, McGill University, Montreal, pp. 9-14.

68. Xiao, Z., Laplante, A.R., 2003. Characterization of gravity recoverable platinum group minerals in a drill ore sample from Ni Rim South. Report, June 9, 2003.

69. Xiao, Z., Laplante, A. R., 2003a. Characterization of gravity recoverable platinum group minerals in an ore sample from Raglan mill. Report, March 12, 2003.

70. Xiao, Z., Laplante, A. R., 2003b. Characterization of gravity recoverable platinum group minerals in an ore sample from Clarabelle mill. Report, November, 2003.

71. Xiao, Z., Laplante, A. R., 2004. A review of characterizing and recovering the platinum group minerals. Mineral Engineering, Vol. 17 (9-10), pp. 961-979.

72. Zhou, Z., Zhang, D., 1975. Heavy mineral separation for platinum-group minerals in platinum-bearing chromite deposits. Acta. Geol. Sin. (2), pp. 187-193, in Chinese with English abstracts.

73. Zientek, M. L., Cooper, R. W., Corson, S. R., Geraghty, E. P., 2002. Platinum-group element mineralization in the Stillwater complex, Montana. In Cabri, L. J. (Ed.). The geology, geochemistry, mineralogy and mineral beneficiation of platinum-group elements. Canadian Institute of Mining, Metallurgy and Petroleum. CIM special vol. 54, pp. 459-482.

Appendix 1-Raglan Metallurgical Balance, Upgrading the Five Coarsest for Pt

Size, µm	Product	Mass (g)	Mass (%)	Grade (g/t)	Unit	Rec. (%)	Enrichment
+600	Conc.	2.06	10.72	0.6	6.43	10.7	1.0
	Tailing	17.15	89.28	0.6	53.57	89.3	
	Total	19.21	100.00	0.6	60	100.0	
425-600	Conc.	2.03	10.24	1.8	18.44	20.4	2.0
	Tailing	17.79	89.76	0.8	71.81	79.6	
	Total	19.82	100.00	0.9	90.24	100.0	
300-425	Conc.	2.25	14.35	1.1	15.78	20.8	1.5
	Tailing	13.43	85.65	0.7	59.96	79.2	
	Total	15.68	100.00	0.8	75.74	100.0	
212-300	Conc.	1.76	14.55	0.7	10.18	14.5	1.0
	Tailing	10.34	85.45	0.7	59.82	85.5	
	Total	12.1	100.00	0.7	70	100.0	
150-212	Conc.	0.77	9.63	1.9	17.81	13.2	1.4
	Tailing	7.23	90.38	1.3	117.49	86.8	
	Total	8.00	100.00	1.4	135.29	100.0	

Appendix 1-Raglan Metallurgical Balance, Upgrading the Five Coarsest for Pd

Size, µm	Product	Mass (g)	Mass (%)	Grade (g/t)	Unit	Rec. (%)	Enrichment
+600	Conc.	2.06	10.72	7.8	83.64	36.9	3.4
	Tailing	17.15	89.28	1.6	142.84	63.1	
	Total	19.21	100.00	2.3	226.49	100.0	
425-600	Conc.	2.03	10.24	11.3	115.74	35.9	3.5
	Tailing	17.79	89.76	2.3	206.44	64.1	
	Total	19.82	100.00	3.2	322.18	100.0	
300-425	Conc.	2.25	14.35	12.7	182.24	41.5	2.9
	Tailing	13.43	85.65	3.0	256.95	58.5	
	Total	15.68	100.00	4.4	439.19	100.0	
212-300	Conc.	1.76	14.55	12.6	183.27	30.2	2.1
	Tailing	10.34	85.45	5.0	423.00	69.8	
	Total	12.1	100.00	6.1	606.27	100.0	
150-212	Conc.	0.77	9.63	11.9	114.54	20.7	2.2
	Tailing	7.23	90.38	4.9	438.32	79.3	
	Total	8.00	100.00	5.5	552.86	100.0	

Appendix 1-Raglan Table 1 Metallurgical Balance of Stage 1

Size (µm)	CONCENTRATE				TAILS				FEED			
	Weight (g)	% Weight	Grade (g/t)	Rec. (%)	Weight (g)	% Weight	Grade (g/t)	Rec. (%)	Weight (g)	% Weight	Grade (g/t)	Dist'n (%)
850	0.00	0.00	0.0	0.00	0	0.00	0.00	0.00	0	0.00	0.00	0.00
600	19.21	22.13	0.6	0.27	9587	17.62	0.45	99.73	9606	17.63	0.45	11.52
425	19.82	22.83	0.9	0.32	9366	17.22	0.60	99.68	9385	17.22	0.60	15.01
300	15.68	18.06	0.8	0.29	6385	11.74	0.65	99.71	6401	11.75	0.65	11.08
212	12.10	13.94	0.7	0.21	5721	10.52	0.70	99.79	5733	10.52	0.70	10.69
150	8.00	9.21	1.4	0.39	3977	7.31	0.70	99.61	3985	7.31	0.70	7.44
106	4.21	4.85	1.4	0.27	3313	6.09	0.65	99.73	3317	6.09	0.65	5.75
75	2.85	3.28	14	2.90	2270	4.17	0.60	97.10	2273	4.17	0.62	3.73
53	2.17	2.50	33	4.57	2510	4.61	0.60	95.43	2512	4.61	0.63	4.20
37	1.28	1.47	74	7.11	1762	3.24	0.70	92.89	1764	3.24	0.75	3.54
25	0.68	0.78	84	4.04	1587	2.92	0.85	95.96	1588	2.91	0.89	3.74
15	0.82	0.94	35	0.33	7926	14.57	1.10	99.67	7927	14.55	1.10	23.29
Total	86.82	100.00	4.1	0.96	54403	100.00	0.68	99.04	54490	100.00	0.69	100.00

Appendix 1-Raglan Table 2 Metallurgical Balance of Stage 2

Size (μm)	CONCENTRATE				TAILS				FEED			
	Weight (g)	% Weight	Grade (g/t)	Rec. (%)	Weight (g)	% Weight	Grade (g/t)	Rec. (%)	Weight (g)	% Weight	Grade (g/t)	Dist'n (%)
300	7.64	7.90	1.4	1.96	1032	3.94	0.50	98.04	1040	3.96	0.51	2.57
212	23.18	23.98	1.1	1.12	3902	14.91	0.55	98.88	3925	14.94	0.55	10.60
150	26.77	27.70	0.9	1.11	3584	13.69	0.60	98.89	3610	13.74	0.60	10.62
106	16.02	16.58	1.2	0.94	2884	11.02	0.70	99.06	2900	11.04	0.70	9.96
75	9.51	9.84	1.5	1.02	1917	7.33	0.70	98.98	1927	7.33	0.70	6.62
53	6.08	6.29	6.8	2.79	2199	8.40	0.65	97.21	2205	8.40	0.67	7.19
37	3.81	3.94	22.5	5.76	2001	7.64	0.70	94.24	2005	7.63	0.74	7.26
25	1.70	1.76	52.5	8.05	1359	5.19	0.75	91.95	1360	5.18	0.81	5.41
15	1.94	2.01	58.4	1.39	7295	27.87	1.10	98.61	7297	27.78	1.12	39.76
Total	96.65	100.00	4.4	2.06	26173	100.00	0.77	97.94	26270	100.00	0.78	100.00

Appendix 1-Raglan Table 3 Metallurgical Balance of Stage 3

Size (µm)	CONCENTRATE				TAILS				FEED			
	Weight (g)	% Weight	Grade (g/t)	Rec. (%)	Weight (g)	% Weight	Grade (g/t)	Rec. (%)	Weight (g)	% Weight	Grade (g/t)	Dist'n (%)
212	0.00	0.00	0.0	0.00	0	0.00	0.00	0.00	0	0.00	0.00	0.00
150	2.50	2.97	1.4	2.76	247	1.03	0.50	97.24	249	1.03	0.51	0.70
106	15.26	18.14	1.0	2.03	1846	7.67	0.40	97.97	1861	7.70	0.40	4.16
75	27.11	32.22	0.8	1.45	2942	12.22	0.50	98.55	2969	12.29	0.50	8.24
53	18.71	22.24	1.5	1.46	3792	15.75	0.50	98.54	3811	15.77	0.50	10.62
37	10.07	11.97	8.3	4.54	2930	12.17	0.60	95.46	2940	12.17	0.63	10.17
25	4.92	5.85	7.8	4.15	1479	6.14	0.60	95.85	1484	6.14	0.62	5.11
15	5.57	6.62	36.8	1.86	10840	45.03	1.00	98.14	10846	44.89	1.02	60.99
Total	84.14	100.00	4.7	2.18	24076	100.00	0.74	97.82	24160	100.00	0.75	100.00

Appendix 1-Raglan Table 4 Overall Metallurgical Balance

Size (µm)	First Stage: 100% -850 µm Stage Recov.	Dist'n	Rec. g/t	Second Stage: 49.0% -75 µm Stage Recov.	Dist'n	Rec. g/t	Third Stage: 79.0% -75 µm Stage Recov.	Dist'n	Rec. g/t	Losses g/t	Total Recov. g/t	Total Recov. %
850												
600	0.27	11.52	0.0002								0.0002	0.03
425	0.32	15.01	0.0003								0.0003	0.04
300	0.29	11.08	0.0002	1.96	2.57	0.0004					0.001	0.1
212	0.21	10.69	0.0002	1.12	10.60	0.001					0.001	0.1
150	0.39	7.44	0.0002	1.11	10.62	0.001	2.76	0.70	0.0001	0.01	0.001	0.2
106	0.27	5.75	0.0001	0.94	9.96	0.001	2.03	4.16	0.001	0.03	0.001	0.2
75	2.90	3.73	0.001	1.02	6.62	0.001	1.45	8.24	0.001	0.06	0.002	0.3
53	4.57	4.20	0.001	2.79	7.19	0.002	1.46	10.62	0.001	0.08	0.004	0.5
37	7.11	3.54	0.002	5.76	7.26	0.003	4.54	10.17	0.003	0.07	0.008	1.1
25	4.04	3.74	0.001	8.05	5.41	0.003	4.15	5.11	0.002	0.04	0.006	0.8
15	0.33	23.29	0.001	1.39	39.76	0.004	1.86	60.99	0.008	0.45	0.013	1.7
Total	0.9	100.0	0.007	2.1	100.0	0.016	2.2	100.0	0.016	0.73	0.039	5.1
O/A	0.9	0.9		2.1			2.1					
Yield	0.00159			0.00368			0.00348					
Grade	0.689g/t			0.78g/t			0.75g/t					
Calc.:	0.768g/t											

Appendix 2 Strathcona Table 1A Metallurgical Balance of Platinum for Stage 1

Size (µm)	CONCENTRATE				TAILS				FEED			
	Weight (g)	% Weight	Grade (g/t)	Rec. (%)	Weight (g)	% Weight	Grade (g/t)	Rec. (%)	Weight (g)	% Weight	Grade (g/t)	Dist'n (%)
850	0.00	0.00	0.0	0.00	0	0.00	0.00	0.00	0	0.00	0.00	0.00
600	21.63	22.81	2.0	1.05	11987.2	15.92	0.34	98.95	12009	15.93	0.34	13.07
425	19.7	20.77	2.6	2.01	12342.9	16.39	0.20	97.99	12363	16.40	0.20	8.00
300	15.58	16.43	21.0	10.86	8659.23	11.50	0.31	89.14	8675	11.51	0.35	9.56
212	12.58	13.27	52.3	17.22	7906.09	10.50	0.40	82.78	7919	10.50	0.48	12.13
150	8.47	8.93	58.4	14.06	5929.25	7.87	0.51	85.94	5938	7.88	0.59	11.17
106	5.7	6.01	232.5	47.29	5471.31	7.27	0.27	52.71	5477	7.26	0.51	8.90
75	3.66	3.86	226.0	42.84	3942.32	5.24	0.28	57.16	3946	5.23	0.49	6.13
53	3.01	3.17	253.2	30.55	4681.58	6.22	0.37	69.45	4685	6.21	0.53	7.92
37	2	2.11	269.5	38.39	2403.24	3.19	0.36	61.61	2405	3.19	0.58	4.46
25	1.09	1.15	175.6	13.72	3760.66	4.99	0.32	86.28	3762	4.99	0.37	4.43
20	0.59	0.62	131.2	12.31	889.39	1.18	0.62	87.69	890	1.18	0.71	2.00
10	0.82	0.86	65.6	1.39	7321.99	9.72	0.52	98.61	7323	9.71	0.53	12.26
Total	94.83	100.00	56	16.98	75295	100.00	0.35	83.02	75390	100.00	0.42	100.00

Appendix 2 Strathcona Table 2 A Metallurgical Balance of Platinum for Stage 2

Size (μm)	CONCENTRATE				TAILS				FEED			
	Weight (g)	% Weight	Grade (g/t)	Rec. (%)	Weight (g)	% Weight	Grade (g/t)	Rec. (%)	Weight (g)	% Weight	Grade (g/t)	Dist'n (%)
300	6.77	5.78	1.6	24.16	213	0.78	0.16	75.84	219	0.80	0.20	0.47
212	34.07	29.08	1.7	16.18	2471	9.02	0.12	83.82	2505	9.10	0.14	3.74
150	35.52	30.31	9.0	34.09	3867	14.12	0.16	65.91	3903	14.19	0.24	9.93
106	19.69	16.80	19.4	36.06	3565	13.02	0.19	63.94	3584	13.03	0.30	11.20
75	10.73	9.16	30.7	36.96	2554	9.33	0.22	63.04	2565	9.32	0.35	9.43
53	6.83	5.83	54.2	38.08	3169	11.57	0.19	61.92	3175	11.54	0.31	10.28
37	4.62	3.94	78.0	51.43	1891	6.90	0.18	48.57	1896	6.89	0.37	7.41
25	2.6	2.22	97.8	23.80	3256	11.89	0.25	76.20	3259	11.85	0.33	11.30
20	1.35	1.15	62.9	37.20	368	1.34	0.39	62.80	369	1.34	0.62	2.41
10	1.76	1.50	68.2	3.75	6033	22.03	0.51	96.25	6035	21.94	0.53	33.82
Total	117.17	100.00	19.5	24.21	27386	100.00	0.26	75.79	27510	100.00	0.34	100.00

Appendix 2 Strathcona Table 3A Metallurgical Balance of Platinum for Stage 3

Size (µm)	CONCENTRATE				TAILS				FEED			
	Weight (g)	% Weight	Grade (g/t)	Rec. (%)	Weight (g)	% Weight	Grade (g/t)	Rec. (%)	Weight (g)	% Weight	Grade (g/t)	Dist'n (%)
212	0.00	0.00	0.0	0.00	0	0.00	0.00	0.00	0	0.00	0.00	0.00
150	16.47	14.40	0.4	16.79	381	1.52	0.09	83.21	397	1.58	0.10	0.57
106	25.31	22.12	0.7	7.99	1570	6.27	0.13	92.01	1595	6.34	0.14	3.09
75	26.11	22.82	1.5	8.05	3000	11.97	0.15	91.95	3026	12.02	0.16	6.81
53	18.18	15.89	5.5	14.80	4090	16.32	0.14	85.20	4108	16.32	0.16	9.35
37	13.01	11.37	12.6	34.24	2624	10.47	0.12	65.76	2637	10.48	0.18	6.66
25	7.32	6.40	25.7	23.83	4296	17.15	0.14	76.17	4303	17.10	0.18	10.98
20	3.89	3.40	53.1	81.24	199	0.79	0.24	18.76	203	0.81	1.25	3.54
10	4.12	3.60	79.6	7.73	8896	35.50	0.44	92.27	8900	35.36	0.48	59.01
Total	114.41	100.00	9.2	14.61	25056	100.00	0.25	85.39	25170	100.00	0.29	100.00

Appendix 2 Strathcona Table 4A **Overall Metallurgical Balance of Platinum (Standard test, 3 stages)**

Size (µm)	First Stage: 100% -850 µm			Second Stage: 53.6% -75 µm			Third Stage: 80.1% -75 µm				Total	Total
	Stage Recov.	Dist'n	Rec. g/t	Stage Recov.	Dist'n	Rec. g/t	Stage Recov.	Dist'n	Rec. g/t	Losses g/t	Recov. g/t	Recov. %
850												
600	1.05	13.07	0.001								0.001	0.1
425	2.01	8.00	0.001								0.001	0.2
300	10.86	9.56	0.004	24.16	0.47	0.000					0.005	1.1
212	17.22	12.13	0.009	16.18	3.74	0.002					0.011	2.5
150	14.06	11.17	0.007	34.09	9.93	0.012	16.79	0.57	0.000	0.00	0.018	4.2
106	47.29	8.90	0.018	36.06	11.20	0.014	7.99	3.09	0.001	0.01	0.032	7.3
75	42.84	6.13	0.011	36.96	9.43	0.012	8.05	6.81	0.002	0.02	0.024	5.6
53	30.55	7.92	0.010	38.08	10.28	0.013	14.80	9.35	0.004	0.02	0.027	6.3
37	38.39	4.46	0.007	51.43	7.41	0.013	34.24	6.66	0.006	0.01	0.027	6.1
25	13.72	4.43	0.003	23.80	11.30	0.009	23.83	10.98	0.007	0.02	0.019	4.4
20	12.31	2.00	0.001	37.20	2.41	0.003	81.24	3.54	0.008	0.00	0.012	2.8
15	1.39	12.26	0.001	3.75	33.82	0.004	7.73	59.01	0.013	0.15	0.018	4.1
Total	16.2	100.0	0.07	22.6	100.0	0.083	14.5	100.0	0.041	0.24	0.196	44.6
O/A	16.2			18.9			9.5					
Yield	0.00126			0.00426			0.00455					
Grade	0.418g/t			0.34g/t			0.29g/t					
Calc.:	0.438g/t											

Appendix 2 Strathcona Table 5A Metallurgical Balance of Platinum for Stage 4

Size (μm)	CONCENTRATE				TAILS				FEED			
	Weight (g)	% Weight	Grade (g/t)	Rec. (%)	Weight (g)	% Weight	Grade (g/t)	Rec. (%)	Weight (g)	% Weight	Grade (g/t)	Dist'n (%)
212	0	0	0	0	0	0	0	0	0	0	0	0
150	7.54	6.79	0.5	10.18	332.56	1.52	0.10	89.82	340	1.54	0.11	0.68
106	18.63	16.77	0.5	3.57	1544.64	7.04	0.15	96.43	1563	7.09	0.15	4.39
75	28.73	25.87	0.7	4.91	2783.42	12.69	0.14	95.09	2812	12.76	0.15	7.49
53	24.27	21.85	1.6	5.97	3775.98	17.22	0.16	94.03	3800	17.24	0.17	11.74
37	14.92	13.43	3.6	15.93	2168.05	9.89	0.13	84.07	2183	9.90	0.15	6.12
25	7.58	6.83	8.9	14.75	3556.47	16.22	0.11	85.25	3564	16.17	0.13	8.38
20	4.33	3.90	27.4	75.06	303.29	1.38	0.13	24.94	308	1.40	0.51	2.89
10	5.06	4.56	99.9	15.83	7464.52	34.04	0.36	84.17	7470	33.89	0.43	58.32
Total	111.06	100.00	7.3	14.91	21929	100.00	0.21	85.09	22040	100.00	0.25	100.00

Appendix 2 Strathcona Table 6A Overall Metallurgical Balance for Platinum (Four recovery stages)

Size (µm)	First Stage: 100% -850 µm			Second Stage: 53.6% -75 µm			Third Stage: 80.1% -75 µm			Four stage: 78.6% -75 µm				Total	Total
	Stage Recov.	Dist'n	Rec. g/t	Stage Recov.	Dist'n	Rec. g/t	Stage Recov.	Dist'n	Rec. g/t	Stage Recov.	Dist'n	Rec. g/t	Losses g/t	Recov. g/t	Recov. %
850															
600	1.05	13.07	0.001											0.001	0.1
425	2.01	8.00	0.001											0.001	0.2
300	10.86	9.56	0.004	24.16	0.47	0.000								0.005	1.1
212	17.22	12.13	0.009	16.18	3.74	0.002								0.011	2.4
150	14.06	11.17	0.007	34.09	9.93	0.012	16.79	0.57	0.000	10.18	0.68	0.000	0.00	0.019	4.2
106	47.29	8.90	0.018	36.06	11.20	0.014	7.99	3.09	0.001	3.57	4.39	0.000	0.01	0.033	7.4
75	42.84	6.13	0.011	36.96	9.43	0.012	8.05	6.81	0.002	4.91	7.49	0.001	0.02	0.025	5.8
53	30.55	7.92	0.010	38.08	10.28	0.013	14.80	9.35	0.004	5.97	11.74	0.002	0.03	0.029	6.6
37	38.39	4.46	0.007	51.43	7.41	0.013	34.24	6.66	0.006	15.93	6.12	0.002	0.01	0.029	6.6
25	13.72	4.43	0.003	23.80	11.30	0.009	23.83	10.98	0.007	14.75	8.38	0.003	0.02	0.022	5.0
20	12.31	2.00	0.001	37.20	2.41	0.003	81.24	3.54	0.008	75.06	2.89	0.005	0.00	0.018	4.0
15	1.39	12.26	0.001	3.75	33.82	0.004	7.73	59.01	0.013	15.83	58.32	0.023	0.12	0.041	9.2
Total	16.1	100.0	0.07	22.4	100.0	0.083	14.5	100.0	0.041	14.76	100.0	0.037	0.21	0.232	52.6
O/A	16.1	16.1		18.8	18.8		9.4			8.3					
Yield	0.0013			0.0043			0.0045			0					
Grade	0.418g/t			0.34g/t			0.29g/t			0.25g/t					
Calc.:	0.441g/t														

Appendix 2 Strathcona Table 1B Metallurgical Balance of Palladium for Stage 1

Size (µm)	CONCENTRATE				TAILS				FEED			
	Weight (g)	% Weight	Grade (g/t)	Rec. (%)	Weight (g)	% Weight	Grade (g/t)	Rec. (%)	Weight (g)	% Weight	Grade (g/t)	Dist'n (%)
850	0	0	0	0	0	0	0	0	0	0	0	0
600	21.63	22.81	3.5	2.44	11987.2	15.92	0.25	97.56	12009	15.93	0.26	6.91
425	19.7	20.77	2.2	0.66	12342.9	16.39	0.52	99.34	12363	16.40	0.52	14.52
300	15.58	16.43	15.8	5.95	8659.23	11.50	0.45	94.05	8675	11.51	0.48	9.31
212	12.58	13.27	64.4	19.99	7906.09	10.50	0.41	80.01	7919	10.50	0.51	9.11
150	8.47	8.93	90.8	23.17	5929.25	7.87	0.43	76.83	5938	7.88	0.56	7.46
106	5.7	6.01	377.4	44.52	5471.31	7.27	0.49	55.48	5477	7.26	0.88	10.86
75	3.66	3.86	344.6	45.06	3942.32	5.24	0.39	54.94	3946	5.23	0.71	6.29
53	3.01	3.17	369.9	31.80	4681.58	6.22	0.51	68.20	4685	6.21	0.75	7.87
37	2	2.11	338.8	33.89	2403.24	3.19	0.55	66.11	2405	3.19	0.83	4.49
25	1.09	1.15	192.2	8.12	3760.66	4.99	0.63	91.88	3762	4.99	0.69	5.80
20	0.59	0.62	115.6	7.77	889.39	1.18	0.91	92.23	890	1.18	0.99	1.97
10	0.82	0.86	48.6	0.58	7321.99	9.72	0.93	99.42	7323	9.71	0.94	15.40
Total	94.83	100.00	79	16.78	75295	100.00	0.49	83.22	75390	100.00	0.59	100.00

Appendix 2 Strathcona Table 2 B Metallurgical Balance of Palladium for Stage 2

Size (µm)	CONCENTRATE				TAILS				FEED			
	Weight (g)	% Weight	Grade (g/t)	Rec. (%)	Weight (g)	% Weight	Grade (g/t)	Rec. (%)	Weight (g)	% Weight	Grade (g/t)	Dist'n (%)
300	6.77	5.78	0.84	5.6868	10.42	212.56	0.78	0.23	49	89.58	219	0.80
212	34.07	29.08	0.8	28.619	7.64	2471	9.02	0.14	346	92.36	2505	9.10
150	35.52	30.31	5.5	195.72	18.03	3867	14.12	0.23	890	81.97	3903	14.19
106	19.69	16.80	8.4	165.99	15.70	3565	13.02	0.25	891	84.30	3584	13.03
75	10.73	9.16	27.8	298.29	27.37	2554	9.33	0.31	792	72.63	2565	9.32
53	6.83	5.83	52.8	360.62	28.90	3169	11.57	0.28	887	71.10	3175	11.54
37	4.62	3.94	80.3	370.99	38.01	1891	6.90	0.32	605	61.99	1896	6.89
25	2.6	2.22	112.8	293.28	15.53	3256	11.89	0.49	1596	84.47	3259	11.85
20	1.35	1.15	69.9	94.365	28.63	368	1.34	0.64	235	71.37	369	1.34
10	1.76	1.50	65.0	114.4	2.16	6033	22.03	0.86	5189	97.84	6035	21.94
Total	117.17	100.00	16.5	1928	14.38	27386	100.00	0.42	11479	85.62	27510	100.00

Appendix 2 Strathcona Table 3B **Metallurgical Balance of Palladium for Stage 3**

Size (µm)	CONCENTRATE				TAILS				FEED			
	Weight (g)	% Weight	Grade (g/t)	Rec. (%)	Weight (g)	% Weight	Grade (g/t)	Rec. (%)	Weight (g)	% Weight	Grade (g/t)	Dist'n (%)
212	0	0	0	0	0	0	0	0	0	0	0	0
150	16.47	14.40	0.5	7.5762	11.71	381	1.52	0.15	57	88.29	397	1.58
106	25.31	22.12	0.8	19.995	8.92	1570	6.27	0.13	204	91.08	1595	6.34
75	26.11	22.82	1.7	44.126	6.54	3000	11.97	0.21	630	93.46	3026	12.02
53	18.18	15.89	3.8	69.629	7.85	4090	16.32	0.20	818	92.15	4108	16.32
37	13.01	11.37	9.7	126.46	17.32	2624	10.47	0.23	604	82.68	2637	10.48
25	7.32	6.40	22.2	162.5	12.70	4296	17.15	0.26	1117	87.30	4303	17.10
20	3.89	3.40	51.3	199.56	74.70	199	0.79	0.34	68	25.30	203	0.81
10	4.12	3.60	83.7	344.84	5.18	8896	35.50	0.71	6316	94.82	8900	35.36
Total	114.41	100.00	8.5	974.69	9.03	25056	100.00	0.39	9813	90.97	25170	100.00

Appendix 2 Strathcona Table 4B **Overall Metallurgical Balance of Paladium (Standard test, 3 stages)**

Size (µm)	First Stage: 100% -850 µm			Second Stage: 53.6% -75 µm			Third Stage: 80.1% -75 µm				Total	Total
	Stage Recov.	Dist'n	Rec. g/t	Stage Recov.	Dist'n	Rec. g/t	Stage Recov.	Dist'n	Rec. g/t	Losses g/t	Recov. g/t	Recov. %
850												
600	2.44	6.91	0.001								0.001	0.2
425	0.66	14.52	0.001								0.001	0.1
300	5.95	9.31	0.003	10.42	0.41	0.000					0.003	0.6
212	19.99	9.11	0.011	7.64	2.79	0.001					0.012	2.0
150	23.17	7.46	0.010	18.03	8.09	0.007	11.71	0.60	0.000	0.00	0.018	3.0
106	44.52	10.86	0.029	15.70	7.89	0.006	8.92	2.08	0.001	0.01	0.035	5.9
75	45.06	6.29	0.017	27.37	8.13	0.011	6.54	6.25	0.002	0.02	0.029	4.9
53	31.80	7.87	0.015	28.90	9.31	0.013	7.85	8.23	0.003	0.03	0.031	5.1
37	33.89	4.49	0.009	38.01	7.28	0.013	17.32	6.77	0.005	0.02	0.027	4.6
25	8.12	5.80	0.003	15.53	14.09	0.011	12.70	11.86	0.006	0.04	0.020	3.3
20	7.77	1.97	0.001	28.63	2.46	0.003	74.70	2.48	0.008	0.00	0.012	2.1
15	0.58	15.40	0.001	2.16	39.55	0.004	5.18	61.74	0.014	0.25	0.018	3.1
Total	16.6	100.0	0.10	14.1	100.0	0.070	9.0	100.0	0.039	0.39	0.208	34.9
O/A	16.6			11.7			6.5					
Yield	0.00126			0.00426			0.00455					
Grade	0.590g/t			0.49g/t			0.43g/t					
Calc.:	0.595g/t											

Appendix 2 Strathcona Table 5B Metallurgical Balance of Palladium for Stage 4

Size (μm)	CONCENTRATE				TAILS				FEED			
	Weight (g)	% Weight	Grade (g/t)	Rec. (%)	Weight (g)	% Weight	Grade (g/t)	Rec. (%)	Weight (g)	% Weight	Grade (g/t)	Dist'n (%)
212	0	0	0	0	0	0	0	0	0	0	0	0
150	7.54	6.79	0.7	9.92	332.56	1.52	0.14	90.08	340	1.54	0.15	0.63
106	18.63	16.77	0.5	4.05	1544.64	7.04	0.14	95.95	1563	7.09	0.14	2.75
75	28.73	25.87	0.9	5.06	2783.42	12.69	0.18	94.94	2812	12.76	0.19	6.44
53	24.27	21.85	1.8	5.33	3775.98	17.22	0.21	94.67	3800	17.24	0.22	10.22
37	14.92	13.43	3.7	18.80	2168.05	9.89	0.11	81.20	2183	9.90	0.13	3.58
25	7.58	6.83	10.2	8.31	3556.47	16.22	0.24	91.69	3564	16.17	0.26	11.36
20	4.33	3.90	32.8	62.58	303.29	1.38	0.28	37.42	308	1.40	0.74	2.77
10	5.06	4.56	122.9	12.19	7464.52	34.04	0.60	87.81	7470	33.89	0.68	62.24
Total	111.06	100.00	8.8	11.98	21929	100.00	0.33	88.02	22040	100.00	0.37	100.00

Appendix 2 Strathcona Table 6B **Overall Metallurgical Balance for Palladium (Four recovery stages)**

Size (µm)	First Stage: 100% -850 µm			Second Stage: 53.6% -75 µm			Third Stage: 80.1% -75 µm			Four stage: 78.6% -75 µm				Total	Total
	Stage Recov.	Dist'n	Rec. g/t	Stage Recov.	Dist'n	Rec. g/t	Stage Recov.	Dist'n	Rec. g/t	Stage Recov.	Dist'n	Rec. g/t	Losses g/t	Recov. g/t	Recov. %
850															
600	2.44	6.91	0.001											0.001	0.2
425	0.66	14.52	0.001											0.001	0.1
300	5.95	9.31	0.003	10.42	0.41	0.000								0.003	0.6
212	19.99	9.11	0.011	7.64	2.79	0.001								0.012	2.0
150	23.17	7.46	0.010	18.03	8.09	0.007	11.71	0.60	0.000	9.92	0.63	0.000	0.00	0.018	3.1
106	44.52	10.86	0.029	15.70	7.89	0.006	8.92	2.08	0.001	4.05	2.75	0.000	0.01	0.036	6.2
75	45.06	6.29	0.017	27.37	8.13	0.011	6.54	6.25	0.002	5.06	6.44	0.001	0.02	0.031	5.3
53	31.80	7.87	0.015	28.90	9.31	0.013	7.85	8.23	0.003	5.33	10.22	0.002	0.04	0.033	5.7
37	33.89	4.49	0.009	38.01	7.28	0.013	17.32	6.77	0.005	18.80	3.58	0.002	0.01	0.030	5.2
25	8.12	5.80	0.003	15.53	14.09	0.011	12.70	11.86	0.006	8.31	11.36	0.003	0.04	0.023	4.1
20	7.77	1.97	0.001	28.63	2.46	0.003	74.70	2.48	0.008	62.58	2.77	0.006	0.00	0.019	3.2
15	0.58	15.40	0.001	2.16	39.55	0.004	5.18	61.74	0.014	12.19	62.24	0.028	0.20	0.046	8.0
Total	17.2	100.0	0.10	14.7	100.0	0.070	9.0	100.0	0.039	11.86	100.0	0.044	0.32	0.252	43.7
O/A	17.2	17.2		12.1	12.2		6.7			7.7					
Yield	0.0013			0.0043			0.0045			0					
Grade	0.590g/t			0.49g/t			0.43g/t			0.37g/t					
Calc.:	0.576g/t														

Appendix 3 Nickel Rim South Table 1A Metallurgical Balance of Platinum for Stage 1

Size (µm)	CONCENTRATE				TAILS				FEED			
	Weight (g)	% Weight	Grade (g/t)	Rec. (%)	Weight (g)	% Weight	Grade (g/t)	Rec. (%)	Weight (g)	% Weight	Grade (g/t)	Dist'n (%)
850	850	0.00	0.00	0.0	0.00	0	0.00	0.00	0.00	0	0.00	0.00
600	600	16.52	19.14	2.8	0.50	3974.64	16.12	2.32	99.50	3991	16.13	2.32
425	425	17.93	20.78	3.3	0.58	3789.37	15.37	2.66	99.42	3807	15.39	2.66
300	300	16.24	18.82	3.9	0.63	2916.54	11.83	3.41	99.37	2933	11.85	3.41
212	212	12.46	14.44	13.8	1.75	2762.57	11.21	3.49	98.25	2775	11.22	3.54
150	150	8.26	9.57	24.8	3.01	2039.61	8.27	3.23	96.99	2048	8.28	3.32
106	106	5.59	6.48	111.4	9.44	1766.23	7.16	3.38	90.56	1772	7.16	3.72
75	75	3.6	4.17	396.0	27.47	1161.84	4.71	3.24	72.53	1165	4.71	4.45
53	53	2.75	3.19	759.1	31.39	1277.94	5.18	3.57	68.61	1281	5.18	5.19
37	38	1.63	1.89	1089.8	40.94	603.57	2.45	4.25	59.06	605	2.45	7.17
25	25	0.7	0.81	883.6	11.17	973.69	3.95	5.05	88.83	974	3.94	5.68
20	20	0.32	0.37	498.2	8.01	359.01	1.46	5.10	91.99	359	1.45	5.54
10	10	0.29	0.34	142.2	0.26	3027.71	12.28	5.15	99.74	3028	12.24	5.16
Total	Total	86.29	100.00	84	7.91	24653	100.00	3.43	92.09	24739	100.00	3.72

Appendix 3 Nickel Rim South Table 2 A Metallurgical Balance of Platinum for Stage 2

Size (μm)	CONCENTRATE				TAILS				FEED			
	Weight (g)	% Weight	Grade (g/t)	Rec. (%)	Weight (g)	% Weight	Grade (g/t)	Rec. (%)	Weight (g)	% Weight	Grade (g/t)	Dist'n (%)
300	6.65	5.91	7.3	7.81	336	1.57	1.70	92.19	342	1.60	1.81	0.87
212	23.67	21.03	7.0	7.86	1045	4.90	1.85	92.14	1069	4.98	1.96	2.95
150	27.43	24.37	12.3	8.10	1801	8.44	2.12	91.90	1828	8.52	2.27	5.84
106	20.9	18.57	23.4	8.02	2736	12.82	2.05	91.98	2757	12.85	2.21	8.58
75	14.29	12.69	66.1	15.76	2214	10.38	2.28	84.24	2228	10.39	2.69	8.43
53	9.32	8.28	174.7	23.64	2435	11.41	2.16	76.36	2444	11.40	2.82	9.69
37	5.51	4.89	503.3	53.11	1338	6.27	1.83	46.89	1344	6.26	3.89	7.35
25	2.46	2.19	885.3	29.80	2103	9.86	2.44	70.20	2106	9.82	3.47	10.28
20	1.17	1.04	1232.9	39.71	637	2.98	3.44	60.29	638	2.97	5.69	5.11
10	1.17	1.04	929.6	3.74	6693	31.37	4.18	96.26	6694	31.21	4.34	40.89
Total	112.57	100.00	98.5	15.61	21337	100.00	2.81	84.39	21450	100.00	3.31	100.00

Appendix 3 Nickel Rim South Table 3A Metallurgical Balance of Platinum for Stage 3

Size (µm)	CONCENTRATE				TAILS				FEED			
	Weight (g)	% Weight	Grade (g/t)	Rec. (%)	Weight (g)	% Weight	Grade (g/t)	Rec. (%)	Weight (g)	% Weight	Grade (g/t)	Dist'n (%)
212	0.00	0.00	0.0	0.00	0	0.00	0.00	0.00	0	0.00	0.00	0.00
150	1.55	1.86	8.1	9.85	96	0.51	1.20	90.15	97	0.51	1.31	0.24
106	15.81	19.00	7.9	9.83	905	4.82	1.27	90.17	920	4.88	1.38	2.42
75	26.18	31.47	10.3	9.01	1904	10.14	1.43	90.99	1930	10.23	1.55	5.67
53	19.01	22.85	28.5	11.51	2761	14.71	1.51	88.49	2780	14.74	1.69	8.93
37	10.92	13.13	91.2	29.64	1565	8.33	1.51	70.36	1576	8.36	2.13	6.37
25	4.9	5.89	230.1	22.23	2496	13.29	1.58	77.77	2501	13.26	2.03	9.62
20	2.50	3.01	490.5	45.48	720	3.84	2.04	54.52	723	3.83	3.73	5.11
10	2.32	2.79	799.6	5.71	8330	44.36	3.68	94.29	8332	44.18	3.90	61.64
Total	83.19	100.00	74.0	11.67	18777	100.00	2.48	88.33	18860	100.00	2.80	100.00

Appendix 3 Nickel Rim South Table 4A Overall Metallurgical Balance of Platinum (Standard test, 3 stages)

Size (µm)	First Stage: 100% -850 µm			Second Stage: 61.75% -75 µm			Third Stage: 84.4% -75 µm				Total	Total
	Stage Recov.	Dist'n	Rec. g/t	Stage Recov.	Dist'n	Rec. g/t	Stage Recov.	Dist'n	Rec. g/t	Losses g/t	Recov. g/t	Recov. %
850												
600	0.50	10.08	0.002								0.002	0.1
425	0.58	11.03	0.002								0.002	0.1
300	0.63	10.88	0.003	7.81	0.87	0.002					0.005	0.1
212	1.75	10.67	0.007	7.86	2.95	0.008					0.015	0.4
150	3.01	7.39	0.008	8.10	5.84	0.016	9.85	0.24	0.001	0.01	0.025	0.7
106	9.44	7.17	0.025	8.02	8.58	0.023	9.83	2.42	0.007	0.06	0.054	1.5
75	27.47	5.64	0.058	15.76	8.43	0.044	9.01	5.67	0.014	0.14	0.116	3.2
53	31.39	7.23	0.084	23.64	9.69	0.076	11.51	8.93	0.029	0.22	0.189	5.3
38	40.94	4.72	0.072	53.11	7.35	0.129	29.64	6.37	0.052	0.12	0.253	7.1
25	11.17	6.02	0.025	29.80	10.28	0.101	22.23	9.62	0.059	0.21	0.185	5.2
20	8.01	2.16	0.006	39.71	5.11	0.067	45.48	5.11	0.064	0.08	0.138	3.9
15	0.26	17.00	0.002	3.74	40.89	0.051	5.71	61.64	0.097	1.61	0.150	4.2
Total	8.2	100.0	0.29	15.7	100.0	0.515	11.6	100.0	0.323	2.45	1.133	31.6
O/A	8.2	8.2		14.3	14.4		9.0					
Yield	0.00349			0.00525			0.00000					
Grade	3.717g/t			3.31g/t			2.80g/t					
Calc.:	3.581g/t											

Appendix 3 Nickel Rim South Table 5A Metallurgical Balance of Platinum for Stage 4

Size (µm)	CONCENTRATE				TAILS				FEED			
	Weight (g)	% Weight	Grade (g/t)	Rec. (%)	Weight (g)	% Weight	Grade (g/t)	Rec. (%)	Weight (g)	% Weight	Grade (g/t)	Dist'n (%)
212	0.00	0.00	0.0	0.00	0	0.00	0.00	0.00	0	0.00	0.00	0.00
150	1.72	1.34	3.0	4.83	85.29	0.51	1.20	95.17	87	0.52	1.24	0.25
106	14.49	11.25	5.0	5.89	837.79	5.02	1.39	94.11	852	5.07	1.45	2.89
75	40.36	31.35	5.6	8.82	1734.87	10.39	1.34	91.18	1775	10.55	1.44	5.96
53	39.31	30.53	8.4	7.84	2581.61	15.47	1.50	92.16	2621	15.58	1.60	9.83
37	18.01	13.99	16.5	12.99	1438.45	8.62	1.38	87.01	1456	8.66	1.57	5.33
25	7.43	5.77	58.9	13.89	2222.55	13.32	1.22	86.11	2230	13.26	1.41	7.36
20	3.68	2.86	239.4	54.88	646.80	3.88	1.12	45.12	650	3.87	2.47	3.75
10	3.75	2.91	1234.5	16.75	7143.89	42.80	3.22	83.25	7148	42.49	3.87	64.62
Total	128.75	100.00	53.4	16.08	16691	100.00	2.15	83.92	16820	100.00	2.54	100.00

Appendix 3 Nickel Rim South Table 6A Overall Metallurgical Balance for Platinum (Four recovery stages)

Size (µm)	First Stage: 100% -850 µm			Second Stage: 61.7% -75 µm			Third Stage: 84.4% -75 µm			Four stage: 84.1% -75 µm				Total	Total
	Stage Recov.	Dist'n	Rec. g/t	Stage Recov.	Dist'n	Rec. g/t	Stage Recov.	Dist'n	Rec. g/t	Stage Recov.	Dist'n	Rec. g/t	Losses g/t	Recov. g/t	Recov. %
850															
600	0.50	10.08	0.002											0.002	0.1
425	0.58	11.03	0.002											0.002	0.1
300	0.63	10.88	0.003	7.81	0.87	0.002								0.005	0.1
212	1.75	10.67	0.007	7.86	2.95	0.008								0.015	0.4
150	3.01	7.39	0.008	8.10	5.84	0.016	9.85	0.24	0.001	4.83	0.25	0.000	0.01	0.025	0.7
106	9.44	7.17	0.025	8.02	8.58	0.023	9.83	2.42	0.007	5.89	2.89	0.004	0.07	0.059	1.6
75	27.47	5.64	0.058	15.76	8.43	0.044	9.01	5.67	0.014	8.82	5.96	0.013	0.14	0.129	3.5
53	31.39	7.23	0.084	23.64	9.69	0.076	11.51	8.93	0.029	7.84	9.83	0.019	0.23	0.208	5.7
37	40.94	4.72	0.072	53.11	7.35	0.129	29.64	6.37	0.052	12.99	5.33	0.017	0.12	0.270	7.4
25	11.17	6.02	0.025	29.80	10.28	0.101	22.23	9.62	0.059	13.89	7.36	0.026	0.16	0.211	5.8
20	8.01	2.16	0.006	39.71	5.11	0.067	45.48	5.11	0.064	54.88	3.75	0.052	0.04	0.190	5.2
15	0.26	17.00	0.002	3.74	40.89	0.051	5.71	61.64	0.097	16.75	64.62	0.273	1.36	0.423	11.6
Total	8.1	100.0	0.29	15.3	100.0	0.515	11.6	100.0	0.323	15.94	100.0	0.405	2.12	1.538	42.1
O/A	8.1	8.0		14.1	14.1		8.9			11.1					
Yield	0.0035			0.0052			0.0000			0					
Grade	3.717g/t			3.31g/t			2.80g/t			2.54g/t					
Calc.:	3.653g/t														

Appendix 3 Nickel Rim South Table 1B Metallurgical Balance of Palladium for Stage 1

Size (μm)	CONCENTRATE				TAILS				FEED			
	Weight (g)	% Weight	Grade (g/t)	Rec. (%)	Weight (g)	% Weight	Grade (g/t)	Rec. (%)	Weight (g)	% Weight	Grade (g/t)	Dist'n (%)
850	0.00	0.00	0.0	0.00	0	0.00	0.00	0.00	0	0.00	0.00	0.00
600	16.52	19.14	2.7	0.46	3974.64	16.12	2.38	99.54	3991	16.13	2.38	9.56
425	17.93	20.78	4.5	0.65	3789.37	15.37	3.24	99.35	3807	15.39	3.25	12.43
300	16.24	18.82	4.0	0.69	2916.54	11.83	3.21	99.31	2933	11.85	3.21	9.48
212	12.46	14.44	13.8	1.61	2762.57	11.21	3.81	98.39	2775	11.22	3.85	10.76
150	8.26	9.57	37.2	3.71	2039.61	8.27	3.91	96.29	2048	8.28	4.04	8.33
106	5.59	6.48	167.1	12.39	1766.23	7.16	3.74	87.61	1772	7.16	4.26	7.58
75	3.6	4.17	494.3	31.57	1161.84	4.71	3.32	68.43	1165	4.71	4.84	5.67
53	2.75	3.19	943.3	35.86	1277.94	5.18	3.63	64.14	1281	5.18	5.65	7.27
37	1.63	1.89	1328.7	45.33	603.57	2.45	4.33	54.67	605	2.45	7.90	4.81
25	0.7	0.81	992.3	12.15	973.69	3.95	5.16	87.85	974	3.94	5.87	5.75
20	0.32	0.37	493.4	7.73	359.01	1.46	5.25	92.27	359	1.45	5.68	2.05
10	0.29	0.34	140.5	0.25	3027.71	12.28	5.34	99.75	3028	12.24	5.35	16.30
Total	86.29	100.00	105	9.09	24653	100.00	3.67	90.91	24739	100.00	4.02	100.00

Appendix 3 Nickel Rim South Table 2 B Metallurgical Balance of Palladium for Stage 2

Size (µm)	CONCENTRATE				TAILS				FEED			
	Weight (g)	% Weight	Grade (g/t)	Rec. (%)	Weight (g)	% Weight	Grade (g/t)	Rec. (%)	Weight (g)	% Weight	Grade (g/t)	Dist'n (%)
300	6.65	5.91	7.2	8.65	336	1.57	1.50	91.35	342	1.60	1.61	0.74
212	23.67	21.03	8.8	10.92	1045	4.90	1.62	89.08	1069	4.98	1.78	2.56
150	27.43	24.37	12.9	9.50	1801	8.44	1.87	90.50	1828	8.52	2.04	5.01
106	20.9	18.57	28.0	9.59	2736	12.82	2.02	90.41	2757	12.85	2.22	8.23
75	14.29	12.69	85.9	20.42	2214	10.38	2.16	79.58	2228	10.39	2.70	8.09
53	9.32	8.28	213.8	28.43	2435	11.41	2.06	71.57	2444	11.40	2.87	9.44
37	5.51	4.89	540.4	55.14	1338	6.27	1.81	44.86	1344	6.26	4.02	7.27
25	2.46	2.19	933.9	32.49	2103	9.86	2.27	67.51	2106	9.82	3.36	9.52
20	1.17	1.04	1255.5	41.00	637	2.98	3.32	59.00	638	2.97	5.62	4.82
10	1.17	1.04	911.8	3.24	6693	31.37	4.76	96.76	6694	31.21	4.92	44.32
Total	112.57	100.00	108.6	16.46	21337	100.00	2.91	83.54	21450	100.00	3.46	100.00

Appendix 3 Nickel Rim South Table 3B **Metallurgical Balance of Palladium for Stage 3**

Size (μm)	CONCENTRATE				TAILS				FEED			
	Weight (g)	% Weight	Grade (g/t)	Rec. (%)	Weight (g)	% Weight	Grade (g/t)	Rec. (%)	Weight (g)	% Weight	Grade (g/t)	Dist'n (%)
212	0.00	0.00	0.0	0.00	0	0.00	0.00	0.00	0	0.00	0.00	0.00
150	1.55	1.86	9.8	13.12	96	0.51	1.05	86.88	97	0.51	1.19	0.21
106	15.81	19.00	8.6	12.09	905	4.82	1.09	87.91	920	4.88	1.22	1.99
75	26.18	31.47	15.5	14.15	1904	10.14	1.29	85.85	1930	10.23	1.48	5.09
53	19.01	22.85	32.1	13.63	2761	14.71	1.40	86.37	2780	14.74	1.61	7.96
37	10.92	13.13	89.9	31.56	1565	8.33	1.36	68.44	1576	8.36	1.97	5.53
25	4.9	5.89	217.8	22.53	2496	13.29	1.47	77.47	2501	13.26	1.89	8.42
20	2.50	3.01	447.2	46.57	720	3.84	1.78	53.43	723	3.83	3.32	4.27
10	2.32	2.79	768.5	4.76	8330	44.36	4.28	95.24	8332	44.18	4.49	66.54
Total	83.19	100.00	73.5	10.87	18777	100.00	2.67	89.13	18860	100.00	2.98	100.00

Appendix 3 Nickel Rim South Table 4B Overall Metallurgical Balance of Paladium (Standard test, 3 stages)

Size (µm)	First Stage: 100% -850 µm Stage Recov.	Dist'n	Rec. g/t	Second Stage: 61.7% -75 µm Stage Recov.	Dist'n	Rec. g/t	Third Stage: 84.4% -75 µm Stage Recov.	Dist'n	Rec. g/t	Losses g/t	Total Recov. g/t	Total Recov. %
850												
600	0.46	9.56	0.002								0.002	0.0
425	0.65	12.43	0.003								0.003	0.1
300	0.69	9.48	0.003	8.65	0.74	0.002					0.005	0.1
212	1.61	10.76	0.007	10.92	2.56	0.010					0.017	0.4
150	3.71	8.33	0.012	9.50	5.01	0.016	13.12	0.21	0.001	0.01	0.030	0.8
106	12.39	7.58	0.038	9.59	8.23	0.027	12.09	1.99	0.007	0.05	0.072	1.9
75	31.57	5.67	0.072	20.42	8.09	0.057	14.15	5.09	0.021	0.13	0.150	3.9
53	35.86	7.27	0.105	28.43	9.44	0.093	13.63	7.96	0.032	0.20	0.230	5.9
37	45.33	4.81	0.088	55.14	7.27	0.138	31.56	5.53	0.052	0.11	0.277	7.1
25	12.15	5.75	0.028	32.49	9.52	0.107	22.53	8.42	0.056	0.19	0.191	4.9
20	7.73	2.05	0.006	41.00	4.82	0.068	46.57	4.27	0.059	0.07	0.133	3.4
15	0.25	16.30	0.002	3.24	44.32	0.050	4.76	66.54	0.094	1.87	0.145	3.7
Total	9.4	100.0	0.37	16.1	100.0	0.568	10.8	100.0	0.321	2.64	1.255	32.3
O/A	9.4	9.4		14.5	14.6		8.3					
Yield	0.00349			0.00525			0.00441					
Grade	4.019g/t			3.46g/t			2.98g/t					
Calc.:	3.890g/t											

Appendix 3 Nickel Rim South Table 5B Metallurgical Balance of Palladium for Stage 4

Size (µm)	CONCENTRATE				TAILS				FEED			
	Weight (g)	% Weight	Grade (g/t)	Rec. (%)	Weight (g)	% Weight	Grade (g/t)	Rec. (%)	Weight (g)	% Weight	Grade (g/t)	Dist'n (%)
212	0.00	0.00	0.0	0.00	0	0.00	0.00	0.00	0	0.00	0.00	0.00
150	1.72	1.34	3.3	6.29	85.29	0.51	1.00	93.71	87	0.52	1.05	0.21
106	14.49	11.25	5.3	7.90	837.79	5.02	1.06	92.10	852	5.07	1.13	2.17
75	40.36	31.35	6.8	11.69	1734.87	10.39	1.20	88.31	1775	10.55	1.33	5.31
53	39.31	30.53	10.3	10.49	2581.61	15.47	1.34	89.51	2621	15.58	1.47	8.71
37	18.01	13.99	17.9	15.74	1438.45	8.62	1.20	84.26	1456	8.66	1.41	4.62
25	7.43	5.77	46.0	11.54	2222.55	13.32	1.18	88.46	2230	13.26	1.33	6.68
20	3.68	2.86	169.6	46.28	646.80	3.88	1.12	53.72	650	3.87	2.07	3.04
10	3.75	2.91	1164.2	14.21	7143.89	42.80	3.69	85.79	7148	42.49	4.30	69.26
Total	128.75	100.00	49.8	14.46	16691	100.00	2.27	85.54	16820	100.00	2.64	100.00

Appendix 3 Nickel Rim South Table 6B Overall Metallurgical Balance for Palladium (Four recovery stages)

Size (µm)	First Stage: 100% -850 µm			Second Stage: 61.7% -75 µm			Third Stage: 84.4% -75 µm			Four stage 84.1% -75 µm				Total	Total
	Stage Recov.	Dist'n	Rec. g/t	Stage Recov.	Dist'n	Rec. g/t	Stage Recov.	Dist'n	Rec. g/t	Stage Recov.	Dist'n	Rec. g/t	Losses g/t	Recov. g/t	Recov. %
850															
600	0.46	9.56	0.002											0.002	0.0
425	0.65	12.43	0.003											0.003	0.1
300	0.69	9.48	0.003	8.65	0.74	0.002								0.005	0.1
212	1.61	10.76	0.007	10.92	2.56	0.010								0.017	0.4
150	3.71	8.33	0.012	9.50	5.01	0.016	13.12	0.21	0.001	6.29	0.21	0.000	0.01	0.030	0.8
106	12.39	7.58	0.038	9.59	8.23	0.027	12.09	1.99	0.007	7.90	2.17	0.004	0.05	0.077	2.0
75	31.57	5.67	0.072	20.42	8.09	0.057	14.15	5.09	0.021	11.69	5.31	0.016	0.12	0.166	4.3
53	35.86	7.27	0.105	28.43	9.44	0.093	13.63	7.96	0.032	10.49	8.71	0.024	0.20	0.253	6.6
37	45.33	4.81	0.088	55.14	7.27	0.138	31.56	5.53	0.052	15.74	4.62	0.019	0.10	0.296	7.7
25	12.15	5.75	0.028	32.49	9.52	0.107	22.53	8.42	0.056	11.54	6.68	0.020	0.15	0.211	5.5
20	7.73	2.05	0.006	41.00	4.82	0.068	46.57	4.27	0.059	46.28	3.04	0.037	0.04	0.170	4.4
15	0.25	16.30	0.002	3.24	44.32	0.050	4.76	66.54	0.094	14.21	69.26	0.256	1.55	0.401	10.4
Total	9.5	100.0	0.37	16.3	100.0	0.568	10.8	100.0	0.321	14.27	100.0	0.377	2.23	1.631	42.3
O/A	9.5	9.4		14.7	14.7		8.3			9.8					
Yield	0.0035			0.0052			0.0044			0.0077					
Grade	4.019g/t			3.46g/t			2.98g/t			2.64g/t					
Calc.:	3.858g/t														

Appendix 4 Clarabelle Table 1A Metallurgical Balance of Platinum for Stage 1

Size (µm)	CONCENTRATE				TAILS				FEED			
	Weight (g)	% Weight	Grade (g/t)	Rec. (%)	Weight (g)	% Weight	Grade (g/t)	Rec. (%)	Weight (g)	% Weight	Grade (g/t)	Dist'n (%)
850	0.00	0.00	0.0	0.00	0	0.00	0.00	0.00	0	0.00	0.00	0.00
600	15.52	14.92	5	4.77	7854	13.71	0.20	95.23	7870	13.71	0.21	3.80
425	18.39	17.67	80	21.77	8865	15.47	0.60	78.23	8883	15.48	0.77	15.68
300	18.28	17.57	101	28.38	6637	11.58	0.70	71.62	6655	11.59	0.97	14.96
212	16.24	15.61	152	55.97	6465	11.28	0.30	44.03	6481	11.29	0.68	10.16
150	11.58	11.13	208	54.56	5019	8.76	0.40	45.44	5030	8.76	0.88	10.19
106	7.93	7.62	323	57.91	4654	8.12	0.40	42.09	4661	8.12	0.95	10.20
75	5.6	5.38	438	78.19	3421	5.97	0.20	21.81	3426	5.97	0.92	7.23
53	4.2	4.04	408	51.38	4055	7.08	0.40	48.62	4059	7.07	0.82	7.69
37	3.29	3.16	438	50.03	2878	5.02	0.50	49.97	2882	5.02	1.00	6.64
25	1.53	1.47	286	23.74	2343	4.09	0.60	76.26	2344	4.08	0.79	4.25
20	0.61	0.59	147	8.48	968	1.69	1.00	91.52	969	1.69	1.09	2.44
10	0.88	0.85	34	1.02	4138	7.22	0.70	98.98	4139	7.21	0.71	6.75
Total	104.05	100.00	163	39.21	57296	100.00	0.46	60.79	57400	100.00	0.76	100.00

Appendix 4 Clarabelle Table 2 A Metallurgical Balance of Platinum for Stage 2

Size (µm)	CONCENTRATE				TAILS				FEED			
	Weight (g)	% Weight	Grade (g/t)	Rec. (%)	Weight (g)	% Weight	Grade (g/t)	Rec. (%)	Weight (g)	% Weight	Grade (g/t)	Dist'n (%)
300	15.19	12.97	1.2	11.63	346	1.34	0.40	88.37	361	1.39	0.43	1.40
212	26.96	23.02	3.8	27.61	1343	5.18	0.20	72.39	1370	5.26	0.27	3.31
150	23.75	20.27	8.0	17.70	2208	8.52	0.40	82.30	2232	8.57	0.48	9.56
106	18.26	15.59	24.6	39.72	3408	13.15	0.20	60.28	3427	13.16	0.33	10.08
75	12.52	10.69	45.1	49.46	2885	11.13	0.20	50.54	2897	11.13	0.39	10.17
53	8.66	7.39	80.5	67.29	3389	13.08	0.10	32.71	3398	13.05	0.30	9.23
37	5.84	4.99	126.0	55.25	2980	11.50	0.20	44.75	2986	11.47	0.45	11.87
25	3.03	2.59	187.0	40.57	2767	10.68	0.30	59.43	2770	10.64	0.50	12.44
20	1.47	1.25	203.0	54.95	815	3.15	0.30	45.05	817	3.14	0.66	4.84
10	1.46	1.25	107.0	5.14	5771	22.27	0.50	94.86	5773	22.18	0.53	27.10
Total	117.14	100.00	32.3	33.67	25913	100.00	0.29	66.33	26030	100.00	0.43	100.00

Appendix 4 Clarabelle Table 3A Metallurgical Balance of Platinum for Stage 3

Size (μm)	CONCENTRATE				TAILS				FEED			
	Weight (g)	% Weight	Grade (g/t)	Rec. (%)	Weight (g)	% Weight	Grade (g/t)	Rec. (%)	Weight (g)	% Weight	Grade (g/t)	Dist'n (%)
212	0.00	0.00	0.0	0.00	0	0.00	0.00	0.00	0	0.00	0.00	0.00
150	4.24	4.16	0.8	7.69	204	0.88	0.20	92.31	208	0.90	0.21	0.67
106	20.18	19.78	1.4	18.17	1272	5.52	0.10	81.83	1293	5.59	0.12	2.36
75	29.59	29.00	1.5	7.85	2604	11.30	0.20	92.15	2634	11.38	0.21	8.60
53	20.68	20.27	7.2	28.59	3720	16.15	0.10	71.41	3740	16.16	0.14	7.92
37	12.9	12.64	17.1	40.60	3227	14.01	0.10	59.40	3240	14.00	0.17	8.26
25	6.88	6.74	46.5	48.86	3349	14.54	0.10	51.14	3356	14.50	0.20	9.96
20	3.58	3.51	88.4	66.66	791	3.44	0.20	33.34	795	3.44	0.60	7.22
10	3.97	3.89	118.0	12.95	7870	34.16	0.40	87.05	7874	34.03	0.46	55.00
Total	102.02	100.00	15.2	23.58	23038	100.00	0.22	76.42	23140	100.00	0.28	100.00

Appendix 4 Clarabelle Table 4A Overall Metallurgical Balance of Platinum (Standard test, 3 stages)

Size (µm)	First Stage: 100% -850 µm Stage Recov.	Dist'n	Rec. g/t	Second Stage: 49.0% -75 µm Stage Recov.	Dist'n	Rec. g/t	Third Stage: 79.0% -75 µm Stage Recov.	Dist'n	Rec. g/t	Losses g/t	Total Recov. g/t	Total Recov. %
850												
600	4.77	3.80	0.001								0.001	0.2
425	21.77	15.68	0.026								0.026	3.6
300	28.38	14.96	0.032	11.63	1.40	0.001					0.033	4.5
212	55.97	10.16	0.043	27.61	3.31	0.004					0.047	6.5
150	54.56	10.19	0.042	17.70	9.56	0.007	7.69	0.67	0.000	0.00	0.049	6.8
106	57.91	10.20	0.045	39.72	10.08	0.017	18.17	2.36	0.001	0.01	0.063	8.7
75	78.19	7.23	0.043	49.46	10.17	0.022	7.85	8.60	0.002	0.02	0.066	9.2
53	51.38	7.69	0.030	67.29	9.23	0.027	28.59	7.92	0.006	0.02	0.063	8.7
37	50.03	6.64	0.025	55.25	11.87	0.028	40.60	8.26	0.009	0.01	0.063	8.7
25	23.74	4.25	0.008	40.57	12.44	0.022	48.86	9.96	0.014	0.01	0.043	6.0
20	8.48	2.44	0.002	54.95	4.84	0.011	66.66	7.22	0.014	0.01	0.027	3.7
15	1.02	6.75	0.001	5.14	27.10	0.006	12.95	55.00	0.020	0.14	0.027	3.7
Total	40.9	100.0	0.30	33.9	100.0	0.145	23.4	100.0	0.067	0.22	0.508	70.2
O/A	40.9	40.9		20.0	20.0		9.2					
Yield	0.00181			0.00450			0.00441					
Grade	0.755g/t			0.43g/t			0.28g/t					
Calc.:	0.723g/t											

Appendix 4 Clarabelle Table 5A Metallurgical Balance of Platinum for Stage 4

Size (µm)	CONCENTRATE				TAILS				FEED			
	Weight (g)	% Weight	Grade (g/t)	Rec. (%)	Weight (g)	% Weight	Grade (g/t)	Rec. (%)	Weight (g)	% Weight	Grade (g/t)	Dist'n (%)
212	0.00	0.00	0.0	0.00	0	0.00	0.00	0.00	0	0.00	0.00	0.00
150	5.08	5.11	0.5	5.67	211	0.98	0.20	94.33	216	1.00	0.21	1.18
106	21.3	21.44	0.4	5.80	1383	6.42	0.10	94.20	1405	6.49	0.10	3.87
75	27.51	27.69	0.9	8.89	2537	11.77	0.10	91.11	2565	11.85	0.11	7.33
53	20.4	20.53	2.7	13.02	3681	17.08	0.10	86.98	3701	17.10	0.11	11.14
37	11.55	11.62	5.7	18.23	2953	13.70	0.10	81.77	2964	13.69	0.12	9.51
25	5.75	5.79	14.9	27.27	2856	13.25	0.08	72.73	2862	13.22	0.11	8.27
20	3.28	3.30	43.4	61.88	877	4.07	0.10	38.12	880	4.07	0.26	6.06
10	4.49	4.52	131.0	29.43	7052	32.72	0.20	70.57	7057	32.59	0.28	52.63
Total	99.36	100.00	9.8	25.62	21551	100.00	0.13	74.38	21650	100.00	0.18	100.00

Appendix 4 Clarabelle Table 6A Overall Metallurgical Balance for Platinum (Four recovery stages)

Size (µm)	First Stage: 100% -850 µm			Second Stage: 49.0% -75 µm			Third Stage: 79.0% -75 µm			Four stage: 80.06% -75 µm				Total	Total
	Stage Recov.	Dist'n	Rec. g/t	Stage Recov.	Dist'n	Rec. g/t	Stage Recov.	Dist'n	Rec. g/t	Stage Recov.	Dist'n	Rec. g/t	Losses g/t	Recov. g/t	Recov. %
850															
600	4.77	3.80	0.001											0.001	0.2
425	21.77	15.68	0.026											0.026	3.8
300	28.38	14.96	0.032	11.63	1.40	0.001								0.033	4.8
212	55.97	10.16	0.043	27.61	3.31	0.004								0.047	6.9
150	54.56	10.19	0.042	17.70	9.56	0.007	7.69	0.67	0.000	5.67	1.18	0.000	0.00	0.050	7.3
106	57.91	10.20	0.045	39.72	10.08	0.017	18.17	2.36	0.001	5.80	3.87	0.000	0.01	0.063	9.3
75	78.19	7.23	0.043	49.46	10.17	0.022	7.85	8.60	0.002	8.89	7.33	0.001	0.01	0.067	9.9
53	51.38	7.69	0.030	67.29	9.23	0.027	28.59	7.92	0.006	13.02	11.14	0.003	0.02	0.065	9.6
37	50.03	6.64	0.025	55.25	11.87	0.028	40.60	8.26	0.009	18.23	9.51	0.003	0.01	0.066	9.7
25	23.74	4.25	0.008	40.57	12.44	0.022	48.86	9.96	0.014	27.27	8.27	0.004	0.01	0.047	6.9
20	8.48	2.44	0.002	54.95	4.84	0.011	66.66	7.22	0.014	61.88	6.06	0.007	0.00	0.033	4.9
15	1.02	6.75	0.001	5.14	27.10	0.006	12.95	55.00	0.020	29.43	52.63	0.027	0.06	0.054	7.9
Total	43.5	100.0	0.30	37.6	100.0	0.145	23.4	100.0	0.067	25.35	100.0	0.044	0.13	0.552	81.1
O/A	43.5	43.4		21.2	21.3		9.8			6.5					
Yield	0.0018			0.0045			0.0044			0.0046					
Grade	0.755g/t			0.43g/t			0.28g/t			0.18g/t					
Calc.:	0.681g/t														

Appendix 4 Clarabelle Table 1B Metallurgical Balance of Palladium for Stage 1

Size (µm)	CONCENTRATE				TAILS				FEED			
	Weight (g)	% Weight	Grade (g/t)	Rec. (%)	Weight (g)	% Weight	Grade (g/t)	Rec. (%)	Weight (g)	% Weight	Grade (g/t)	Dist'n (%)
850	0.00	0.00	0.0	0.00	0	0.00	0.00	0.00	0	0.00	0.00	0.00
600	15.52	14.92	0.2	0.06	7854.20	13.71	0.50	99.94	7870	13.71	0.50	10.49
425	18.39	17.67	2.2	0.66	8864.95	15.47	0.70	99.34	8883	15.48	0.70	16.67
300	18.28	17.57	8.3	3.68	6637.03	11.58	0.60	96.32	6655	11.59	0.62	11.03
212	16.24	15.61	27	12.05	6464.67	11.28	0.50	87.95	6481	11.29	0.57	9.81
150	11.58	11.13	46	15.01	5018.67	8.76	0.60	84.99	5030	8.76	0.70	9.46
106	7.93	7.62	88	23.07	4653.51	8.12	0.50	76.93	4661	8.12	0.65	8.07
75	5.60	5.38	144	44.00	3420.76	5.97	0.30	56.00	3426	5.97	0.53	4.89
53	4.20	4.04	153	24.07	4054.66	7.08	0.50	75.93	4059	7.07	0.66	7.13
37	3.29	3.16	161	26.90	2878.38	5.02	0.50	73.10	2882	5.02	0.68	5.25
25	1.53	1.47	88	6.67	2342.82	4.09	0.80	93.33	2344	4.08	0.86	5.36
20	0.61	0.59	41	3.57	967.90	1.69	0.70	96.43	969	1.69	0.73	1.88
10	0.88	0.85	13	0.31	4138.40	7.22	0.90	99.69	4139	7.21	0.90	9.97
Total	104.05	100.00	39	10.72	57296	100.00	0.58	89.28	57400	100.00	0.65	100.00

Appendix 4 Clarabelle Table 2 B Metallurgical Balance of Palladium for Stage 2

Size (µm)	CONCENTRATE				TAILS				FEED			
	Weight (g)	% Weight	Grade (g/t)	Rec. (%)	Weight (g)	% Weight	Grade (g/t)	Rec. (%)	Weight (g)	% Weight	Grade (g/t)	Dist'n (%)
300	15.19	12.97	0.9	11.63	346	1.34	0.30	88.37	361	1.39	0.33	0.95
212	26.96	23.02	1.7	14.58	1343	5.18	0.20	85.42	1370	5.26	0.23	2.53
150	23.75	20.27	3.0	13.89	2208	8.52	0.20	86.11	2232	8.57	0.23	4.13
106	18.26	15.59	5.0	8.20	3408	13.15	0.30	91.80	3427	13.16	0.33	8.98
75	12.52	10.69	10.1	17.98	2885	11.13	0.20	82.02	2897	11.13	0.24	5.67
53	8.66	7.39	21.1	21.23	3389	13.08	0.20	78.77	3398	13.05	0.25	6.94
37	5.84	4.99	45.1	30.65	2980	11.50	0.20	69.35	2986	11.47	0.29	6.93
25	3.03	2.59	71.6	20.72	2767	10.68	0.30	79.28	2770	10.64	0.38	8.44
20	1.47	1.25	88.0	28.40	815	3.15	0.40	71.60	817	3.14	0.56	3.67
10	1.46	1.25	49.0	1.11	5771	22.27	1.10	98.89	5773	22.18	1.11	51.76
Total	117.14	100.00	10.4	9.77	25913	100.00	0.43	90.23	26030	100.00	0.48	100.00

Appendix 4 Clarabelle Table 3B Metallurgical Balance of Palladium for Stage 3

Size (µm)	CONCENTRATE				TAILS				FEED			
	Weight (g)	% Weight	Grade (g/t)	Rec. (%)	Weight (g)	% Weight	Grade (g/t)	Rec. (%)	Weight (g)	% Weight	Grade (g/t)	Dist'n (%)
212	0.00	0.00	0.0	0.00	0	0.00	0.00	0.00	0	0.00	0.00	0.00
150	4.24	4.16	1.9	11.65	204	0.88	0.30	88.35	208	0.90	0.33	0.62
106	20.18	19.78	0.8	4.06	1272	5.52	0.30	95.94	1293	5.59	0.31	3.55
75	29.59	29.00	1.0	3.65	2604	11.30	0.30	96.35	2634	11.38	0.31	7.24
53	20.68	20.27	2.1	3.75	3720	16.15	0.30	96.25	3740	16.16	0.31	10.35
37	12.9	12.64	5.2	9.41	3227	14.01	0.20	90.59	3240	14.00	0.22	6.36
25	6.88	6.74	16.1	9.93	3349	14.54	0.30	90.07	3356	14.50	0.33	9.96
20	3.58	3.51	36.3	35.37	791	3.44	0.30	64.63	795	3.44	0.46	3.28
10	3.97	3.89	68.4	4.13	7870	34.16	0.80	95.87	7874	34.03	0.83	58.64
Total	102.02	100.00	6.6	6.04	23038	100.00	0.46	93.96	23140	100.00	0.48	100.00

Appendix 4 Clarabelle Table 4B Overall Metallurgical Balance of Paladium (Standard test, 3 stages)

Size (µm)	First Stage: 100% -850 µm			Second Stage: 49.0% -75 µm			Third Stage: 79.0% -75 µm				Total	Total
	Stage Recov.	Dist'n	Rec. g/t	Stage Recov.	Dist'n	Rec. g/t	Stage Recov.	Dist'n	Rec. g/t	Losses g/t	Recov. g/t	Recov. %
850												
600	0.06	10.49	0.000								0.000	0.0
425	0.66	16.67	0.001								0.001	0.1
300	3.68	11.03	0.003	11.63	0.95	0.001					0.003	0.5
212	12.05	9.81	0.008	14.58	2.53	0.002					0.009	1.6
150	15.01	9.46	0.009	13.89	4.13	0.003	11.65	0.62	0.000	0.00	0.012	2.1
106	23.07	8.07	0.012	8.20	8.98	0.004	4.06	3.55	0.001	0.02	0.016	2.7
75	44.00	4.89	0.014	17.98	5.67	0.005	3.65	7.24	0.001	0.03	0.020	3.4
53	24.07	7.13	0.011	21.23	6.94	0.007	3.75	10.35	0.002	0.05	0.020	3.4
37	26.90	5.25	0.009	30.65	6.93	0.010	9.41	6.36	0.003	0.03	0.022	3.7
25	6.67	5.36	0.002	20.72	8.44	0.008	9.93	9.96	0.005	0.04	0.015	2.6
20	3.57	1.88	0.000	28.40	3.67	0.005	35.37	3.28	0.006	0.01	0.011	1.8
15	0.31	9.97	0.000	1.11	51.76	0.003	4.13	58.64	0.012	0.27	0.015	2.4
Total	11.7	100.0	0.07	8.8	100.0	0.046	6.0	100.0	0.029	0.45	0.146	24.4
O/A	11.7	11.7		7.8	7.8		4.9					
Yield	0.00181			0.00450			0.00441					
Grade	0.653g/t			0.48g/t			0.48g/t					
Calc.:	0.597g/t											

Appendix 4 Clarabelle Table 5B Metallurgical Balance of Palladium for Stage 4

Size (μm)	CONCENTRATE				TAILS				FEED			
	Weight (g)	% Weight	Grade (g/t)	Rec. (%)	Weight (g)	% Weight	Grade (g/t)	Rec. (%)	Weight (g)	% Weight	Grade (g/t)	Dist'n (%)
212	0.00	0.00	0.0	0	0.00	0	0.00	0.00	0	0.00	0	0.00
150	5.08	5.11	0.3	1.52	3.48	211.23	0.98	0.20	42	96.52	216	1.00
106	21.3	21.44	0.4	8.52	2.99	1383.42	6.42	0.20	277	97.01	1405	6.49
75	27.51	27.69	1.0	27.51	5.14	2537.29	11.77	0.20	507	94.86	2565	11.85
53	20.4	20.53	1.6	32.64	4.25	3680.74	17.08	0.20	736	95.75	3701	17.10
37	11.55	11.62	2.8	32.34	5.19	2952.93	13.70	0.20	591	94.81	2964	13.69
25	5.75	5.79	8.2	47.15	7.63	2855.94	13.25	0.20	571	92.37	2862	13.22
20	3.28	3.30	27.3	89.54	33.80	876.90	4.07	0.20	175	66.20	880	4.07
10	4.49	4.52	101.0	453.49	9.68	7052.19	32.72	0.60	4231	90.32	7057	32.59
Total	99.36	100.00	7.0	692.72	8.85	21551	100.00	0.33	7131	91.15	21650	100.00

Appendix 4 Clarabelle Table 6B Overall Metallurgical Balance for Palladium (Four recovery stages)

Size (µm)	First Stage: 100% -850 µm			Second Stage: 49.0% -75 µm			Third Stage: 79.0% -75 µm			Four stage: 80.06% -75 µm				Total	Total
	Stage Recov.	Dist'n	Rec. g/t	Stage Recov.	Dist'n	Rec. g/t	Stage Recov.	Dist'n	Rec. g/t	Stage Recov.	Dist'n	Rec. g/t	Losses g/t	Recov. g/t	Recov. %
850															
600	0.06	10.49	0.000											0.000	0.0
425	0.66	16.67	0.001											0.001	0.1
300	3.68	11.03	0.003	11.63	0.95	0.001								0.003	0.6
212	12.05	9.81	0.008	14.58	2.53	0.002								0.009	1.9
150	15.01	9.46	0.009	13.89	4.13	0.003	11.65	0.62	0.000	3.48	0.56	0.000	0.00	0.012	2.5
106	23.07	8.07	0.012	8.20	8.98	0.004	4.06	3.55	0.001	2.99	3.65	0.000	0.01	0.017	3.3
75	44.00	4.89	0.014	17.98	5.67	0.005	3.65	7.24	0.001	5.14	6.84	0.001	0.02	0.021	4.3
53	24.07	7.13	0.011	21.23	6.94	0.007	3.75	10.35	0.002	4.25	9.83	0.001	0.03	0.022	4.3
37	26.90	5.25	0.009	30.65	6.93	0.010	9.41	6.36	0.003	5.19	7.96	0.001	0.03	0.024	4.7
25	6.67	5.36	0.002	20.72	8.44	0.008	9.93	9.96	0.005	7.63	7.90	0.002	0.03	0.018	3.5
20	3.57	1.88	0.000	28.40	3.67	0.005	35.37	3.28	0.006	33.80	3.39	0.004	0.01	0.015	3.0
15	0.31	9.97	0.000	1.11	51.76	0.003	4.13	58.64	0.012	9.68	59.88	0.021	0.19	0.035	7.0
Total	13.9	100.0	0.07	10.7	100.0	0.046	6.0	100.0	0.029	8.76	100.0	0.032	0.33	0.177	35.2
O/A	13.9	13.9		9.2	9.2		5.8			6.3					
Yield	0.0018			0.0045			0.0044			0.0046					
Grade	0.653g/t			0.48g/t			0.48g/t			0.36g/t					
Calc.:	0.503g/t														

Appendix 5 Mass Balance of measuring the stream GRPGM for the Survey #1 at Clarabelle Mill

The mass balance of hydrosizing results for the ball mill discharge

Size , µm	Product	Mass (g)	Mass (%)	Grade (0z/st)	Unit	Rec. (%)	Enrichment
+600	Conc.	1.38	45.70	0.0150	0.69	71.6	1.6
	Tailing	1.64	54.30	0.0050	0.27	28.4	
	Total	3.02	100.00	0.0096	0.96	100.0	
425-600	Conc.	1.78	29.62	1.4700	43.54	79.7	2.7
	Tailing	4.23	70.38	0.1580	11.12	20.3	
	Total	6.01	100.00	0.5466	54.66	100.0	
300-425	Conc.	2.19	15.03	0.0140	0.21	9.7	0.6
	Tailing	12.38	84.97	0.0230	1.95	90.3	
	Total	14.57	100.00	0.0216	2.16	100.0	
212-300	Conc.	1.99	11.15	1.1300	12.60	82.5	7.4
	Tailing	15.85	88.85	0.0300	2.67	17.5	
	Total	17.84	100.00	0.1527	15.27	100.0	
150-212	Conc.	1.13	4.98	75.7900	377.11	85.7	17.2
	Tailing	21.58	95.02	0.6610	62.81	14.3	
	Total	22.71	100.00	4.3993	439.93	100.0	

Ball mill discharge ---Standard KC Operation Mass Balance

Size (µm)	CONCENTRATE				TAILS				FEED			
	Mass (g)	Mass (%)	Grade (Pt oz/st)	Pt Rec %	Mass (g)	Mass (%)	Grade (Pt oz/st)	Pt Rec %	Mass (g)	Mass (%)	Grade (Pt oz/st)	Au Dist'n %
600	3.02	3.02	0.0096	3.15	162	1.36	0.0055	96.85	165	1.37	0.006	0.09
425	6.01	6.00	0.5466	49.63	445	3.72	0.0075	50.37	451	3.74	0.015	0.68
300	14.57	14.55	0.0216	3.42	889	7.44	0.0100	96.58	903	7.50	0.010	0.94
212	17.84	17.81	0.1527	10.21	1712	14.34	0.0140	89.79	1730	14.37	0.015	2.74
150	22.71	22.67	4.3993	79.15	2025	16.95	0.0130	20.85	2047	17.00	0.062	12.94
106	13.45	13.43	2.6000	48.03	2102	17.60	0.0180	51.97	2116	17.57	0.034	7.46
75	11.50	11.48	20.5600	87.77	1267	10.61	0.0260	12.23	1278	10.61	0.211	27.61
53	4.86	4.85	35.5900	78.74	1015	8.50	0.0460	21.26	1020	8.47	0.215	22.52
38	2.84	2.84	30.2100	62.88	618	5.17	0.0820	37.12	620	5.15	0.220	13.99
25	1.49	1.49	8.9300	27.42	457	3.83	0.0770	72.58	459	3.81	0.106	4.97
20	0.47	0.47	2.1200	7.09	185	1.55	0.0700	92.91	186	1.54	0.075	1.43
-20	1.40	1.40	0.2090	0.65	1065	8.92	0.0420	99.35	1067	8.86	0.042	4.62
Total	**100.16**	**100.00**	**6.500**	66.74	**11942**	**100.00**	**0.027**	**33.26**	**12042**	**100.00**	**0.081**	**100.00**

Ball mill discharge--- Variable Speed KC Operation Mass Balance

Size (µm)	CONCENTRATE				TAILS				FEED			
	Mass (g)	Mass (%)	Grade (Pt oz/st)	Pt Rec %	Mass (g)	Mass (%)	Grade (Pt oz/st)	Pt Rec %	Mass (g)	Mass (%)	Grade (Pt oz/st)	Au Dist'n %
212	14.30	14.45	0.011	2.00	1149	13.21	0.0067	98.00	1162.84	13.23	0.007	2.97
150	27.78	28.07	0.050	10.30	1920	22.08	0.0063	89.70	1947.47	22.15	0.007	5.10
106	23.67	23.92	0.290	20.59	1891	21.75	0.0140	79.41	1914.46	21.78	0.017	12.62
75	15.04	15.20	1.090	48.28	1098	12.63	0.0160	51.72	1112.66	12.66	0.031	12.85
53	7.55	7.63	4.420	70.77	862	9.91	0.0160	29.23	869.08	9.88	0.054	17.85
38	4.92	4.97	9.110	86.23	511	5.88	0.0140	13.77	516.03	5.87	0.101	19.68
25	3.07	3.10	8.740	84.31	384	4.42	0.0130	15.69	387.15	4.40	0.082	12.05
20	0.96	0.97	9.060	81.18	134	1.55	0.0150	18.82	135.39	1.54	0.079	4.06
-20	1.67	1.69	5.990	29.55	745	8.57	0.0320	70.45	746.92	8.50	0.045	12.82
Total	**98.96**	**100.00**	**1.501**	**56.23**	**8693**	**100.00**	**0.0133**	**43.77**	**8792**	**100.00**	**0.030**	**100.00**

Primary fine --- Standard KC Operation Mass Balance

Size (µm)	CONCENTRATE Mass (g)	Mass (%)	Grade (Pt oz/st)	Pt Rec %	TAILS Mass (g)	Mass (%)	Grade (Pt oz/st)	Pt Rec %	FEED Mass (g)	Mass (%)	Grade (Pt oz/st)	Au Dist'n %
600	17.64	15.54	0.03	0.66	1413	12.64	0.0522	99.34	1430	12.67	0.052	14.50
425	22.36	19.70	0.50	25.68	2023	18.10	0.0160	74.32	2045	18.12	0.021	8.53
300	25.73	22.66	1.71	60.55	1918	17.16	0.0149	39.45	1943	17.22	0.037	14.17
212	17.17	15.12	3.24	57.00	1780	15.93	0.024	43.00	1797	15.92	0.054	19.08
150	13.03	11.48	3.81	84.05	1109	9.92	0.008	15.95	1122	9.94	0.053	11.54
106	6.91	6.09	6.22	81.37	790	7.07	0.012	18.63	797	7.06	0.066	10.32
75	4.55	4.01	8.57	83.09	485	4.34	0.016	16.91	490	4.34	0.096	9.17
53	2.72	2.40	6.86	73.49	456	4.08	0.015	26.51	459	4.07	0.055	4.96
38	1.67	1.47	3.96	50.66	305	2.73	0.021	49.34	307	2.72	0.042	2.55
25	0.87	0.77	1.95	23.42	205	1.84	0.027	76.58	206	1.83	0.035	1.41
20	0.26	0.23	0.58	3.39	107	0.96	0.041	96.61	107	0.95	0.042	0.89
-20	0.61	0.54	0.19	0.79	583	5.22	0.025	99.21	584	5.17	0.025	2.88
Total	**113.52**	**100.00**	**2.379**	52.78	**11174**	**100.00**	**0.022**	**47.22**	**11288**	**100.00**	**0.045**	**100.00**

Primary fine --- Variable Speed KC Operation Mass Balance

Size (µm)	CONCENTRATE Mass (g)	Mass (%)	Grade (Pt oz/st)	Pt Rec %	TAILS Mass (g)	Mass (%)	Grade (Pt oz/st)	Pt Rec %	FEED Mass (g)	Mass (%)	Grade (Pt oz/st)	Au Dist'n %
212	28.14	22.97	0.021	2.33	1053	22.87	0.0237	97.67	1080.85	22.88	0.024	30.34
150	35.05	28.61	0.011	4.46	947	20.58	0.0084	95.54	982.23	20.79	0.008	9.93
106	22.12	18.06	0.039	10.04	671	14.59	0.0116	89.96	693.56	14.68	0.012	10.28
75	15.30	12.49	0.192	40.91	425	9.23	0.0100	59.09	440.19	9.32	0.016	8.56
53	8.90	7.26	0.379	52.97	423	9.18	0.0071	47.03	431.45	9.13	0.015	7.58
38	5.78	4.72	0.843	75.71	299	6.51	0.0052	24.29	305.20	6.46	0.021	7.66
25	3.98	3.25	1.321	83.58	229	4.98	0.0045	16.42	233.05	4.93	0.027	7.48
20	1.30	1.06	2.059	81.21	79	1.72	0.0078	18.79	80.60	1.71	0.041	3.92
-20	1.94	1.58	1.882	30.51	476	10.34	0.0175	69.49	477.87	10.11	0.025	14.24
Total	**122.51**	**100.00**	**0.201**	**29.28**	**4602**	**100.00**	**0.0129**	**70.72**	**4725**	**100.00**	**0.018**	**100.00**

SAG U/F --- Standard KC Operation Mass Balance

Size (µm)	CONCENTRATE Mass (g)	Mass (%)	Grade (Pt oz/st)	Pt Rec %	TAILS Mass (g)	Mass (%)	Grade (Pt oz/st)	Pt Rec %	FEED Mass (g)	Mass (%)	Grade (Pt oz/st)	Au Dist'n %
600	8.06	8.52	0.007	1.17	474	3.97	0.0093	98.83	482	4.01	0.009	1.75
425	10.92	11.54	0.116	11.45	806	6.76	0.0122	88.55	817	6.80	0.014	4.35
300	16.13	17.05	0.130	9.70	934	7.83	0.0209	90.30	950	7.91	0.023	8.48
212	14.17	14.97	0.421	33.82	1227	10.29	0.010	66.18	1241	10.33	0.014	6.91
150	14.03	14.83	0.584	34.56	1128	9.46	0.014	65.44	1142	9.50	0.021	9.30
106	8.12	8.58	0.606	21.62	1206	10.11	0.015	78.38	1214	10.10	0.019	8.92
75	8.76	9.26	2.240	63.95	1032	8.66	0.011	36.05	1041	8.66	0.029	12.03
53	5.36	5.66	1.950	43.54	1157	9.70	0.012	56.46	1162	9.67	0.021	9.41
38	3.82	4.04	1.490	33.37	891	7.47	0.013	66.63	894	7.44	0.019	6.69
25	2.44	2.58	1.570	11.09	890	7.46	0.035	88.91	892	7.42	0.039	13.54
20	0.75	0.80	1.140	13.84	238	2.00	0.022	86.16	239	1.99	0.026	2.43
-20	2.07	2.18	0.308	1.54	1942	16.29	0.021	98.46	1944	16.18	0.021	16.18
Total	**94.63**	**100.00**	**0.672**	24.94	**11924**	**100.00**	**0.016**	**75.06**	**12019**	**100.00**	**0.021**	**100.00**

SAG U/F --- Variable Speed KC Operation Mass Balance

Size (µm)	CONCENTRATE Mass (g)	Mass (%)	Grade (Pt oz/st)	Pt Rec %	TAILS Mass (g)	Mass (%)	Grade (Pt oz/st)	Pt Rec %	FEED Mass (g)	Mass (%)	Grade (Pt oz/st)	Au Dist'n %
212	10.96	11.59	0.010	1.70	665	8.39	0.0095	98.30	676.16	8.43	0.010	5.24
150	21.08	22.30	0.053	7.32	1087	13.71	0.0130	92.68	1108.42	13.81	0.014	12.43
106	20.28	21.45	0.109	12.22	1202	15.16	0.0132	87.78	1222.70	15.24	0.015	14.73
75	14.00	14.81	0.186	22.65	1059	13.35	0.0084	77.35	1072.65	13.37	0.011	9.37
53	10.46	11.06	0.321	31.65	895	11.29	0.0081	68.35	905.82	11.29	0.012	8.64
38	7.52	7.95	0.693	51.88	780	9.83	0.0062	48.12	787.12	9.81	0.013	8.18
25	5.32	5.63	1.320	83.85	237	2.99	0.0057	16.15	242.61	3.02	0.035	6.82
20	1.77	1.87	2.500	70.35	278	3.51	0.0067	29.65	280.14	3.49	0.022	5.12
-20	3.15	3.33	2.770	24.12	1726	21.77	0.0159	75.88	1729.38	21.55	0.021	29.47
Total	**94.54**	**100.00**	**0.368**	**28.34**	**7930**	**100.00**	**0.0111**	**71.66**	**8025**	**100.00**	**0.015**	**100.00**

Cyclone Overflow --- Standard KC Operation Mass Balance

Size (µm)	CONCENTRATE Mass (g)	Mass (%)	Grade (Pt oz/st)	Pt Rec %	TAILS Mass (g)	Mass (%)	Grade (Pt oz/st)	Pt Rec %	FEED Mass (g)	Mass (%)	Grade (Pt oz/st)	Au Dist'n %
600	1.03	1.20	0.01	100.00	0	0.00	**0**	0.00	1	0.01	0.005	0.00
425	1.52	1.77	0.01	100.00	0	0.00	**0**	0.00	2	0.01	0.009	0.01
300	4.67	5.42	0.01	4.33	171	1.70	0.004	95.67	175	1.73	0.004	0.38
212	8.02	9.32	0.01	2.43	501	4.98	0.007	97.57	509	5.01	0.007	1.77
150	13.66	15.87	0.00	0.87	794	7.88	0.006	99.13	807	7.95	0.006	2.33
106	16.17	18.78	0.07	11.32	1176	11.67	0.007	88.68	1192	11.73	0.008	4.73
75	17.03	19.78	0.27	29.26	1245	12.36	0.009	70.74	1262	12.42	0.012	7.79
53	10.74	12.48	0.90	44.18	1505	14.95	0.008	55.82	1516	14.92	0.014	11.02
38	6.24	7.25	1.87	40.89	1207	11.99	0.014	59.11	1214	11.95	0.023	14.35
25	3.60	4.18	2.58	27.34	1165	11.57	0.021	72.66	1169	11.50	0.029	17.14
20	1.05	1.22	3.12	29.99	194	1.92	0.040	70.01	195	1.92	0.056	5.52
-20	2.36	2.74	0.89	3.02	2115	21.00	0.032	96.98	2118	20.85	0.033	34.96
Total	86.09	100.00	0.485	21.04	10073	100.00	**0.016**	**78.96**	**10159**	**100.00**	**0.020**	**100.00**

Cyclone Overflow --- Variable Speed KC Operation Mass Balance

Size (µm)	CONCENTRATE Mass (g)	Mass (%)	Grade (Pt oz/st)	Pt Rec %	TAILS Mass (g)	Mass (%)	Grade (Pt oz/st)	Pt Rec %	FEED Mass (g)	Mass (%)	Grade (Pt oz/st)	Au Dist'n %
212	**4.40**	4.59	**0.014**	2.61	337	**3.83**	**0.0068**	97.39	341.10	3.84	0.007	1.69
150	**15.33**	15.98	**0.026**	8.76	782	**8.90**	**0.0054**	91.24	797.33	8.98	0.006	3.33
106	**21.14**	22.03	**0.013**	3.42	1139	**12.97**	**0.0070**	96.58	1160.60	13.07	0.007	5.94
75	**23.53**	24.53	**0.034**	7.56	1168	**13.30**	**0.0083**	92.44	1192.02	13.42	0.009	7.57
53	**13.19**	13.75	**0.229**	26.58	1388	**15.80**	**0.0060**	73.42	1400.91	15.77	0.008	8.21
38	**7.56**	7.88	**1.020**	52.92	1038	**11.81**	**0.0066**	47.08	1045.14	11.77	0.014	10.53
25	**5.54**	5.77	**1.811**	57.76	813	**9.26**	**0.0090**	42.24	818.85	9.22	0.021	12.56
20	**1.84**	1.92	**3.782**	74.38	235	**2.67**	**0.0102**	25.62	236.67	2.66	0.040	6.77
-20	**3.41**	3.55	**4.596**	26.10	1885	**21.46**	**0.0235**	73.90	1888.38	21.26	0.032	43.41
Total	**95.94**	**100.00**	**0.468**	**32.48**	**8785**	**100.00**	**0.0106**	**67.52**	**8881**	**100.00**	**0.016**	**100.00**

Cyclone Underflow --- Standard KC Operation Mass Balance

Size (µm)	CONCENTRATE Mass (g)	Mass (%)	Grade (Pt oz/st)	Pt Rec %	TAILS Mass (g)	Mass (%)	Grade (Pt oz/st)	Pt Rec %	FEED Mass (g)	Mass (%)	Grade (Pt oz/st)	Au Dist'n %
600	5.98	5.91	0.011	3.37	405	3.40	0.0046	96.63	411	3.42	0.005	0.21
425	8.94	8.83	2.226	70.62	783	6.57	0.0106	29.38	792	6.59	0.036	3.12
300	17.62	17.41	0.268	18.29	1280	10.73	0.0165	81.71	1297	10.79	0.020	2.86
212	19.29	19.06	1.145	44.44	2158	18.10	0.013	55.56	2177	18.11	0.023	5.51
150	21.95	21.68	1.586	43.22	2219	18.61	0.021	56.78	2241	18.64	0.036	8.92
106	13.75	13.58	6.252	64.76	2108	17.68	0.022	35.24	2122	17.65	0.063	14.71
75	7.11	7.02	21.221	74.80	1070	8.97	0.048	25.20	1077	8.95	0.187	22.36
53	2.88	2.85	52.463	75.45	656	5.50	0.075	24.55	658	5.48	0.304	22.19
38	1.52	1.50	45.352	64.01	350	2.93	0.111	35.99	351	2.92	0.306	11.93
25	0.83	0.82	14.277	28.53	252	2.11	0.117	71.47	253	2.10	0.164	4.58
20	0.34	0.34	2.387	5.97	111	0.93	0.116	94.03	111	0.92	0.123	1.51
-20	1.02	1.01	0.260	1.42	533	4.47	0.035	98.58	534	4.44	0.035	2.08
Total	**101.23**	**100.00**	**5.446**	61.10	**11925**	**100.00**	**0.029**	**38.90**	**12026**	**100.00**	**0.075**	**100.00**

Cyclone Underflow --- Variable Speed KC Operation Mass Balance

Size (µm)	CONCENTRATE Mass (g)	Mass (%)	Grade (Pt oz/st)	Pt Rec %	TAILS Mass (g)	Mass (%)	Grade (Pt oz/st)	Pt Rec %	FEED Mass (g)	Mass (%)	Grade (Pt oz/st)	Au Dist'n %
212	11.06	10.48	0.026	1.84	1207	15.91	0.0127	98.16	1217.76	15.84	0.013	5.64
150	34.69	32.87	0.019	1.59	1927	25.41	0.0206	98.41	1962.05	25.51	0.021	14.64
106	30.32	28.74	0.236	18.36	1726	22.76	0.0184	81.64	1756.52	22.84	0.022	14.11
75	16.83	15.95	1.210	48.99	857	11.30	0.0247	51.01	874.23	11.37	0.048	15.05
53	6.14	5.82	5.051	72.83	562	7.40	0.0206	27.17	567.70	7.38	0.075	15.42
38	3.03	2.87	10.370	86.30	326	4.29	0.0153	13.70	328.72	4.27	0.111	13.18
25	1.81	1.72	13.401	84.61	242	3.19	0.0182	15.39	244.07	3.17	0.117	10.38
20	0.61	0.58	11.936	80.28	77	1.02	0.0231	19.72	78.08	1.02	0.116	3.28
-20	1.03	0.98	5.752	25.85	660	8.70	0.0258	74.15	660.88	8.59	0.035	8.30
Total	**105.52**	**100.00**	**1.216**	**46.47**	**7584**	**100.00**	**0.0195**	**53.53**	**7690**	**100.00**	**0.036**	**100.00**

Appendix 6 Clarabelle Survey #1 Result

Clarabelle Survey#1 With Assays

Residual sum of squares: 424.7152 Final Results

	Stream	Absolute Solid Flowrate	Pulp Mass Flowrate Meas	Calc	S.D.	Adjust
1	SAG U/S	929.94	930	929.9	1	-0.1
2	PR Fines	50.02	50	50	1	0
3	Cyc U/F	2905.07	2500	2905.1	500	405.1
4	BM Dis.	2905.07		2905.1		
5	Cyc O/F	979.96		980		

	Stream	Relative Solids Flowrate
1	SAG U/S	100
2	PR Fines	5.38
3	Cyc U/F	312.39
4	BM Dis.	312.39
5	Cyc O/F	105.38

Fraction size distribution data of each stream for survey #1

	SAG U/S				PR Fines			
Size	Meas	Calc	SD.	Adj.	Meas	Calc	SD.	Adj.
850	21.85	21.69	0.5	-0.2	48.66	48.65	0.5	0
600	3.13	3.23	0.5	0.1	6.51	6.52	0.5	0
425	5.31	5.39	0.5	0.1	9.3	9.3	0.5	0
300	6.18	6.29	0.5	0.1	8.84	8.85	0.5	0
212	8.07	8.26	0.5	0.2	8.17	8.18	0.5	0
150	7.43	7.5	0.5	0.1	5.1	5.1	0.5	0
106	7.89	7.93	0.5	0	3.63	3.63	0.5	0
75	6.77	6.74	0.5	0	2.23	2.23	0.5	0
53	7.56	7.46	0.5	-0.1	2.09	2.08	0.5	0
37	5.82	5.79	0.5	0	1.4	1.4	0.5	0
25	5.8	5.83	0.5	0	0.94	0.94	0.5	0
20	1.55	1.47	0.5	-0.1	0.49	0.49	0.3	0
pan	12.64	12.42	0.5	0.2	2.64	2.63	0.3	0
total	100	100			100	100		

Fraction size distribution data of each stream for survey #1 (continued)

	Cyclone U/F				BM Dis (Ball Mill Discharge)				Cyclone O/F			
Size	Meas	Calc	SD.	Adj.	Meas	Calc	SD.	Adj.	Meas	Calc	SD.	Adj.
850	10.53	11.02	0.5	0.5	3.74	3.25	0.5	-0.5	0.01	0.01	0.1	0
600	3.06	2.76	0.5	-0.3	1.32	1.62	0.5	0.3	0.01	0.01	0.1	0
425	5.89	5.64	0.5	-0.3	3.6	3.85	0.5	0.3	0.3	0.29	0.2	0
300	9.65	9.3	0.5	-0.4	7.22	7.57	0.5	0.4	1.43	1.31	0.5	-0.1
212	16.2	15.6	0.5	-0.6*	13.83	14.43	0.5	0.6*	5.01	4.81	0.5	-0.2
150	16.67	16.44	0.5	-0.2	16.37	16.6	0.5	0.2	7.95	7.87	0.5	-0.1
106	15.79	15.68	0.5	-0.1	16.91	17.02	0.5	0.1	11.73	11.69	0.5	0
75	8.01	8.11	0.5	0.1	10.22	10.12	0.5	-0.1	12.42	12.45	0.5	0
53	4.9	5.21	0.5	0.3	8.16	7.85	0.5	-0.3	14.92	15.02	0.5	0.1
37	2.61	2.7	0.5	0.1	4.96	4.87	0.5	-0.1	11.95	11.98	0.5	0
25	1.88	1.78	0.5	-0.1	3.67	3.77	0.5	0.1	11.5	11.47	0.5	0
20	0.83	1.02	0.4	0.2	1.48	1.22	0.5	-0.3	1.92	2.01	0.5	0.1
pan	3.98	4.74	0.5	0.2	8.52	7.83	0.3	0	20.85	21.08		
total	100	100			100	100			100	100		

Assays of size fraction of each stream for survey #1

	SAG U/S			Primary Fines		
Size (um)	Pt oz/st	Pd oz/st	Au oz/st	Pt oz/st	Pd oz/st	Au oz/st
600	0.009	0.014	0.006	0.052	0.023	0.015
425	0.014	0.012	0.006	0.021	0.032	0.007
300	0.023	0.016	0.006	0.037	0.032	0.008
212	0.013	0.015	0.006	0.043	0.036	0.014
150	0.034	0.022	0.015	0.055	0.035	0.013
106	0.012	0.021	0.006	0.068	0.048	0.011
75	0.028	0.028	0.013	0.096	0.064	0.015
53	0.021	0.022	0.007	0.07	0.046	0.009
37	0.019	0.017	0.005	0.046	0.03	0.008
25	0.02	0.024	0.007	0.033	0.04	0.009
20	0.022	0.024	0.006	0.035	0.042	0.014
PAN	0.022	0.034	0.008	0.026	0.044	0.011

Assays of size fraction of each stream for survey #1 (Continued)

	Cylone Underflow			Ball Mill Discharge			Cylone Overflow		
	Pt	Pd	Au	Pt	Pd	Au	Pt	Pd	Au
Size (um)	oz/st	oz/st	oz/st	oz/st	oz/st	oz/st	oz/st	oz/st	oz/st
600	0.005	0.016	0.011	0.006	0.007	0.004	0.006	0.012	0.022
425	0.036	0.015	0.058	0.015	0.012	0.132	0.009	0.015	0.073
300	0.02	0.018	0.056	0.01	0.015	0.194	0.004	0.009	0.007
212	0.026	0.022	0.077	0.015	0.023	0.076	0.005	0.008	0.005
150	0.047	0.028	0.078	0.062	0.029	0.154	0.006	0.01	0.013
106	0.058	0.045	0.125	0.034	0.037	0.048	0.009	0.011	0.009
75	0.194	0.107	0.115	0.211	0.101	0.182	0.015	0.016	0.007
53	0.308	0.173	0.123	0.215	0.098	0.072	0.014	0.02	0.006
37	0.324	0.1	0.043	0.22	0.074	0.03	0.024	0.022	0.007
25	0.154	0.107	0.034	0.106	0.069	0.028	0.008	0.005	0.002
20	0.087	0.071	0.027	0.075	0.061	0.017	0.04	0.045	0.01
PAN	0.036	0.043	0.011	0.042	0.048	0.01	0.031	0.043	0.008

Clarabelle Survey #2 With Assays

Residual sum of squares: 376.9419 Final Results

	Stream	Absolute So Flowrate	Pulp Mass Flowrate Meas	Calc	S.D.	Adjust	
1	SAG U/S	929.99	930	930	1		0
2	PR Fines	49.97	50	50	1		0
3	Cyc U/F	3358.34	2500	3358.3	800	858.3*	
4	BM Dis.	3358.34		3358.3			
5	Cyc O/F	1279.99		1280			
6	RMDis	300.03	300	300	1		0

	Stream	Relative Solids Flowrate
1	SAG U/S	100
2	PR Fines	5.37
3	Cyc U/F	361.12
4	BM Dis.	361.12
5	Cyc O/F	137.63
6	RMDis	32.26

Fraction size distribution data of each stream for survey #2

	SAG U/S				PR Fines				Rod Mill Discharge			
Size	Meas	Calc	SD.	Adj.	Meas	Calc	SD.	Adj.	Meas	Calc	SD.	Adj.
850	26.01	26.08	0.5	0.1	43.12	43.12	0.5	0	22.63	22.65	0.5	0
600	4.22	4.06	0.5	-0.2	6.38	6.37	0.5	0	5.85	5.8	0.5	-0.1
425	5.72	5.63	0.5	-0.1	9.28	9.28	0.5	0	8.74	8.71	0.5	0
300	6.05	6	0.5	-0.1	8.84	8.84	0.5	0	8.48	8.46	0.5	0
212	7.78	7.81	0.5	0	9.16	9.16	0.5	0	8.71	8.72	0.5	0
150	6.9	7.01	0.5	0.1	6.18	6.19	0.5	0	7.3	7.34	0.5	0
106	7.2	7.31	0.5	0.1	4.7	4.71	0.5	0	6.92	6.96	0.5	0
75	6.29	6.33	0.5	0	2.74	2.74	0.5	0	5.87	5.88	0.5	0
53	7.4	7.39	0.5	0	2.85	2.85	0.5	0	6.78	6.78	0.5	0
37	3.5	3.55	0.5	0.1	1.28	1.28	0.5	0	4.63	4.65	0.5	0
25	4.25	4.35	0.5	0.1	1.78	1.79	0.5	0	1.78	1.81	0.5	0
20	2.78	2.52	0.5	-0.3	0.45	0.45	0.3	0	2.45	2.37	0.5	-0.1
pan	11.90	11.96			3.24	3.22			9.86	9.87		
total	100	100			100	100			100	100		

Fraction size distribution data of each stream for survey #2 (Continued)

Size	Cyclone U/F				BM Dis (Ball Mill Discharge)				Cyclone O/F			
	Meas	Calc	SD.	Adj.	Meas	Calc	SD.	Adj.	Meas	Calc	SD.	Adj.
850	15.06	14.81	0.5	-0.2	4.68	4.93	0.5	0.2	0.01	0.01	0.1	0
600	3.84	4.43	0.5	0.6	3.34	2.75	0.5		0.15	0.16	0.1	0
425	7.86	8.17	0.5	0.3	6.39	6.08	0.5	-0.3	0.92	1.02	0.5	0.1
300	11.79	11.98	0.5	0.2	10.41	10.22	0.5	-0.2	2	2.07	0.5	0.1
212	15.44	15.33	0.5	-0.1	14.96	15.07	0.5	0.1	7.43	7.39	0.5	0
150	14.31	13.92	0.5	-0.4	14.52	14.91	0.5	0.4	9.82	9.67	0.5	-0.2
106	11.74	11.34	0.5	-0.4	12.74	13.14	0.5	0.4	12.02	11.87	0.5	-0.2
75	5.93	5.78	0.5	-0.2	7.82	7.97	0.5	0.2	11.89	11.83	0.5	-0.1
53	4.42	4.45	0.5	0	7.04	7.01	0.5	0	13.75	13.76	0.5	0
37	2.49	2.29	0.5	-0.2	3.66	3.86	0.5	0.2	7.89	7.82	0.5	-0.1
25	1.27	0.91	0.5	-0.4	1.95	2.31	0.5	0.4	7.46	7.32	0.5	-0.1
20	0.72	1.25	0.4	0.5	2.91	1.96	0.5	-0.9	3.92	4.28	0.5	0.4
pan	5.13	5.34			9.58	9.79			22.74	22.8		
total	100	100			100	100			100	100		

Assays of size fraction of each stream for survey #2

	SAG U/S			Primary Fines			Rod Mill Discharge		
	Pt	Pd	Au	Pt	Pd	Au	Pt	Pd	Au
Size (um	oz/st	oz/st	oz/st	oz/st	oz/st	oz/st	oz/st	oz/st	oz/st
600	0.007	0.01	0.003	0.019	0.031	0.002	0.008	0.008	0.003
425	0.006	0.015	0.01	0.03	0.04	0.003	0.006	0.007	0.003
300	0.023	0.015	0.006	0.028	0.041	0.004	0.009	0.009	0.145
212	0.012	0.017	0.003	0.032	0.04	0.004	0.011	0.009	0.009
150	0.016	0.016	0.009	0.051	0.041	0.011	0.018	0.009	0.007
106	0.018	0.016	0.007	0.061	0.047	0.014	0.014	0.009	0.008
75	0.024	0.021	0.008	0.061	0.06	0.014	0.015	0.01	0.009
53	0.016	0.019	0.006	0.057	0.052	0.008	0.009	0.01	0.004
37	0.023	0.021	0.007	0.052	0.005	0.01	0.015	0.013	0.008
25	0.02	0.019	0.007	0.032	0.039	0.009	0.018	0.013	0.007
20	0.023	0.023	0.007	0.039	0.047	0.011	0.015	0.015	0.006
Pan	0.017	0.023	0.007	0.031	0.042	0.01	0.013	0.018	0.007

Assays of size fraction of each stream for survey #2 (Continued)

	Cylone Underflow			Ball Mill Discharge			Cylone Overflow		
Size (um	Pt oz/st	Pd oz/st	Au oz/st	Pt oz/st	Pd oz/st	Au oz/st	Pt oz/st	Pd oz/st	Au oz/st
600	0.006	0.012	0.045	0.009	0.028	0.058	0.006	0.012	0.022
425	0.006	0.008	0.049	0.008	0.011	0.018	0.009	0.015	0.073
300	0.018	0.013	0.098	0.017	0.013	0.066	0.004	0.009	0.007
212	0.012	0.016	0.109	0.022	0.012	0.187	0.007	0.009	0.007
150	0.065	0.023	0.124	0.043	0.019	0.132	0.006	0.009	0.01
106	0.07	0.036	0.21	0.055	0.028	0.165	0.006	0.009	0.007
75	0.132	0.057	0.285	0.153	0.054	0.194	0.005	0.009	0.005
53	0.161	0.07	0.087	0.101	0.038	0.073	0.006	0.011	0.005
37	0.502	0.148	0.159	0.301	0.087	0.081	0.01	0.012	0.022
25	0.161	0.075	0.043	0.085	0.042	0.025	0.018	0.016	0.006
20	0.087	0.051	0.021	0.063	0.035	0.018	0.017	0.017	0.006
Pan	0.028	0.03	0.011	0.027	0.029	0.007	0.028	0.026	0.009